CRANFIELD UNIVERSITY

OMKAR VITTHAL GULAVANI

COMPARATIVE ASSESSMENT OF IMPLICIT AND EXPLICIT FINITE ELEMENT SOLUTION SCHEMES FOR STATIC AND DYNAMIC CIVILIAN AIRCRAFT SEAT CERTIFICATION (CS25.561 AND CS25.562)

SCHOOL OF ENGINEERING

PhD THESIS
Academic Year: 2012 - 2013

Supervisor: Dr Kevin Hughes and Professor Rade Vignjevic
MARCH 2013

CRANFIELD UNIVERSITY

SCHOOL OF ENGINEERING

PhD THESIS

Academic Year 2012 - 2013

OMKAR VITTHAL GULAVANI

COMPARATIVE ASSESSMENT OF IMPLICIT AND EXPLICIT FINITE ELEMENT SOLUTION SCHEMES FOR STATIC AND DYNAMIC CIVILIAN AIRCRAFT SEAT CERTIFICATION (CS25.561 AND CS25.562)

Supervisor: Dr Kevin Hughes and Professor Rade Vignjevic

MARCH 2013

dedicated to my parents

ABSTRACT

Due to the competitive nature of airline industry and the desire to minimise aircraft weight, there is a continual drive to develop lightweight, reliable and more comfortable seating solutions, in particular, a new generation slim economy seat. The key design challenge is to maximise the "living space" for the passenger, with strict adherence to the 'Crash Safety Regulations'.

Cranfield University is addressing the needs of airliners, seat manufactures and safety regulating bodies by designing a completely novel seat structure coined as "Sleep Seat". A generous angle of recline (40 degree), movement of "Seat Pan" along the gradient, fixed outer shell of the backrest, and a unique single "Forward Beam" design distinguishes "Sleep Seat" form current generation seats. It is an ultra-lightweight design weighing 8kg (typical seat weight is 11kg). It has to sustain the static (CS 25.561) and dynamic (CS25.562) "Emergency landing" loads as specified by "Certification Specifications (CS).

Apart from maintaining structural integrity; a seat-structure must not deform, which would impede evacuation, should absorb energy so that the loads transferred to Occupants are within human tolerance limits and should always maintain survivable space around the Occupant. All these parameters, which increase a life-expectancy in a 'survivable' crash, can be estimated using either experimental testing or virtual simulation tools such as "Finite Element Analysis (FEA). Design of the "Sleep Seat" is still in its conceptual phase and therefore experimental testing for all the design iterations involved is unrealistic, given a measure of the costs and timescales involved.

Therefore focus of research is to develop practical and robust FE methodologies to assess static and dynamic performances of a seat-structure so as to compare different design concepts based on their strength, seat interface loads (a limit defined by strength of aircraft-floor), maximum deformations and cross-sectional forces.

The first aim of the research is to develop FE methodologies for demonstrating static (9g) compliance i.e. structural adequacy of the seat-structure to sustain

CS25.561 loads. Implicit formulation has been identified to simulate the loadcases in which loads are introduced into the seat-structure without body blocks. Strategies to obtain a converged solution have been discussed. A framework to verify the reliability of FEA results has been demonstrated for a case-study of 'Downward 8.6g' load applied to the triple occupancy seat design. Different solvers have been compared in terms of CPU time required for the case-study.

Case-study is then simulated using explicit formulation. Challenges such as realistic CPU time and quasi-static solution have been addressed. A matrix has been developed to assess the quality of FEA results.

Results of the case-study solved using both the formulations are then compared against those from experimental tests. An acceptable level of agreement between FEA results and test results helped to validate both the FE methodologies developed to evaluate structural performance of the seat when subjected to static certification loads (CS25.561).

For the static loads applied over body blocks, implicit formulations struggle to converge whereas inherent lack of convergence for explicit formulation is advantageous. Therefore, explicit methodology is further extended to simulate loadcases with body blocks and validated against experimental tests thereby addressing all the issues related with virtual simulations pertaining to static compliance of an aircraft seat.

In dynamic compliance, CS 25.562 (Dynamic loads) specifies two different deceleration pulses to be applied to the structure. Seat structure has to withstand a '16g' pulse applied in a combined longitudinal and lateral direction with damaged floor (called as floor-distortion). Whereas a "14g" pulse, is applied in a combined vertical and longitudinal direction.

Literature review showed that earlier attempts have either failed or compromised on separating '16g' and 'floor distortion'. During this research, two different methods are developed and successfully implemented to combine these two loadcases, which is one of the novelties of this research. Going

further, two innovative, practical and economical design solutions have been proposed and evaluated to mitigate the detrimental loads introduced into the seat-structure due to floor-distortion loads.

Instead of merely using FEA as a post-design prediction tool, it has been seamlessly intervened into the design process to derive the optimum and feasible concepts. Using Altair / Optistruct, design of seat-leg has been derived considering combination of critical loads, manufacturability, mass and symmetry of design. Seat-structure with optimised seat-leg design is then evaluated against static and dynamic certification loads using validated FE methodologies. Triple seat-structure under study can withstand both types of loads without disintegrating from the load path, excessive plastic deformation of the components, damaging the seat track and exceeding the allowable deformation limits thus demonstrating '16g compatibility'.

Hypermesh, a product of Altair Engineering is extensively used for pre-processing, Abaqus (Research) 6.9-3 and LSDYNA V9.71 R4.2.1 as solution platforms, Hyperview, Hyperstudy, LsPre-Post and Abaqus / CAE, Abaqus / Viewer for post-processing, and "Optistruct" for optimisation. Wherever possible, spreadsheets are developed using analytical calculations and are used as a "Quick and Simple" design tools. In house programmes for data conversion are developed using "FoxPlus". Bill Of Materials (BOM), boundary conditions, total loads considered, definition of output matrices to extract useful information from FEA, and cards to control the solution progress used in this research are presented in the Appendix section.

Keywords:

Certification By Analysis, LSDYNA V9.71 R4.2.1, Abaqus (Research) 6.9-3, Optistruct, Damaged floor condition, Aircraft Seat

ACKNOWLEDGEMENTS

I am indebted to my supervisor Dr Kevin Hughes for his guidance, help and support throughout this research. He gave me the freedom to try my ideas and helped me in every possible way. I am inspired by his tremendous energy, flexible nature, humbleness and interests in many fields of engineering.

I consider myself fortunate to have had the chance to work under Professor Vignjevic Rade. His brilliance, innovative ideas and ability to foresee problems have been some of the major driving forces for this research.

I would like to thank Mrs Marion Bastable for helping me with all the paper work and offering valuable suggestions.

Had it not been for Eileen and Stephan Cave, my life after University hours would have been boring. Due to their caring and understanding nature, I did not miss my parents.

I would like to express my gratitude to my brother Ashish, for his emotional support

Last but not least, I am thankful to my wife Priyanka, for her patience and support during my write-up

TABLE OF CONTENTS

LIST OF FIGURES

LIST OF TABLES

LIST OF ABBREVIATIONS

ARP	Aerospace Recommended Practice
AS	Aerospace Standard
ATD	Anthropomorphic Test Dummy
CAA	Civil Aviation Authority
CBA	Certification By Analysis
CS	Certification Specification
dof /DOF	Degree of Freedom
DVT	Deep Vein Thrombosis
EASA	European Aviation Safety Agency
FAA	Federal Aviation Administration
FEA	Finite Element Analysis
GASP	General Aviation Safety Panel
HIC	Head Injury Criterion
HPC	High Performance Computing, 856 processor HPXC Cluster available at Cranfield University
IE	Internal Energy
JAA	Joint Aviation Authorities
KE	Kinetic Energy
LHS	Left Hand Side
NASA	National Aeronautics and Space Administration
RHS	Right Hand Side
SNPRM	Supplemental Notice of Proposed Rulemaking
TLF	Tool-less fitting
TSO	Technical Standard Order
VMS	Von Mises Stress in MPa

1 INTRODUCTION

Due to all-inclusive economic development, number of travellers opting for air travel has increased steadily over the last two decades [1]. Naturally, airframe manufacturers are developing airframes to absorb increased demand of more carrying capacity, comfort levels and safety related issues. Therefore, the issues concerned with prevention of occurrence of accidents and improvement in the survival rate, in the event of an accident or emergency landing will be major topics for research in years to come. Failure to initialise measures to deal with increased risk of exposure to accidents and injuries in air travel may only lead to lowering of passenger confidence in air safety.

Efforts should concentrate on reducing fatalities and injuries resulting from accidents and providing survivable space for passengers throughout all the phases of flight. They should address in-flight issues such as turbulence and fire as well as post-crash survivability, which includes crashworthiness, occupant retention, loads transferred to the occupants and rapid evacuation.

Federal Aviation Administration (FAA) and National Aeronautics and Space Administration (NASA) undertook wide range of research activities to address the crashworthiness characteristics of the transport category aircraft, rotorcraft and small general aviation aircraft [2]. The aircraft behaviour and the Occupant characteristics were observed through the inter-related studies comprising of aircraft accident data, static and dynamic analysis of the crash events, full-scale aircraft impacts tests and aircraft-seat tests. A panel General Aviation Safety Panel (GASP) formed in 1978, made recommendations on crashworthiness requirements during the survivable accidents for which the floor remained intact [2].

Findings of these studies summarised as follows, form the foundation of the crashworthiness design standards for civil aircrafts.

- To maximise the Occupant protection, a system's approach in which; every subsystem is considered for crashworthiness design; should be used e.g. when an aircraft impacts the ground, deformation of ground

absorbs some energy. However, this is an uncontrollable variable since the quality of impacted surface usually cannot be selected by the pilot. Then the landing gear and crushing of the fuselage absorb the energy. Since the fuselage is also expected to maintain the 'survivable' and 'protective' shell around the Occupant, crushing must occur outside the protective shell. The seat and restraint systems, last item in the crash sequence to remain in motion; restraint the Occupant within the protective shell without detaching from the floor and provide an additional energy-absorbing stroke to further bring down the Occupant declarative loading below the human tolerance limit. A well-designed Energy absorbing seat functions under most conditions of the impact surface and altitude and is therefore, a highly reliable method of attenuating the Occupant loads [3].

- During a crash event, Occupant's centre of gravity acquires a relative velocity with respective to the airframe because of the extension of the restraint harness, compression of the soft human tissues loaded by the harness, relative movement of the body parts and compression of the seat-cushion before 'bottoming' out. The magnitude of the relative velocity depends on the magnitude and duration of the deceleration pulse and interaction between the connection between an Occupant and the seat structure. In order to maintain the integrity with an airframe, seat structure must either
  - Option I - Possess the capability of sustaining the inertial forces imposed by the deceleration of the Occupant and seat without collapse or
  - Option II - Possess sufficient energy-absorbing capacity to bring the occupant to a complete rest before the structural failure.

'Option I' demands seat structure with a significant strength as the elasticity of the restraint harness and seat-cushion may result in a dynamic overshoot of 1.2 to 2 [3]. Dynamic overshoot is the ratio of output decelerative force to the input decelerative force. Thus to accommodate an input floor pulse of 20g, seat with design strength of 24g to 40g may be necessary to design. In addition, forces

transmitted to the Occupant may be above the human tolerance limit. Therefore, ‘Option I’ is not a practical solution.

‘Option II’ is a practical and an economical design approach as the seat motion behaviour is used to limit the loads transferred to the Occupant. Seat structure would start deforming plastically when the acceleration of the combined mass of the Occupant and seat reaches the pre-designed limit load. Seat then absorbs the energy, without disintegrating from the floor and maintains the Occupant loads below the survivable limits.

Crashworthy aircraft-seat design is a major challenge for the aviation industry since its customers place a greater emphasis on the comfort and appearance of a seat, which they can ‘see’ or ‘feel’; than on its crashworthiness performance, which cannot (and not expected) to be easily demonstrated. Thus, there is a strange relationship between ‘comfort’ and ‘crashworthy design’ of an aircraft seat.

Comfort is reflected in the requirements for a variety of the adjustment knobs as well as a demand for plush upholstery [3, 4]. Various adjustment knobs compete for the space with energy absorbing systems, thus complicating the design of later. Increased cushioning tends to increase the pelvic loads during the download test. Payne has demonstrated increase in the injury potential associated with the amplification effect of the seat cushions by comparing ‘Dynamic Response Indexes’ of different designs of seat cushions [3]. Thus ‘comfort’ and ‘crashworthy design’ are the curves with opposite slope!

A well-designed crashworthy seat would enhance the Occupant protection if it is used and it will only be used if it is ‘comfortable’! Therefore development of a ‘Comfortable AND effective Crashworthy seat’ requires thoughtful integration of specifications and standards, energy absorption concepts, combination of the seat cushions, seat pans, seat legs, restraint systems, human tolerances, fire safety, aesthetic and ergonomic considerations [4].

Thus, seating solutions entail balancing different requirements. The architecture must meet the requirements for reliability, strength, comfort, weight,

manufacturability, cost, and assembly. Development must be accomplished in time to be in sync with airliners critical-path development plan.

Drilling down, analysts must evaluate structural performance and kinematic properties of the restraint system with the objective of harmonising the different constraints and delivering the end-product, which properly function for their intended use and provide safety during emergency landings.

Therefore, design and development of a new aircraft seat is time consuming and costly process, which includes design iterations, development tests, prototyping, full-pledged tests and optimisation. To reduce the time and money involved in physical testing, Finite Element Analysis (FEA) that simulate the testing scenario and predict the static and dynamic behaviour of the structure can be used. FEA shortens build-test-break cycle from months to weeks of computer calculations. It also imparts flexibility, to the designers, of quickly comparing number of design options that is not practical with physical tests due to time and budget involved. It helps to differentiate under-designed as well as over-designed parts. Recent developments in computer hardware (e.g. High Performance Computing, HPC) and simulation software, has made it possible to analyse complex models at low costs.

As a promising step to future, FAA has released a programme called ‘Certification By Analysis (CBA)’, the ultimate goal of which would be to substantiate physical testing by virtual simulations, which would offer significant cost reductions and would encourage more designers to come forward with ground-breaking seat designs [5].

1.1 AIMS AND OBJECTIVES OF THIS RESEARCH

This thesis addresses the need to develop a robust and validated virtual testing methodology using implicit and explicit finite element codes in order to evaluate the static and dynamic certification compliance of a next generation aircraft seat.

Being able to develop a numerical framework that addresses the needs of airliners and seat manufacturers to reduce inherent weight, in addition to comply with safety regulating bodies is essential in order for designers to evaluate different design concepts and arrive at feasible, robust and manufacturable designs in a faster and more economical way.

The outcomes from this research are not only relevant to aircraft sector, but can also be applied to seat designers in automotive and rail sectors where similar technical and numerical simulation problems are encountered.

The objectives of this research are,

- Develop a framework for the analysis led design of a novel seat-structure to demonstrate compliance against Crash Safety regulations. This research will develop robust methodologies when applying different Finite Element formulations to assess the suitability of a chosen configuration through a sound engineering and application of FEA.

- Develop guidelines for an FE analyst to obtain a reliable solution for a highly non-linear (involving all three types on non-linearities i.e. geometric, material and contact) problem when investigating the structural behaviour of complete seat subjected to the crash loads. This will also involve comparison of different numerical techniques based on parameters such as computational time, numerical accuracy and pre-processing (FE model building and assigning boundary conditions) together with efforts required to achieve a satisfactory solution. The guidelines developed should be extended to consider the dynamic crash certification requirements.

- Propose a framework to critically assess the quality of numerical results and to provide confidence in their use as a main design tool during the conceptual design phase, when usually experimental tests are not performed, due to time and cost associated with prototyping/ tooling.

- Demonstrate usefulness of FE procedures developed during this research by evaluating different design concepts and comparing the results against experimental data.

- Develop a methodology for applying numerical optimisation techniques to derive a novel and manufacturable design concept, which would accelerate the design process.

1.2 STRUCTURE OF THE REPORT

Chapter 2 takes an overview of different regulations used during certification. It identifies the static and dynamic requirements of a seat, guidelines to 'define' an acceptable performance of seat-structure during emergency landing conditions and general guidelines of seat designing. It shows different stages of development of an aircraft seat where FEA has been predominantly used by various researchers. It also opens up new potential areas for future research work.

Chapter 3 describes the components involved in the design of "Sleep Seat" and novelty this research. It then presents project plan for this research, which includes milestones and a breakdown of research activities.

Chapter 4 presents application of implicit formulation to solve the loadcases where static loads (CS 25.561) are applied to the seat-structure. The chapter elaborates steps in the implicit solution scheme; challenges such as non-convergence faced during its application and solutions provided by this research. Loadcase of 'Downward 8.6g' applied to the 'triple seat-structure' is chosen as a case-study. The solution obtained is then thoroughly checked against FE quality checks and an exercise to reduce the CPU time (using different solution techniques) has been performed.

Chapter 5 gives development of a methodology for utilising an explicit solution scheme to solve quasi-static problems such as static loads applied to the seat-structure. As the size and complexity of FE models increase, implicit formulation struggles to find a 'converged' solution, whereas 'inherent lack of convergence'

is a major strength of explicit codes. The chapter discusses the steps in the explicit solution scheme, challenges faced during its application and solutions provided by this research. 'Downward 8.6g' loadcase (solved using implicit formulation in Chapter 4) has been solved as a case-study and different quality checks to verify solution have been demonstrated.

Chapter 6 compares the FE results of the 'Downward 8.6g' loadcase solved using implicit and explicit solution schemes. After self-verification of these two schemes, results have been compared against those from experimental tests. A reasonable correlation between results helps to validate both the procedures developed during this research. Methodology is then extended to simulate complex loadcases such as 'Forward 9g' i.e. load applied through body blocks.

Chapter 7 revolves around the FE procedure derived for simulating "Damaged floor Condition'' or 'Seat Pre-deformation', a pre-requisite for dynamic '16g' tests. Three different solution techniques have been applied to solve this loadcase and are compared. Going further, innovative design solutions to reduce the loads introduced by damaged floor into the seat-structure have been developed and evaluated.

Chapter 8 is a bridge between static loads (CS25.561 and damaged floor condition) and dynamics loads (CS 25.562). Design improvements based on static results, though do not guarantee success during ultimate dynamic tests, but at least improve the chances. Therefore, this chapter presents a brief overview of design activities such as identification of deficiencies, application of topology optimisation scheme to lead the design of seat-leg and assessment against static loads. It demonstrates static (9g) compliance of the triple seat-structure.

Chapter 9 focuses on a FE procedure to initiate stresses and strains due to the 'damaged floor condition' into the '16g' loadcase. It provides two different techniques to combine these two loadcases. It discusses element technology, contact algorithm and minimum stable time-step increment criteria used in explicit formulation. Triple Sleep-Seat structure is then analysed for '16g' and

‘14g’ dynamic load according to CS25.562 and ‘16g Compatibility’ is demonstrated.

Chapter 10 concludes this research and provides ideas/areas for future researchers.

Appendix A provides drawbacks of conventional seat tie-down connections (anchorages).

Appendix B provides a list of CONTROL CARDS required in LSDYNA to perform an implicit analysis.

Appendix C provides a list of CONTROL CARDS required in LSDYNA to perform an explicit analysis.

Appendix D provides a list of CONTROL CARDS used in LSDYNA to extract various outputs such as interface loads, cross-sectional forces etc.

Appendix E describes procedure to calibrate ‘ImageJ’, software used to measure deflections of seat-structure after experimental testing.

Appendix F takes an overview of different designs of leg-clamps.

Appendix G provides analytical calculations and results of FE simulations performed for sizing a novel elastomeric leg-clamp developed during this research.

Appendix H reports comparison of contact pressure distribution on modified tool-less fitting, estimated by analytical calculations and FEA. A good agreement between the results indicates sufficient discretisation density and appropriate algorithm used for contact compatibility.

Appendix I describes definition of boundary conditions for floor-distortion performed using Abaqus (Research) 6.9-3 and LSDYNA.

Appendix J describes the procedure to initiate damaged floor condition (initial stresses and strains), in a ‘16g’ dynamic simulation. It provides the programme developed in FOXPlus to convert Abaqus (Research) 6.9-3 output in LSDYNA format.

Appendix K provides mechanical properties of the materials used for various components of the seat-structure.

Appendix L provides nomenclature of the Seat-leg from design viewpoint.

Appendix M describes the FE model of complete seat-structure i.e. nomenclature, bill of materials, contact pairs defined; used to demonstrate static (9g) compliance.

Appendix N provides von mises stress (VMS) plots for major load carrying members of the seat-structure subjected to static certification (CS25.561) loads.

Appendix O provides VMS plots for major load carrying members of the seat-structure, which is subjected to dynamic loads (16g and 14g) according to CS25.562.

Appendix P provides time history plots for the triple seat-structure with three ATDs, for the applied ‘16g’ pulse with damaged floor condition.

2 LITERATURE REVIEW

Post September 11, many people were reluctant to fly and were looking for other modes of transportation. So many airliners either “parked” or “retired” their older air fleet instead of operating with empty seats. This resulted in a negative impact on company balance sheet. Once this downturn in number of boarding was over; airlines met by increased fuel prices and cut throat competition from low cost carriers; thereby further weakening the financial status. In addition, on October 4, 2002, FAA published ‘Supplemental Notice of Proposed Rulemaking (SNPRM)’, which stated that all airplanes (newly manufactured and existing with retrofitting) should have ‘16g’ seats [6]. After re-evaluation, retrofitting requirement was dropped down. However, cost of implementation of new rule was still $33.7 million for passenger seats [7]. Further, due to heavier seats (in order to meet the dynamic conditions proposed by Section 25.562) and added cost of certification of ‘16g’ seats; requirement of 16g seats was received by the airlines with hesitation.

Hence an independent consultancy firm R.G.W. Cherry and Associates Limited was appointed by FAA to study the impact of implementation of ‘16g’ seats over ‘9g’ seats in transport category aircrafts mainly considering the “Cost – Benefit” relationship [7]. The Cherry Report studied accidents in transport category airplane, which occurred from 1984 to 1998 and predicted the benefits to the occupants if ‘16g’ seats had been installed in those airplanes. Findings from this cost analysis showed that the benefit of approximately $76.3 million, as compared to the costs of $33.7 million.

Hence with the background of solid economic and safety advantages FAA finally published the rule on September 20, 2005, which states that [8],

After October 27, 2009, no person may operate a transport category airplane type certificated after January 1, 1958 and manufactured on or after October 27, 2009 in passenger-carrying operations under this part unless all passenger and flight attendant seats on the airplane meet the requirements of Section 25.562 in effect on or after June 16, 1988 [8]. Thus 16g seats were introduced.

What is a 16g seat?

A ‘16g’ seat can withstand static and dynamic loads as specified by Certification Specifications, CS 25.561 and CS 25.562 respectively without

- Generating discontinuity in the load path
- Disintegrating from the aircraft floor
- Deforming in any manner that would hamper or block the rapid evacuation
- Exceeding the human tolerance limit
- Encroaching Occupant survivable envelope

Please note that the CS 25.561 and CS 25.562 are discussed in detail in Section 2.1.3 of this chapter.

Following topics were covered in the literature review presented in the thesis for ‘Master of Science by research’ of the author present report [9]

- Historical overview of accidents statics and causes
- Classification and definition of accidents
- Crashworthiness design principles
- Compliance of ‘Sleep Seat’ against Comfort regulations (Generic Requirements 2)

This chapter has been divided in three phases

- First phase of this chapter focuses on relevant safety standards, evaluation criteria for structural performance of an aircraft seat, limits on Occupant loads, load application procedures and measurement techniques for test results. In the end it also presents general safety design principles to be considered while designing an aircraft-seat.
- Next phase of literature review takes a brief overview of work done by various researchers in developing FEA framework to design and develop an aircraft seat. Work specific to a particular area for example floor distortion or mechanism of implicit and explicit algorithms has been presented in relevant chapters.

- Last phase of this chapter presents areas in which regulating bodies need to do substantial research to enhance the safety sphere accommodating all types of passengers. It presents some ideas for future research.

2.1 OVERVIEW OF SAFETY STANDARDS FOR AN AIRCRAFT SEAT

Three main documents, which cover the topics related to safety regulations that a seat must meet to be installed on a passenger carrier are

- Aerospace Recommended Practice, ARP5526
- Aerospace Standard AS8049
- Certification Specifications, CS

2.1.1 AEROSPACE RECOMMENDED PRACTICE, ARP5526

The Society of Automotive Engineers (SAE) - ARP5526 outlines guidelines, to promote a common platform for design criteria and compliance issues faced by designers during certification of aircraft seats [10]. ARP5526 has been prepared considering the following publications. In case of a conflict between ARP5526 and these documents, ARP5526 takes precedence unless a specific exemption has been released. The publications are

AS8049	Performance Standards for Seats in Civil Rotorcraft, Transport Aircraft, and General Aviation Aircraft [11]
14CFR Part 25	Code of Federal Regulations, Title 14 Part 25 Airworthiness Standards: Transport Category Airplanes. It also considers 14 CFR for Part 23, Part 27, Part 29 and Part 121 [10].
AC 25-17	Advisory Circular by European Aviation Safety Agency (EASA), Transport Airplane Cabin Interiors Crashworthiness Handbook
TSO – C39, C127 and C22	Technical Standard Order (TSO) by Department of Transportation for o Aircraft Seats and births, o Rotorcraft, Transport Airplane and Normal and Utility Airplane Seating systems, Safety Belts
NAS 809	National Aerospace Standard (NAS) by Aerospace Industries Association (AIA), Specification – Aircraft Seats and Berths
NASA-STD-3000	National Air and Space Administration Publication on Man-Systems Integration Standards

Table 2-1 List of documents considered for generating ARP5526 (Aerospace Recommended Practice), a common platform for seat designers for guidelines on design criteria and compliance issues [10].

2.1.2 AEROSPACE STANDARD AS8049

It discusses minimum performance standards, qualification requirements and minimum documentation requirements for the passenger aircraft seats [11]. It provides the guidance for the test procedures, measurements, test equipment and the interpretation of the results to promote uniformity in certification of passenger aircraft seats and to achieve acceptable data. Its goal is to achieve enhanced comfort, serviceability and Occupant safety in air travel. The responsibility of the performance of seating system is divided between the seat

supplier and the installation applicant [11]. It is the seat supplier's duty to achieve the satisfactory performance of the seat as per 'CS' and to provide all the necessary data (prescribed by AS8049) to the installation applicant who in turn must ensure that all the requirements for a safe seat installation have been met [11].

2.1.3 CERTIFICATION SPECIFICATIONS, CS

EASA (European Aviation Safety Agency) is an agency of EU (European Union) which looks after the safety analysis and research of civil aviation [12]. EASA owns the responsibility for airworthiness certification of all aeronautical products and parts developed and used under the EU member States [12]. "Subpart C– Structures" from Certification Specifications for Large Aeroplanes (CS-25), published by EASA, provides static and dynamic requirements that a seat-structure must satisfy, in order to be installed in flight, in sections CS25.561 and CS25.562 respectively [13].

CS 25.561 provides the magnitude and directions of the ultimate loads to be applied to the seat-structure and AS8049 describes the procedure for applying these loads.

A list of additional useful documents is as follows,

Relevant Regulation on Safety requirements from aircraft seat	Content used in this research
Advisory Circular 25.562-1B	Acceptable means of compliance e.g. maximum deformation limits on seat –structure subjected to CS 25.561 and CS 25.562 loads [14]
National Aerospace Standard 809	Guidance for CS25.561 load application point [15]
Aircraft Manufactures requirements	Design philosophy for of Seat-leg and Seat Interface Loads are taken from Boeing Specification D6 36238 [16]
Aircraft Design Survivable Guide Volume IV	Useful design guidelines and crashworthiness principles for aircraft seat design [3]
FAA Technical Report- No. FS-70-592-120A	A useful document to understand advantages of a crashworthy aircraft seat and design ideas to improve its structural performance [17]
FAA Technical Report ADS-24	A document to understand development of crashworthiness principles to maximise life expectancy during a crash [18]
AC 20-146	Acceptable means to comply with dynamic tests using computer modelling [19].

Table 2-2 List of useful documents related with Occupant safety during air travel and their content used in this research. Author of this report strongly encourages reading through these documents to gather a sound understanding of crashworthiness.

The author of this report encourages seat analysts and designers to go through all these documents as they help to understand the crashworthiness design

principles. Parallel documents are available in automotive industry, which should be studied as well to obtain an overall idea of crashworthiness.

2.1.3.1 CS 25.561 – GENERAL [13]

The purpose of static tests is to demonstrate that the seat structure has adequate strength to sustain the Ultimate Inertia Loads acting separately on it, in all the principle loading directions (Figure 2-1). In the event of emergency landing or minor crash, the seat structure must be designed in such a way that each occupant has a reasonable chance of escaping the damaged aeroplane when the proper use of seat belts and other safety provisions is made. The limit on the maximum deformation of seat for each loading condition ensures that seat structure would not yield in any manner that would hamper or block the rapid evacuation of the occupants or encroach into any required passageway [13, 14].

The loads are applied at a slow enough rate (quasi-static) so as to observe the behaviour of the structure for the known loads. It exposes the weak areas and corrective actions can be taken before ultimate dynamic tests.

Seat primary structure, the occupant restraint system and the seat anchorages should be accurately represented. Items that are not part of the primary load carrying structure and omission of which will not alter structural performance of the seat can be excluded from the test article but their weight should be considered when determining the static loads [11].

Out of different designs of the body block supplied by AS8049, a suitable design can be installed in the place of each occupant and should be restrained by the occupant restraint. As long as the load application point complies with AS8049, design of the body block can be refined or modified as per the requirement.

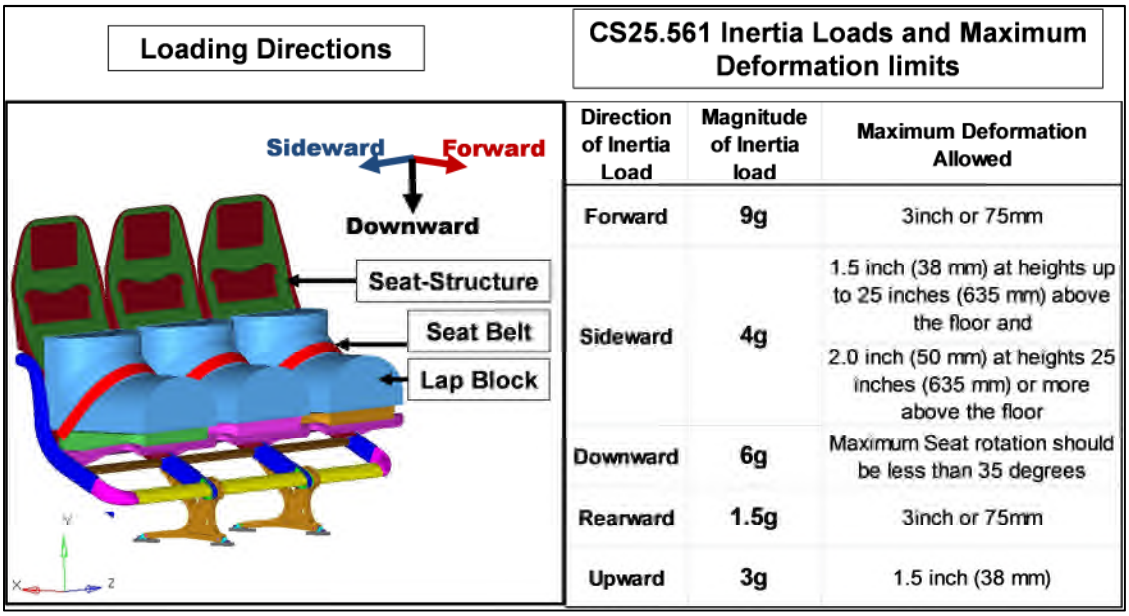

CS25.561 Inertia Loads and Maximum Deformation limits

Direction of Inertia Load	Magnitude of Inertia load	Maximum Deformation Allowed
Forward	9g	3inch or 75mm
Sideward	4g	1.5 inch (38 mm) at heights up to 25 inches (635 mm) above the floor and 2.0 inch (50 mm) at heights 25 inches (635 mm) or more above the floor
Downward	6g	Maximum Seat rotation should be less than 35 degrees
Rearward	1.5g	3inch or 75mm
Upward	3g	1.5 inch (38 mm)

Figure 2-1 LHS Inertial loading directions for Seat-Structure according to CS25.561 [13]. RHS – Magnitude of static inertia load to be applied to the seat-structure in a particular direction along with the maximum deformation limits upon load application [13, 14].

Procedure to apply CS 25.561 loads is as follows [10]

- For the application of down loads (i.e. 'Downward 6g') representative distributed loading of the seat pan must be achieved.
- For the Forward (9g), Sideward (4g) and Upward (3g) loads, the lap block should be placed either on the actual bottom cushion or on a non-rigid block representation of the bottom cushion (Figure 2-1 LHS).
- For the forward facing seats, lap block and the non-rigid foam block placed between the lap block and the back structure should ensure distribution of the rearward loads over the seat-back. In present research, rearward (1.5g) loads have been directly applied to the seat-back structure ensuring uniform distribution thereby minimising the computational cost and time required had the body block and back-cushion been used.

Requirements to demonstrate compliance against CS25.561 [10, 13, 14]

- Seat structure should withstand the static loads without failure in the load path for at least 3 seconds.
- It should not dis-integrate from aircraft floor.
- After the removal of test load, measurements e.g. permanent deformation if any should be made. Maximum permanent deformation of the seat-structure should be within the allowable limit as specified in Figure 2-1RHS in corresponding inertia loading direction.

2.1.3.2 CS25.562 – EMERGENCY LANDING DYNAMIC CONDITIONS [13]

CS 25.562 dynamic loading conditions have been summarised in Figure 2-2 [13, 14].

Parameters	14g – Combined Vertical and Horizontal Peak Floor Deceleration	16g- Combined Longitudinal and lateral Peak Floor Deceleration
Minimum Change in the Velocity to be Demonstrated (mm/s)	Downward vertical velocity of 10700	Forward longitudinal velocity 13400
Maximum Time for the Peak Floor Deceleration, t1 (s)	0.08	0.09
Minimum Floor Deceleration level to be demonstrated, G (g)	14	16
Deform the floor	NO	YES

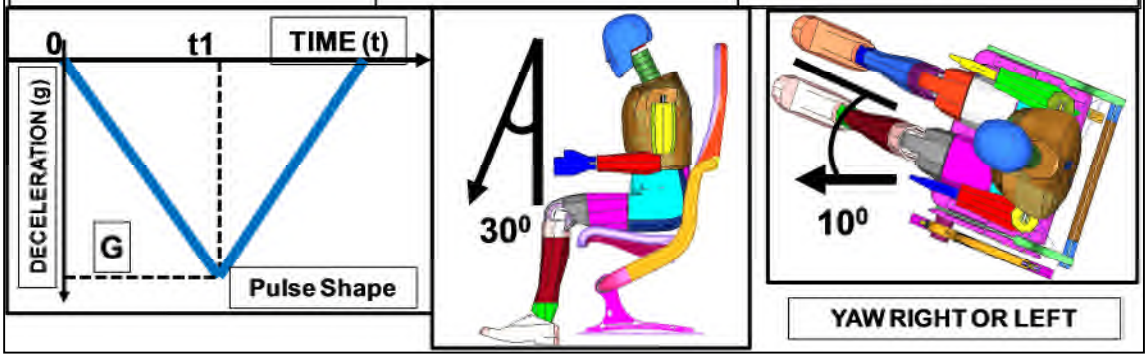

Figure 2-2 Dynamic loads the seat has to withstand as specified in CS25.562 along with the shape of the pulse to be applied and initial orientation of the seat-structure as required by a specific load case [13, 14]

Procedure for dynamic qualification of an aircraft-seat is as follows,

“14g”, as a single row test, determines the performance of the system in a test environment where the predominant impact force component is along the spinal column of the Occupant and is combined with a forward impact force

component as a result of 30 degree pitch angle [5, 13]. This test evaluates the structural adequacy of the seat, critical pelvic or lumbar column compressive forces and the permanent deformation of the seat under downward and forward combined impact loading [5]. An 'Anthropomorphic Test Dummy, ATD' representing a 50^{th} percentile male as defined in 49 CFR Part 572 should be used to simulate the Occupant

"16g", as a single row test, determines the performance of the system in a test environment where the predominant impact force component is along the longitudinal axis of the aircraft and is combined with a lateral impact force component as a result of 10 degree yaw orientation [5]. This test evaluates the structural adequacy of the seat, behaviour of the pelvic restraint and the corresponding loads experienced and the permanent deformation of the seat under forward and lateral combined impact loading. In addition, it yields the data on the time histories of ATD head displacement, velocity and acceleration and the trajectory of the head movement. It also gives the load imposed by the seat on the floor or seat anchorages (seat interface loads), which are useful to check if the loads are within the structural capability of the seat-floor.

As an additional test, two seats are at placed at a distance separated by seat pitch and are subjected to "16g" dynamic load with or without floor deformation [10]. The purpose of this test is to evaluate the maximum and minimum bounds on head and femur injury for the $\pm$10 degree yaw orientation. If the same test is used to demonstrate the structural performance then floor deformation is required prior to "16g" pulse.

Submarining indicators such as electronic transducers may be added at the anterior surface of the ilium of the dummy pelvis. If this is not possible then careful review of the images from high-speed camera should be performed to determine the position of pelvis restraint throughout the test sequence.

Requirements to demonstrate compliance against CS25.562 [13, 14]

- Seat structure should withstand the dynamic loads without failure in the primary load path or without ripping-off from aircraft floor.

- Maximum permanent deformation of the seat-structure should be not in any manner block or hamper evacuation process.
- Head impact should not exceed the Head Injury Criterion (HIC) of 1000 units.
- Where upper torso belts are used, tension loads in individual straps must not exceed 1750 pounds (7789N). If dual straps are used for restraining the upper torso, the total strap tension loads must not exceed 2000 pounds (8897N).
- The maximum compressive load measured between the pelvis and the lumbar column of the ATD must not exceed 1500 pounds (6670N).
- The upper torso restraint straps (where installed) must remain on the occupant's shoulder during the impact.
- The lap safety belt must remain on the occupant's pelvis during the impact.
- Axial compressive load in each femur should not exceed 2250 pounds (10016N).
- Cushion and restraint system should minimise submarining of the occupant and slippage of the restraint.

Transport Airplane Directorate (TAD-96-002) from ARP5526 - Appendix A provides general guidelines for 'Seat-to-Seat Installation tests for Compliance with the HIC in Transport Airplanes' for a typical passenger seat [10]. The aim of the procedure is to standardise the approach to estimate seat-to-seat HIC using only two tests defined in Section 25.562.

Evaluation of the HIC should be conducted with a 50^{th} percentile male ATD. Procedure to determine the head impact area is as follows

- ❖ For dynamically certified seats like 'Sleep Seat', head-strike envelop is a three- dimensional space through which the dummy's head may traverse when tested in accordance with dynamic conditions specified in Section 25.562. '16g' dynamic condition ((horizontal-yaw test) may produce the critical head-path than '14g' pulse (vertical test).

- ❖ Dynamic deflection of the seat backs of the forward row seats makes it difficult to accurately predict the head strike zone of the aft row seated

ATD. The three potential zones within the ±10 degree yaw range of impact point, considered for the head strike are (Figure 2-3)

- Right hand side of the Seat back (Zone I)
- Centre of the Seat back , which may include a food-tray, telephone handset, or video display.(Zone II)
- Left hand side of the Seat back (Zone III)

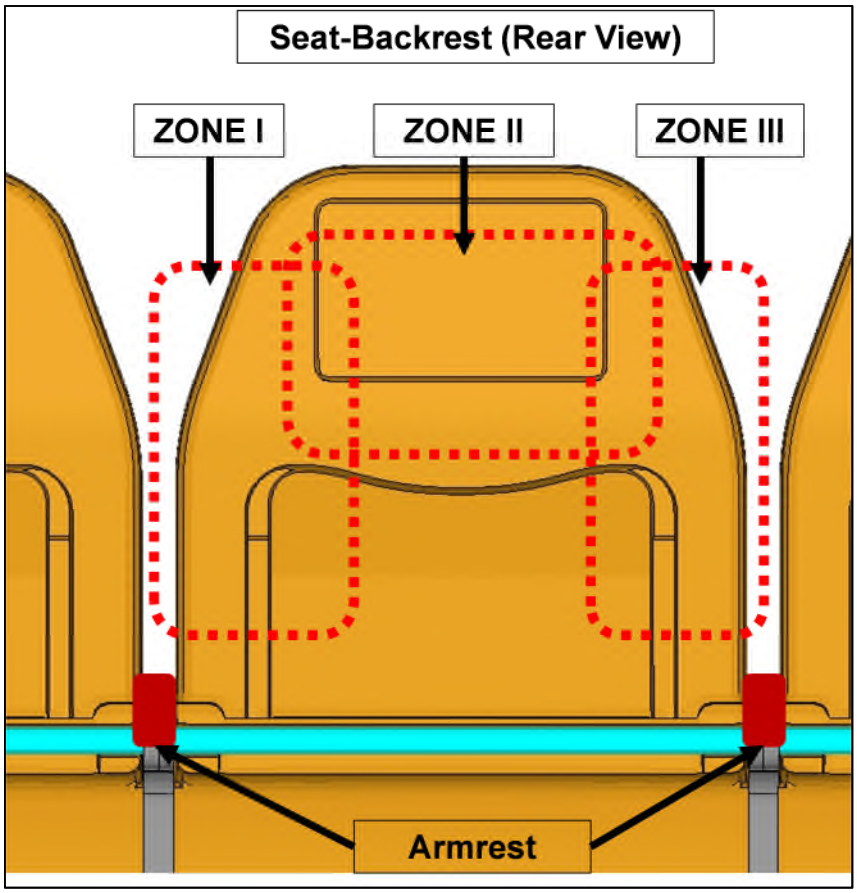

Figure 2-3 Zone I, II and II, within the ±10 degree yaw range of impact point, are considered for the head strike zone test [10]

The recliner mechanism can affect the stiffness of the seat back on the side it is located. Seat-to-seat HIC evaluation test for 'Zone I' and 'Zone II' can be accomplished in a single double row test with two instrumented dummies in the aft row.

Effect of Seat Pitch, The HIC assessment test should be performed, as a minimum, to record the responses for the three head strike zones described

above. The seat pitch range for a particular passenger seat can be certified for HIC evaluation in a minimum of two tests [10].

- Minimum Seat Pitch severely loads the head impact 'Zone II' with 'No Yaw' impact orientation.
- Maximum Seat Pitch severely loads the head impact 'Zone I' and 'Zone III' evaluated with critical yaw $\pm$ 10 degree orientation. This is because the head will strike the seat back at the lower point and potentially at the arm rest.

Envelop of Occupant Height, The regulation CS25.562 does not require assessment of the HIC for a range of different size ATDs. 'Zone II' may contain the structure with significantly varying stiffness e.g. food tray table, stiff telephone hand-set and comparatively flexible video display. To illustrate, a 50th percentile male ATD may barely miss a telephone handset whereas a under same impact conditions, a taller dummy's head (e.g. 95th percentile male dummy) may hit it. Therefore, it becomes necessary to examine the area of the seat-back in the 'vicinity' of the 'initial point of contact' of the head of the 50th percentile male ATD to provide a consistent level of protection against the head impact in Zone II [10].

'Vicinity' is a rectangular area of 152.4*304.8 mm^2 (6*12 inch^2) on the seat back centred on the 'initial point of contact' [10]. Additional test to evaluate HIC are encouraged to be performed if this area contains stiffer items than those at the 'initial point of contact'.

- ❖ For the seats installed in the 'taper section' of the Airplane, yaw angle due to taper can be neglected for HIC evaluation. However, for structural evaluation of such seats 'additional' yaw angle due to taper must be considered.
- ❖ Floor deformation (Seat-track distortion) may be excluded for evaluation of HIC.
- ❖ The double row Seat-to-seat HIC tests can be performed with no ATD in the forward row seat.

- ❖ Occupant to Occupant strikes (for opposite facing seats) should be prohibited. The mechanism behind such strikes and the related injury criteria is unknown and is beyond the scope of the seat dynamic performance standards evaluations.
- ❖ Head strikes with sharp objects need not be evaluated as their presence is prohibited in the head-strike path.
- ❖ De-lethalisation of the 'head impact area' can be proved by either
    - o Perform the testing as per CS25.562 and show that the HIC is less than 1000 in addition to the elimination of sharp penetrating edges or
    - o Use a bowling ball as described in Advisory Circular (AC 25-17) or an approved head component tester and establish HIC.

For the test, significant measuring points are identified from virtual simulations and their positions are measured in longitudinal, vertical and lateral directions relative to the fixed points on the test fixtures. These measurements are taken before and after the tests.

In case of a "16g" dynamic test, if the pre-test measurements are made before the seat-track-pre-deformation, post-test measurements should be made relative to the fixed points on the un-deformed configuration. Conversely, if the pre-test measurements are made after the seat-track-pre-deformation, post-test measurements should be made before removal of floor deformation.

2.1.4 REQUIREMENTS OF TEST FIXTURE

A test fixture positions the aircraft seat on the sled or drop carriage of test facility and takes place of aircraft's floor. It does not need to simulate the flexibility of the aircraft's floor [10]. It holds the seat tracks and provides the capability of floor deformation. In the simulation of "Sleep Seat", weight, stiffness and geometry of the seat track has been considered.

The standard AS8049 specifies the guidelines for electronic and photographic instrumentation [11]. Electronic Instrumentation; containing transducers, different data channels and a provision to convert analogue data to digital data;

measures the test environment and records the data for the comparison of structural pass/fail criteria. Photographic instrumentation consists of high-speed cameras (nominal speed 1000 frames per second), still-imaging system, photographic calibration boards or scales and different camera lens. It documents the overall response of the test article such as behaviour of ATD and pelvis restraint, permanent deformation of seat (if any), integrity of the load path and connection to the floor.

Please note that evaluation of the Occupant loads does not fall under the scope of this research and hence has not been performed.

2.1.5 GUIDELINES FOR A SAFER SEAT DESIGN

Some of the safety guidelines according to ARP5526 to be considered while seat designing are,

2.1.5.1 SEAT BACK HANDHOLD IN TURBULENCE

A handhold support provides support for a person standing in upright in an aisle in moderately rough air. In the absence of adequate supplemental rail or handgrip, the upper-aisle corner of the seat back should provide either a surface to grip or push against. A seat-back used as a handhold should

- Not break-over when a force of 111N (25 pounds) is applied at the top centre of the seat-back in a direction perpendicular to it.
- Be at least 840mm (33inch) above the floor, when the seat-back is in reclined position.

Anchorage of the restraint-system should provide a self-orientating (free rotation and self-aligning) features and should be designed to minimise an incorrect installation and inadvertent disconnection of the restraints. The report also discusses in detail,

- Examples of various causes of seat-belt misalignment and
- Procedure to the test the belt for inadvertent disengagement

ARP5526 supplies guidelines for location, storage and easy accessibility of the life vest or Life Jackets that should be provided at each seating position.

Means should be provided to prevent in-plane reading items from becoming a 'flying hazard' during emergency landing conditions of Section CS25.561 and specified flight and ground load condition.

Moving parts accessible to the Occupant for example leg-rest, food tray, deployable video should have restricted motion and should be shielded so that the shearing hazards are minimised. Edges that would penetrate the occupant's skin should be avoided.

Head injury for an Occupant making more than 18^0 angle with the vertical plane containing the airplane centreline must be protected by

- By eliminating injurious objects in the 'striking radius', also called as 'arc of travel 'of the head of an occupant; should be avoided.

  - The radius of 'arc of travel', representing the extremity of the Occupant's head should be 710mm (28in). The centre of this radius should be 460mm (18in) forward and upward of the intersection of the seat-back and seat-bottom and should be at 35 degree to the seat-bottom (Figure 2-4).

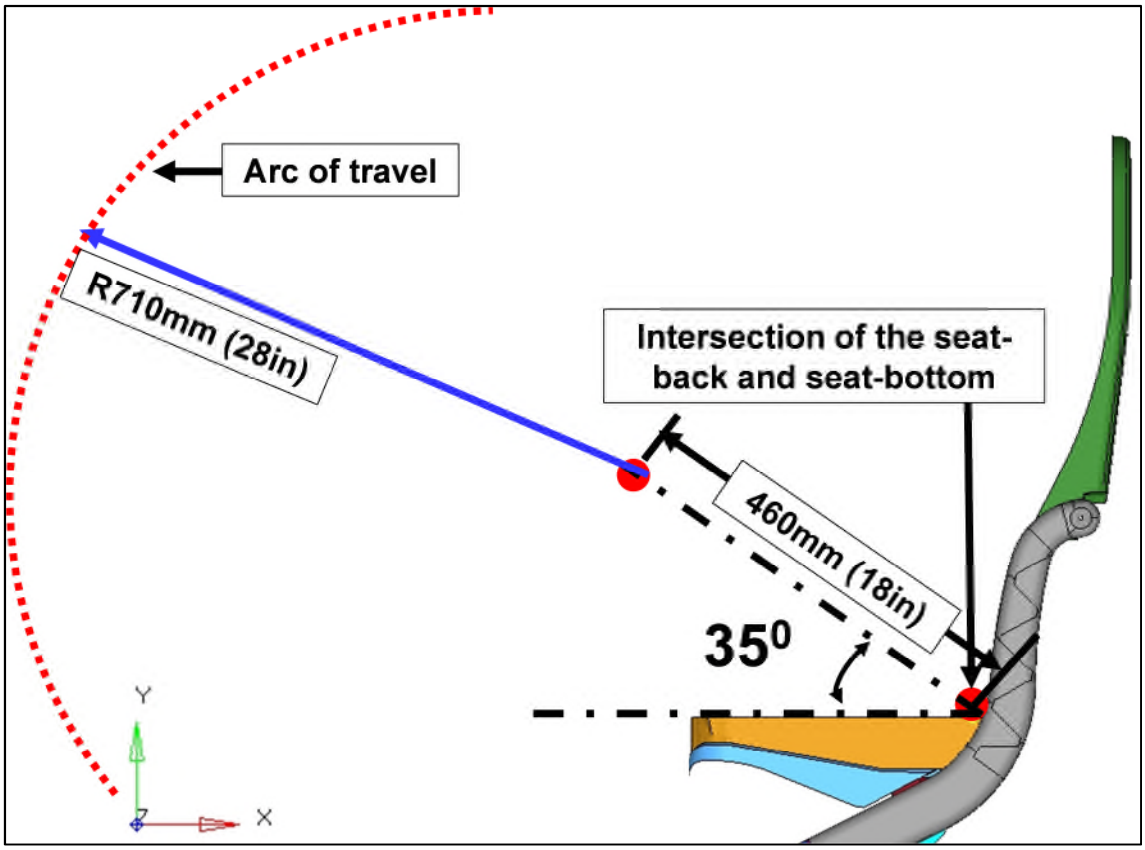

Figure 2-4 Definition of 'striking radius' or 'arc of travel' [10]. Injurious objects should be eliminated within arc of travel to prevent Head injury for an Occupant

- All surfaces of the passenger accommodation and the areas of the seat-back within the 'arc of travel'; should be smooth and of large radius. They should be padded to at least 25mm (1in) radius with at least 12.5mm (0.5in) of firm padding. The padding should be designed in such a way that the head would deflect past them rather striking with a direct blow.
- No structural member should occur where it may penetrate or strike the throat.
- Seat-back should pivot so as to move forward during emergency landing so that the Occupant seating behind would strike a glancing blow on the back of the front seat-structure.
- Design of the primary structural components of seat should ensure easy inspection to detect wear, deterioration or any other condition that would degrade safety.

- Seat anchorage should have anti-rattle design to reduce wear on the seat track or fittings.
- The cushion, covering and padding, upholstery and all other exposed material should have self-extinguishing properties.

2.1.5.2 MATERIALS

For the major load carrying members of the seat structure, designer should select the materials that offer the best strength-to-weight ratio yet maintaining sufficient ductility for energy absorption [3]. The degree of ductility in these parts depends on whether the seat structure is designed to absorb the energy through large plastic deformation of the basic structure or by a separate energy absorber. For a seat structure without additional energy absorber, a ductile material with a minimum 10 percent elongation is recommended [3]. Castings should be avoided in the primary load-path as their quality is more difficult to reproduce and verify [3].

2.1.5.3 STRUCTURAL CONNECTIONS

Fatigue is generally not considered in the design of an aircraft-seat as high-loading of the fitting is a one-time event. A good aircraft engineering practice dictates that the bolts less than 0.25inches (roughly M6 bolts) should be avoided because of the ease with which they can be over-torqued [3]. As the seat-structure has to undergo large deformations while maintaining the continuity in the load-path, bolts should have a minimum elongation of 10 percent in the longitudinal and transverse directions. Welded connections though 100 percent efficient; depend upon the skill of the welder, the process and inspection procedure followed. Since they may result in stress concentrations and misaligned parts, the cross-sectional area of the parent material in the vicinity of a welded joint should be 10 percent greater than the area calculated by design. Magnesium alloys should not used due to flammability issues.

2.2 ROLE OF FEA IN AIRCRAFT SEAT DEVELOPMENT

Knowledge of the conditions critical to Occupant's survival during a crash event is a must to improve the aircraft crash safety. A possibly large number of different environments for an aircraft crash exist and experimental testing of all of these configurations is not either possible or feasible [2]. Furthermore, a well-defined experimental testing program requires a thorough understanding of the seat behaviour through multiple virtual simulations. FE models, once validated; reduce the necessity of fabrication and testing of design optimisations or small modifications made to the seat structure.

Lankarani et al have described applications of the non-linear FEA for the aircraft Occupant and seat crashworthiness studies [2]. The authors have identified potential solutions for problems like protection against the head impact for bulkhead-seats, criteria for the certification of side-facing seats and crashworthiness of the 32G commuter seat [2]. Using FEA tools, lumbar loads could be limited under 1500lb (6650N) through a careful design of seat-leg for a commuter seat for the occupants ranging from 5^{th} percentile adult female to a 95^{th} percentile adult male.

Hooper addressed the issue of the aircraft crashworthiness by reviewing the accident statistics and the regulatory requirements related to the dynamic seat testing for the Part23, Part25 and the Commuter aircraft [4]. The author has extended the discussion to a systematic approach for seat-designing using computer modelling techniques and shown that much of the development time can be squeezed through the use of nonlinear FEA tools over experimental testing. The author has used software called MARC, to develop the force-deflection characteristics of a S-beam leg.

Bhonge in his thesis based on dynamic seat certification methodology has justified use of FEA in support of aircraft seat certification process over expensive physical testing [5]. The author has successfully reduced 66 seat configurations to 11 configurations for certification testing, using a validated FE methodology. The author could substantiate the physical testing by FEA for the business jet seat (case study discussed in his thesis). In addition, effect of

different geometries and densities of seat-cushions and take-off and landing positions, on Occupant loads and on structural performance of the seat , are substantiated using FEA.

Olivares in his report on ‘Certification by Analysis, ‘CBA I and II’ provides an overview of numerical modelling practices combined with components tests to solve aircraft crashworthiness problems [20].

- CBA I focuses on the development of component test methods, validation procedures for metallic components used in seat-structure, seat-belt webbing and seat-cushion modelling.
- CBA II focuses on crashworthiness performance of composite aircraft structures.

Ayyar performed computer simulation (using MADYMO) to investigate variation of HIC and neck loads with varying: dummy sizes and types, seat-pitch and break-over resistance of seat-back [21]. Experimental testing for exploring the safety provided by an aircraft seat for all these variants would have required significant amount of investment in terms of money and resources. The author found computer simulations as a better alternative.

Olschinka et al has demonstrated suitability of LS-DYNA simulation tool to predict crash behaviour of an aircraft seat and used it as an accompanying development tool during certification [22]. The authors have calculated and evaluated three different seats for

- Seat Interface Loads i.e. loads introduced in the aircraft-floor due to aircraft seats,
- Head trajectories and Occupant loads (HIC, femur compressive loads)
- Energy absorption mechanism
- Stress distribution in the seat structure

Dhole in his thesis on the development and validation of FE model of a transport category of aircraft seat subjected to dynamic loads (Part 25.562) has used LSDYNA explicit code to study the behaviour of a typical aircraft seat under dynamic loading [23]. The author has documented material models,

element formulations and contact models in LSDYNA commonly used by seat-analysts. Validated FE models helped him to build the confidence in FE methodology and to arrive at a conclusion that virtual simulations are helpful in designing an aircraft seat.

Shanahan has provided an informative summary of basic crashworthiness principles and examples of their effective use in helicopter designs [24]. The author has discussed various crash injuries and measures to ensure safe designs through: strengthened container, integrity of restraint systems with floor, energy absorbing design, protective shell around the Occupant and evacuation.

Barth in his PhD thesis has investigated the contribution of viscous injury (arriving from inertial loading to the heart and aorta) from vertical impact in survivable aircraft accidents [25]. The author has created computer models to assess the injury potential and compared them with real accident autopsies to determine that the spine injury is more critical than viscous injury in vertical impacts.

Sicma Aero Seat SA, a French company providing seating solutions, relies on virtual simulation tools for evaluating structural performance of aircraft seats, improve seat designs, cut certification costs and reduce product delivery times [26]. FEA has helped them to reduce the number of seats that initially fail and find the best solution faster for a failed seat by providing a better understanding of failure phenomenon.

With the above examples, it can be seen that various designers and FE analysts have used FEA to evaluate structural performance of a seat structure, predominantly against dynamic crash regulations (CS 25.562). Additionally Lankarani et al. [2] have used FEA to perform an extensive study on bio-mechanics of occupant injuries and occupant protection during different automotive and aircraft crash scenarios. However, in the area of assessing the structural performance of a seat against static regulations (CS 25.561) and the seat pre-deformation loadcase using FEA, the available literature is very limited. Further research is required to propose well-defined guidelines for

- FE model building of complete seat structure for simulating Static CS25.561 loads.
- Representing experimental loading procedure (e.g. using body blocks, floor-distortion) in FE modelling
- Obtaining a converged solution for a non-linear (involving all three types on non-linearities i.e. geometric, material and contact) FE model of a complete seat-structure using implicit formulation.
- Initiating the pre-deformation loadcase in the 'Dynamic 16g' as specified in the CS25.562
- Obtaining a quasi-static solution for complex nonlinear problems using explicit formulation
- Critically assessing the quality of numerical results
- Reducing the computational time by choosing appropriate numerical algorithm

This research is aimed at addressing these issues.

Conclusion – Chapter 2

Aerospace Recommended Practice ARP5526 is the most important document to be used during seat certification as it involves findings from the most relevant regulations such as Aerospace Standard AS8049 (which defines static and dynamic load application procedures), Certification Specifications CS25.561 and CS25.562 and Advisory Circular AC25.562-1B.

CS25.561 specifics six static inertia loads to be applied separately in six different co-ordinate directions while CS25.562 specified two dynamic loads (16g with damaged floor condition and 14g) that a seat-structure has to withstand without disintegrating from the load path or deform excessively thereby hampering the evacuation in the event of emergency landing. Maximum limits on permanent deformation of seat-structure and Occupant loads when subjected to certification loads are specified in AC25.562-1B. A summary of general design guidelines for an aircraft-seat are as follows,

- Injurious objects or sharp radii must not be present within head impact area of an occupant
- Means should be provided to prevent in-plane reading items becoming a ‘flying hazard’ during emergency landing conditions
- Bolts less than 0.25inches (roughly M6 bolts) should be avoided because of the ease with which they can be over-torqued.
- Ductile material should be used for major load carrying members as they can absorb energy thereby reducing occupant loads

A brief overview of FEA used by various researchers and companies offering seating solutions, during seat designing has been provided. It can be observed that due to a close correlation between FEA and experimental tests results, costs associated with prototyping and physical testing, failure rate and development time can be significantly reduced.

This research would address the shortcomings of earlier researchers in the areas such as, building well-defined procedures : to simulate CS 25.561 and CS 25.562 crash tests, to assess the quality of numerical results, to reduce the computational time involved and to use numerical results as a main design driving tool in the absence of physical test results.

3 INTRODUCTION TO SEAT AND PROJECT PLAN

In Chapter 1 objectives of this research are laid out and in Chapter 2, safety standards are discussed. In this chapter, the architecture of 'Sleep Seat' and novelties of this research will be discussed and a step-wise procedure to achieve the objectives will be presented.

To balance the increasing demands of air-travellers and decreasing profit margins; airliners want to maximise on-board capacity, without sacrificing comfort and safety. This has opened new skies for the seat developers. Cranfield University is working in collaboration with its industrial partner "BlueSky Designers Limited, UK (hereafter called as BlueSky or Industry)" to address these needs by designing a completely novel seat structure coined as "Sleep Seat. The configuration represented in Figure 3-1 RHS is for 9 abreast A340, with the separation between seat legs of 527mm.The main components of the "Sleep Seat" are Seat-leg, Forward beam, Seat-pan, boomerang and the backrest panel (Figure 3-1 LHS).

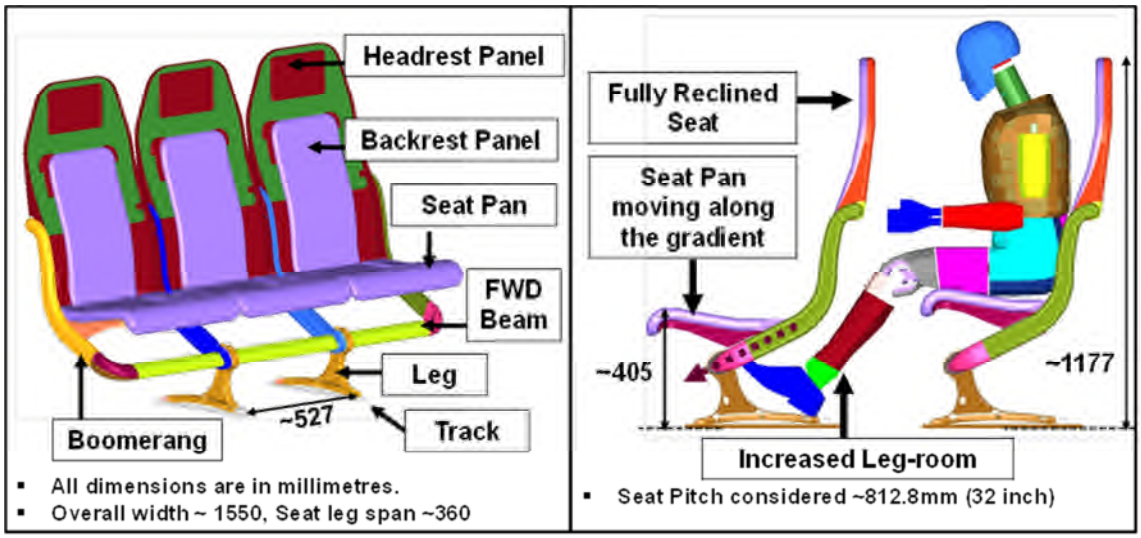

Figure 3-1 LHS Nomenclature of the "Sleep Seat", RHS - Unique Single Forward Beam design along with movement of the Seat Pan along the gradient increases the leg-room for the Occupant seating behind even with a fully reclined Front Seat (due to fixed outer shell of the backrest). Courtesy – BlueSky Designers Limited, UK [28]

3.1 FUNCTIONING OF SLEEP SEAT

Fixed backrest (A, in Figure 3-2) has a slot (C), through which movable backrest (H) slides. 'H' is attached to Seat-Pan (E) using bolted connections. Seat-pan can move along the gradient through the guided track (G); mounted inside the boomerang (D); operated by an electric motor (Not shown in the Figure). Synchronised motion of movable-backrest (through slot C) and seat-pan (along the gradient) generates an angle of recline for the passenger comfort.

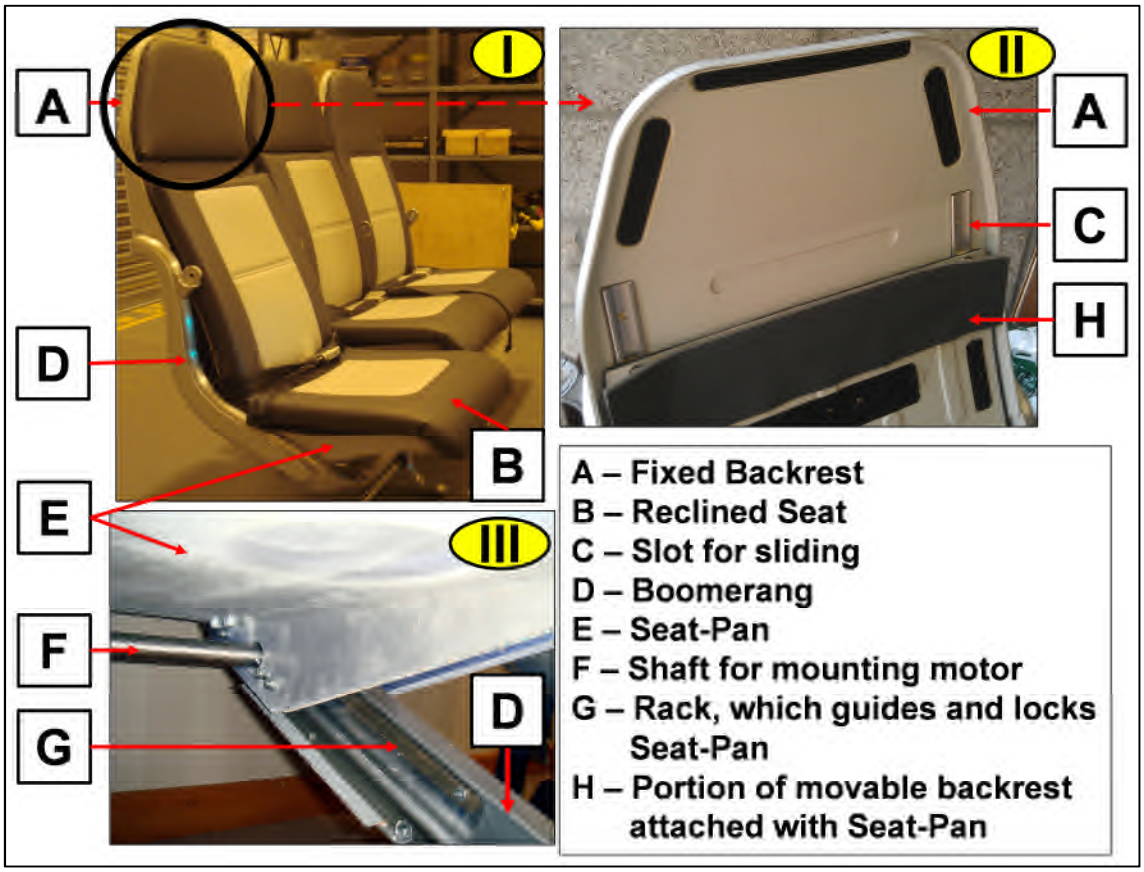

Figure 3-2 One seat (extreme left) reclined (backrest remains fixed) while other two seats in take-off position. II – Fixed seat backrest, A without back-cushion. Movable backrest, H moves through the slots (C) for creating an angle of recline. III – View from bot tom of the seat showing rack and pinion arrangement (G) mounted inside the boomerang (D) for movement of the Seat-Pan (E). Courtesy – BlueSky Designers Limited, UK

Armrest and Seat-belt (not shown in figure) are mounted on the boomerang, which is bolted to "Forward Beam (FWD beam)". Curved 'Corner' piece is used

to connect Side-boomerang with FWD Beam (Figure 3-3), which is bolted to the seat legs.

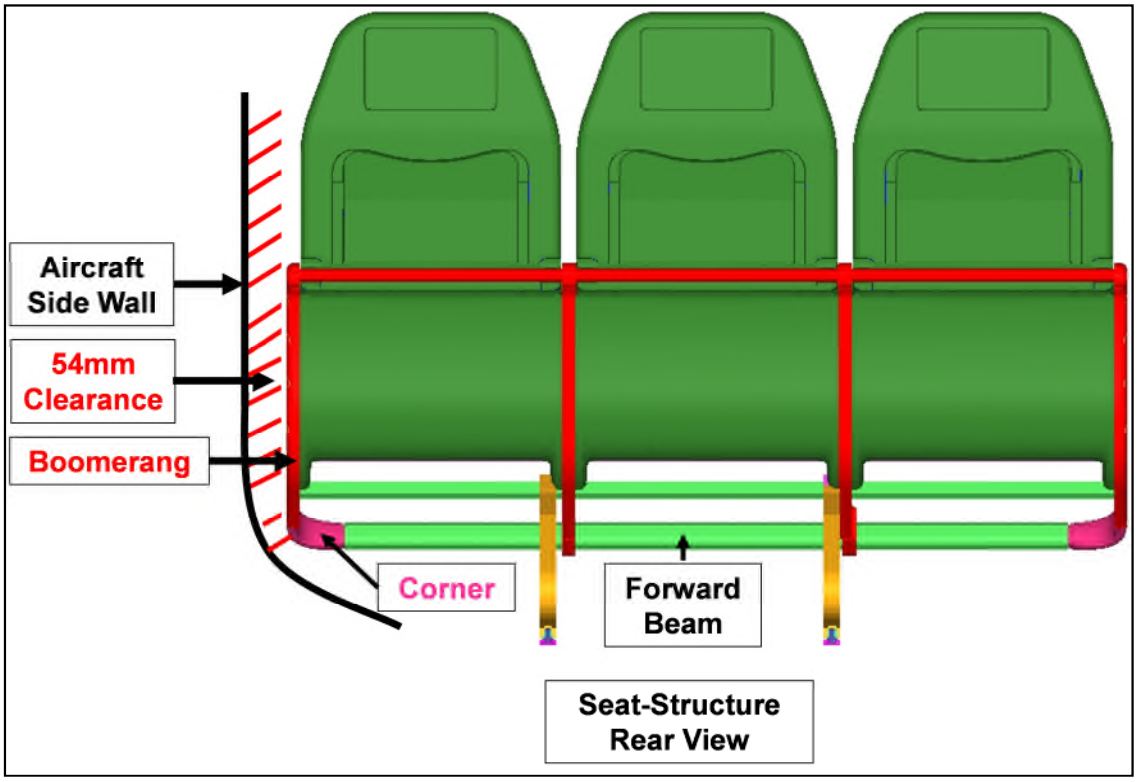

Figure 3-3 54mm clearance to be maintained from aircraft-side wall for 9 abreast A340 seating configuration. Therefore curved 'Corner' piece is used to connect Side bommerangs with Forward beam. Courtesy – BlueSky Designers Limited, UK

Corner piece helps to maintain the required clearance zone of 54mm from aircraft side-wall [Figure 3-3]. Seat-structure is anchored to the Seat-track using tool-less fittings (via Seat-leg), design of which is modified to enable relative movement between seat-structure and seat track, thereby preventing damage to the structure due to '10 degree Roll' applied during floor-distortion loads (explained in detail in Section 7.4.3).

3.1.1 SEAT ANCHORAGES – TOOL-LESS FITTINGS (TLF)

Using "flexible or variable cabin configuration", airlines should be able to quickly shuffle different configurations to absorb fluctuations in number of passengers e.g. many late night-scheduled aircrafts need to convert certain passenger

cabins into cargo [29]. In addition, for a large aircraft with many seats, major assembly time is invested in installing seats in the fuselage. Naturally, airliners would like to reduce this initial installation time. A step taken by initial designers was to provide a track, which run fore and aft along the entire floor of the major cabins of the aircraft. These tracks have a “lip design” at the top surface and enlarged cutouts at regular intervals (one inch) for placing seat assembly into track (Figure 3-4).

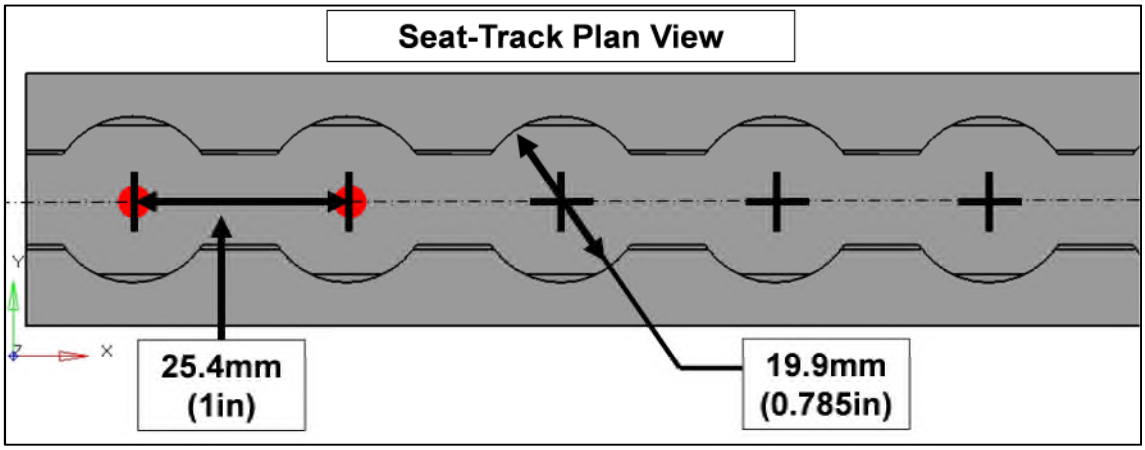

Figure 3-4 Seat track crown segment (Plan view). Regular interval of one inch is provided throughout the length of track for easy installation of seat-structure at desired locations [29, 66].

With the help of adjustable track fasteners, it is possible to reposition or to remove the seats and/or cargo. Track fasteners are typically installed using Allen wrench or hex head wrench. This process suffers from following drawbacks [29],

- Torque tool, which is used to rotate the threaded fastener, has a very little operating area.
- Due to congested area, an element of fatigue is introduced into the operator. Hence, it is difficult to determine whether fastener is adequately secured in place.

Considering all these drawbacks of current seat installing connections, for anchoring ‘Sleep seat’ to track, tool-less fittings (TLF) developed by Ancra International Lic (Figure 3-5, Part number 49623-10 and 49648-10) are used [30].

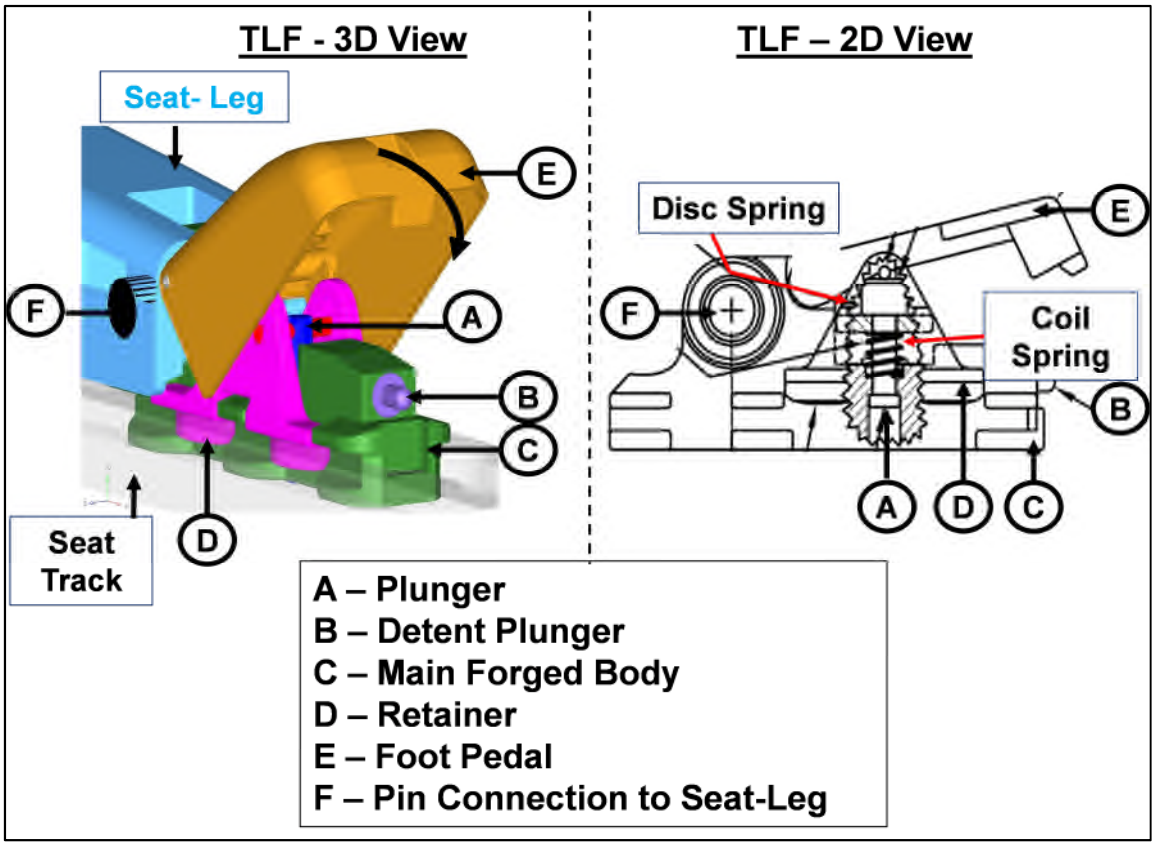

Figure 3-5 LHS – 3D View of Ancra Tool Less Fittings (TLF) used to fasten 'Sleep Seat' to the Seat-track (before assembly). RHS - Ancra rear tool less-fitting (part Number 49623). TLF consists of main forged body, C with three integrated studs engaging with Seat-track lips. Retainer, D has two shear plungers and the entire assembly is held together with two springs (disc and coil). Pressing of Foot-pedal E presses Plunger A, against Seat-track. Foot-pedal is held in position by detent plunger B, when assembled. Courtesy – BlueSky Designers Limited, UK

TLF are easy to operate and easy to implement [30]. These fittings ensure proper positing, prevent rattling and vibration caused due to aircraft operation. This eradicates irritating in-plane noise and loosening of the track [29]. With a press of a knob (Detent plunger B in Figure 3-5 RHS), fasteners can be disengaged from track thereby dramatically decreasing switchover time between different passenger compartments.

Further investigation of methods of attaching seat structure to the track showed the use of tool-less fittings is quite beneficial and even Boeing uses the same practice [29, 30, 57].

The assembly procedure of these fittings can be explained with the help of Figure 3-5. During sliding (half-inch forward) of TLF through track, coil spring lifts retainer (D), disc spring, washer, dowel pin and foot pedal (E). Once the fitting is in position, foot pedal is pressed, which ensures that the retainer is in contact with the seat-track. This assembly procedure compresses the disc spring, which has much higher spring rate than that of coil spring. As the foot pedal reaches its locking position, detent plunger (B) engages into the hole of foot pedal. Further compression of coil spring provides anti-rattle feature.

For removing the seat, foot pedal is pressed to relieve the disc spring force. With the help of a tool, “B” is pushed forward, which disengages TLF from track. Thus, it can be sensed that the installing and dismantling procedure of TLF is quite easy and quick offering seamless shift between Premium to Economy seats on all the flights and a quick make over from passenger jet to partial cargo for late night flights.

Sleep seat would be launched in double and triple configurations. Three different variants based on the movement of seat pan are

- *Basic Economy Seat* for short haul (1-2 hours) domestic or regional flights. No movement of seat-pan, hence a fixed-position seat without any reclining.
- *Normal Economy Seat* for medium haul (2-5 hours) continental flights. Three-inch forward motion of seat pan will provide reclined position to relax.
- *Premium Economy Seat* for long haul (> 5 hours) international flights. Seat pan movement of three-inch forward and six-inch downward will offer a generous 40 degrees angle of recline.

The potential targets for “Sleep Seat” include A320/A330/A340 and Boeing 767. The designs would be tailored as per the needs of particular airliner e.g. more outboard, different seat spacing, different seat track spacing.

Based on the requirement from BlueSky; a triple seat configuration (Figure 3-1 LHS) from “Basic Economy Class”, has been considered for the present

research. A double occupancy ‘Sleep Seat’ (dual structure) has been used (sometimes) while developing FE procedures. Due to reduced number of parts, less modelling effort is required to build a FE model of dual seat than that for ‘triple’ seat. This would reduce the model debugging time along with computational costs.

3.2 NOVELTIES OF THIS RESEARCH

The design of the seat is mainly driven by aesthetics, comfort and weight matrix fixed by BlueSky designers.

3.2.1 FEATURES OF SEAT-DESIGN IDEA BY BLUESKY

- ✓ The seat pan can move three-inches forward and six-inches downward along the gradient, creating an unrivalled space for the leg spread, in addition to creating a 40 degree generous recline (when compared to 32/34 degrees for current seats) (Figure 3-1 RHS) [28].

- ✓ Outer shell of the backrest is fixed even when the seat is fully reclined. This means when the passengers in the front seat recline, they do not protrude into the space of the passengers sitting behind (Figure 3-2)!

- ✓ Conventional seats have twin beams at shin level under the seat pan that restricts access to the valuable space under the seat. Some designs of ‘Sleep seat’ feature a unique single Forward beam, which eradicates this undercarriage, thereby maximising the space in the tight confines of economy class. This feature significantly reduces the part count, assembly time and the costs involved.

- ✓ Sleep seat is aimed to be an ultra-lightweight design weighing less than 8kg (typical seat weighs around 11kg) [Input from BlueSky].

- ✓ Sleep seat will be a “16g” seat, which means it will satisfy the structural requirements as specified by CS 25.561 and CS 25.562 and occupant loads would be under human tolerance limit. Please note that the ‘Complete 16g’ seat is a goal of the overall project. Aim of this research

is to obtain a ‘16g compatible’ seat i.e. demonstrate ‘static compliance’ (against CS25.561 loads) and derive a design that can sustain dynamic loads (CS 25.562) with damaged floor condition; without dis-continuity in the load path.

Role of this research is

- To provide means for assessing the structural performance of the seat against crash safety regulations,
- To suggest design changes if poor performance is observed. However, design changes should be within the boundaries drawn by aesthetics and comfort and should not deviate from the features outlined in Section 3.2.1 of this report.

Therefore, novelties of this research would be

- ✓ Guidelines for FE model building of complete seat structure for simulating Static CS25.561 loads and dynamic CS25.562 loads
- ✓ Guidelines for representing experimental loading procedure (e.g. using body blocks, floor-distortion) in FE modelling
- ✓ Guidelines for obtaining a converged solution for a non-linear (involving all three types on non-linearities i.e. geometric, material and contact) FE model of a complete seat-structure using implicit formulation.
- ✓ Guidelines for obtaining a quasi-static solution for complex nonlinear problems using explicit formulation
- ✓ Guidelines for critically assessing the quality of numerical results

Literature review has shown that earlier efforts to simulate ‘damaged floor condition (DFC)’ and then initiate associated stresses and strains in a dynamic ‘16g’ simulation were not successful [5, 22]. This research aims to develop methodologies, for simulating ‘damaged floor condition’ and initiation of stress, strains and deformed geometry in a ‘16g’ loadcase. Going further, economical and practical design solutions would also be proposed to reduce the high loads introduced by DFC into the seat-structure.

Along with developing simulation procedures, this research would also present detailed

- ✓ Guidelines for selecting a particular formulation (implicit or explicit) for a particular loadcase specified by CS25.561 and CS25.562
- ✓ Overview of Element Technology, modelling of rigid bodies and Contacts algorithms for both implicit and explicit formulations
- ✓ Guidelines for extracting useful information such as interface loads, cross-sectional loads from FE results
- ✓ Techniques to optimise simulation run times
- ✓ Optimisation techniques to derive a feasible solution

Aim of this report is to be a useful document for the 'Certification By Analysis', a programme undertaken by Federal Aviation Administration (FAA). The methodologies developed would also aid the virtual development of seats used in railways, automobiles and agricultural equipment.

3.2.2 PROJECT PLAN

The project plan designed for this research reflects a formalised framework for the "New Product Development" Process, aims and objectives of this research and SIX well defined "Development Stages (DS)" for the concept, design and prototype consolidation (Figure 3-6). Project milestone have been further categorised into the detailed activities to avoid otherwise chaotic mixing of various parameters.

Abbreviations form the Figure 3-6 -

- DS – Development Stage
- FEA – Finite Element Analysis
- Static Compliance – Compliance against loads as specified by CS 25.561
- "16g" compatible – Seat structure that can sustain dynamic loads (CS 25.562)

'Downward 8.6g' loadcase has been selected as a case-study to be solved with implicit formulation as well as with explicit formulation as

- It does not involve a complex body block and seat belt mechanism thereby simplifying FE model building and boundary conditions,
- It is planned to be tested experimentally

Though CS25.561 specifies ‘6g’ inertia load multiplied by occupant mass of approximately 77kg to be applied in downward direction per seat; in tests, ‘8.6g’ factor and 111kg mass is considered per seat pan due to the requirement posed by a particular airline (input from BlueSky).

In early design phase, experimental testing is costlier and hence FEA has been used as the main decision making tool for modifying the geometry and selecting the material grades. However, reliability of FEA results is of utmost importance to arrive at a realistic design. Keeping this in this mind, verification framework is developed and executed at all the stages to critically assess the output of FEA. If FE methodology at a particular stage satisfies these checks, only then it is adopted for comparing the design concepts.

The main body of coming Chapters reflect research activities undertaken to meet the objectives and chapter conclusions demonstrate achievement of milestones as outlined in the self-explanatory project plan (Figure 3-6).

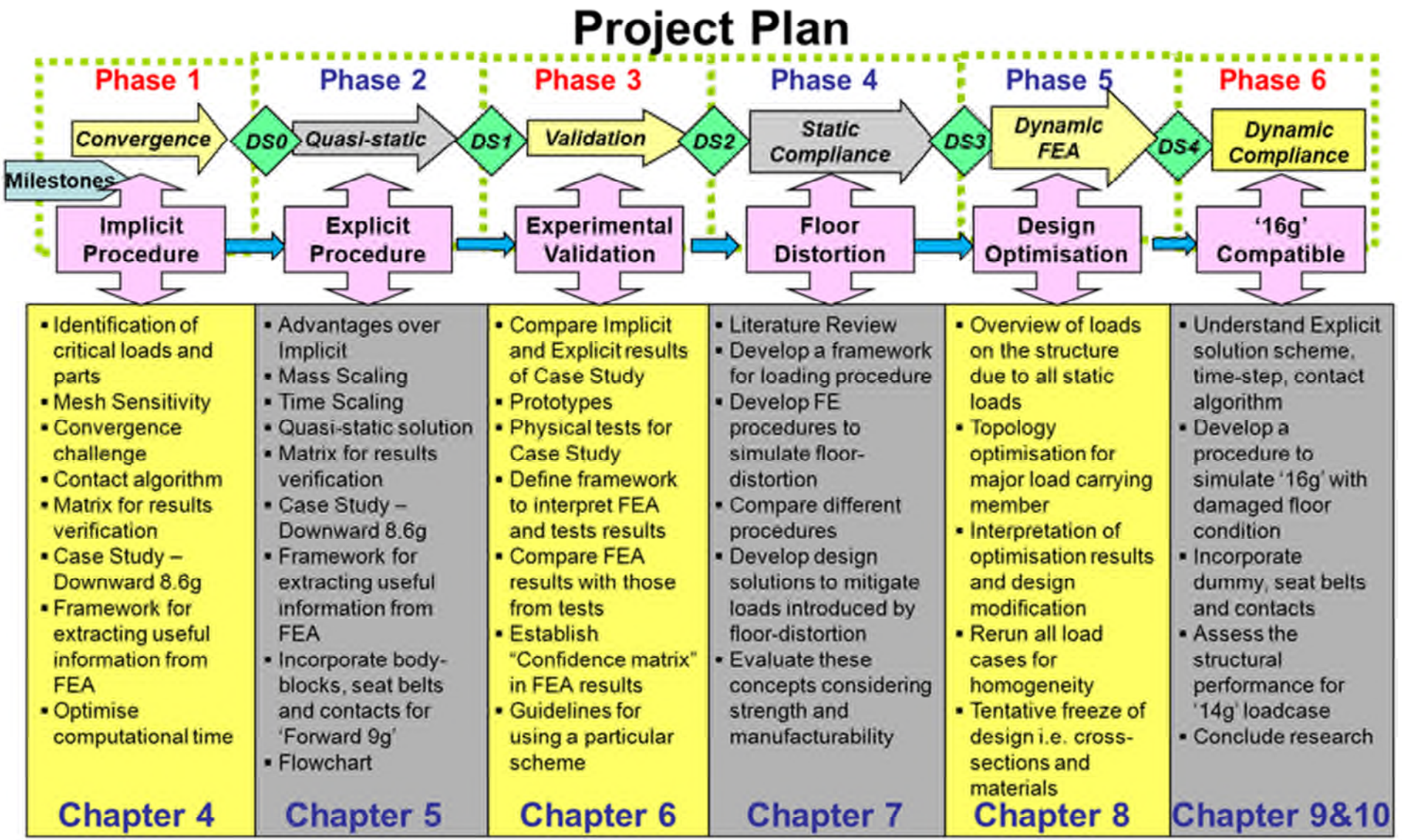

Figure 3-6 Methodology adopted for this research

4 IMPLICIT FORMULATION TO SIMULATE CS25.561

As per the project plan discussed in Chapter 3, different solution algorithms to simulate the loadcases specified in CS25.561 and CS25.562 will be discussed in depth, in coming chapters. The solution schemes used to solve various loadcases specified by CS25.561are,

- Implicit Solution Scheme (Discussed in Chapter 4)
- Explicit Dynamic Integration Scheme ((Discussed in Chapter 5)
- Implicit/Explicit automatic Switch (Discussed in chapter 7)

The mechanism, advantages and disadvantages, challenges faced by analysts in usage, techniques to overcome these challenges and a results verification framework for the implicit solution scheme will be discussed in coming sections of this chapter.

The consideration of FE model of the complete seat-structure subjected to loads as per CS25.561 leads to a nonlinear analysis.

4.1 WHAT IS A NONLINEAR ANALYSIS?

The finite element equilibrium equation for a linear static analysis of a structural problem is given by [31]

$$[K]\{U\}=\{R\} \qquad \textbf{Equation 4-1}$$

Where, the nodal displacement response {U} is a linear function of the applied nodal load vector {R} and [K] is the element stiffness matrix.

The assumptions of the linearity and their entry into the equation 4-1 can be identified as follows.

- The first assumption that the displacements of the FE assemblage are infinitesimally small enters into the evaluation of matrix [K] and the load vector {R} because all the integrations are performed over the original reference volume of the finite elements and the strain-displacement matrix {B} of each element is assumed to be constant and independent of the element displacements [31].

- The assumption of linear elastic material is implied in the use of constitutive relation i.e. constant stress-strain matrix [C].
- The assumption that the boundary condition remain unchanged (i.e. degree of freedom, which was unrestrained initially remains unrestrained through the solution unlike becoming restrained at a certain load level-situation arising during a contact problem) is reflected in the use of constant constraint relations for the complete response.

Violation in any of these assumptions results into a non-linear problem.

4.1.1 ALGORITHMS TO SOLVE THE NON-LINEAR PROBLEM

The essence of solving a general non-linear problem is to find the state of equilibrium of a body corresponding to the applied loads. The equilibrium conditions of a system of finite elements representing the body under consideration can be expressed as

$R-F=0$ [31] **Equation 4-2**

Where

R lists the externally applied nodal point forces in a particular configuration

$R = R_b + R_s + R_c$

R_b, R_s, R_c are the element body forces, element surfaces forces and applied nodal concentrated loads respectively.

F lists the nodal point forces corresponding to the element stresses in that particular configuration. For m elements,

$F = \sum_m \int_{V^{(m)}} B^{(m)T} \tau^{(m)} dV^{(m)}$ [31] **Equation 4-3**

Where,

$B^{(m)}$ is the strain-displacement matrix, which defines the element strains in terms of complete array of FE assemblage of nodal point displacements.

$\tau^{(m)}$ are the element stresses due to internal nodal forces for the configuration under study

- Nonlinear relationship between displacement increment and strain increment i.e. nonlinearity associated with component '$B_{(m)}$' is called as *geometric nonlinearity*.
- Nonlinear relationship between stress and stain i.e. nonlinearity associated with component 'τ' is called as *material nonlinearity*.
- Dependence of {R} on the displacements in the current configuration gives rise to *boundary nonlinearity* e.g. contact interface pairs transferring the load or nonlinear external load.

Evaluation of the structural performance of the complete "Sleep Seat" according to CS25.561 and CS25.562 is a classic example of complex combination of all types of non-linearities namely large displacement, large rotations, large strains and changing boundary conditions.

For a general non-linear analysis, element stresses as well as the volume of the body for the current applied load is are unknown. Therefore the Equation 4-2 must express the equilibrium of the system throughout the complete history of load application taking due account of all nonlinearities. For a dynamic analysis, vector R also includes inertia and damping forces.

In a dynamic analysis and static analysis with material time effects, the time variable is required to be properly incorporated in the modelling of the actual physical situation. Considering these aspects and an assertion that a "dynamic analysis is basically a static analysis including inertia effects", generally time variable is used to describe the load application and the response history, in almost all the commercial non-linear solvers. However, in a static analysis (i.e. without time dependency) other than the definition of the load level (e.g. without creep effects), time is only a convenient variable, which denotes different intensities of load application and corresponding configurations.

The equilibrium configuration for a highly non-linear problem is established in a step-by-step incremental fashion. The approach in an incremental solution scheme is the solution of the system at discrete time $t+\Delta t$ from the known equilibrated configuration at t for a suitably chosen time increment Δt based on either accuracy (implicit) or stability (explicit).

In implicit formulation, spatial approximation is applied at time-step $t+\Delta t$, which is a backward difference approximation [5]. The information at time $t+\Delta t$ depends on information at previous time intervals (t, $t-\Delta t$...) and current time as well (i.e. $t+\Delta t$). Implicit methods are generally unconditionally stable i.e. even for large values of time (load) increments calculations do not blow up (but may hamper the accuracy) [40].

Hence, considering equation 4-2 at time $t+\Delta t$,

$$R_{t+\Delta t} - F_{t+\Delta t} = 0 \qquad \textbf{Equation 4-4}$$

(Assuming $R_{t+\Delta t}$ is independent of deformations). Based on the assumption that the solution at time t is known,

$$F_{t+\Delta t} = F_t + \Delta F \qquad \textbf{Equation 4-5}$$

Where, ΔF is the increment in the nodal point forces corresponding to the increment in element displacements and stresses from time t to $t+\Delta t$. This vector is “approximated” using a tangent stiffness matrix K_t, which corresponds to the geometric and material co-ordinates at time t.

$$\Delta F \cong K_t\, U \qquad \textbf{Equation 4-6}$$

Where U is a vector of incremental nodal point displacements,

$$K_t = \partial / \partial_t \, (F_t / U_t) \qquad \textbf{Equation 4-7}$$

Tangent stiffness matrix, K_t corresponds to the derivative of the internal element nodal point forces F_t with respect to the nodal point displacement U_t. Substituting Equation 4-5 and Equation 4-6 in Equation 4-4 and solving for U, an approximation to the displacements at time $t+\Delta t$ is calculated. The displacements are approximate as the source of error enters into the solution

during calculation of K_t. Depending on the approximation used in calculating K_t, solution may be subjected to significant errors or may even become unstable. Therefore, in practice, it becomes necessary to use an iterative step-by-step load increment procedure to evaluate Equation 4-6 to sufficient accuracy (called as convergence) to obtain a reliable FE solution.

In this research Abaqus (Research) 6.9-3 is used to solve the static non-linear FE model of "Sleep seat' subjected to CS25.561 loads. The widely used iteration method, Newton-Raphson technique (known as Newton's method in calculus) is used to solve the nonlinear FE model of 'Sleep seat' [33].

The convergence (equilibrium) criteria used is the default setting in Abaqus (Research) 6.9-3 [33] i.e.

- Force residual tolerance, R_a is set to 0.5% of an average force in the structure, averaged over time.
- Even if R_a is within the tolerance, the last displacement correction, C_a should be less than 1% of the increment displacement.

If the FE model involves contact pairs (as in 'Sleep Seat'), open-close changes in contact and stick-slip changes in friction, lead to abrupt changes in the stiffness. To illustrate,

- For the contact openings, contact force is set to zero leading to a force discontinuity,
- For contact closure, discontinuity arises if the penetration error (difference between the actual penetration and the penetration estimated using contact-pressure over-closure relation) is smaller than the contact compatibility tolerance times the incremental displacement.
- In stick-to-slip transitions, the frictional force is set to a lower value leading to force residual.

To make sure that sufficient accuracy is obtained in the contact behaviour, 'Severe Discontinuity Iterations' SDIs, which check various contact irregularities against the corresponding tolerances are performed by the Abaqus [33]. For a

given load increment, it continues to iterate until the SDIs are within the acceptable tolerance and equilibrium tolerances are satisfied.

The solution is accepted as a 'Converged Solution" only when both the convergence checks are satisfied and then the next load increment is applied.

As it can be concluded that in each 'equilibrium' iteration of a nonlinear analysis, formation of structure's stiffness matrix, its inversion and solution of system of equilibrium equations is performed, computational cost of each iteration nearly equals to the cost of performing a complete linear analysis. Therefore, computational expense to achieve a "Converged Solution" for a complete nonlinear problem is very high and lies in the calculation and factorisation of the tangent stiffness matrix.

4.1.2 SELECTION OF CONTACT COMPATIBILITY ALGORITHM

For present research non-linear variation of the penalty method is used, in which penalty stiffness increases linearly between regions of constant low initial stiffness and constant high final stiffness, giving overall non-linear pressure over closure relationship [33].

Different zones in the "Contact Pressure Over-closure" relationship (Figure 4-1) can be explained as

- Inactive Contact region (AB): The contact pressure is zero for clearances greater than Zero.
- Initial contact region (BC): Linear variation of contact pressure with penalty stiffness equal to that of underlying element stiffness (K_i) allowing maximum penetration of 1% of a characteristic element length (l), which is calculated by Abaqus (Research) 6.9-3 [33].
- Stiffening region (CD): Quadratic variation of contact pressure for the penetrations in the range of "l" to "3l". The penalty stiffness increase linearly from K_i to K_f. K_f is equal to 100 times the representative underlying element stiffness.
- Final constant contact-stiffness region (DE): For the penetrations greater than "3l", there is a linear variation of contact pressure with a slope of K_f.

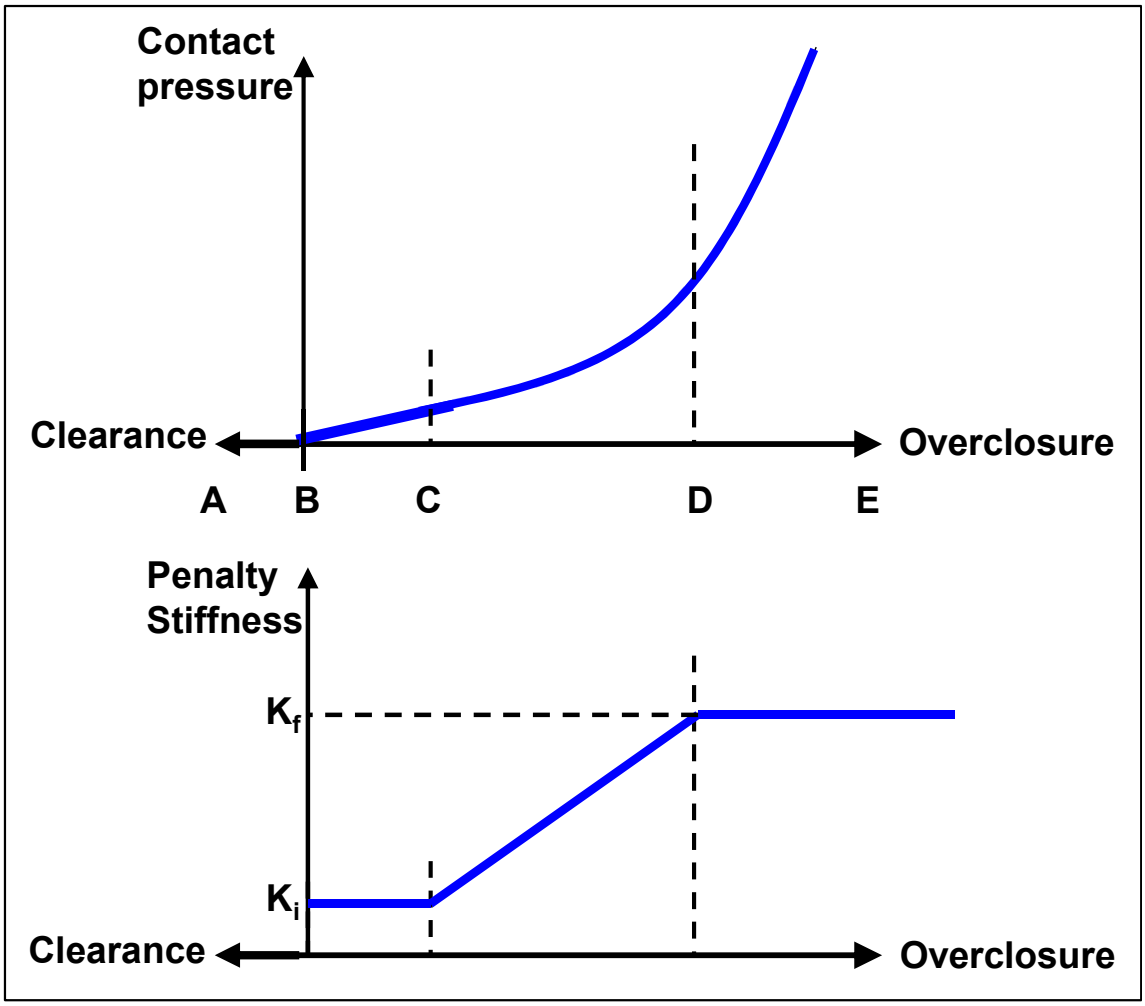

Figure 4-1 Non-linear variation of the penalty stiffness used in Abaqus (Research) 6.9-3 [33]

The advantage of using non-linear variation of penalty stiffness is quite apparent. The low initial stiffness results in better convergence of Newton iterations and better robustness, while the higher final penalty stiffness keeps the penetrations at an acceptable levels as the contact pressure builds up.

In the author's thesis for MSc by research, following characteristics of a nonlinear problem are discussed in detail [9].

- Iteration and incremental scheme used in a non-linear analysis
- Guidelines discretising the contact interfaces

4.2 CHALLENGES FACED WHILE USING IMPLICIT FORMULATION AND PROPOSED SOLUTION

The major challenges in obtaining a solution using implicit time integration formulation are

- Initialising the solution
- Achieving a 'converged' solution
- Controlling CPU time and disk-space requirements

The first two challenges are inter related and are the most daunting tasks in front of an analyst. A detailed study undertaken during this research to understand the mechanism behind these problems and solutions sought are provided in coming sections. The third aspect of controlling CPU time and disk-space requirement is related with

- The identification of correct element type and density for a FE discretisation of a component i.e. mesh sensitivity study. It has been explained in Section 4.6.2 of author's thesis for MSc by research [9].
- The identification of load increment steps and a suitable solution technique (presented in the Section 4.6 of this chapter).

With this brief background, following section gives a list of various convergence problems faced and solutions applied during non-linear FEA of the complete seat.

4.2.1 RIGID BODY MOTION

This is the most common, most talked and yet the most challenging issue in front of the analyst [9, 40]. It occurs when the system has inadequate supports and structure is free to "float" is space. Generally solvers report this error with singular stiffness matrix or with very large displacement [41, 42]. A care should been taken to ensure that appropriate support conditions are applied to suppress unconstrained motion. This is a basic step in any structural FEA.

The real challenge comes when various contact pairs are defined and parts are supposed to be held only through contact. Often frictional sticking is effectively used to constrain rigid body motion. However, to generate friction; contact pressure has to develop, which is not possible when surfaces are not in contact at the beginning of the simulation! (Figure 4-2 LHS) Therefore, for initial conditions, friction is not an effective tool. So inactive contact constraints cause unrestrained rigid body motion. Additional reasons for rigid body motion and corresponding preventive techniques are,

4.2.1.1 INITIAL CLEARANCE AND SIGNIFICANT DISSIMILAR MESH DENSITIES FOR CONTACT PAIRS

FE models for individual components are built and then assembled as per the CAD references. Due to the “Geometry Idealisation” and use of finite elements with straight sides; contact pairs normally have initial clearances (Figure 4-2 LHS). In addition, contact pairs suffer from mismatching element densities and dissimilar curvatures (Figure 4-2 RHS). Significant mismatch between element densities at the contact interface results either, in the failure of the one surface detecting its interacting surface or occurrence of the contact interaction entirely within the bounds of a single element. If the contact occurs at very few points, contact compatibility conditions are applied to a small number of slave nodes. Though the analyst may be successful in obtaining a converged solution, post-processing of these results reveals an uneven pattern (peak and valley) of contact pressure on the contact surface due to the high concentration of constraints at small number of elements. These results may lead to an inappropriate indication of a localised structural failure.

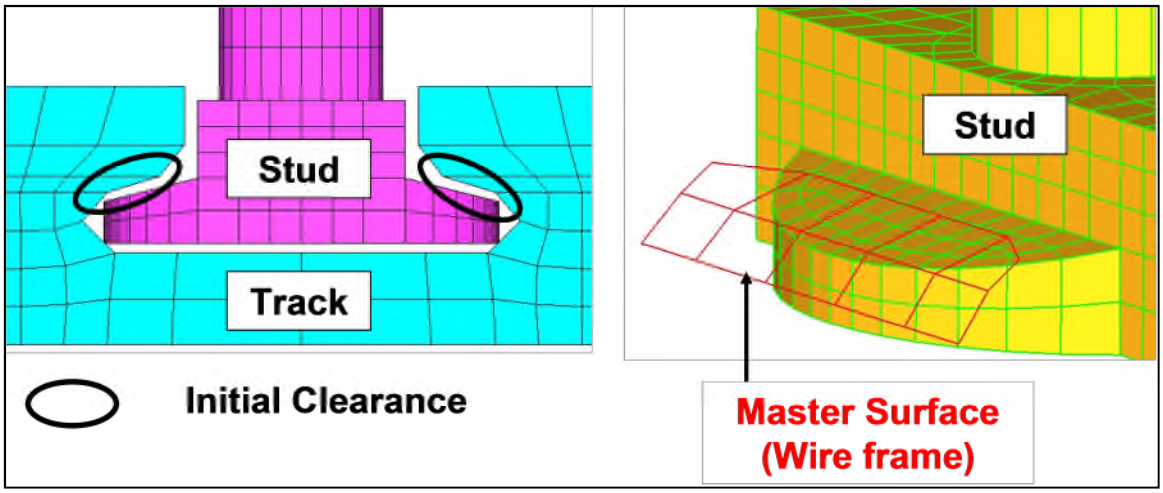

Figure 4-2 Causes of non-convergence or failure of the implicit solution algorithm to initiate. LHS Initial clearance in the components leads to rigid body motion, RHS - Inappropriate mesh densities at the contact interface fail to establish a proper contact conditions.

To avoid these problems, mesh should refine so as to spread the interaction across multiple element faces. Wherever possible, surfaces, which are likely to come in contact with each other, should be positioned such that no gap exists between them during initial configuration e.g. as illustrated in Figure 4-3, inner profile of the seat track (shown by wire frame) and the corresponding mating surface of the stud, are in contact with each other i.e. 'Just touching', in the undeformed configuration.

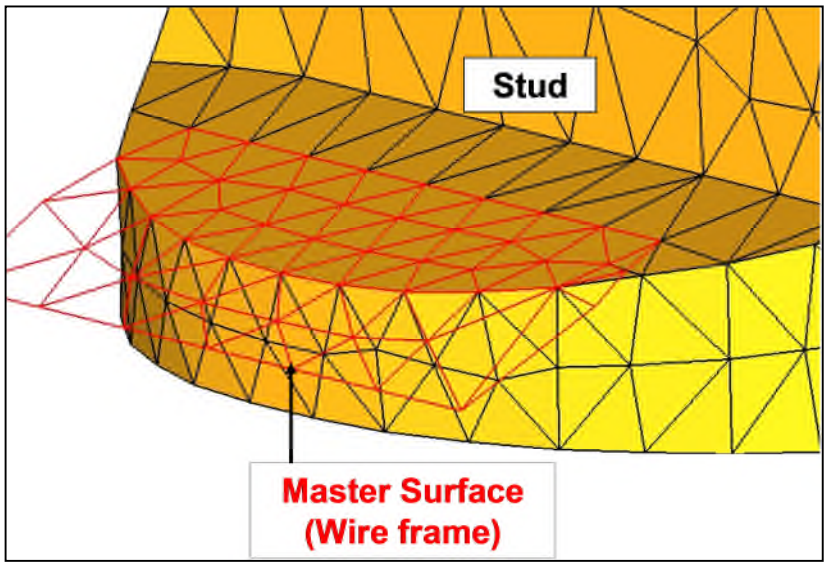

Figure 4-3 Discretisation strategy at the contact interface to obtain a 'converged' solution. Small differences in the mesh density of the interacting surfaces and contact surfaces in 'just touching' initial configuration.

4.2.1.2 UNINTENDED INITIAL PENETRATION

Abaqus (Research) 6.9-3 interprets this case as an interference fit and tries to resolve it during the first increment [33]. This generates very high and unrealistic stresses during the initial time step thereby corrupting the final results. Care should be taken while developing the mesh for surfaces in contact so as, to avoid initial penetrations. A detailed discussion on effects of initial penetrations and clearances on the solution of nonlinear problems and strategies to build a mesh without initial penetrations and clearances is available in Section 7.5 of author's MRes thesis [9].

Abaqus (Research) 6.9-3 can automatically adjust slave surface to remove initial penetrations without straining the elements. However, it may distort the mesh and may develop new unphysical regions of stress-concentration.

4.2.2 VOLUME BASED STABILISATION

The instability of a nonlinear problem may be of a geometric nature such as buckling or of a material nature such as material softening. Manifestation of such instabilities in the global load-displacement response with a negative slope

can be accounted by employing bucking or collapse analysis procedures. However, in a non-linear FEA of complete seat, instabilities are localised i.e. strain energy is transferred locally from one part to its neighbouring part and global solution methods such as buckling or collapse modelling may not work. These types of problems needs to be solved either dynamically or by using artificial dashpots.

Abaqus addresses such class of problems by adding a volume proportional viscous damping to the model [33]. If the local region becomes unstable; fraction of strain energy then released due to increased local velocities; is dissipated by the applied damping. This fraction is called as 'Dissipated Energy Fraction (DEP)', default value of which is 2.0E-4. This is applied to all the contact pairs equally in normal and tangential direction.

In automatic stabilisation, viscous force of form

$F_v = cM^*v$ **Equation 4-8**

is added to the global equilibrium equations

$P\text{-}I\text{-}F_v = 0$ **Equation 4-9**

Where

F_v is the viscous force

c is a damping factor

M* is an artificial mass matrix calculated with unit density

v is the vector of nodal velocities

P is the externally applied load

I is the internal nodal force generated due to element stresses

If the convergence behaviour is problematic then DEP should be increased or if the artificial damping is distorting the solution then it should be decreased (Post-analysis check). Therefore, this becomes a manual trial and error process until

a converged solution is obtained and ratio of energy dissipated by viscous damping (ALLSD) to the total strain energy (ALLIE) is minimal.

In the present research, adaptive automatic stabilisation scheme has been used. Under this scheme, Abaqus automatically calculates the damping factor required based on convergence history and ratio of ALLSD to ALLIE which is limited to 0.05 on the global level for the whole model [33]. Variation of the damping factor with time provides an effective approach. Artificial stabilisation energy always increases while strain energy may decrease. Therefore, Abaqus (Research) 6.9-3 maintains for the ratio of incremental value of the stabilisation energy to the incremental value of the strain energy for each increment; below the accuracy tolerance. In addition, analyst should ensure that the viscous forces are small compared with the overall forces in the model.

One important advantage of this automatic stabilisation scheme is that it is active only for the duration of step, for which it is specified. It does not propagate to subsequent steps automatically. In the present research, this characteristic is used to avoid effect of viscous damping on final solution. Total load is applied in two load steps. In first step, only 5% of load was applied with adaptive stabilisation to establish initial contact. In the next step, remaining load is applied without artificial damping. Solution behaves well as the contact is established in first load step.

4.2.3 CONTACT BASED STABILISATION

Rigid body motion should be stabilised through appropriate FE modelling techniques. However, during design iterations; when geometries of one or two components change; exact positioning of all contact surfaces becomes difficult and rather time consuming, as the complete seat structure has a large number of contact pairs involved. In addition, modelling of “Zero Gap” in geometry does not ensure “Initially touching” contact pairs in FEA because of mathematical approximations in the solver and internal formulations of master and slave segments (in case of surface to surface interface definitions).

Contact stabilisation scheme can be employed to control such rigid body motions where accurate positioning of multiple bodies is not possible during their FE modelling. Under this scheme, viscous damping is applied to the slave nodes for the relative motion of the contact pair. The ratio of contact damping dress (CDSTRESS) to the true value of the contact stress (CPRESS) should be minimal [33].

4.2.4 CONTACT DIAGNOSTICS TOOL – ABAQUS (RESEARCH) 6.9-3

It is a powerful visualisation tool to,

- Check the initial contact conditions,
- Track contact status over the solution history

Since it is a visualisation tool, the contact pair causing fluctuations can be readily seen (Figure 4-4). This offers a great deal of simplicity to rectify the problem. Diagnostic information is also available in data file (*.dat) and in message file (*.msg) [33].

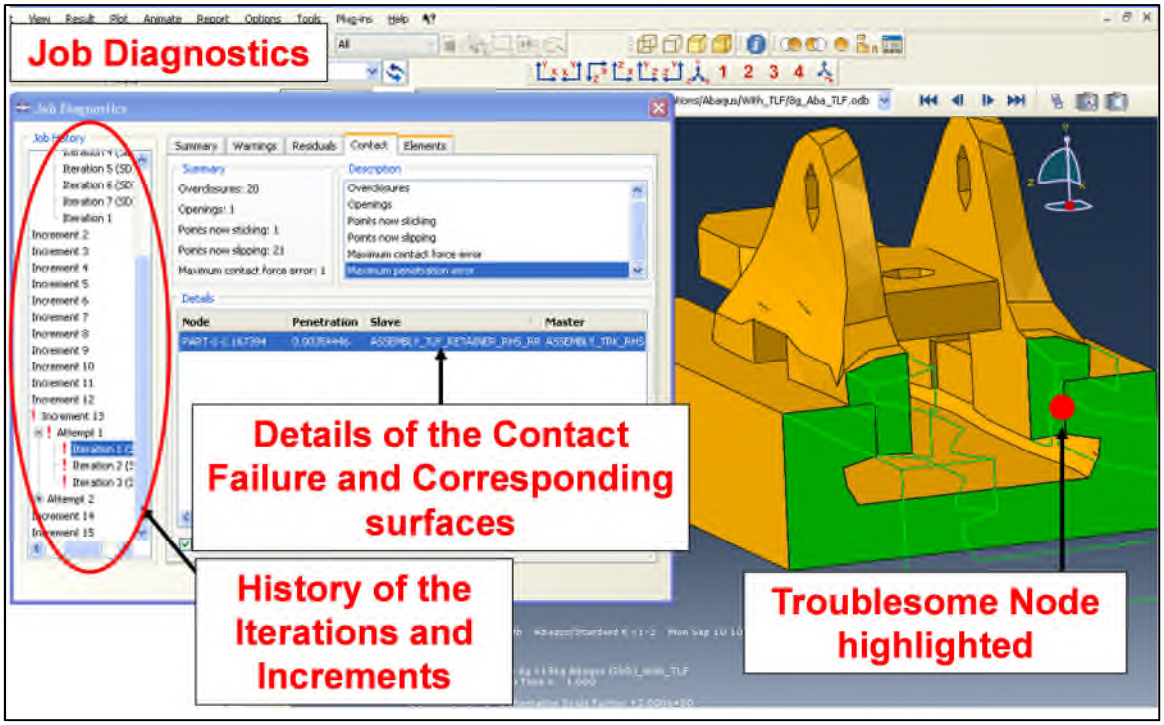

Figure 4-4 Job diagnostic tool for 'visualising' history of load increments and iterations. It helps to highlight a particular portion in the FE model, which leads to a troublesome contact behaviour or failure of the solution [33].

Using output database file (*.odb); initial strain-free adjustments of the nodal positions to remove over-closures; performed by Abaqus at time zero; can be viewed using output variable STRAINFREE [33]. A symbol plot of this variable in the visualisation module of Abaqus (Research) 6.9-3 shows, how the individual nodes have been adjusted and a contour plot of this variable shows the magnitude of the adjustment.

COPEN (Contact Opening) variable helps to identify the contact over-closure (negative value of COPEN) and initial clearances (positive value of COPEN). A detailed information on the initial contact status (open or closed), clearance distance for each constraint point on slave segment and internally generated contact element number conjugate with each slave node or segment; is written to *.dat file. Since internally generated contact elements are not user-defined, they do not appear in the input database. Therefore, if an error or warning message refers to them, it becomes difficult to locate them.

If an analysis terminates or cutback in the load increment is applied because the limit on maximum number of SDIs is exceeded, the contact diagnostics gives insight into how to tackle the problem. The number of contact status changes (open or over-closure) against number of iterations in an increment can be plotted. If the changes are tending towards zero then just increasing the allowed number of SDI will resolve the problem. It proved to be very handy in the “Forward 9g” simulations that failed due to excessive SDI. Allowed number of SDI was increased from 12 to 18 and initial contact conditions were resolved. If the contact changes are not tending towards Zero, either the FE model should be revised or parameters of the contact algorithm should be altered.

Contact chattering can be easily detected through diagnostic tool. Under such circumstances, same node or constraint appears in the diagnostic summary of every iteration, swinging between an over-closure and opening.

Using diagnostic tool, a non-convergence of equilibrium iterations (residual forces) can be traced back to a poorly defined contact pair. In such cases, switch between master and slave surfaces or changing the discretisation to

surface –to-surface or refining the mesh on slave segment; are some of the potential solutions.

The discussion on rigid body motion (Section 4.2.1) and remedies to overcome, is also applicable to FE models solved using LSDYNA/Implicit. In addition, following sections discuss additional techniques required to debug a failed simulation while using LSDYNA/Implicit.

4.2.5 DUMP SEARCH DIRECTIONS TO DATABASE

This is a very powerful visualisation tool available in LSDYNA environment. Nonlinear search directions can be written to ”D3ITER” database by specifying D3ITCTL on *CONTROL_IMPLICIT_SOLUTION control card [35]. “D3ITER” file can be opened with LS-PREPOST to examine the search directions [36]. If the search directions are orientated in the wrong direction (may be due to singularity) corrective action can be taken to ensure progress of the simulation.

4.2.6 MEMBRANE FORMULATION FOR ‘DUMMY’ SHELL ELEMENTS

In structural analysis, a huge cluster of rigid body modes or zero eigenvalues can be a consequence of wrapping a solid part with very thin elements. Such a practice is commonly used to connect shell elements to solid elements, derive surface stresses and to avoid contact failure at the solid-shell interface [37]. Very thin ‘dummy’ shell elements add very little mass or stiffness to the model, which is desirable so as not influence the ‘structural’ solution but, can be a ‘bottleneck’ in initialising the implicit solution, if appropriate element formulation is not used. If a common shell formulation i.e. linear shell with six dof (degrees-of-freedom) per node is used for ‘dummy’ shell elements, they will have negligible stiffness associated with rotational dof that is absent in solid elements. Thus they add nearly three zero eigenvalues per node attached to shell element leading to solution failure.

As a remedy, ‘membrane’ element formulation should be used (in LSDYNA/Implicit) for such ‘dummy’ shell elements so as to prevent additional of unnecessary rotational dofs [37]. Abaqus (Research) 6.9-3 has a dedicated

algorithm ‘Shell-to-Solid coupling’ to handle connections between shell and solid elements [33].

4.3 RECOMMENDATIONS TO OBTAIN A CONVERGED NONLINEAR SOLUTION

A summary of techniques used to achieve a satisfactory solution using implicit formulation is as follows

- Total load should be divided in number of increments. For the complete seat structure, first load increment should be of order of 10^{-3}. This helps to establish firm contacts initially and stabilises the solution. Automatic time-stepping (i.e. automatic load increment) option is recommended. It ensures appropriate load increment depending on the degree of nonlinearity of the system [31-33].
- A refined mesh ensuring adequate discretisation on the contact pair should be used. Contact pairs with abrupt geometry changes or sharp concave or convex contours should be thoroughly checked for initial penetrations.
- Contact pairs with sharp edges and individual segments intersecting at an edge should be smoothed manually as well as using default smoothing algorithms provided by the solver. For a node-to-surface discretisation, smoothening of the master segment should be done to have continuous surface normals. In case, sharp fold lines need to be preserved (i.e. to override default smoothing of master segment), two separate contact pairs should be defined by breaking the master surface into two surfaces and using same slave surface [33].
- To avoid the failure of the solution during initial stages due to rigid body motion, sufficient restraints should be provided and contact pairs should be in “Just touching” position.
- Springs with very small amount of stiffness (usually one thousandth of lowest stiffness in the model) can be used. For such springs can attach parts to one another or can be grounded. Due to very low stiffness assigned, their effect on the results is negligible.

- Contact stabilisation tool can be used to damp the excessive relative motion between sliding interfaces.
- Adaptive automatic stabilisation scheme should be employed to arrest the local unphysical instabilities.
- Friction can be used to restrain the excessive sliding of the interfaces.
- For bending dominated problems, interface stiffness should be reduced to avoid very stiff interface model, which may otherwise lead to excessive iterations [33, 34].
- Before submitting the full-fledged analysis, a data-check run should be performed. The data written in the output and message files should be thoroughly checked for various parameters, to name a few: overview of any contact openings, excessive adjustments in node positioning and nodes missing the master surface in tied contact. It provides an insight into the potential instabilities and saves valuable computer resources and time.
- In Abaqus (Research) 6.9-3, contact diagnostic tool is a very effective and efficient visualisation tool to analyse the contact conditions throughout the length of the analysis [33].
- For complex nonlinear problems, a quasi-static solver can be employed instead of traditional Newton-Raphson scheme. Quasi-static solver is based on improvisation of tangent stiffness matrix to reduce its reformulations (as done with Newton-Raphson method) and is robust due to built-in line search algorithm [32, 33]. This aspect is discussed in detail in Section 4.6.2, where BFGS method using quasi-static solver has been used to simulate the CS 25.561 static loads applied to the seat structure.
- For very complicated large structures involving all types of nonlinearities, explicit direct integration with damping can be employed to obtain a quasi-static solution with sufficient accuracy.

4.4 APPLICATION OF METHODOLOGY – 'DOWNWARD' LOADCASE

The guidelines developed in earlier sections of this chapter have been 'put to test' for simulating the 'Downward 8.6g' loadcase applied to the FE model of the 'triple' Sleep-seat structure. Though the regulation (CS25.561) states '6g' load in downward direction, actually 8.6g of load is applied in downward direction to be in line with the experimental testing (results from FEA and those from experimental testing are compared in Section 6.2 of this report).

The problem has been attempted using implicit formulation of two different commercial codes: Abaqus (Research) 6.9-3, LSDYNA (Implicit) V9.71 R4.2.1. The FE model, boundary conditions and material definition used for these two different simulations is same. Newton-Raphson method can be activated in LSDYNA by setting ILIMIT equal to 1 on *CONTROL_IMPLICIT_SOLUTION [35]. The settings of the control cards required to accomplish an implicit simulation using LSDYNA/Implicit are explained in Appendix B of this report.

The FE model has 18190 nodes and 194612 elements. Linear solid elements and shell elements are used to model the seat leg and the components represented with mid-surface geometry (such as boomerang, seat-pan and Forward beam) respectively. The maximum aspect ratio of 4.69 is observed for seven elements located in the aft upper quadrant of the Forward beam. The vertically downward force of 9364.63N (as per the test procedure considering ~111kg per seat with 8.6g inertia load) has been uniformly distributed over each seat-pan and the bottom surface of each of the Seat-track has been constrained for all degree-of-freedom (Figure 4-5). Bill of material is present in 'Appendix M', which provides a tabular summary of materials used for various components of seat structure and contact pairs defined. Mechanical material properties are present in 'Appendix K'.

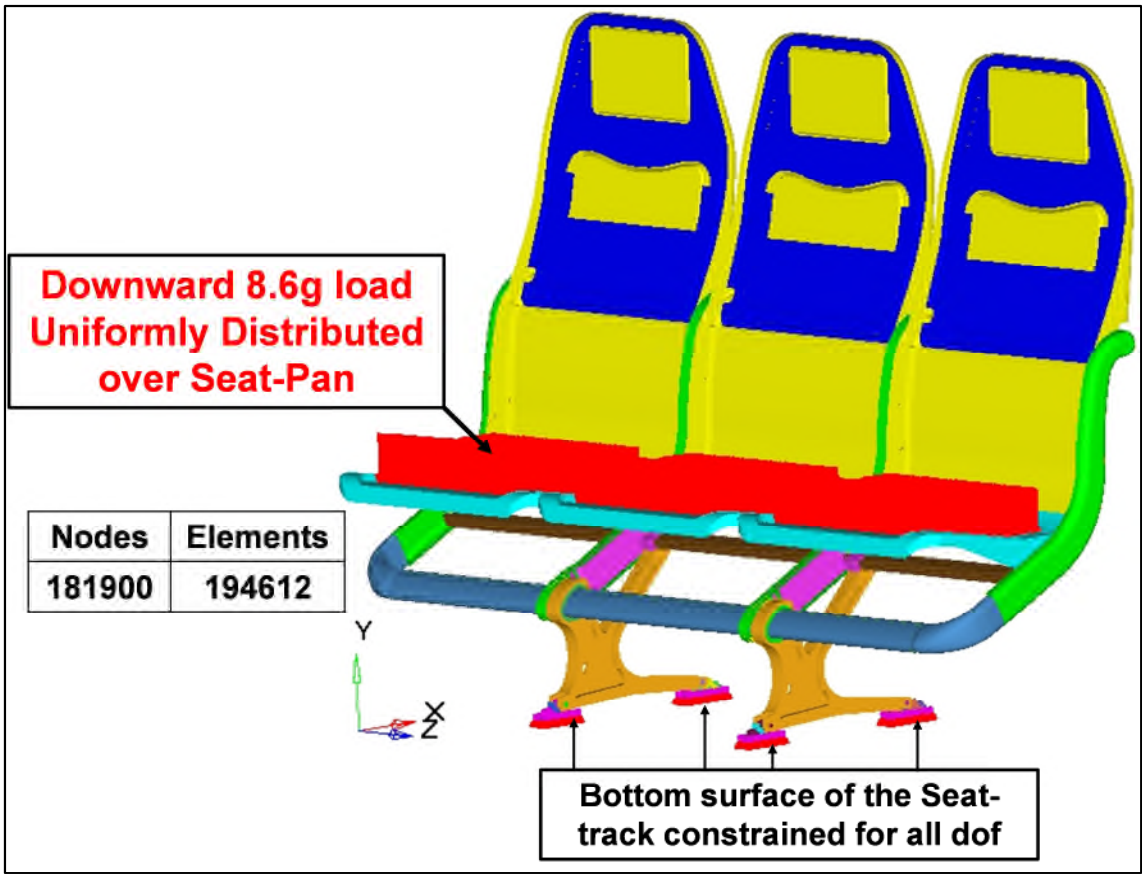

Figure 4-5 Boundary conditions for 'Downward 8.6g' loadcase simulated using Abaqus (Research) 6.9-3

Abaqus and LSDYNA commercial codes are used as solvers due to their widespread use in the industry and ability to handle large-scale nonlinear problems [41, 43].

Abaqus (Research) 6.9-3 required 13 load increments to achieve the 100% of load with 62 iterations (equilibrium iterations with severe discontinuity equations). CPU time is 2163s with 16 processors (two Intel E5-2660 (Sandy Bridge) CPU's equivalent to 16 CPU cores).

LSDYNA/Implicit (V9.71 R4.2.1) required 12 load increments to achieve the 100% of load with 64 iterations. CPU time is 899s with 16 processors. The difference in load increments and the solution time between two solvers can be because of,

- Different techniques for handling and distributing elements

- Difference in solution technique as Abaqus (Research) 6.9-3 uses Newton-Raphson method while LSDYNA/Implicit uses Newton-Raphson with line search algorithm. Since, the later solution technique is more stable than the previous one, it requires less load increments and hence less CPU time.

Findings from the study conducted to 'reduce' the CPU time are presented in Section 4.6 in this chapter.

4.5 FRAMEWORK FOR VERIFYING FEA RESULTS

Though the solutions are obtained with both the solvers (Abaqus (Research) 6.9-3 and LSDYNA/Implicit), it is essential to verify their quality. Following section demonstrates that the FEA results for 'Downward 8.6g' satisfy all the quality checks thereby ensuring a reliable solution.

Please note that the results are discussed (in this section 4.5) only from FEA reliability standpoint and no interpretation has been made for design parameters such as stress or displacement. This loadcase has been solved by two another solution techniques namely LSDYNA/Explicit and 'LSDYNA-Implicit/Explicit Automatic Switching' presented in chapter number 5. The results from these four methods are then compared (for parameters such as stress, displacement, interface loads etc.) with one another as well as with those from experimental testing (Section 6.2.1).

The first step after obtaining a FEA solution for a structural problem should be thorough checking of displacement contours, for the displacements in unexpected directions or at unexpected regions and/or of surprisingly small or large magnitudes. Then the displacement plot should be animated with different scale factors and with different frame rates for all the time frames of the analysis. This helps to check for any failure in the contact mechanism for the interior parts of the structure and hour-glassing. This immediately reveals the load increment at which a particular contact fails (if any).

If nothing is obviously wrong with these visual checks then the analyst should proceed to detailed quantitative checks and results interpretation.

4.5.1 FORCE EQUILIBRIUM CHECK

The procedure to extract the components of the reaction forces for 'Abaqus Implicit Method' and 'LS-DYNA Implicit or Explicit Method' is provided in the Appendix D.1 of this report.

It can be seen that two solution techniques used to solve the problem of 'Sleep Seat' subjected to the 'Downward 8.6g' load, satisfy the force equilibrium check i.e. reaction force should approximately balance the applied force (Table 4-1). This indicates that the

- Loads were not applied to the constrained nodes and
- The applied loads and the recovered reaction forces are in the same co-ordinate system (Global co-ordinate system in present case).

Commercial Code	**Abaqus/ Standard**			**LSDYNA-Implicit**		
	Components of the reaction force, N					
	Fx	**Fy**	Fz	Fx	**Fy**	Fz
Applied Force, N						
Fx = 0, **Fy = 28093.8**, Fz = 0	1.60E-3	**28110.6**	1.98e-3	0.20e-3	**28117.3**	2.85e-3

Table 4-1 Force equilibrium check is satisfied by the simulation of 'Downward 8.6g' load applied to the 'Sleep seat' solved using Abaqus (Research) 6.9-3 and

The small imbalance in the reaction force and applied force can be attributed to the automatic stabilisation and contact stabilisation schemes used to aid convergence.

4.5.2 DISTRIBUTION OF THE CONTACT PRESSURE

The representative plot of contact pressure has been produced (Figure 4-6) for the interface definition between main body of the tool-less fitting and upper lip of

the seat-track. This is the most critical interface definition for the 'Downward 8g' as the maximum interface load is transferred through it. The uniform distribution of the contact pressure without any peaks and valleys ensures that

- The density used for discretisation at the interface is sufficient.
- The algorithm used for ensuring contact compatibility is appropriate.
- Interface definition is spread over a reasonable area as the slave nodes are not sticking or chattering along the master surface.
- No initial interpenetrations are present at the interface.

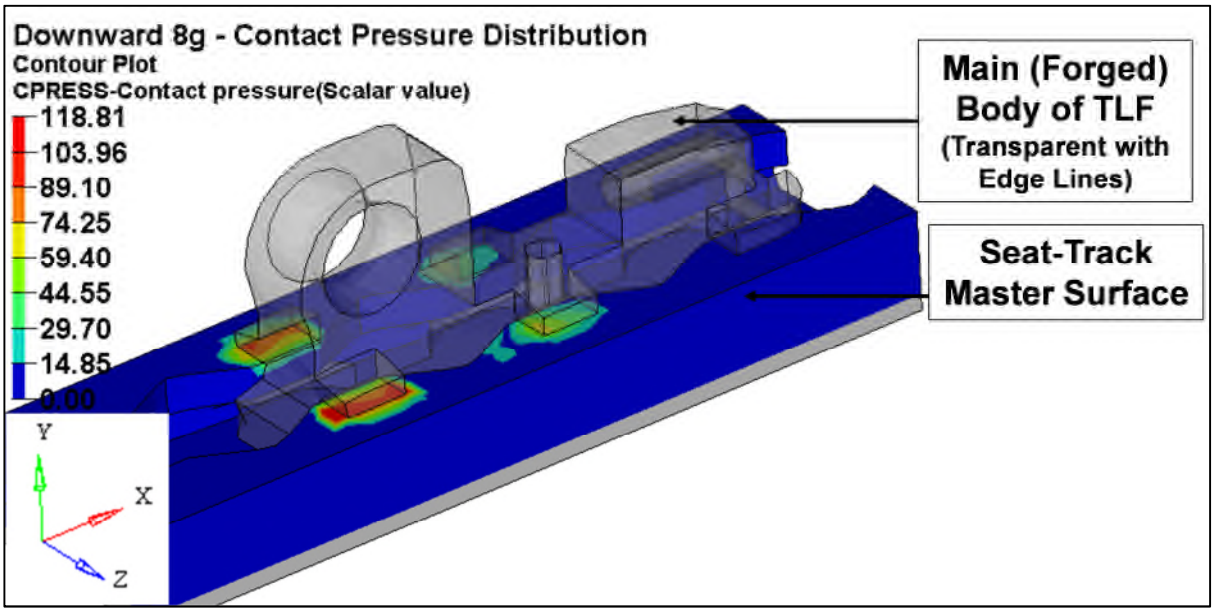

Figure 4-6 Uniform distribution of the contact pressure at the interface between main body of the tool-less fitting and seat-track verifies the procedure used for implementing the contact compatibility condition. Loadcase - Downward 8.6g applied to the FE model of 'Triple' seat-structure. Solver used - Abaqus (Research) 6.9-3

4.5.3 RATIO OF STABILISATION STRAIN ENERGY TO TOTAL STRAIN ENERGY

As explained in Section 4.2.2 of this report, energy dissipated by viscous damping (artificial stabilisation strain energy, ALLSD) should be less than 5% of the total strain energy (ALLIE) [33]. Output for both the energies can be requested in the 'History Output' section of the Abaqus **STEP* definition.

As the ALLSD is 0.27% of the ALLIE, the FE simulation of the ‘Downward 8.6g’ load applied to the ‘Sleep Seat’; satisfies the ‘Stabilisation Energy’ check (Table 4-2).

ALLSD, N-mm	ALLIE,N-mm	Actual Ratio, %	Limit, %
194.91E+03	0.54E+03	0.27	5

Table 4-2 Ratio of the Artificial Stabilisation Energy (ALLSD) to the Total Strain Energy (ALLIE), Loadcase - Downward 8.6g applied to the FE model of 'Triple' seat-structure. Solver used - Abaqus (Research) 6.9-3

4.5.4 RATIO OF CONTACT DAMPING STRESS TO CONTACT STRESS

As explained in Section 4.2.3 of this report, contact stabilisation schemes can be used to stabilise the troublesome contact pairs. The ratio of contact damping pressure (CDPRESS) to the contact pressure (CPRESS) should be low.

The most critical interface for ‘Downward 8.6g’ loadcase i.e. the interface definition between main body of the tool-less fitting and upper lip of the seat-track (Section 4.5.2), has been chosen to monitor the ratio of CDPRESS to CPRESS. Output for both the energies can be requested in the ‘History Output’ section of the Abaqus (Research) 6.9-3 ‘Step’ definition [33].

As the CDPRESS is 0.0013% of the CPRESS (Table 4-3), the FE simulation of the ‘Downward 8.6g’ load applied to the ‘Sleep Seat’; satisfies the ‘Contact Stabilisation’ check. The ratio is negligible, which indicates that

- The contact surfaces of the un-deformed configuration are in ‘Just touching’ condition, which has helped to establish the contact during initial load increment.
- Sufficient restraints have been provided in the model to prevent the rigid body motion.

Interface Location	CDPRESS, N/mm^2	CPRESS, N/mm^2	Actual Ratio, %
RHS Rear	0.08453	6459.96	0.0013

Table 4-3 Ratio of the Contact Damping Pressure (CDPRESS) to the Contact Pressure (CPRESS) Interface – Main Forged Body of the tool-less fitting and the Seat-track, Loadcase - Downward 8.6g applied to the FE model of 'Triple' seat-structure. Solver used - Abaqus (Research) 6.9-3

4.6 TECHNIQUES TO REDUCE COMPUTATIONAL TIME

Once a procedure to obtain a 'converged' solution for the complex and highly-nonlinear implicit problem was established, an additional study was performed to 'reduce' the CPU time required for the solution. The FE model of the seat subjected to 'Downward 8.6g' load (same model as described in Section 4.4 of this chapter, referred as 'previous simulation' in this section) is chosen for this study and the commercial codes used are 'Abaqus (Research) 6.9-3' and LSDYNA (Implicit formulation). The target is to achieve the CPU time of 899s with 16 processors as observed with LSDYNA/Implicit (Section 4.4).

4.6.1 ADJUST INITIAL LOAD – INCREMENT BASED ON CONVERGENCE HISTORY

The load increment history of the previous simulation is studied and it is observed that initial load increment can be increased as the number of SDIs is less than 5 in first load increments [33]. This indicates that the FE model of the seat does not strongly suffer from 'rigid body motion' or 'contact' related issues. Therefore, first-step load increment is increased from 1% to 15% of the total load (by trial and error) for all the simulations performed.

4.6.2 EFFECT OF SOLUTION TECHNIQUE ON COMPUTATIONAL TIME

The problem has been solved using three different solution techniques, which are readily available in the commercial softwares [41, 43]

i. Full Newton-Raphson
ii. Full Newton with line search algorithm
iii. Quasi-Newton

Another class of solution methods based on 'Arc length technique' has not been explored due to their suitability for buckling and snap-through problems [33].

With reference to Table 4-4

- The initial load increment (First time-step) used for Solution techniques B, C, D, E, F and G is 15% of the total load.
- Solution technique C i.e. 'Full Newton method with line search' can be activated in Abaqus (Research) 6.9-3 by editing 'General Solution controls' and setting N^{ls} (maximum number of line search iterations) equal to a number between 0 to 5 [33]. Zero (0) indicates 'Full Newton' method and '5' indicates 'Quasi-Newton method' i.e. solution technique D.
- Solution technique G i.e. 'LSDYNA - Quasi-Newton with BFGS updates', is a default incremental-iterative numerical algorithm implemented in LSDYNA [35].
- Solution technique F, 'LSDYNA- Full Newton + Line search' can be activated by setting ILIMIT equal to 1 on *CONTROL_IMPLICIT_SOLUTION and E i.e. 'Full Newton' by adding LSTOL=9999.0 to the same control card [35].

4.6.2.1 DISCUSSION OF RESULTS

Figure 4-7 shows the displacement (magnitude) plots obtained for the seat-structure subjected to 'Downward 8.6g' loads and solved using different solution techniques. It can be observed that the differences in the deflection magnitudes are insignificant. Therefore, it can be concluded that the change of solution scheme does not affect the simulation results.

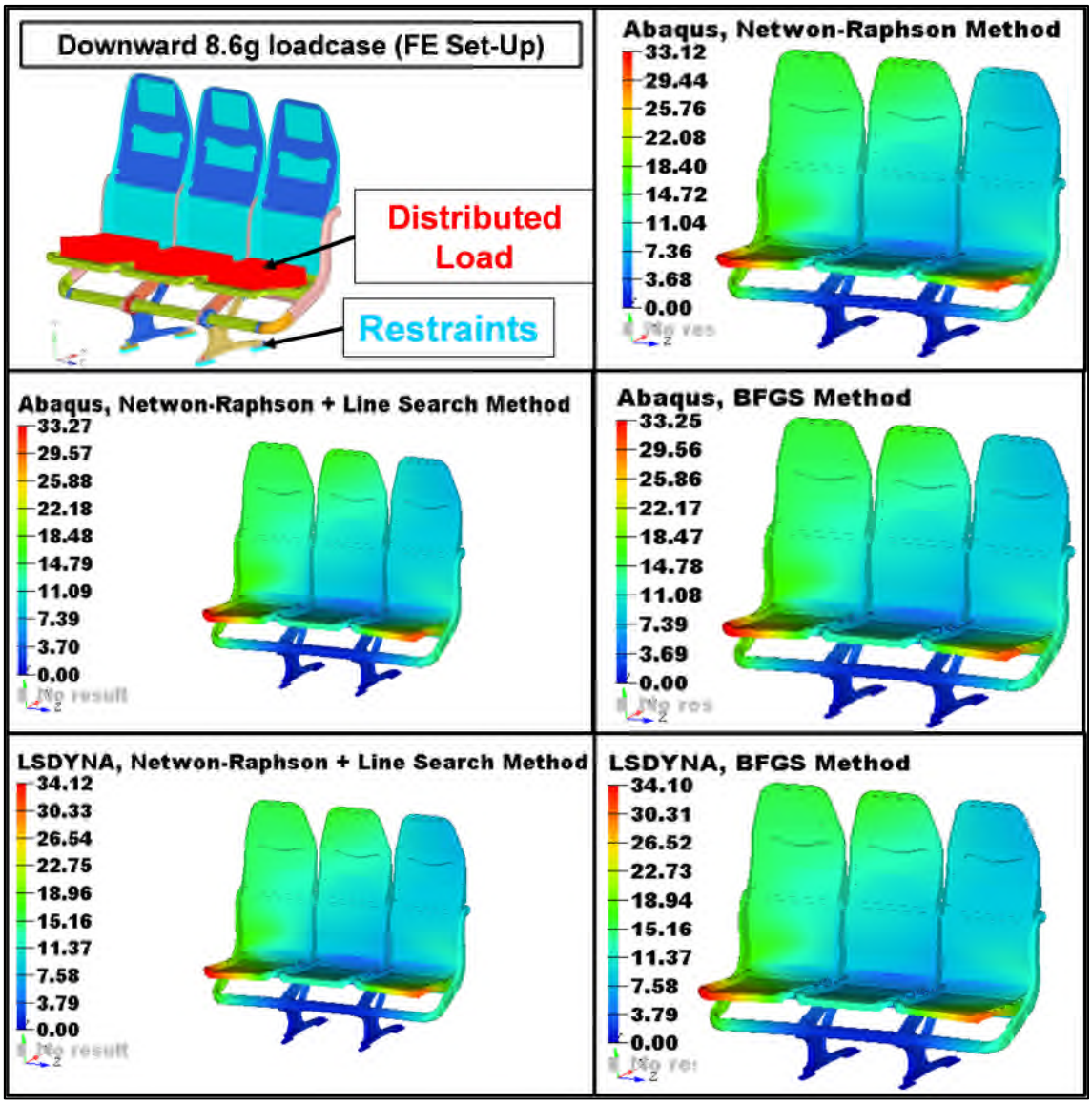

Figure 4-7 Magnitude and the contours of the displacement (magnitude) for the 'Triple Seat Assembly' subjected to 'Downward 8.6g' loads and solved using different solution techniques. It can be observed that the different solution techniques do not have any significant impact on the results obtained.

Please note that only displacement contours are presented in this chapter. The case-study has been solved by two another solution techniques namely 'Explicit time integration scheme' and 'Implicit/Explicit Automatic Switching' in chapter number 5. The results from different time integration schemes are then compared (for parameters such as stress, displacement, interface loads etc.) with one another as well as with those from experimental testing (Section 6.2.1) to validate the FEA methodology developed during this research.

Increase in the initial load increment (from 1% to 15%) has resulted in reducing the CPU time from 2163s to 1433s (Solution A and B respectively) as the total load increments required to achieve 100% of load reduced from 13 to 9. An attempt to further increase the 'initial load increment' to 20% of the total load failed to find a converged solution; resulting in a 'cut-back' in load increment.

Robustness of Full Newton or Quasi-Newton can be improved by including a 'line search' algorithm. During equilibrium iterations, where residuals are large (greater than solution convergence tolerances), the 'line search' algorithm 'corrects' the solution by line search scale factor, S^{ls} [41, 43].

An iterative procedure is used to estimate the value of S^{ls} that minimises the component of residual vector in the direction of correction vector. These iterations require a pass through element loop increasing the computational cost per iteration. However, as the solution divergence is prevented, less iterations are required to obtain a converged solution, which reduces the CPU time. The decrease in solution time from 1433s to 1393s (CPU time for 'B' and 'C' respectively, Table 4-4) with approximately same memory requirement (6.2GB) highlights this fact. The number of equilibrium iteration required for obtaining a converged solution reduced from 9 to 8.

A solution technique based on Newton method suffers from following shortcomings,

- The method becomes computationally very expensive per iteration as tangent stiffness matrix must be formed and solved at each iteration.
- Modified Newton-Raphson method, in which the tangent stiffness matrix is updated only after the convergence is obtained in the current load increment; is suitable for mild-nonlinear problems e.g. problems involving softening behaviour with monotonic straining [33].
- As the problem size increases, the "Direct" solution of tangent stiffness matrix dominates the entire computational cost.

Therefore methods based on "iterative" improvements of tangent stiffness matrix known as quasi-Newton or secant stiffness or matrix update; are increasingly used for solving the nonlinear system of equations [31-33, 35].

Among the quasi-Newton methods, the BFGS (Broyden, Fletcher, Goldfarb, Shanno) method; which is simple to programme and very effective for solving large FE problems; is used by Abaqus (Research) 6.9-3 and LsDyna [33, 35].

Characteristics of BFGS solver using quasi-Newton method

- The method is robust and for a large FE model involving multiple degree-of-freedoms, the inverse of the secant stiffness matrix (essentially tangent stiffness matrix) can be obtained by updating the preceding tangent stiffness matrix. The inverted secant matrix is used for certain number of pre-defined iterations (e.g. default 10 maximum iterations in LsDyna and 8 in Abaqus (Research) 6.9-3), but is constantly improved after each iteration using an inexpensive rank two update. If the convergence is not reached after specified maximum number of iterations or if divergence is detected, a new tangent stiffness matrix is formed and inverted and the process is continued. Thus equation solving cost of secant step is significantly reduced, which more than pays for the computational expense for generating the inverse of secant stiffness matrix.
- Line search is an integral part of the solution method.

It can be observed from Table 4-4 that the CPU time required with 'Full Newton + Line search' method is 1393s whilst that with 'quasi-Newton' method is 1324s (Solution C and D respectively). The memory requirement for Quasi-Newton methods is higher than that for Newton-Raphson methods due to updates of secant stiffness matrix. The equilibrium iterations required for obtaining a converged solution dropped from 8 to 6.

So far, FEA results obtained with Abaqus (Research) 6.9-3 using different solution techniques are discussed. Same logic applies to the results obtained with LSDYNA/Implicit solver with respective solution techniques. Difference in the CPU time is observed for the same solution technique when used with two different commercial codes (e.g. CPU time to solve FE model of 'Sleep Seat' subjected to 'Downward 8.6g' with 'Quasi-Newton with BFGS updates' with Abaqus (Research) 6.9-3 is 1324s whereas that with LSDYNA/Implicit is 853s).

Serial Number	Solution Technique	CPU time, s	Memory Required, ~GB
A	**Previous Simulation** - Abaqus – Full Newton, First time-step = 1% of the total load	2163	6.20
B	Abaqus – Full Newton, First time-step = 15% of the total load	1433	6.20
C	Abaqus – Full Newton + Line search	1393	6.24
D	Abaqus – Quasi-Newton with BFGS updates	1324	6.55
E	LSDYNA – Full Newton	No Solution	Not applicable
F	LSDYNA- Full Newton + Line search	899	4.51
G	LSDYNA - Quasi-Newton with BFGS updates	853	5.83

Table 4-4 Comparison of different solution techniques based on CPU time and memory requirements (in gigabytes, GB) Loadcase - Downward 8.6g applied to the FE model of 'Triple' seat-structure. Solvers used - Abaqus (Research) 6.9-3 and LSDYNA/Implicit

4.6.2.2 EFFICIENT SOLUTION TECHNIQUE SUGGESTED

- Quasi-Newton is a hybrid method, which combines the efficiency of the modified Newton-Raphson method with the reliability of the full Newton-Raphson method.
- BFGS updates help to reduce the total number of load increments thereby reducing the CPU time.

To conclude, Quasi-Newton solver with BFGS updates is recommended to solve complex nonlinear problems such as a seat structure subjected to static inertia loads as per CS25.561. The decision to use a particular commercial code should be taken based on hardware resources available and computational cost.

4.6.3 MEMORY SETTINGS FOR LSDYNA/IMPLICIT

For an explicit problem to be solved using MPP-DYNA, memory is allocated on the command line using 'memory' keyword.

*KEYWORD memory1=XXXm memory2=YYYm [37]

Where, XXX and YYY are the number of megawords (8 bytes for double precision) of allocated memory. The amount of 'memory1' is assigned to the core used for decomposing the specified job, whereas 'memory2' is assigned for the remaining cores.

However, for an implicit simulation to be run using LSDYNA, the 'memory2' specification should not be used [37]. The imbalance of memory (i.e. 'memory1' and 'memory2') causes an imbalance in the intensive computational during linear algebra phase. The FE model under study (Section 4.4) is solved using 16 processors by specifying two types of memory specifications with solution technique 'G' (Table 4-4).

I. memory1=400m memory2=80m
II. memory=100m

With a balanced memory allocation for each core, CPU time drops from 853s to 827s (Table 4-5).

Downward 8.6g, Triple Seat structure, LSDYNA/Implicit Solution Technique 'G'	
Type of memory allocation	**CPU time, s**
memory1=400m memory2=80m	**853**
memory=100m	**827**

Table 4-5 Allocation of appropriate memory type reduces the CPU time for a FE model of 'Sleep Seat' subjected to 'Downward 8.6g' solved using LSDYNA/Implicit default nonlinear solver.

Conclusion - Chapter 4

The simulation of the FE model of the complete 'Sleep Seat-structure' subjected to loads as per CS25.561 is a classic problem involving large displacement, large rotation and large strains i.e. all types of nonlinearities namely geometric, contact, and material.

The essence of solving a general non-linear problem is to estimate the value for tangent stiffness matrix; K_t. Depending on the approximation used in calculating K_t, solution may be subjected to significant errors or may even become unstable. Therefore, in practice, it becomes necessary to use an iterative step-by-step load increment procedure to evaluate K_t to sufficient accuracy (called as convergence) to obtain state of equilibrium of a body corresponding to the applied loads. The major computational cost per iteration lies in the calculation and factorisation of the tangent stiffness matrix. The major challenges in obtaining a solution using implicit formulation are

- Initialising the solution
- Achieving a 'converged' solution
- Controlling CPU time and disk-space requirements

A detailed study was then undertaken to develop techniques to deal with non-convergence and a following guidelines are proposed by this research,

- Initial Clearance and significant dissimilar mesh densities along contact interfaces should be avoided.
- A refined mesh ensuring adequate discretisation on the contact pair should be used. Contact pairs with abrupt geometry changes or sharp concave or convex contours should be thoroughly checked for initial penetrations.
- Springs with very small amount of stiffness (usually one thousandth of lowest stiffness in the model) should be attached to 'ground' the parts held only by contact. Due to very low stiffness assigned, their effect on the results is negligible.
- Adaptive automatic stabilisation scheme (in Abaqus (Research) 6.9-3) should be employed to arrest the local unphysical instabilities.
- Non-linear variation of the penalty method should be used to ensure contact compatibility. The low initial stiffness results in better convergence of Newton iterations and better robustness, while the higher final penalty stiffness keeps the penetrations at an acceptable levels as the contact pressure builds up.

The methodology developed in this chapter for FE model building, modelling of contact compatibility condition and incorporating stabilisation techniques in the solution scheme is then 'put to test' to solve a real-life problem i.e. to obtain a 'converged' solution the complex nonlinear problem of the FE model of triple seat-structure subjected to Downward 8.6g (load used in experimental testing) using two different commercial codes namely Abaqus (Research) 6.9-3 and LSDYNA/Implicit. Both the method yielded solutions for the problem. To assess the quality of the solutions, following guidelines are recommended by this research

- Reaction force should approximately balance the applied force.
- Energy dissipated by viscous damping (artificial stabilisation strain energy) should be less than 5% of the total strain energy.

- Distribution of the contact pressure should be uniform without any peaks and valleys ensures
- The ratio of contact damping pressure to the contact pressure should be low

It was observed that the **FE methodology developed in this chapter to solve a highly nonlinear problem using implicit formulation yields a 'converged' solution, which satisfies all the quality checks.**

Going further, an exercise to reduce the CPU time was performed for the case-study undertaken, which yields following

- Adjust the initial load increment based on convergence history.
- 'Quasi-Newton with BFGS updates' technique is recommended by this research to reduce the CPU time.
- The imbalance of memory in LSDYNA (i.e. 'memory1' and 'memory2') causes an imbalance in the intensive computational during linear algebra phase. Therefore balanced memory settings (only 'memory1') should be used for implicit calculations.

5 EXPLICIT DYNAMIC INTEGRATION FOR A QUASI-STATIC ANALYSIS

In Chapter 4, FE methodology to obtain a converged solution by implicit formulation, for 'Downward 8.6g' load applied to the 'Sleep seat' in accordance with CS25.561, was developed, implemented and verified. However, as the size and complexity of nonlinear problem increases (e.g. 'Forward 9g' loadcase demands use of body blocks and seat belts), implicit solution algorithms face the problems of huge amount of efforts required to build FE model (particularly at the contact interfaces so that they are in initial contact before the solution begins) and in many cases offer non-convergent solutions. Therefore, the explicit dynamic algorithm, which can handle large FE models with all the non-linearities and does not face convergence problems, is an attractive option for such kind of quasi-static problems. It is often less expensive computationally and more reliable than an implicit quasi-static solution technique [33].

Therefore, in this chapter methodology to simulate the static inertia loads (CS25.561) applied to the seat-structure using explicit dynamic integration has been developed and applied to solve the 'Downward 8.6g' loadcase (a case study solved in Chapter 4 using implicit formulation). In addition, a section of this chapter is devoted to demonstrate FE quality checks that must be performed to ensure a quasi-static finish when an explicit formulation is applied to solve the static/ quasi-static problems.

5.1 USE OF EXPLICIT FORMULATION FOR QUASI-STATIC PROBLEM – A LITERATURE REVIEW

Literature review has been performed considering a seat-structure has

- Large number of nonlinear contacts
- Bolted connections
- Large deformations (similar to processes such as hot rolling, hydroforming etc.)

One of the early areas in which, the codes based on explicit time integration were successfully used to simulate basically quasi-static process, was the sheet

metal stamping process. One of the first successful attempts to apply this technique for the deep drawing of a hemispherical cup and automobile radiator top was demonstrated by Honecker and Mattiasson in 1989 [46, 47, 48]. Because of robustness of the technique and its suitability for large scale problems, it was widely used for the metal forming simulations. For a medium-sized sheet metal forming process, Rebelo et al found that the explicit method was about ten times faster than the implicit one [40]. For a larger problem the difference is even more pronounced.

In metal forming processes, work-piece is formed between displacement-controlled rigid tools, making it easier in the FE simulations to control the unwanted inertia effects through prescribed displacement or velocity. However, in the evaluation of the structural performance of the seat, where prescribed forces are applied, stiffness of the structure (undergoing plastic deformations), changes considerably during the loading. This often leads to the uncontrollable accelerations and velocities making it quite challenging to have quasi-static finish [40]. Adaptive loading procedure, in which the loading rate is adapted to meet the target prescribed velocity-norm as a function of time, is proposed by Mattiasson to solve the force-driven, quasi-static problems by the means of explicit dynamic algorithm [40]. The usefulness of this method is demonstrated for drawing and hydroforming simulations. However, the algorithm involves lot of numerical parameters to control and several attempts are required to arrive at the optimised values of these parameters for the best performance and hence not been further explored in present research.

Yu et al. used explicit dynamic solution scheme to analyse the bolted steel connection subjected to combination of shear, tension and bending (complicated loading condition) at an ambient and elevated temperatures. The authors have compared the explicit FEA results with those from implicit and the test and have found good-correlation [41].

Xu et al. used an explicit dynamic FE programme called LSDYNA to evaluate the performance of a “Child restraint anchorage system” used in the automobile seat structure (Regulation used – FMVSS225) [42]. Experimental procedures

mandated to satisfy the FMVSS225 requirements are essentially static in nature. The authors averaged the response (i.e. displacement for their case) at 100% of the load and the final stabilised value and compared it with that from the physical testing. They found good co-relation thereby demonstrating the usefulness of explicit dynamic integration scheme for solving quasi-static problems.

Other areas in which explicit algorithm is used to solve highly nonlinear and complex quasi-static processes are

- Hot ring rolling process [43].
- Tubular hydroforming process [36]
- Bending of a mobile phone [37]

Patwardhan et al. have chosen LSDYNA, an explicit dynamic code to simulate the quasi-static loadcase FMVSS 207/210 that is applicable to automotive seating systems. The authors have considered the effect of, mass and boundary conditions of body blocks and element formulations and mechanical properties of seat belt, on the solution. They could obtain reliable results, which correlated well with those from physical testing [38].

Hessenberger et al. has simulated FMVSS210 for the driver cab using Abaqus (Research) 6.9-3 (implicit) and LSDYNA (explicit). The authors encountered problems such as local instabilities due to large deformations, very small load increments leading to high CPU times and considerable effort to define all the interface definitions with implicit formulation. With carefully chosen load application procedure the authors could achieve a balanced solution state with explicit formulation and observed good correlation between LSDYNA simulations and the tests. The authors recommend using explicit formulation to simulate such loadcases to save the overall time for modelling, simulation and correction [39].

Though the above examples show the different applications of technique of using ‘Explicit formulation for a quasi-static problem’, they do not discuss the methodology used and quality checks performed in detail. This report presents

a general methodology developed that is useful to evaluate a structural performance of seats (aircraft or automobile) and other components subjected to complex static loading conditions. In addition, a detailed framework to assess the reliability of results obtained with such a technique has been presented.

5.2 ADVANTAGES OF EXPLICIT FORMULATION FOR QUASI-STATIC PROBLEM

Advantages of using an explicit dynamic solution scheme for solving a complicated quasi-static problem are

- ✓ The greater ease with which complicated contact conditions are resolved [33]. Implicit algorithm continues to iterate till severe discontinuities (open-close changes in contact and stick-slip changes in friction) are within the tolerance and equilibrium tolerances (ensuring force and moment equilibrium) are satisfied. If the contact pairs are not in initial touching contact, the model encounters zero stiffness (rigid body motion) leading to a numerical singularity. For the FE model of the seat structure undergoing conceptual design iterations(therefore new discretisation for each iteration), involving more than forty contact pairs and subjected to complex loading conditions (so that the pattern of the initial slip directions is not clear), it is not possible to bring all the contact pairs in the initial contact. Such a FE model with weakly determined contact conditions propagates into excessive severe discontinuity iterations and either fails to initialise or find a converged solution.

  In Explicit algorithm, contact changes are treated as kinematic constraints so that after the completion of an increment, displacements and velocities of the nodes involved in contact are adjusted to be kinematically correct [40]. Further, size of the time increment is only dependent on element dimensions and material properties and not on the complexity of the analysis. Hence solution time is generally not affected by complex contact conditions thereby saving CPU time and need to check for convergence [40].

- ✓ In explicit method, the computational cost is proportional to the number of elements and roughly inversely proportional to the smallest characteristic length in the FE model [41, 43]. Therefore mesh refinement increases the computational cost e.g. if a three-dimensional FE model with uniform, square elements is refined by a factor of two in all the directions, computational cost would increase by a factor 2^3 (as a result of increase in number of elements) and by a factor of 2^1 (as a result of the decrease in the dimension of the smallest element). Therefore the total computational cost of the analysis would increase by a factor of 2^4. Disk space and memory requirements are directly proportional to the number of elements and are independent of element dimensions; thus these requirements would go up by a factor of 2^3 [41, 43]. Hence predicting the increase in computational cost with the mesh refinement is straightforward for the explicit procedure. However, cost is more difficult to predict for an implicit method since it arises from a problem dependent relationship between element connectivity and complex non-linearities. Literature shows that for many problems solved using implicit method; computational cost is roughly proportional to the square of the number of degrees of freedom [33]. Thus the mesh refinement by a factor of two in all the directions increases the number of degrees of freedom by approximately 2^3, causing increase in the computational cost by a factor of roughly $(2^3)^2$. Though the actual increment in the disk space and memory requirements is difficult to predict, it increases roughly in the same manner. For a relatively uniform mesh, explicit method exhibits great cost savings (computational cost, disk space and memory requirements) over the implicit method as the FE model size increases [41, 48].
- ✓ For the same simulation, explicit procedure requires much less disk space and memory than that required by the implicit procedure [40].
- ✓ For certain quasi-static problems such as seat structures subjected to loads using body blocks, implicit solution schemes require large number of iterations to find a converged solution. Each of these iterations

involves larger wavefronts. Convergence difficulties lead to more iterations per increment and reduced increment size resulting in, huge memory requirements and higher computational costs and time. For the same quasi-static problems, explicit dynamic integration scheme determines the solution by explicitly advancing the kinematic state from the end of previous increment. Even though analysis may require a large number of small time increments, it can be more efficient than that with implicit scheme, which requires many iterations [43].

- ✓ In terms of ease of use, explicit algorithm often continues to produce the results even if the analysis has encountered into difficulties such as failed contact pairs. This makes it lot easier for the analyst to diagnose the root cause of the abruptly terminated analysis. In implicit algorithm, considerable efforts are required to read through the system generated message files and locate the cause of the failure.

To conclude, Inherent lack of convergence problem is the main advantage of explicit FE techniques.

5.3 CHALLENGES IN APPLYING EXPLICIT FORMULATION FOR QUASI-STATIC PROBLEM

Core objective of the explicit solution method is to model high-speed impact events in which the inertia plays a dominant role in the solution [31-33, 35]. Out-of-balance forces are propagated as stress waves (for a structural problem) in the neighbouring elements while solving for the dynamic equilibrium. Therefore, the challenges in applying the explicit dynamic procedure to quasi-static problems are

5.3.1 COMPUTATIONAL ECONOMY

By definition, it is safe to perform a quasi-static process in its natural time-scale i.e. the actual time taken for a physical process, so that the velocities are zero at the conclusion of analysis. In the static analysis, the lowest structural mode dominates the response [32]. Hence, the knowledge of the frequency and corresponding period of the lowest mode helps to estimate the time required to

obtain a pure static response. Natural frequencies and corresponding mode shapes are estimated using Modal analysis. As a ‘thumb rule’, simulation time should be at least ten to fifty times larger than the period of the first mode [33].

To illustrate, consider a simulation of ‘Downward 8.6g’ load applied to the ‘triple’ seat structure (same FE model solved using implicit formulation in Section 4.4). The frequency of the first mode (when bottom surface of the seat-track is restrained for all dofs) is approximately 17Hz. Therefore, the simulation time should be at least 0.80s (100% load achieved in 0.60s using ‘thumb rule’ and a holding time approximately 0.20s). Minimum stable time increment calculated by LSDYNA code is approximately 1.935E-7s [35].

The number of time-steps required to complete this loadcase would be (considering the minimum stable time increment remains same throughout the simulation) over 4 million. As an illustration, the time required for 5000 time-steps using 16 processors (on High Performance Computing facility at Cranfield University) is approximately 266s.

Thus the total Computational time (CPU time) required to accomplish this solution would be approximately 62hours! It is impractical to have such long solution times during the conceptual design phase.

5.3.2 MINIMUM CONTRIBUTION FROM DYNAMIC EFFECTS

To obtain an economical solution, the event needs to be accelerated in some way. Such a numerical acceleration causes static equilibrium to evolve into the state of dynamic equilibrium, in which solution is dominated by inertial forces (unphysical and undesirable effect). The characteristics of the scheme of applying an explicit algorithm for solving a quasi-static problem are summarised in Figure 5-1.

Characteristics of Explicit Formulation for solving a Quasi-Static problem

Advantages

- ✓ **Inherent lack of Convergence**
- ✓ **Easy handling of complex contact conditions**

Challenges	Solutions	Checks
Achieving Realistic Computational time	**Improve the minimum stable time increment by** ➢ **Optimum mesh density** ➢ **Mass scaling** **Artificially accelerate the event by** ➢ **Time Scaling**	✓ **Sufficient number of elements along contact interface** ✓ **KE/IE < 5%** ✓ **Loading reflected in time histories of KE and IE**
Controlling unwanted inertia effects	**Damp-out the unwanted vibrations**	✓ **Damping applied to dominant eigenmodes** ✓ **Damping inactive during rigid body modes**

Figure 5-1 Advantages, challenges, probable solutions and quality checks while applying an explicit algorithm for solving a quasi-static problem

Therefore the goal is to model the Quasi-static process using an explicit dynamic integration scheme in the shortest time period with negligible inertia forces.

5.4 METHODOLOGY TO OVERCOME CHALLENGES

The computer time involved in running a simulation with explicit time integration scheme is [31-33, 35]

a) Directly proportional to the size of the FE model
b) Inversely proportional to the minimum stable time increment
c) Directly proportional to the time period of the loading process

In case of an aircraft seat-structure, consideration of the major load carrying members and their interaction results in the large three-dimensional FE model

and little can be done to reduce the size so as to have a significant impact on run time.

If the minimum stable size increment is increased, total number of increments required to reach the termination time reduces and hence the simulation time reduces. The minimum stable size increment depends on the characteristic length of the smallest element in the model and the material density.

In case of the “Sleep Seat”, the optimum element size for each of the components has been established through “Mesh Sensitivity Study” i.e. the maximum element size which balances the optimum CPU time and an acceptable solution and therefore the possibility of further coarsening the discretisation and thereby reducing the simulation time is minimal.

To conclude, to speed up the simulation, either time period of the event, T should be artificially reduced and/or material density should be increased.

5.4.1 ARTIFICIALLY SCALING THE RATE OF LOADING TO SHORTEN THE SIMULATION TIME

Application of loads over shorter period of time than that of actual process is called as “Load factoring” or “Scaling of the Loading rate” or “Time Scaling”. A good initial estimate of how much the load rate can be increased may be gained by the examination of the structural response of the component and by limiting the ratio of Kinetic Energy (KE) to Internal Energy (IE) less than 5% [33]. There is no clear guideline available to confirm this figure and hence the judgement depends on the experience of the analyst. The advantage of this method is that the mass properties of the structure are unchanged so that the mass dependent loads and body forces need not be factored [40]. Limitation of this method is that it cannot be directly applied to the analysis involving rate-sensitive constitutive theories as the duration of the analysis and the rate of loading is altered due to the speeding up the analysis [33].

If speed of the process is increased too much, resultant velocity of the components may raise the KE to the same order as that of the strain energy or work done [40]. These undesirable inertia effects (for a quasi-static simulation)

can be very high thereby predicting an erroneous response and contact stability may be affected due to noisy oscillations leading to the complete failure of the simulation. Therefore, time period should be reduced sensibly.

The approach to determine an acceptable simulation time is to run series of analyses with various termination times in the order of smallest to largest, since the solution time is directly proportional to the termination time. Examination of the results such as variation of the KE, IE, and their ratio, recovery of reaction forces and overall behaviour of the structure are some of the indicators to find the “Golden mean” between speeding up the analysis and still obtaining an acceptable static solution using an explicit direct integration scheme. Starting with the shortest termination time and increase it from there; at some point, the solutions will become similar for two consecutive termination times; indicating that the solutions are converging on a quasi-static solution.

5.4.1.1 GRADUALLY RAMPING THE LOAD AND HOLDING IT CONSTANT

For a quasi-static solution with explicit dynamic integration scheme the load should be increased gradually and held constant for some time so as to achieve a response close to the static response [47, 48].

5.4.2 SCALING THE MASS OF THE STRUCTURE TO INCREASE STABLE TIME INCREMENT

The key to the computational efficiency and accuracy of the explicit dynamic procedure is the use of discrete mass matrix used in the equilibrium equations [39]. Hinging on this provision, the other possible equivalent to “Time Scaling” would be to use a technique known as “Mass Scaling”. It involves artificially increasing the material density ρ, which decreases the elastic sound speed and increases the stable time increment. As the global stability limit is increased, fewer increments are required to perform the same analysis thereby reducing the cost of the solution.

The advantage of the mass scaling technique is that the rate at which the material is loaded is not affected by the changes in the mass density [40]. This allows inclusion of the rate-dependent materials and any other rate-dependent

components such as dashpots in the analysis [33, 48]. Due to increase in the minimum stable time increment, natural time period can be preserved.

Though mass scaling is an attractive option to treat the quasi-static problems effectively, its influence on the inertial effects is exactly the same as artificially increasing the loading rate. The only difference to the approach is that the speed-up as a result of mass scaling is the square root of the mass scaling factor, whereas the speed-up due to the scaling of the loading rate is proportional to the load rate scale factor.

5.4.3 INTER-RELATION BETWEEN "MASS SCALING" AND "NATURAL TIME PERIOD"

Mass scaling helps to increase minimum stable time increment. However, increase in mass decreases frequency of first mode thereby increasing the natural time period and hence the simulation time! This may either nullify the resultant effect of mass scaling (due to increased simulation time) or introduce inertia effects (if the simulation time is kept constant as that for model without mass scaling).

Hence use of 'Mass scaling' and 'Time Scaling' requires lot of trial and error simulations to derive the suitable scaling factors to achieve a solution with maximum efficiency and reasonable confidence in the results.

5.4.4 DAMPING TO ELIMINATE UNWANTED VIBRATIONS

For simulating the effect of static loads applied to the "Sleep Seat" according to CS 25.561 using explicit dynamic integration scheme, both the methods i.e. 'Mass scaling' and 'Time scaling' are used in combination to obtain a computationally economical solution. This generates a need to develop a procedure for eliminating undesirable and non-physical inertia effects; due to sudden application of force.

One method is to use dynamic relaxation in which all the nodal velocities are factored by a number less than but close to unity at the end of every time increment [33, 35, 48]. It removes the KE from the model by reducing the

velocity of every node in succession. However, it can be used only to initialise a system to a prescribed geometry or for applying a preload which produces only small elastic strains. For the seat structures undergoing large deformations and rotations, this method cannot be used [35].

Damping dissipates the energy gradually diminishing the amplitude of oscillations. The amount of damping depends on the velocity of motion, frequency of vibration and material. If the fictitious system damping matrix is applied globally to structure and displacements are computed as a function of time, the method amounts to immersing the structure in a viscous fluid, which damps strong geometric nonlinearities such as sudden excitation of the lower modes ensuring a desired quasi-static finish [32].

Thus the solution of a quasi-static problem using explicit dynamic algorithm.is treated as a solution of the critically damped dynamic system. Therefore the problem is to find the dominant eigenvalue in the structure related to the “pseudo-dynamic” response of the structure for the applied static load and then estimate the appropriate amount of frequency dependent damping.

5.4.4.1 METHOD TO ESTIMATE THE CORRECT DAMPING FACTOR

For the structures subjected to the less rapid process (such as application of static loads according to CS25.561), most of the KE resides in the lower eigen-frequency domain [32, 33, 49]. Since frequency dependent damping is required; Rayleigh’s damping also known as viscous damping or proportional damping; is appropriate option to use [32]. Energy dissipated per cycle is proportional to the frequency and to the square of amplitude.

For Quasi-static problems solved using Rayleigh damping, the damping matrix ([C]) is expressed as a linear combination of the mass matrix ([M]) and stiffness matrices ([K]) [32, 35]:

$$[C] = \alpha^*[M] + \beta^*[K] \qquad \textbf{Equation 5-1}$$

$$\xi = \tfrac{1}{2}^*((\alpha/\omega) + \beta\omega) \qquad \textbf{Equation 5-2}$$

where,

α is mass proportional Rayleigh damping coefficient

β is stiffness proportional Rayleigh damping coefficient

ξ is critical damping factor

ω, 2π f angular velocity, f is the frequency of first mode (in the present case)

α[M] contribution damps predominantly lowest modes, while β[K] contribution damps highest modes heavily. Since solution of a quasi-static problem using explicit central difference scheme requires

- ✓ a critically damped dynamic system i.e. ξ = 1
- ✓ damping of only lowest mode i.e. consideration of only α[M] and ignoring β[K]

Therefore Equation 5-2 becomes,

1 = ½*(α/ω)

α=2*ω

α=4*π*f **Equation 5-3**

Thus the appropriate amount of damping factor required to damp the unwanted vibration effects induced in a quasi-static analysis is 4π times the frequency of first eigen-mode (or lower dominant eigen mode).

In present analysis, LSDYNA explicit formulation code has been used for this study. For standard nonlinear analysis, LS-DYNA implements “Rayleigh damping” at element level [35]. This is done for numerical convenience, since in the explicit method, internal forces are generated by integrating stresses over the element area and not using stiffness matrix [K]. Mass damping in LS-DYNA, which includes *DAMPING_GLOBAL and *DAMPING_PART_MASS, is intended to damp low-frequency structural modes but it has the added effect of damping rigid body modes [35].

Thus parts that undergo significant rigid body motion should either be excluded from mass damping OR the mass damping should be turned off during the time the part undergoes rigid body motion.

5.4.5 FLOWCHART TO USE EXPLICIT FORMULATION FOR SIMULATING AN QUASI-STATIC PROBLEM

Figure 5-2 summarises the major steps required to obtain a solution for an Quasi-static problem using an explicit dynamic integration scheme.

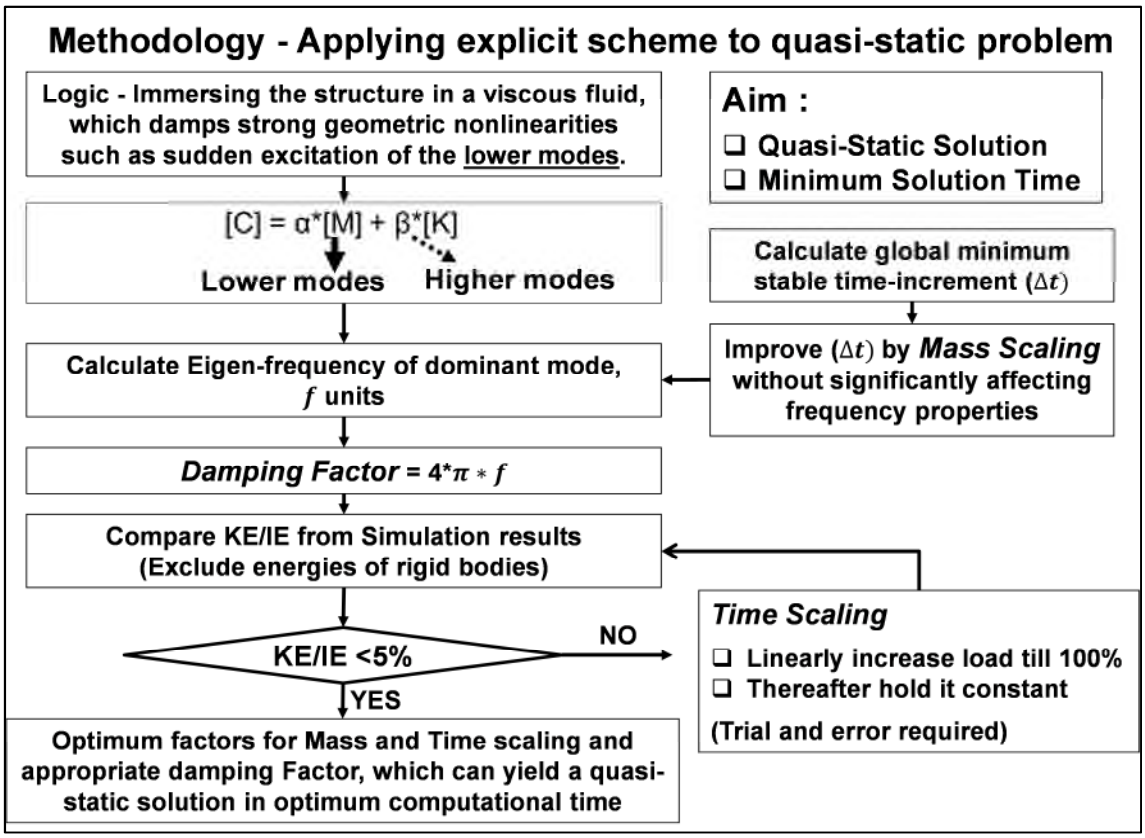

Figure 5-2 Flowchart summarising major steps required to obtain a solution for an Quasi-static problem using an explicit dynamic integration scheme along with results verification checks.

5.5 APPLICATION OF METHDOLOGY – 'DOWNWARD 8.6G'

The guidelines developed in earlier sections of this chapter have been 'put to test' for simulating 'Downward 8.6g' load applied to the FE model of the 'triple' Sleep-seat structure. The FE model, boundary conditions and material definitions used for this exercise are same as that used in Section 4.4, where implicit formulation is used to estimate the structural response of the seat.

5.5.1 MASS SCALING AND USE OF DT2MS

The mass of the seat structure is approximately 26kg and minimum stable time increment calculated by LSDYNA is 1.935E-7s. With this time-step, the time required to achieve a solution for the FE model under study would be approximately 62hours! (As explained in Section 5.3.1 of this chapter)

Therefore, it is important to improve the minimum stable time-step. To start with, the mass of the seat-structure has been uniformly scaled-up by a factor of '5'. This scaling factor is held constant through-out this research in order to control the unwanted inertia effects. This helped to improve the time-step to 3.543E-7s. However, as the frequency of the dominant mode (mode number II) is now 9.8Hz (17Hz without mass scaling); natural time-period to run quasi-static simulation would be approximately 1.2s (against 0.8s without mass scaling). Thus the total simulation time would be now 50 hours, which is still high!

The smallest time-step occurs in the tool-less fittings and then in seat-track. Both of these components are aerospace certified and hence are safe against the loads as specified in CS25.561 and CS25.562. These components could have been treated as rigid so as to bypass them during solution phase. However, in order to be consistent with the FE model solved using implicit formulation (Section 4.4), tool-less fitting and seat-track are considered to be deformable in this analysis.

In order to further improve the global compute time increment, DT2MS parameter from *CONTROL_TIMESTEP can be effectively used [42]. With DT2MS there are two possibilities [50-52],

- DT2MS < 0 (e.g. -1.11E-6s used for present simulation of 'Downward 8.6g load), LSDYNA add mass to each of the elements whose timestep is below IDT2MSI and ensures that element's updated time-step is equal to IDT2MSI.
- DT2MS > 0, LSDYNA add mass to each of the element whose timestep is below DT2MS and removes the mass from elements whose initial timestep is above DT2MS. This option has not been used in this research.

Care should be taken so as to have minimum effect of such 'adjustment' of global compute time-step (by addition of mass) on the solution accuracy. It is suggested to limit the percentage of added mass due to DT2MS to 5% [33]

For this simulation, the DT2MS has been set to -1.111E-6s, which gives a minimum stable time increment of approximately 1E-6s (1 microsecond). Note – For LSDYNA code, minimum stable time increment is a product of IDT2MSI and TSSFAC [35]. TSSFAC is a scale factor for time-step set to 0.90 for stability reasons. With a time-step of 1E-6s, the maximum percentage of added mass is 2.6 (Figure 5-3) and solution time with natural time-period would reduce from 50 hours to 18 hours (with same 16 processors).

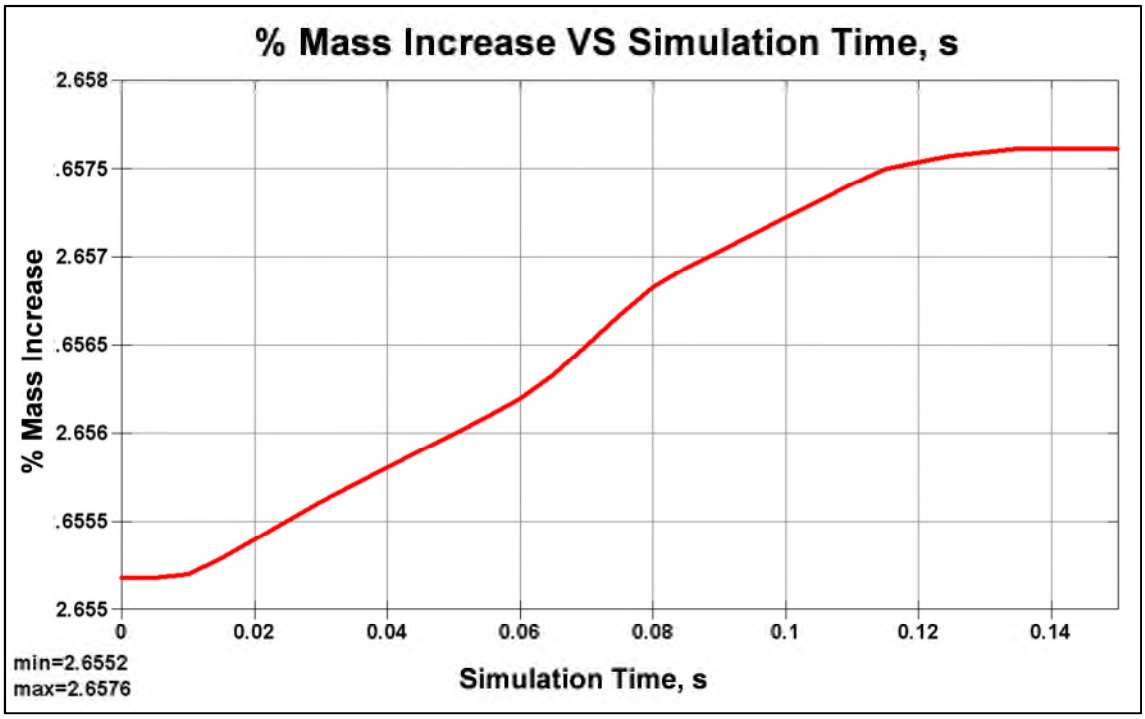

Figure 5-3 For a DT2MS specified as -1.11E-06s, maximum percentage of added mass is 2.66%, which is less than the allowable limit of 5% [33]. Thus effect of specifying DT2MS on solution accuracy and on frequency of first mode vibration of would be insignificant. However, the increase in global minimum time increment (due to DT2MS it becomes 1E-06s instead of 0.354E-6s) would be beneficial in reducing CPU time.

Further reduction in solution time is achieved using 'time-scaling' as explained in the section 5.5.3. Once the 'mass scaling' exercise has been accomplished next natural progression would be estimation of damping factor.

5.5.2 ESTIMATION OF DAMPING FACTOR

Initially, behaviour of the seat structure when subjected to 'Downward 8.6g' load using explicit scheme without damping has been studied. 100% load is linearly achieved (starting from 0N at 0s) in 0.1s and held constant for 0.05s thereafter. It can be observed from Figure 5-4 that the Kinetic Energy is a considerable proportion of Internal Energy indicating presence of high inertia effects (undesirable for a quasi-static solution).

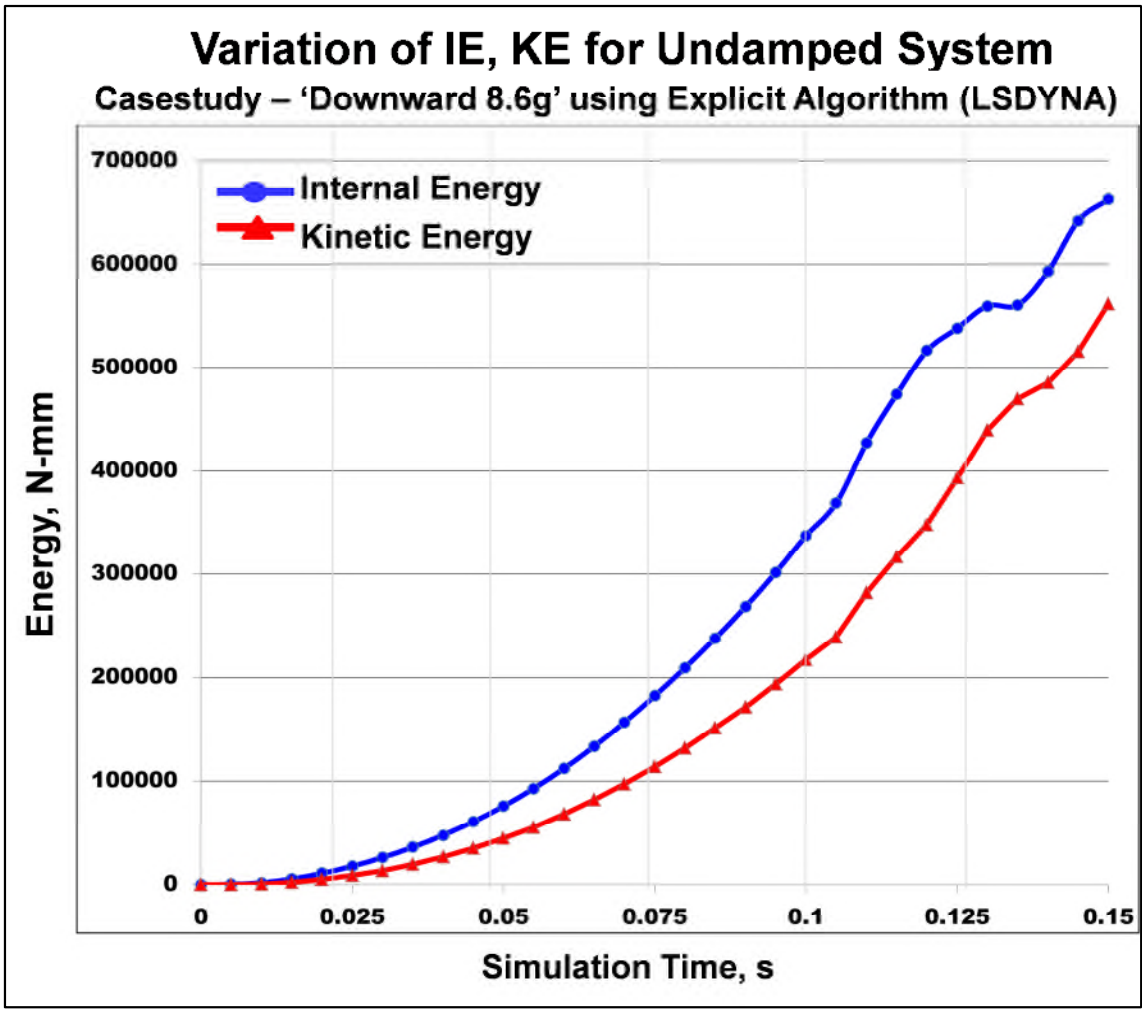

Figure 5-4 Time history of the Internal Energy (IE) and Kinetic Energy (KE) for the 'Downward 8.6g' load applied to the 'triple' seat-structure solved using explicit formulation (without any damping). Since KE is a considerable proportion of IE and continuously increasing, solution is not quasi-static.

Hence, estimation of the correct damping factor to critically damp the unwanted vibrations induced due to the sudden application of 'Downward 8.6' load is necessary. The procedure outlined in Figure 5-2 for estimating such a damping factor is demonstrated in following paragraphs.

To perform an eigenvalue analysis using LSDYNA following procedure should be adopted,

- Activate the implicit method by specifying IMFLAG equal to '1' on *CONTROL_IMPLICIT_GENERAL and

- Specify number of eigenvalues to extract under NEIG on *CONTROL_IMPLICIT_EIGENVALUE [35]

LSDYNA uses ‘Block Shift and Invert Lanczos’ code from ‘Boeing’s Extreme Mathematical Library’ to extract the eigenvalues, which are automatically written to an auxiliary binary database called ‘D3EIGV’ [35]. This file can be opened using LSPRE-POST to view eigenvalues and corresponding mode shapes. A summary of eigenvalue analysis is printed to ‘eigout’ file.

The computational time required for calculating the three mode shapes and corresponding eigen-frequencies is 83s with 8 processors. Observing Figure 5-4, sudden application of downward loads would activate mode shape ‘2’. Hence, this frequency needs to be critically damped to achieve a quasi-static finish for the ‘Downward 8.6g’ loadcase simulated using explicit time integration scheme.

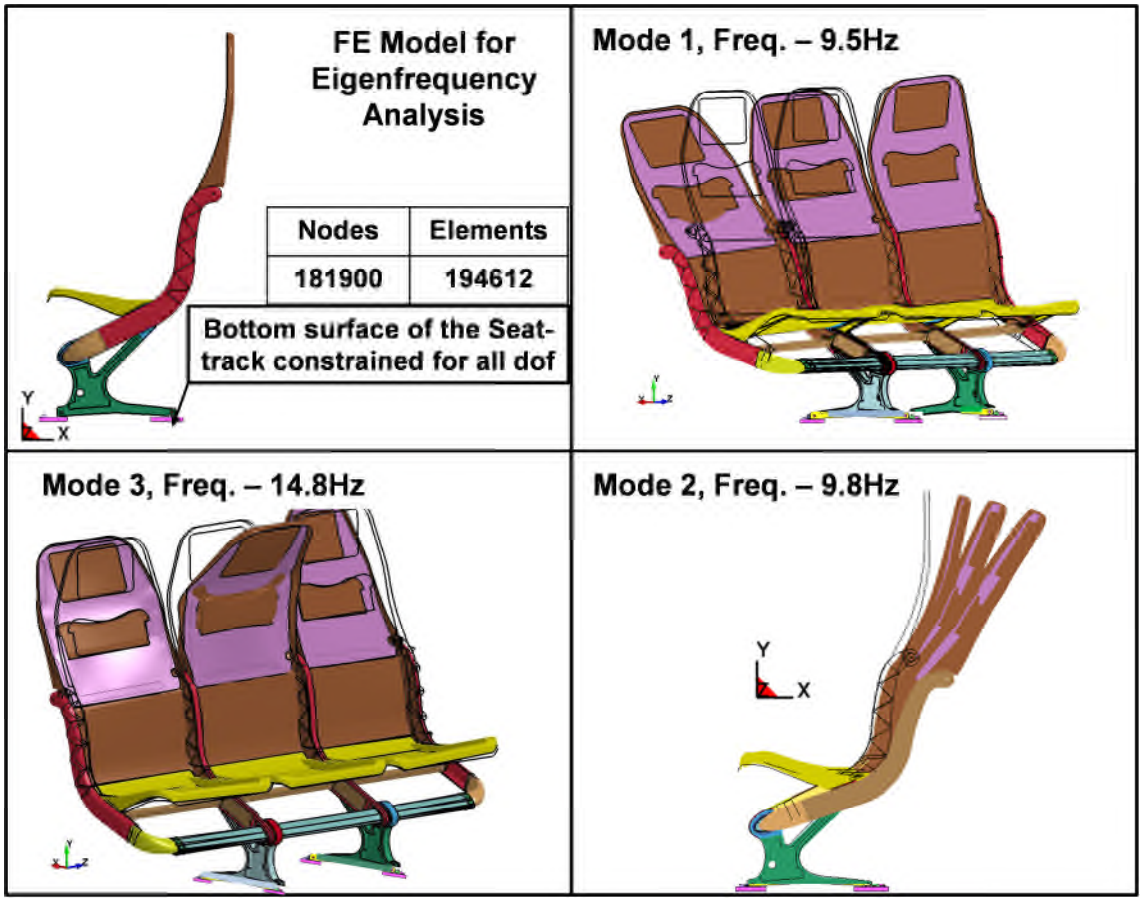

Figure 5-5 FE set for Eigenfrequency analysis of triple seat structure. Bottom surface of the seat-track is constrained for all dofs. The mode shape (2) corresponding eigen-frequency of 9.8Hz (bending about lateral axis i.e. Z) may be activated due to sudden application of downward loads. Hence, this frequency needs to be damped to achieve a quasi-static solution for 'Downward 8.6g 'loadcase using an explicit formulation.

Using Equation 5-3, damping factor (VALDMP) required for 'Downward 8.6g' loadcase simulation can be calculated as 123units, which is set to 150 considering the changes in stiffness due to applied 'Downward 8.6g' load.

5.5.3 TIME SCALING TO LIMIT CPU TIME

Natural time-period to accomplish the simulation of 'Downward 8.6g' load applied to the seat-structure using explicit time integration would be approximately 1.3s, which can be calculated as follows,

- For a seat-structure under study (uniformly mass scaled by 5) dominant eigenmode, which would be activated for the applied 'Downward 8.6g' load, is approximately 9.8Hz. Corresponding time period is 0.1s.
- According to the 'thumb rule', simulation time should be at least 10 times of period of dominant eigenmode [35].
- Hence, 100% load should be achieved in 1s or more and then should be held constant for some time (say 0.3s) to stabilise the response. Such a loading process spread over 1.3s would yield a quasi-static solution.

However, with a time-step of 1E-6s, CPU time would be approximately 19 hours with 16 processors (for the FE model considered for this study, 5000 time increments take approximately 266s), which is very high. The only option remaining (after mass scaling and use of DT2MS) is 'time scaling' i.e. accelerating the loading process as discussed in Section 5.4.1 and holding the load constant for some time period to stabilise the response.

Four different simulations are performed with difference in time for achieving 100% load and holding constant load then after are studied in this research (Table 5-1). FE model (same as that used in Section 4.4), boundary conditions, uniform mass scaling factor (5), and DT2MS (-1.2E-7s) used is same for all the four simulations. Those are run on 16 processors with same memory settings and same damping factor i.e. VALDMP 150. Table 5-1 shows different time-periods used for simulations and corresponding CPU times required. Figure 5-5 plots KE time-history of all the four simulations. Please note that IE for four simulations performed are not plotted in Figure 5-5 so as to easily visualise the differences in KE. The parameter used for comparison is the maximum ratio of KE to IE ($(KE/IE)_{MAX}$), which indicates a quasi-static finish.

Serial Number	Time to achieve 100% load, s	Time for which load is held constant, s	Total simulation time, s	CPU Time, s
A	0.03	0.015	0.045	2334
B	0.06	0.03	0.09	4688
C	0.10	0.05	0.15	7821
D	0.15	0.05	0.20	10400

Table 5-1 Three different time increment schemes used to solve the 'Downward 8.6g' load applied to the 'triple' seat-structure are explained and computaional time is compared.

It can be observed from Table 5-1 and Figure 5-5 that

- Simulation A required 2334s of CPU time. However, $(KE/IE)_{MAX}$ is approximately 7%, indicating presence of high amount of inertia effects. This shows that both the ‘load increment time’ and ‘constant load time’ should be increased to achieve a quasi-static finish.
- Simulation B required 4688s of CPU time. Though the KE approximately follows the loading sequence, $(KE/IE)_{MAX}$ is approximately 5.6%, which is above the allowable limit of 5%.
- Using learning from simulation A and B, 100% load is achieved in 0.1s and then after held constant for 0.05s for Simulation C. This simulation took just over two hours.
  - $(KE/IE)_{MAX}$ is approximately 1.3% indicating insignificant inertia effects.
  - Further, KE does not increase i.e. it stabilise when the load is held constant indicating that the structural is in static equilibrium.

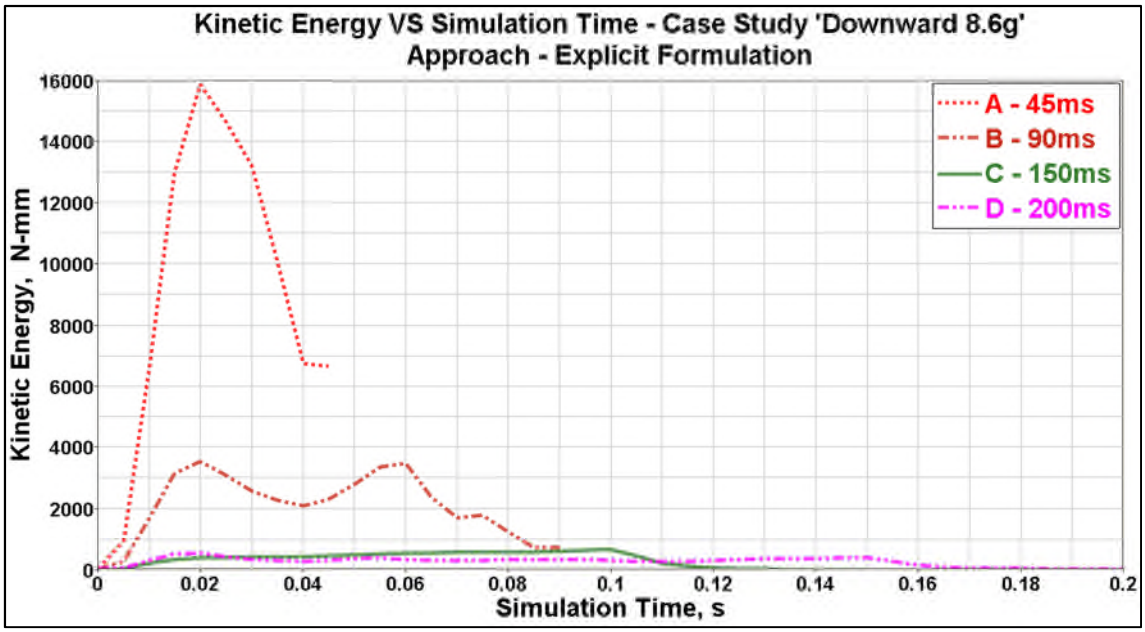

Figure 5-6 Kinetic Energy, N-mm VS Simulation Time, s plots for four different simulations (A, B, C and D explained in Table 5-1). Case Study 'Downward 8.6g' applied to the 'triple' seat-structure solved using explicit formulation. Simulation scheme C gives acceptable quasi-static solution with reasonable CPU time.

- In Simulation D, 100% load is achieved in 0.15s and then after held constant for 0.05s so that the total simulation time is 0.2s.
  - $(KE/IE)_{MAX}$ is approximately 0.9%. KE stabilises when the load is held constant.
  - However, the CPU time for this loading procedure is approximately 10400s (33% increment over that of Simulation C).

Note - For all the cases, maximum percentage ratio of added mass (due to DT2MS) to original seat mass (i.e. seat mass scaled-up uniformly by a factor of 5) is approximately 2.6%.

Considering the foregoing discussion, loading procedure used in simulation 'C' i.e. achieve 100% load in 0.1s and hold it constant for another 0.05s; is identified as an 'optimal' procedure to simulate the 'Downward 8.6g' load applied to the present design of the 'triple' seat-structure using an explicit time integration scheme.

The displacement and stress results obtained by this method and CPU time and disc-space required are compared with those from other methods as well as with results of experimental testing in Chapter 6. In coming sections of present chapter, a framework to verify the quality these FEA results has been developed and demonstrated.

5.6 FRAMEWORK FOR VERIFICATION OF FEA RESULTS

Stress and deformed shape of the seat structure are of ultimate interest of this simulation. However, before in-depth interpretation of the FEA results, a scaled-up displacement plot for the structure should be animated and thoroughly checked for any missing contact definition, untied regions, missing boundary conditions and hour-glassing. Upon satisfactory visual check, the results should be considered for next assessment.

Another must check for a quasi-static problem solved using explicit formulation is, to ensure that the solution is nearly static. In the absence of experimental test data, the most logical and common way to evaluate the appropriateness of the quasi-static response is careful examination of the various model energies.

5.6.1 FORCE EQUILIBRIUM CHECK

The total downward force (F_Y) applied for triple Occupancy is equal to

Mass considered per Seat ~ 111kg

Downward acceleration considered = 8.6 times gravitational force

Therefore, applied force in vertically downward direction,

$F_Y = 111*9.81*8.6*3$

~ 28093.88N

The reaction force in vertical direction is approximately 28057.1N. Therefore the solution satisfies force equilibrium check (Figure 5-6). The procedure to extract a reaction force for a LSDYNA simulation has been explained in Appendix D.1.

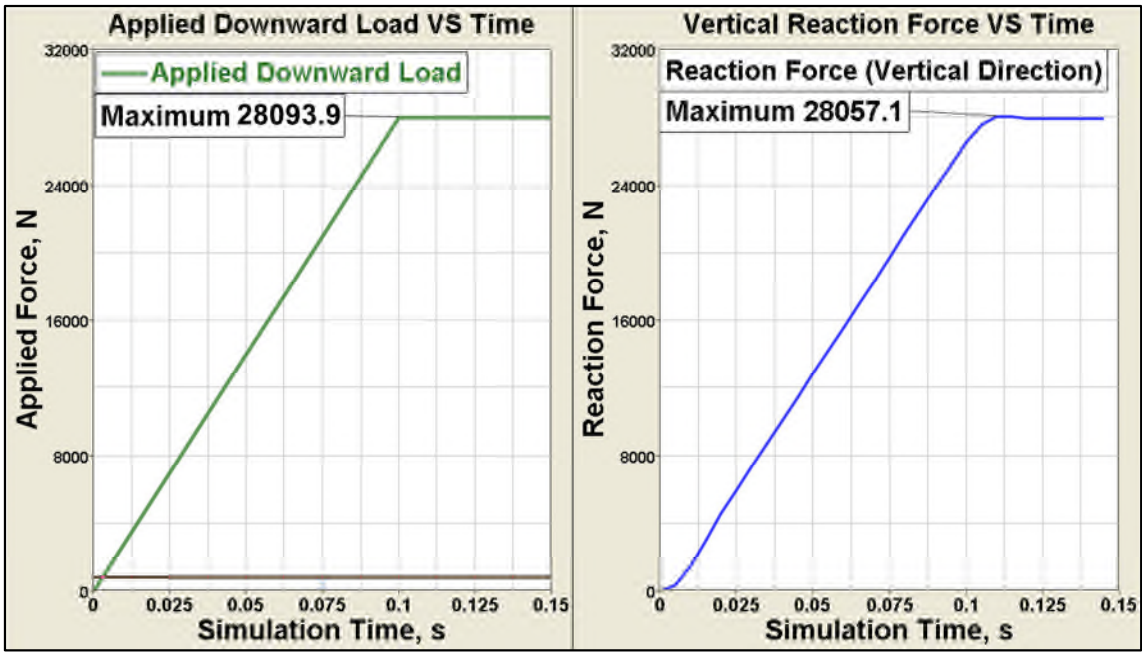

Figure 5-7 The 'Downward 8.6g' loadcase solved using LSDYNA/Explicit code satisfies the reaction force equilibrium check.

A major pitfall of using explicit dynamic algorithm to simulate quasi-static problem is that post-failure resistance of the structure may be over-estimated as inertial force balances the applied load. However, for a static solution, upon failure of the structure, discontinuity is developed in the load path and loads are not transferred to the boundary and reaction force show the corresponding drop. Hence, force equilibrium check must be performed.

5.6.2 ENERGY BALANCE CHECK

The energy balance for the explicit direct integration is given by [35]

Where,

$$E_{int} + E_{ifs} + E_{damp} + E_{kin} + E_{hrg} = W_{ext} + E^{0}_{int} + E^{0}_{kin} \qquad \textbf{Equation 5-4}$$

E_{int} is current IE

E_{ifs} is current dissipated sliding energy due to contact

E_{damp} is current dissipated damping energy

E_{kin} is current KE

E_{hrg} is current hourglass energy

W_{ext} Is work done by externally applied forces

E^0_{int} is initial IE

E^0_{kin} is initial KE

Total Energy = $E_{int} + E_{ifs} + E_{damp} + E_{kin} + E_{hrg}$ i.e. RHS of Equation 5-13

Initial Total Energy + External Work = $E^0_{int} + E^0_{kin}$ i.e. LHS of Equation 5-13

Energy ratio also known as 'Energy balance'; is defined as the ratio of the 'Total energy' to the sum of 'Initial Total Energy' and 'External Work done'. If the energy balance is not equal to 'Unity (1)' then FE results should be suspected with an error [37]. If it is greater than unity then energy is being introduced artificially in the model for example either by a numerical instability or by a sudden detection of an artificial penetration through a contact segment. An energy balance less than a unity indicates that the energy is being artificially absorbed either by excessive hour-glassing or for stabilisation of ill conditioned contact surface [35, 53, 54]. 'Downward 8.6g' loadcase solved using LSDYNA/Explicit code satisfies the energy balance check (Figure 5-7)

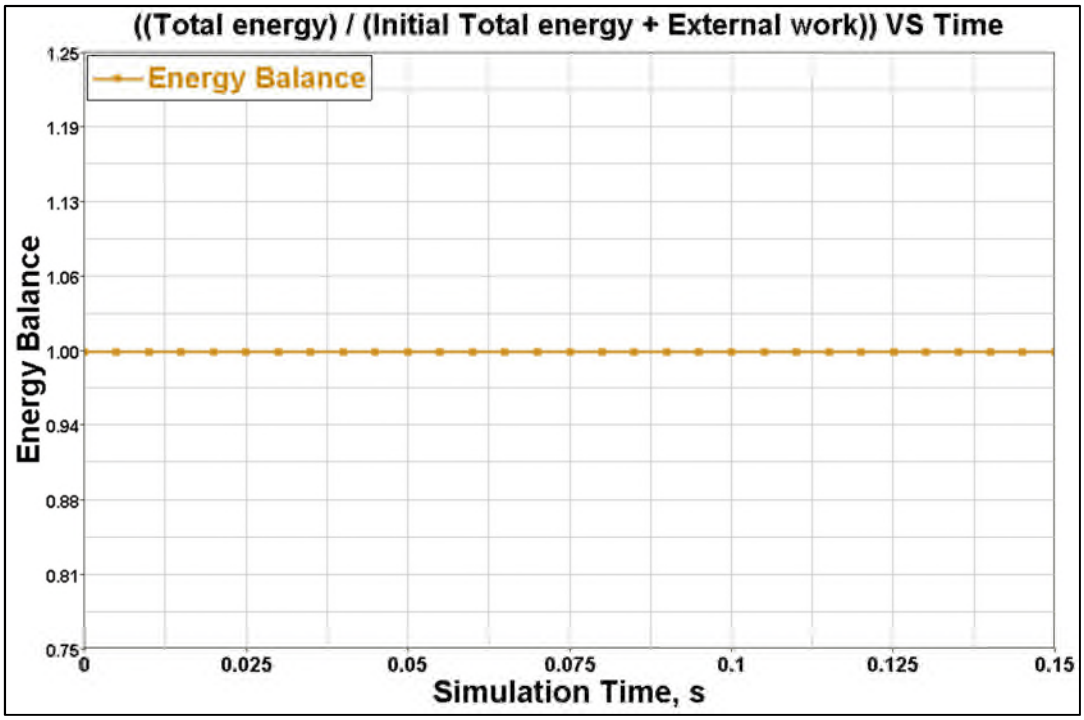

Figure 5-8 'Downward 8.6g' loadcase solved using LSDYNA/Explicit code satisfies the energy balance check i.e. Energy balance = 1 [35]

5.6.3 RATIO OF KINETIC ENERGY TO INTERNAL ENERGY

As the inertial forces are negligible in a quasi-static analysis, the Kinetic Energy (KE) of the deforming material should not exceed a small fraction (typically maximum limit 5% to 10%) of its Internal Energy (IE) throughout most of the process [33, 40-46, 54]. The ratio of KE to IE should be less than 0.1% at the steady state [33].

For a meaningful comparison between the KE to IE, energies associated with any rigid bodies with mass should not be considered as only deformable bodies are of interest.

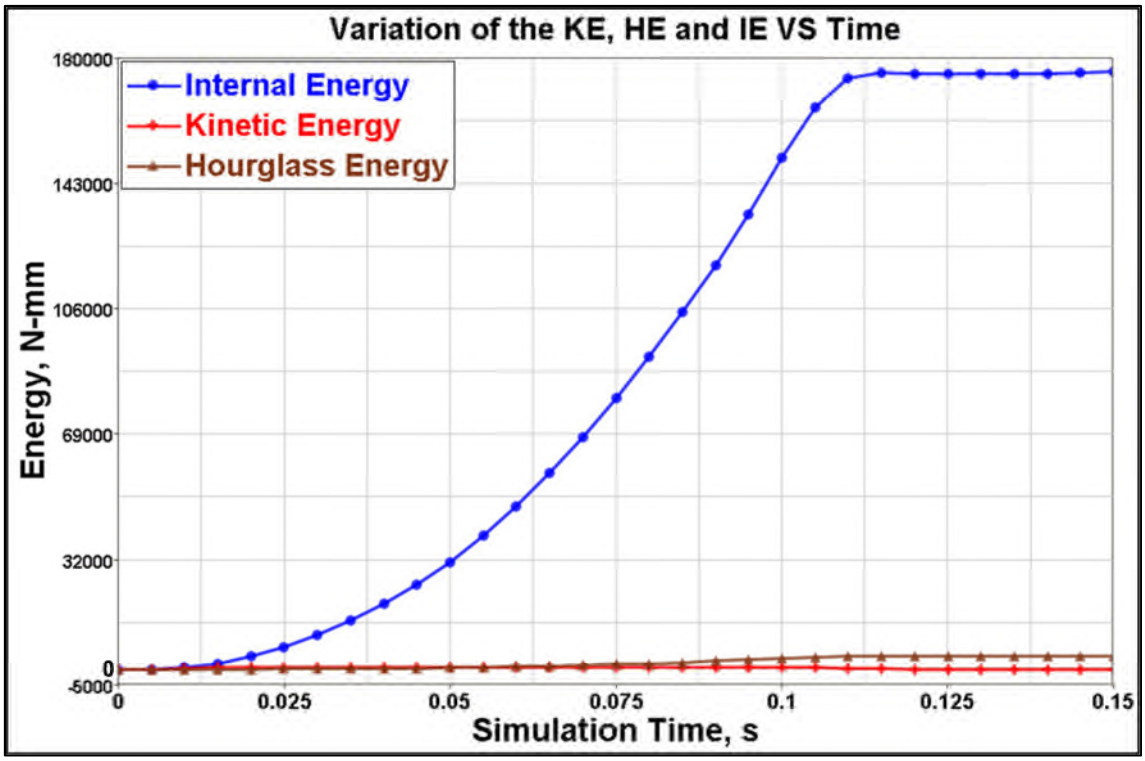

Figure 5-9 Loadcase - 'Downward 8.6g' solved using LSDYNA explicit formulation. Ratio of maximum Kinetic Energy (KE) to Internal Energy (IE) is approximately 0.43%. Ratio of Hourglass Energy (HE) to IE is ~ 2%. As both the ratios are less than the allowable limit of 5%, the solution is essentiallly quasi-static and without excessive artificial hourglass energy.

In the present simulation for 'Downward 8.6g' loadcase, maximum KE is approximately 750N-mm whereas the corresponding IE is approximately 151625N-mm (Figure 5-8). Therefore $(KE/IE)_{MAX}$ is approximately 0.5%.

The value of the KE at the end of simulation i.e. at t=0.15s; is approximately 15.35N-mm and the value of the IE at the end of simulation is approximately 176265N-mm. Therefore the percentage ratio of the KE to IE is approximately 0.009%.

As the ratio of KE to IE is well within the tolerance (maximum ratio < 5%), the response can be considered as a 'Quasi-Static' response i.e. with negligible inertia effects.

Though the ratio of KE to IE is a good primary indicator of the calibre of the quasi-static analysis performed, it is not adequate. Two energies should be

studied individually for any oscillations or noise. Energy ratio can not reveal such behaviour. In many cases, though the condition of energy ratio is satisfied, the KE may show considerable oscillations and the model could experience significant plasticity. The smooth loading pattern should be replicated in the energy histories. If the KE does not indicate quasi-static response, velocities histories of particular parts should be carefully studies as they may reveal the oscillating regions of the model thereby causing high kinetic energies.

5.6.4 VARIATION OF IE

Variation in the IE should reflect the loading rate i.e. time rate of change of IE should be negligible at the steady state as compared to that at load rise time.

'Downward 8.6g' load distributed uniformly over seat-pan is linearly ramped from 0 to 100% in 0.1s and then held constant for another 0.05s thus resulting into a total simulation time of 0.15s. This is reflected in the IE plot of the solution i.e. IE linearly increases from 0s to 0.11s and is then constant till 0.15s (Figure 5-8). The small increase in the IE from 0.1s to 0.11s may be due to the inertia of the structure. Thus the time rate of change of IE is negligible at the steady state as compared to that at load rise time. As there are no sudden jumps in the IE, there is no sudden detection of the undesirable penetrations between contact surfaces.

5.6.5 VARIATION OF THE KE

Variation of Kinetic Energy should reflect the loading sequence and the damping applied. As the load in increased from 0s to 0.1s; the KE increases in that period (Figure 5-9) and reaches its maximum (approximately 750N-mm at 0.1s) when the load reaches its maximum (100% of load at 0.1s).

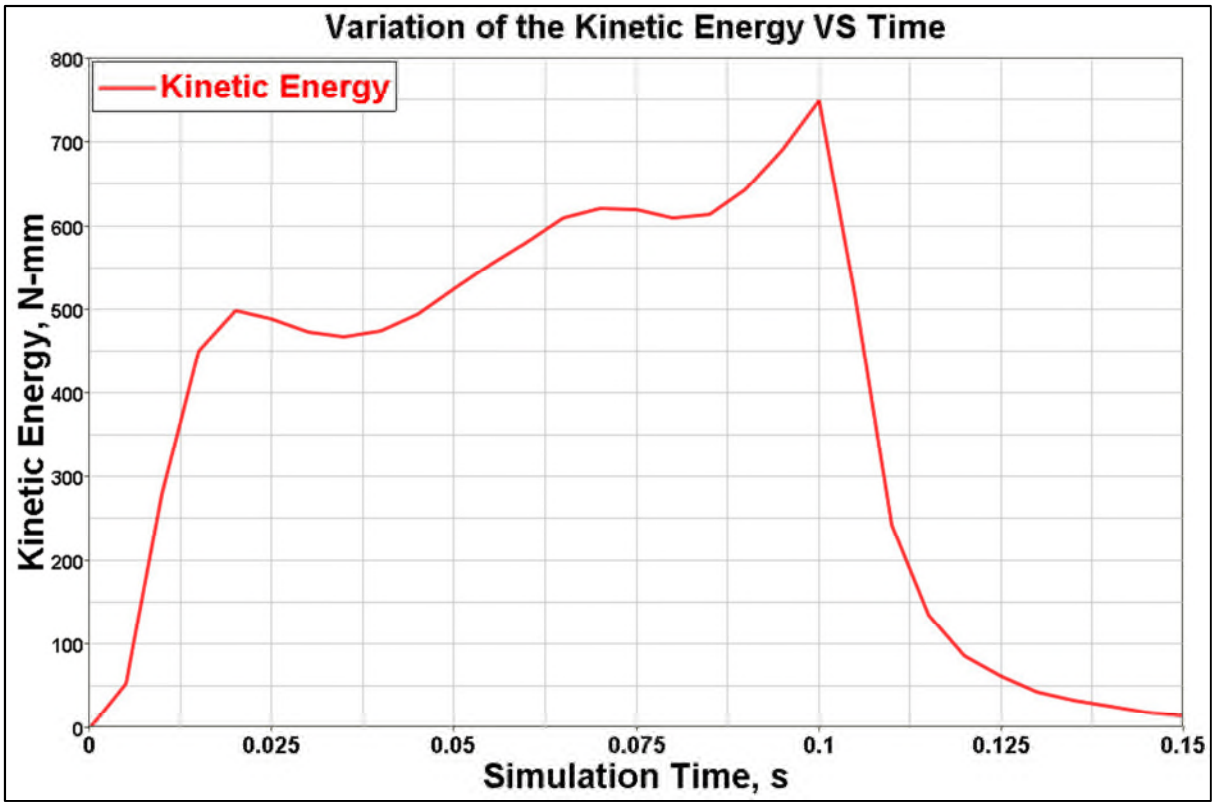

Figure 5-10 Time history plot of KE of the 'triple' seat-structure subjected to 'Downward 8.6g' load and solved using LSDYNA explicit formulation. KE of the rigid bodies has not been considered.

The load is held constant after 0.1s till 0.15s. Therefore there should not be further increase in the Kinetic Energy. It should decrease gradually to zero due to the constant damping applied to the structure. The behaviour of the KE of the seat structure under-study satisfies this requirement as the KE exponentially reduces from approximately 750N-mm to 15.4N-mm during 0.1s to 0.15s (Figure 5-8). This also indicates that no discontinuity is developed in the load path during the loading sequence. In case of the discontinuity in the load path, the structure keeps moving due to the load and KE increases monotonically.

However the variation of KE is not linear as per the loading sequence. The reason can be explained as follows,

- The damping force provided for minimising the unwanted structural oscillations is based on the vibrational characteristics of the un-deformed

(i.e. before load application) seat structure and is provided at the start of the simulation.

- However, during the course of the simulation, due to the changes in the geometry, material response and contact conditions; the vibrational characteristics of the deformed structure change (a seat structure subjected to CS25.561 loads would become stiffer than the un-deformed structure resulting in increased first mode frequency). Hence the magnitude of damping force that required is higher for the deformed structure whereas simulation continues to use lower value of the damping force. This results in non-linear increase in the KE even when the load is linearly ramped in a quasi-static solution obtained with explicit time integration.
- As a remedy, intermittent Eigen values can be calculated using a separate analysis and the damping characteristics can be defined accordingly. This technique has not been used during the present research as; the proportion of KE with respect to the IE of the structure under study is negligible.

Kinetic energies for all the parts of the FE model of the 'Sleep Seat' have been checked and no severe oscillations in the KE are observed indicating

- A stable process and
- Absence of any highly localised oscillations.

5.6.6 RATIO OF HOURGLASS ENERGY TO INTERNAL ENERGY

The maximum ratio of Hourglass Energy (HE) to the 'IE' should be within 5% [41, 43]. The maximum HE is approximately 3857N-mm whereas the maximum IE is approximately 176265N-mm (Figure 5-8). Therefore the maximum ratio of the HE to the IE is approximately 2%.

As the ratio of HE to IE is well within the tolerance (maximum ratio < 5%), the discretisation density, the selection of element types and the hourglass stabilisation algorithm is satisfactory.

5.6.7 TIME HISTORY OF INTERFACE ENERGY

If the FE model contains the interface definitions with friction, the 'Interface Sliding Energy (ISE)' must be positive [38]. Negative ISE indicates either the presence of undetected initial interpenetrations or sudden artificial penetration through contact segment during the course of the simulation.

If the slope of the IE curve is, equal in magnitude and opposite in direction that of the negative ISE curve; the problematic area is normally localised. This argument follows the logic that the impact of the 'negative' ISE on the overall 'IE' is low as the 'IE' is positive. In such cases IE of the components modelled with the shell elements should be checked and ISE of the individual contact pairs should be investigated.

As the sliding interface definitions with friction are present in the FE model of the 'Sleep Seat'; ISE must be positive. A time history of the ISE confirms that this requirement is satisfied (Figure 5-10). It also indicates,

- No undeleted initial interpenetrations or
- No contact failure at a particular time-step (as no negative value is present in the time-history).

ISE of the individual contact pairs have been checked and the behaviour of the interface has been found satisfactory throughout the simulation.

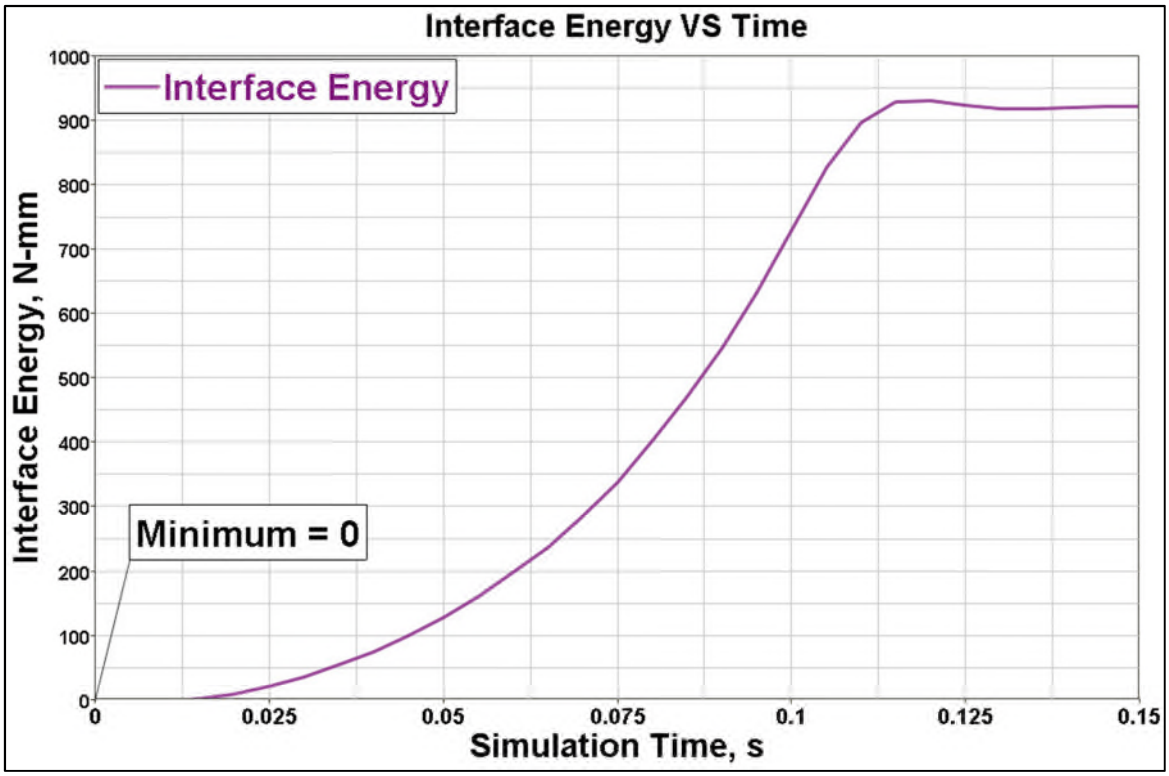

Figure 5-11 Time history plot of Interface energy of the 'triple' seat-structure subjected to 'Downward 8.6g' load and solved using LSDYNA explicit formulation. Positive values of the IE throughout the simulation time indicates no undeleted initial interpenetrations or no contact failure at a particular time-step

Conclusion – Chapter 5

The aim of this chapter is to develop a robust FE methodology for using an explicit dynamic time integration scheme to obtain an acceptable solution for a quasi-static problem. 'Downward 8.6g' load applied to the FE model of the 'triple' Sleep-seat structure has been chosen as a case-study. This problem was solved using an implicit formulation in previous chapter (number 4). The FE model, boundary conditions and material definitions used are kept same for both the formulations.

The advantages of explicit scheme over implicit are,

- Inherent lack of convergence issues,
- Easy handling of complex contact conditions and
- Lower memory and disk space requirements.

Explicit scheme has been successfully used to solve quasi-static processes such as metal forming and hydroforming, which involve nonlinearities. Being a displacement driven loading procedure, the inertia effects can be monitored in such simulations. However, for seat-structures involving complex combination geometric, contact and material non-linearities and a force driven loading process, it is quite challenging

- To limit the influence of unwanted inertia effects on the solution accuracy and
- To obtain a reliable solution in a reasonable CPU time.

The methodology proposed by this research utilises 'Mass scaling (artificial increase of material density, which improves the minimum stable time increment) and 'Time Scaling (artificial reduction in simulation time)' to reduce the CPU time. Mass proportional damping along with a progressive loading sequence (i.e. linearly ramp the load from 0 to 100% and hold it constant thereafter to stabilise the response) has been effectively used to control the unwanted inertia effects.

A matrix to assess the quality of the FEA results obtained by such a scheme has been developed, which includes following guidelines,

- Force equilibrium check must be performed
- Energy ratio, the ratio of the 'Total energy' to the sum of 'Initial Total Energy' and 'External Work done'; should be unity.
- Maximum ratio of Kinetic Energy to Internal Energy should be within 5%.
- Maximum ratio of Hourglass Energy to Internal Energy should be within 5%.
- Variation of Kinetic Energy and Internal Energy should reflect the loading sequence
- If the FE model contains the interface definitions with friction, the 'Interface Sliding Energy' must be positive

Methodology is successfully in reducing the CPU time required for 'Downward 8.6g' loadcase, from 62hours (natural time scale) to approximately over 2hours

yet offering a quasi-static solution. A detailed flowchart of these techniques is provided along with FE results quality checks.

In the next chapter (number 6), the results from both of these solution schemes (i.e. implicit and explicit) are compared against each other.

6 VALIDATION

“Downward 8.6g” load applied to the ‘triple’ seat-structure was solved using implicit formulation in Chapter 4 and explicit formulation in chapter 5. In this chapter results from both of these solution schemes are compared based on

I. Overall displacement and deformed shape of the structure
II. Von Mises stress, VMS induced in Forward beam and Seat-leg
III. Reaction forces
IV. Forces acting on the critical cross-sections
V. Seat Interface Loads
VI. CPU time Disk-space required

After comparing the results, guidelines are provided on using these solution schemes for assessing the structural performance of a seat. FEA results of the ‘Downward 8.6g’ loadcase are compared against those from experimental testing, which is performed by the BlueSky. The role of Cranfield University was of an observer without any direct access to test facilities. In the last portion of the chapter, FE procedure for using explicit time integration to solve a quasi-static FE model has been extended to simulate ‘Forward 9g’ loadcase. The complexity lies in incorporating body blocks, seat belts and loading mechanism. All these issues are discussed and solutions are provided.

6.1 DIFFERENT SOLUTION TECHNIQUES (NOMENCLATURE)

A	Abaqus Implicit Method	'Full Newton' solution technique of Abaqus (Research) 6.9-3 [33]
B	Abaqus Implicit Q-Method	'Quasi-Newton' solution technique of Abaqus (Research) 6.9-3 [33]
C	LS-DYNA Implicit BFGS Method	'Nonlinear solution technique with BFGS updates' in LSDYNA when the 'Implicit Analysis' flag is activated [35]
D	LS-DYNA Implicit N-Method	'Full Newton solution technique with line search' in LSDYNA when the 'Implicit Analysis' flag is activated [35]
E	LS-DYNA Explicit Method	The default 'Solution Technique' used by LS-DYNA for an Explicit analysis [35]

The results obtained with solution technique B (Abaqus (Research) 6.9-3), C (LSDYNA/Implicit) and E (LSDYNA/Explicit) are used for the comparison.

6.1.1 OVERALL DISPLACEMENT AND DEFORMED SHAPE OF THE STRUCTURE

Displacement plot for the FE model of the 'Sleep Seat' after applying 'Downward 8.6g' load simulated by method B, C and E leads to the following remarks (Figure 6-1),

- The contour of the overall displacement and the deformed shape of the structure are approximately same for all the methods.
- The magnitude of the maximum overall displacement shows a variation of +2.6% considering the 33.25 as base value (i.e. 33.25mm is the maximum displacement obtained with Abaqus (Research) 6.9-3, Method B).

- The reason between the difference in the results obtained by Abaqus (Research) 6.9-3 and the LS-DYNA environment could be because of difference between the contact algorithms and the element formulations.
- The solution with LS-DYNA/Explicit (method E) shows a small increment in the maximum displacement over that observed with LS-DYNA/Implicit because of the inertia effects introduced in the system. A small difference of approximately 1.5mm between the results shows that inertia effects are not significant.

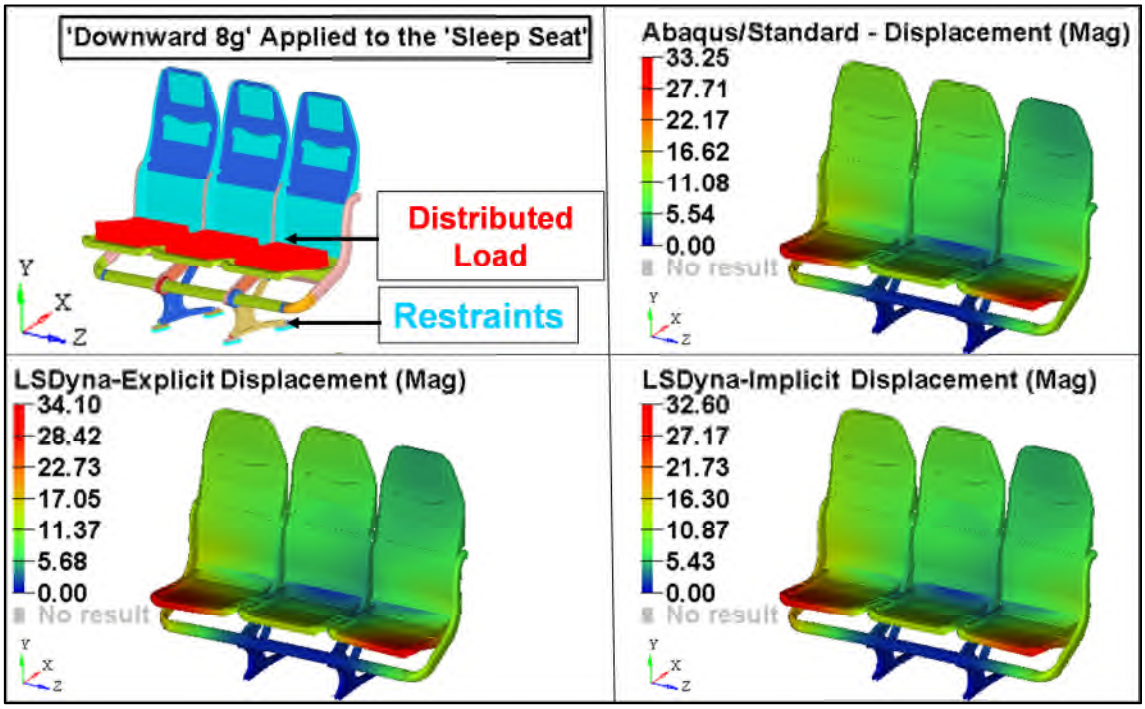

Figure 6-1 Magnitude and the contour of the resultant overall displacement for the 'Triple Seat Assembly' as a result of application of 'Downward 8.6g' loads performed by Method B, C and E as explained in Section 6.1 of this chapter

6.1.2 VMS IN THE FORWARD BEAM AND SEAT-LEG

While comparing the methods B, C and E on the basis of stress levels induced, all the stress components for all the individual components of the 'Sleep Seat' have been considered and have been found to be within a reasonable tolerance. However, VMS contours of only 'Forward Beam' and 'Seat-leg' have been produced and compared in this report to keep it brief. Being the major load carrying members, they experience high stress levels compared to other

components. Unrealistic highly localised stresses (contact noise) if any, have been ignored and are not reported here.

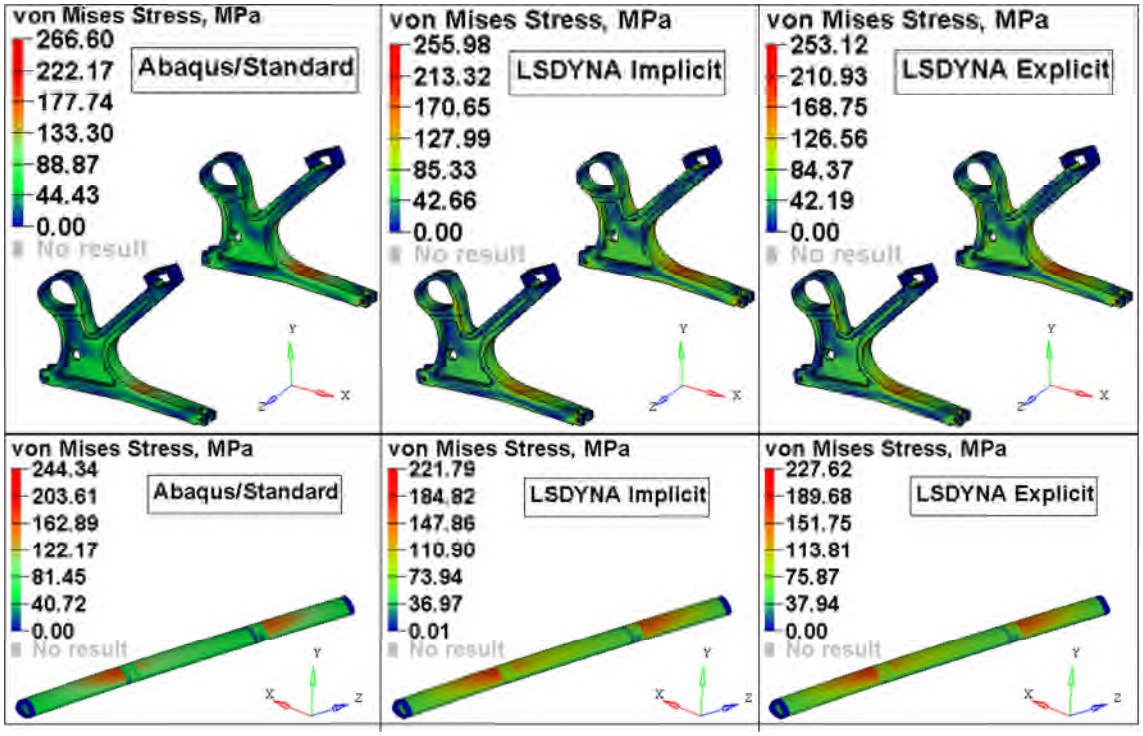

Figure 6-2 Magnitude and the contour of the VMS for Forward beam and Seat-Leg as a result of application of 'Downward 8.6g' loads performed by Method B, C and E as explained in Section 6.1 of this chapter

The remarks on the VMS plots of the FE model of the 'Sleep Seat' after applying 'Downward 8.6g' load simulated by method B, C and E can be summarised as (Figure 6-2),

- The overall distribution of the VMS on the subassembly of the Forward beam and the Seat-leg is approximately same for all the methods.
- The difference between the maximum values of the VMS occurring in Forward beam and Seat-leg for two different environments of LSDYNA (Implicit and Explicit) is not significant.
- The difference in the results obtained by Abaqus (Research) 6.9-3 and the LS-DYNA environment could be because of difference between the contact algorithms and the element formulations.

6.1.3 COMPARISON OF FORCES ACTING AT A CROSS-SECTION

Cross-Sections for extracting the forces and moments acting on them are chosen based on

- Their role in ensuring the continuity in the load path and
- The high stress levels induced when subjected to loads as per CS 25.561 and CS 25.562 (based on previous FEA results)

Thus, three Cross-Sections chosen for the study are (Figure 6-3)

- Cross-section of the boomerang RHS near the seat belt anchorage point
- Cross-Section of the Forward Beam near any one of the bolted connection between Forward Beam and Seat-Leg
- Cross-section of the Seat-Leg in the lower aft foot-section, which is in between the Seat anchorage points and the stiff central web of the leg

The procedure to extract the components of the forces acting at a cross-section for ‘Abaqus Implicit Method’ and ‘LS-DYNA Implicit or Explicit Method’ is provided in the Appendix D.3 of this report.

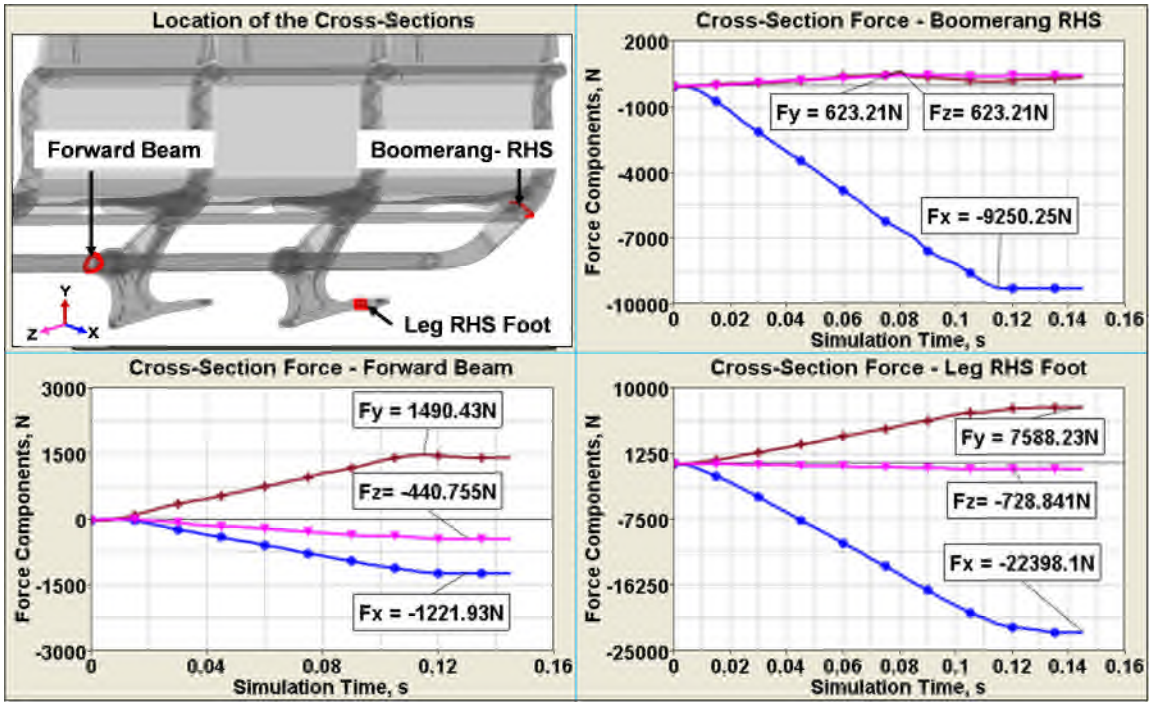

Figure 6-3 Time variation of the cross-sectional forces acting on the 'Boomerang-RHS', 'Leg RHS Foot' and 'Forward Beam', recovered from Abaqus (Research) 6.9-3, Method B. Loadcase – Downward 8.6g

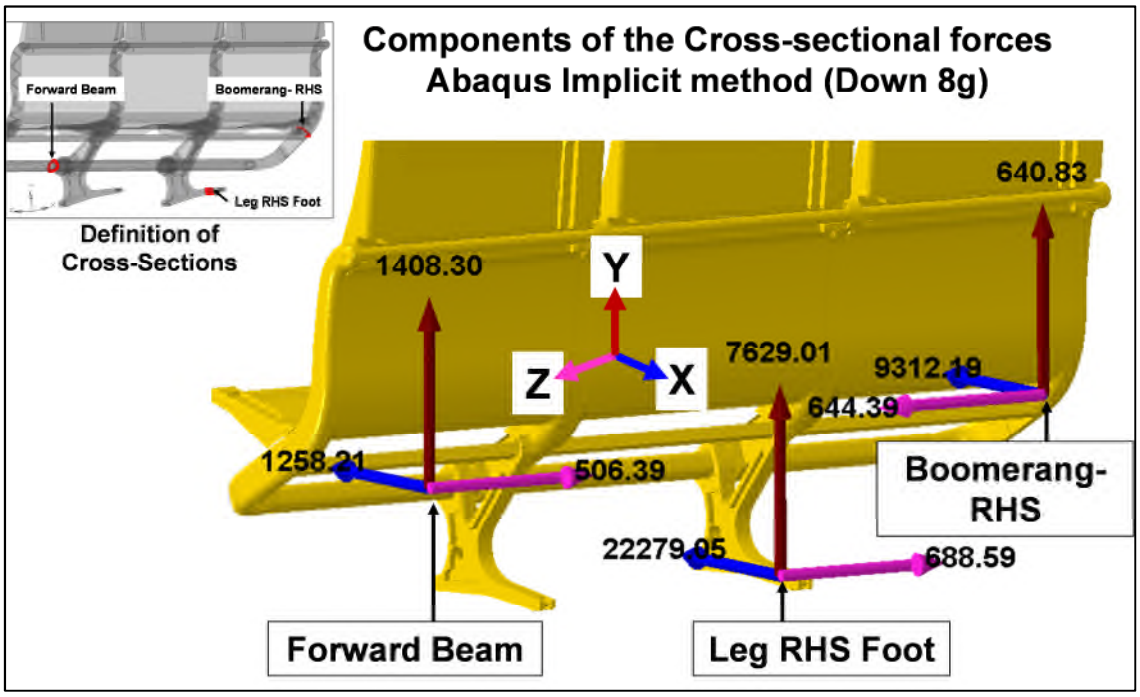

Figure 6-4 Components of the components of the cross-sectional forces acting on the 'Boomerang-RHS', 'Leg RHS Foot' and 'Forward Beam', recovered from LS-DYNA/Explicit, Method E. Loadcase – Downward 8.6g

It can be seen from the Figure 6-3, Figure 6-4 and Table 6-1 that the difference between the components of the cross-sectional forces obtained by three different solution techniques is not significant.

Location of the Cross-Section	X, Y and Z Components of the Cross-Sectional Forces, N								
	Abaqus – Implicit (B)			LSDYNA-Implicit (C)			LS-DYNA Explicit (E)		
	Fx	Fy	Fz	Fx	Fy	Fz	Fx	Fy	Fz
Boomerang RHS	-9312.19	640.83	643.39	-9225.30	650.69	639.23	-9250.25	623.21	623.21
Leg RHS Foot	-22279.05	7629.01	-688.69	-22120.88	7615.23	-696.97	-22398.10	7588.23	-728.84
Forward Beam	-1258.21	1408.30	-506.39	-1276.50	1393.40	-493.25	-1221.93	1490.43	-440.76

Table 6-1 Comparison of the Components of the Forces acting on various Cross-Sections, calculated by Solution Techniques B, C and E as explained in Section 5.1 of this chapter. Minor differences are observed in the respective values. Loadcase – Downward 8.6g

6.1.4 COMPARISON OF INTERFACE FORCES

The procedure to extract the components of the interface forces for 'Abaqus Implicit Method' and 'LS-DYNA Implicit or Explicit Method' is provided in the Appendix D.4of this report.

For the 'Downward 8.6g' load, the final load transfer is through the interface between main body of the tool-less fitting (TLF) and the Seat-track. Hence, the interface forces acting between the upper lip of the tool-less fitting and the seat track are considered for the comparative study.

The observations from the Table 6-2 are

- The differences between X, Y and Z components of the interface forces obtained by three different algorithms used to solve the loadcase of 'Downward 8.6g' are not significant.
- Right hand side TLF is subjected to more 'downward' load compared to that on Left-Hand side due to more overhang. This fact is reflected in the interface loads e.g. the vertical interface load F_Y, acting on both the RHS-Front and RHS-Rear TLF is greater than that on LHS-Front and LHS-Rear TLF.
- Main body of the rear TLF is supported by the retainer, which has shear plungers, which positively engage with the Seat-track carrying the lateral component of the force (F_Z). Therefore, the F_Z acting on the rear TLF (main body) should be minimal. This is reflected in the interface loads as F_Z is approximately 40N.
- However as per the airline regulations, TLF (retainer) in the front side should not have any shear-plunger. Therefore, the main body of the TLF experiences the lateral load due to the out-of-plane bending on the seat structure. This is reflected in the interface loads as F_Z for front TLF is higher than that for rear and is approximately 1400N.

Interface Definition	X, Y and Z Components of the Interface Forces, N								
	Abaqus - Implicit			LSDYNA-Implicit			LS-DYNA Explicit		
	F_X	F_Y	F_Z	F_X	F_Y	F_Z	F_X	F_Y	F_Z
RHS Front	-2389.68	-5023.55	1305.66	-2412.70	-5107.33	1299.70	-2499.17	-5197.23	1357.40
RHS Rear	2190.23	-7228.23	40.26	2200.12	-7301.21	39.56	2250.32	-7351.11	43.43
LHS Front	-2039.93	-3460.40	-1463.40	-2057.93	-3393.53	-1501.50	-2151.91	-3577.53	-1531.50
LHS Rear	1876.80	-5963.39	40.22	1875.70	-5903.93	39.32	1901.84	-5813.34	44.42

Table 6-2 Comparison of the Components of the Interface forces acting on the interfaces between various tool-less fittings and seat-track, calculated by Solution Techniques B, C and E as explained in Section 6.1 of this chapter. Discretisation algorithm used – Surface to Surface. Minor differences are observed in the respective values. Loadcase – Downward 8.6g

6.1.5 COMPARISON OF THE REACTION FORCES

The procedure to extract the components of the reaction forces for 'Abaqus Implicit Method' and 'LS-DYNA Implicit or Explicit Method' is provided in the Appendix D.1 of this report.

It can be seen that all three solution techniques used to solve the problem of 'Sleep Seat' subjected to the 'Downward 8g' load, satisfy the force equilibrium check (Table 6-3).

6.1.6 COMPARISION OF COMPUTATIONAL TIME

The best (i.e. 827s lowest from Table 4-5) Computational time (CPU time) observed for implicit formulation (LSDYNA - Quasi-Newton with BFGS updates), has been considered for this study. For explicit formulation, time associated with 'Solution Scheme C' (7821s, from Table 5-1 i.e. achieve 100% load in 0.1s and hold it constant for another 0.05s), which yields an acceptable quasi-static finish has been considered.

Significant difference can be seen between CPU times (Table 6-4). The reason being

- Same FE model has been used for implicit and explicit calculations. The model was basically built considering the implicit algorithm (mesh grading considering stress concentration) and hence resulted in a very small stable time increment for explicit algorithm (though the uniform mass scaling of '5' was used to increase the time-step) and hence very high CPU time.
- Furthermore, motive behind using explicit formulation; to develop a FE procedure, which can yield acceptable quasi-static finish for the problems such as a seat-structure subjected to static loads as per CS25.561; is successful. The advantages of this scheme are more pronounced while simulating complex nonlinear loadcases with body-blocks e.g. 'Forward 9g', where even after considerable man-hours of FE model building, implicit formulation either fails or struggles to find a converged solution.

- A further study can be undertaken to reduce the CPU time by coarsening the FE discretisation and mass scaling for explicit solution schemes.

Applied Force	X, Y and Z Components of the Reaction Forces, N								
	Abaqus - Implicit			LSDYNA-Implicit			LS-DYNA Explicit		
	F_X	F_Y	F_Z	F_X	F_Y	F_Z	F_X	F_Y	F_Z
Fx, Fz = 0, Fy = 28093.8	1.60E-3	28110.6	1.98e-3	0.20e-3	28117.3	2.85e-3	2.10e-3	28057.1	1.70e-3

Table 6-3 Comparison of the Components of the Reaction forces calculated by different Solution Techniques – Downward 8.6g

Solution Technique	CPU time, s	Memory Required, ~GB
LSDYNA - Quasi-Newton with BFGS updates	853	5.83
LSDYNA - Explicit	7821	4.48

Table 6-4 Comparison of the CPU time and memory required (in gigabytes, GB) to solve case-study of 'Downward 8.6g' loadcase using implicit formulation and explicit formulation. Though CPU time is very high for explicit scheme (as compared to that for implicit), it is mainly due to the same FE model considered for both the schemes.

6.1.7 CONCLUDING REMARKS

- The objective of this exercise was to compare the solutions obtained for case-study i.e. 'Downward 8.6g' applied to the 'triple seat-structure'; using implicit formulation (Chapter 4) and explicit formulation (Chapter 5).
- Abaqus (Research) 6.9-3 and LS-DYNA (Implicit) were used as solvers for implicit solution scheme whereas LSDYNA (Explicit) for explicit solution scheme.
- The methods are compared against each other based on six important parameters:
    - Overall displacement and the deformed shape,
    - VMS induced in the major load carrying members
    - Cross-sectional forces
    - Reaction forces
    - Seat Interface loads and
    - CPU time and disk-space required
- Based on these parameters the structural responses of the 'Sleep Seat' under study, estimated by these three methods is within reasonable tolerance.
- Significant difference is observed in the CPU times (827s with implicit formulation i.e. LSDYNA with quasi-Newton solver 7821s with LSDYNA / Explicit). The reason being
    - FE model built considering the implicit algorithm (fine discretisation to avoid contact failures) was used for explicit simulation resulting in a very small stable time increment and very high CPU time.
    - A further study can be undertaken to reduce the CPU time by coarsening the FE discretisation and/or mass scaling for explicit solution schemes

To conclude, this research has developed three different methods to solve the static loadcases i.e. seat-structure subjected to CS25.561 inertia loads, which can yield acceptable solutions. Any these methods can be used and tailored to suit the available software and hardware.

In next section results from Abaqus (Research) 6.9-3 (Method A, Implicit Solution Scheme) and LSDYNA/Explicit (Method E, Explicit Solution Scheme) are compared against those from experimental testing.

6.2 EXPERIMENTAL TESTING AND VALIDATION

Development tests are performed by BlueSky designers through external agency and the test results are shared with the author of this report.

In Experimental testing, load was applied with the help of body blocks. The total load applied was approximately 28093 N (111kg per seat pan multiplied by 8.6g inertia load in downward direction).

FE model consists of 181900 nodes and 194612 elements with approximately 1038495dofs. Material definitions and geometry of all the components (except Seat-Pan); considered is consistent with that of prototype to be tested (given in Appendix K). A summary of assumptions made in FE model are,

- No failure of the joints during testing (as either tied together or connected by multi-point constraints, MPC),
- Load in uniformly distributed over the seat-pan in FE model as described in ARP5526 [10] as well as considering
  - There is no play in the joints used in the test set-up for load application, which comprises of hydraulic cylinder (A), vertical members (B) and body blocks, D (Figure 6-5).
  - Piston of the hydraulic cylinder, vertical beams and body-blocks do not deform under loading.

Figure 6-5 shows experimental set-up and FE model to assess the behaviour of the triple seat–structure subjected to ‘8.6g’ load in vertically downward direction.

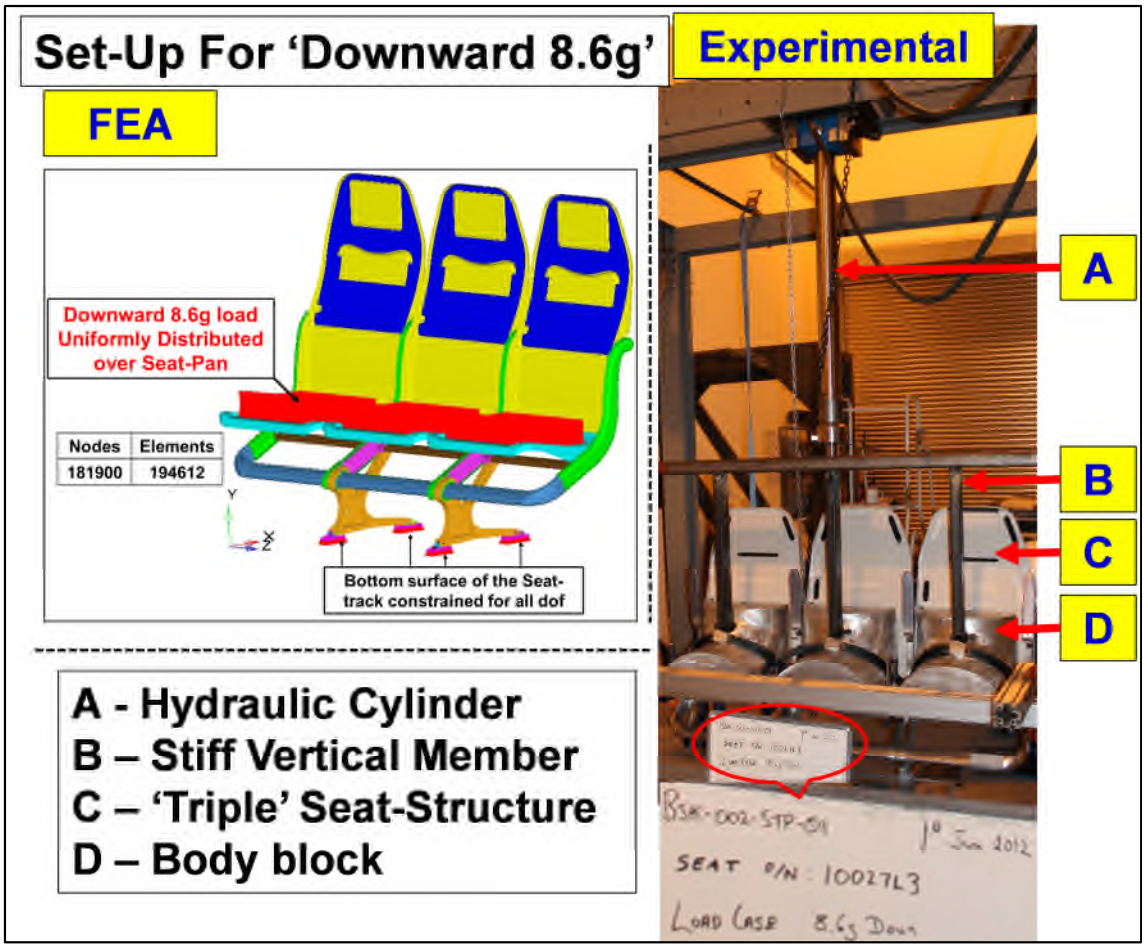

Figure 6-5 Set-up for 'Downward 8.6g' load applied to triple Sleep-Structure LHS - FE Model (Solvers – Abaqus (Research) 6.9-3, LSDYNA), Load is Uniformly distributed over Seat-Pan RHS - Experimental Test Set-Up, Load applied through Body blocks

6.2.1 COMPARISON OF THE RESULTS

A Java-based, public domain image processing program; 'ImageJ' is used to post-process the displacement results obtained from experimental testing. It developed at the National Institutes of Health [55]. It can be downloaded on any computer with a Java5 or later virtual machine. It can read many image formats such as PNG, BMP, JPEG and TIFF and can measure distance and angles. The procedure to calibrate (or to set the reference scale) 'ImageJ' has been given in Appendix E.

Interpretation of FE results and those from experimental testing (Figure 6-6, Figure 6-7 and Table 6-5) leads to following remarks,

- An acceptable correlation is observed in the kinematic behaviour (such as no discontinuity in the load path, integrity with the seat-track, Figure 6-6) predicted by FEA and recorded during the physical testing (Snaps at regular interval from FEA and test videos are not provided in this report as the total displacement of the structure is very low (~30mm) and hence it is difficult to differentiate the deformed plot observed at different time-history. Final deformed shape of the structure is provided instead.
- Flattening of the lower aft section of the leg was observed both in FEA results (method A and B) as well as in test results.
- Difference between deformed shapes of Seat-Pan observed is due to the fact that during experimental testing, seat-pans were not available and hence stiff plywood was used instead. However, in FE model, Seat-pan made up of Al6082T6 and thickness of 3.6mm is used.
- Vertical downward displacement of 'Point I' (Figure 6-7, U_{2I}) is 7.22mm and 7.61mm observed in FE results of 'Method A' and 'Method B' respectively. Whereas U_{2I} observed in test results is 8.71mm.
- 'Method A' and 'Method B' predicted 8.56mm and 8.87mm of vertical downward displacement of 'Point II' (U_{2II}) respectively whereas the 9.84mm was observed in test results.

- An acceptable agreement between FEA results (from two methods) and test results helped

  - To validate the following assumptions made during FE model building
    - ✓ Applying the load directly to the seat-pan instead of using body-blocks
    - ✓ Tied contacts or MPC at the locations given in Section 6.2 (as no failure of the joint was observed in the tests).

  - To validate both FE procedures developed to use implicit formulation and explicit formulation for demonstrating the static compliance (CS25.561) of an aircraft seat.

Notes –

- Displacement contours obtained by ‘Method E’ i.e. explicit formulation, are not presented in this report (only their magnitude is provided in Table 6-5) to keep it brief.
- ‘Point I’ is on Forward Beam, located inward approximately 30mm from LHS end (looking from rear of the seat-structure)
- ‘Point II’ is on Forward Beam, located inward approximately 30mm from RHS end (looking from rear of the seat-structure).

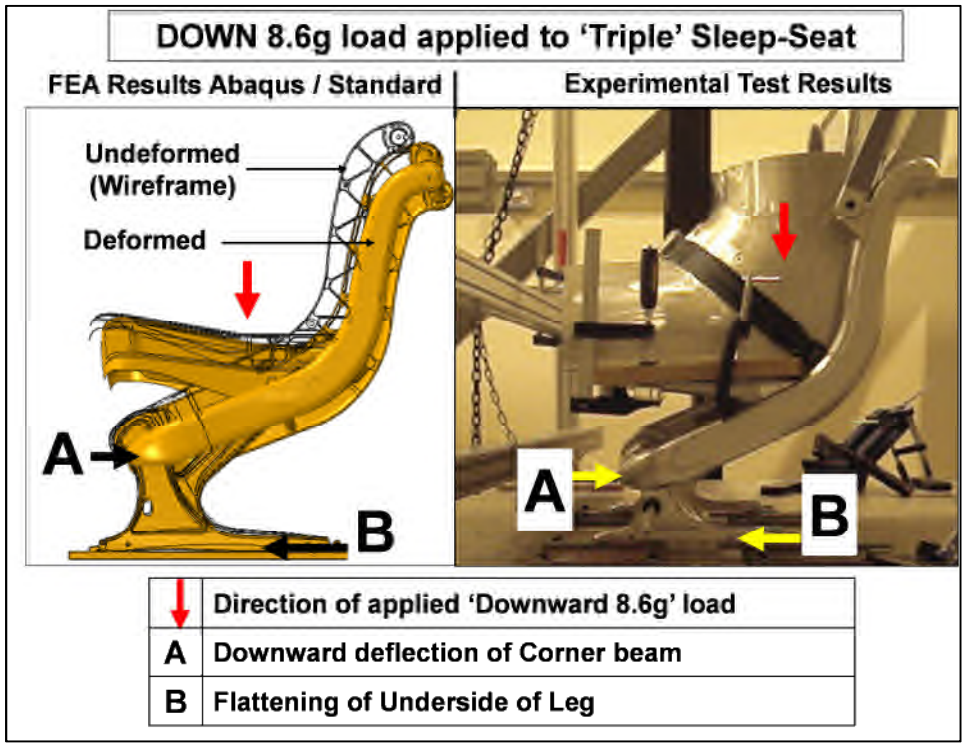

Figure 6-6 An acceptable correlation is observed, in the kinematic behaviour (such as deflection of Point A and flattening of leg-underside at B); of 'triple' Sleep-Seat-Structure subjected to 'Downward 8.6g' load, between the results predicted by FEA (Abaqus (Research) 6.9-3) and those from experimental tests, thereby boosting confidence in the FE procedure adopted for this research. The difference in seat-pan deflection is due to different designs used in FEA and experimental tests.

Parameter	Implicit Formulation (Method A)	Explicit Formulation (Method E)	Experimental
Discontinuity in the load path	NO	NO	NO
Separation from Seat-track	NO	NO	NO
Permanent Strain	NO	NO	NO (Visual observation)
Displacement of Point I, mm	7.2	7.6	8.7
Displacement of Point II, mm	8.5	8.8	9.8

Table 6-5 Comparison of FEA results (obtained with two different formulations: Implicit (Method A) and Explicit (Method B)) against experimental results. Loadcase - 'Downward 8.6g' load applied to the 'Triple' seat-structure. Displacement contour plots are provided in Figure 6-7

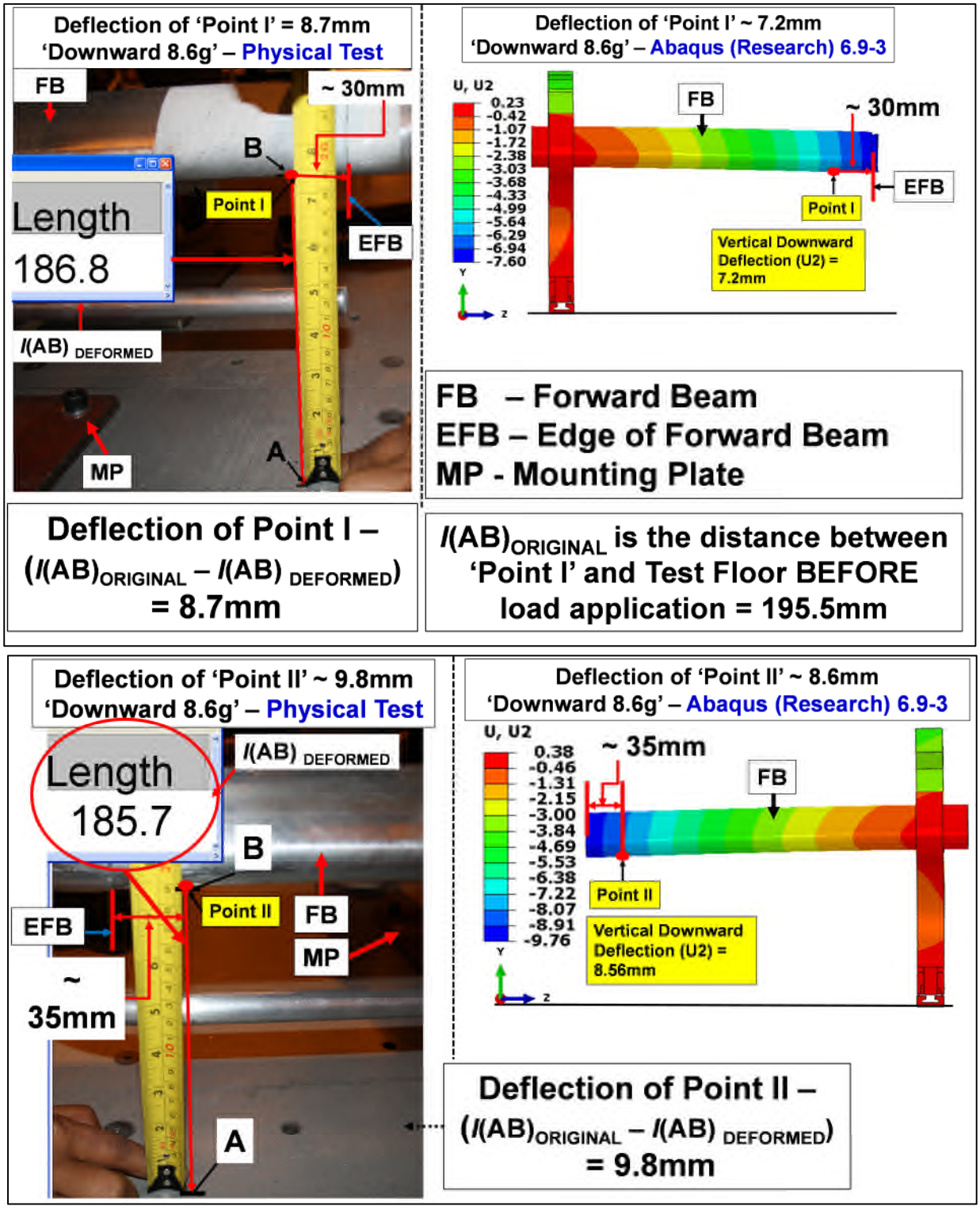

Figure 6-7 A close correlation between the vertical downward displacements of Point 'I' and 'II' on the Forward beam observed from FEA (Abaqus (Research) 6.9-3) and experimental tests helps to validate the FE procedures (application of implicit and explicit formulation) developed in this research to demonstrate static compliance (CS25.561) of a seat-strucutre by simulation Loadcase – 'Downward 8.6g' applied to 'Triple' seat-structure

6.3 DEVELOPMENT OF FE PROCEDURE TO SIMULATE LOADCASES WITH LAP BLOCKS

After a reasonable correlation between FEA results and test results, next task is to upgrade the methodology to include additional complexities such as body blocks and seat-belts, which are essential for introducing loads such as 'Forward 9g' i.e. the 9g inertia load applied in 'Forward' direction; in the seat-structure (Figure 6-8).

CS25.561 is extremely brief in details and contains no information on how the test is performed and hence additional documents must be considered to derive the actual loading procedure by the test labs. Combination of seat, body blocks and seat belt is quite challenging to analyse as

- Body blocks are not tied to the seat-structure or seatbelts, contact and slipping between all the parts occur. Therefore, seat, body block and seat-belt form a complex kinematic system, which is challenging to represent in FE model. In addition, due to large deformations of the structure, the distribution of the applied load to the anchorage points depends on the configuration under load. Hence, for accurate computational results correct modelling of the loading mechanism, associated kinematics, FE modelling of parts considering severe element distortions and interface definitions over large portions is essential.
- Use of static implicit simulations involves time consuming FE model building (definition of interface pairs and parts 'just in contact' at the beginning of the solution) during pre-processing and local instabilities due to excessive deformations during solution phase, thus failing to obtain a converged solution.

The challenges in deriving an appropriate FE modelling technique to simulate 'Forward 9g' load are,

- To develop a loading procedure consistent with physical testing
- FE representation of body blocks (e.g. material properties)
- To select an appropriate element for FE modelling the seat belt,

6.3.1 'FORWARD 9G' LOADING PROCEDURE

Normally during experimental testing, the 'Forward 9g' load is applied with the help of a hydraulic cylinder, A (Figure 6-8). It is bolted (connection C) to a stiff horizontal section B, which in turn is connected with the body block D, with two joints E (a pinned connection) and F (a bolted joint). Pinned joint E ensures a pull in horizontal direction irrespective of the structural response of the seat. Rotation of the Seat-pan may apply a shear load or bending moment to the piston of the hydraulic cylinder leading to its failure. However, presence of pin joint E provides a relative motion (releases rotational degree of freedom thereby avoiding loading of piston of cylinder) between seat-structure and cylinder avoiding damage of later.

Body blocks are rested on the Seat-Pan and are restrained with the help of Seat-belts G, which in turn are connected to the boomerangs through a D clamp (not shown in Figure 6-8)

The major challenge during FE modelling is to ensure a horizontal pull. It can be ensured by three different techniques,

1. Using multi-point constraints to connect the load application point to the seat-belt anchorage points i.e. eliminating the need to consider body blocks and seat belts, and restraining the master node for all degrees-of-freedom except longitudinal. In this method, though the load is applied in a horizontal direction, it fails to capture the kinematics associated with rotation of the seat-pan due to the weight of the body block and associated change in the angle of rotation (due to movement of seat-belt over body-block) that is introduced in the belt anchorages. This simplification is not representative of the loading conditions of test so has been disregarded.
2. Another method could be constraining body blocks in all directions except longitudinal and imposing an enforced displacement on them, which would generate an equivalent 'Forward 9g' load. Again, this mechanism fails to capture the kinematic of the test sequence and for the reasons given above is also not a viable modelling approach.

3. A combination of 1D seat belt elements, slip-ring and a rigid support to hold the slip-ring has been developed during this research to be consistent with the loading sequence (Figure 6-9).

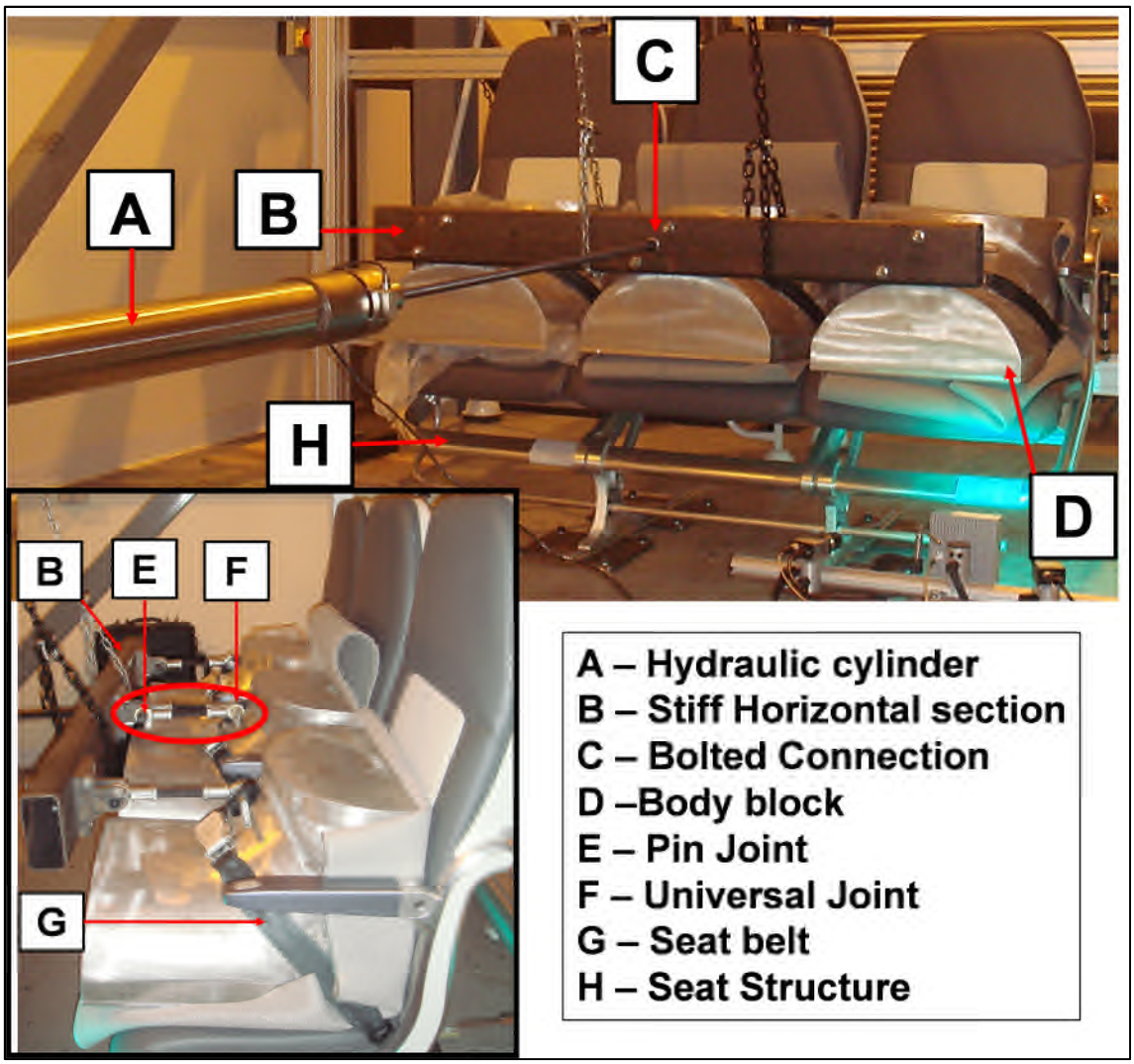

Figure 6-8 Experimental set-up for 'Forward 9g' loadcase. Courtesy – BlueSky Designers Limited, UK

1D seat belt elements represent the piston of the hydraulic cylinder and the load is applied at the free end, A, which is restrained in all the directions except longitudinal. Then a slipring is defined at a common node of two elements (Element A and B from Figure 6-9 LHS). Common node is automatically constrained to follow the slipring node [35]. Slipring is attached to a rigid plate

restrained for all degrees-of-freedom to represent the attachment of the hydraulic cylinder to the test-ring.

Slipping allows continuous sliding of the 1D seat-belt elements even through a sharp change of angle (representing pin Joint E in Figure 6-8). Figure 6-9 RHS shows that even after a considerable rotation of the Seat-Pan, 'Forward 9g' load, is still applied in the longitudinal direction.

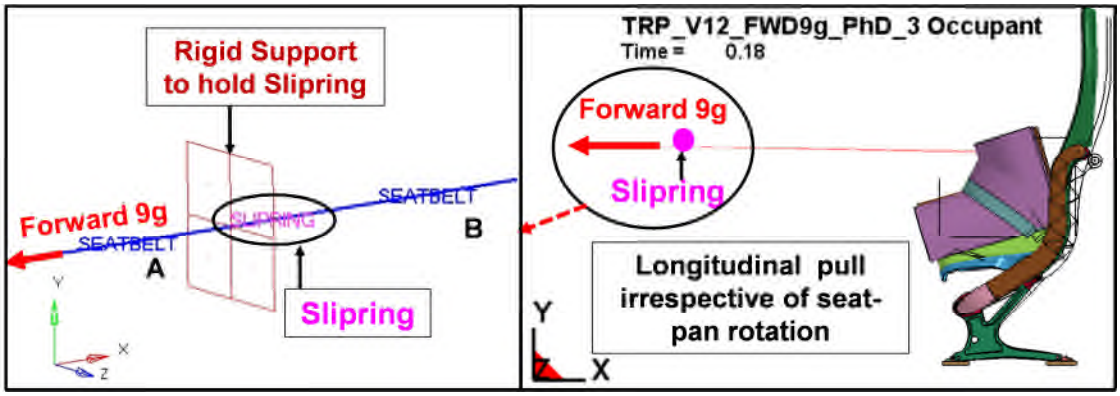

Figure 6-9 LHS - A combination of 1D seat belt elements, slip-ring and a rigid support to hold the slip-ring, used to apply a 'Forward 9g' load. RHS - loading direction remains longitudinal for 'Forward 9g' irrespective of the structural response of the seat, which is consistent with the experimental testing. Un-deformed configuration displayed in 'Edge-view'.

Thus the FE set-up developed to apply the 'Forward 9g' load to the seat-structure is consistent with that observed during experimental test.

6.3.2 FE REPRESENTATION OF LAP BLOCK

The technical drawings defining the dimensions of the body block used for a two point lap belt restraint system can be found in ARP5526, which has a mass of 32kg and is constructed from aluminium (Figure 6-10 LHS) [10].

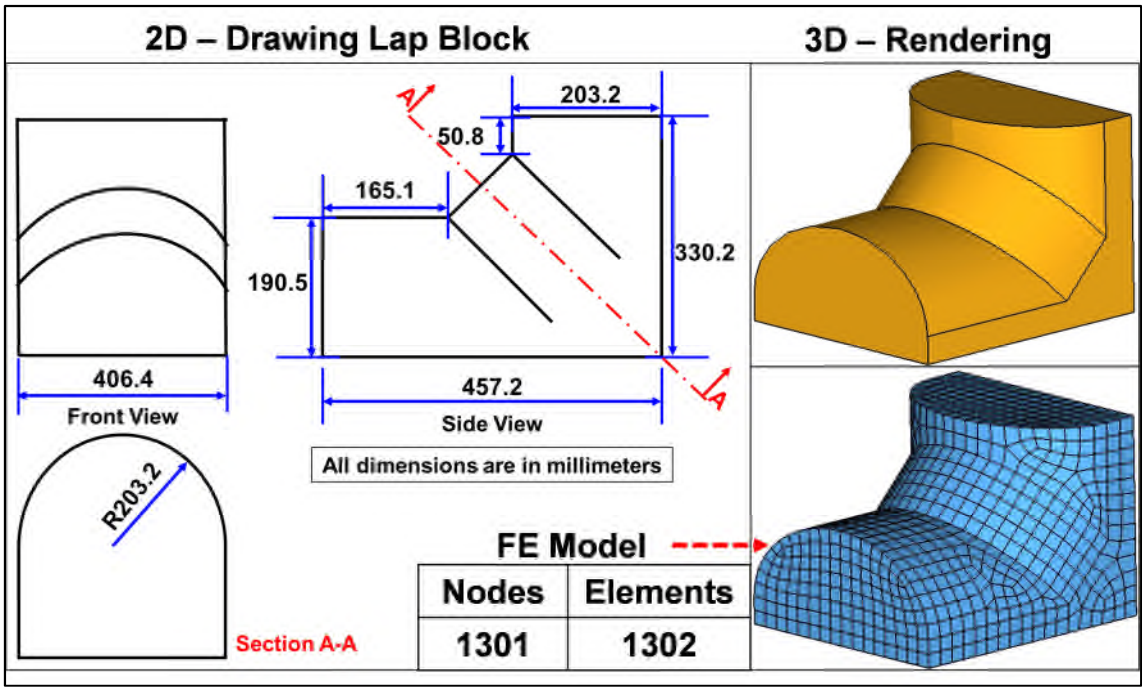

Figure 6-10 Lap block dimensions [10] and FE model with shell elements

As the stiffness of the block is greater than the seat structure, no deformation occurs under load, which supports the assumption that they can be considered as a rigid body and can be represented with shell elements with an appropriate rigid material model [35, 47, 48].

Since explicit dynamic time integration has been used to solve this quasi-static problem, effect of mass of lap block on the magnitude of load introduced in the structure, is an interesting phenomenon to study [38]. Therefore, four simulations were performed for the Forward 9g load case for different lap block masses, which were achieved by adjusting the density on *MAT_RIGID in LSDYNA [6]. The metric for comparison was the maximum displacement of the seat-structure (Table 6-6), which was compared against the upper allowed limit, as defined in the standards [14]:

- For a lap-block of 32kg, the maximum resultant displacement is 47.7mm, which is below the allowable upper limit of 75mm, thus indicating a safe design against the Forward 9g load case [7].
- However as body block mass is reduced, the structure is either at the borderline displacement limit (for 5kg), or exceeds the maximum allowed

deformation requirements (>75mm) for a mass between 0.1 and 0.5kg, and would therefore not pass the certification requirements.

The reasons behind these contrasting outputs is in the usage of explicit time integration scheme for modelling a static test in which there is a large mass (of body block) being moved. For computational efficiency, the loading rate is speeded up. The high inertia of the block (when a block with 32kg of mass is used) causes a delay in force picking up in the belt and hence on seat, which results in the over estimation of seat stiffness and a corresponding reduction in the perceived maximum displacement than occurs in reality.

If the loading time is increased, eventually all of the applied load may be transferred to the seat-structure with a penalty of high computational time. In addition, controlling the inertia of body blocks would be a great challenge.

Hence lighter block should be used in FE simulation which helps to quickly transfer the applied load to the seat-structure.

Serial Number	Mass of lap block, kg	Maximum Displacement of seat-structure, mm
Simulation 1	32 (as in physical test)	47.7 (Safe)
Simulation 2	5.0	74.5 (Border)
Simulation 3	0.5	80.5 (Unsafe)
Simulation 4	0.1	80.7 (Unsafe)

Table 6-6 Comparison of the maximum displacements of the 'triple' seat-structure subjected to 'Forward 9g' load with different masses of the lap-blocks. Solver – LS-DYNA /Explicit

The Kinetic Energy (KE) associated with a body block is a good measure of the mass effect on simulation accuracy. As the mass is reduced, so is its inertia (and KE), thereby stabilising the response (Figure 6-11). Therefore, a lighter body block should be used so as to transfer approximately all the load to the structure. As the displacements converge for the two lightest body blocks, a

mass of 0.1kg has been chosen (assigned through TM on *PART_INERTIA) [35].

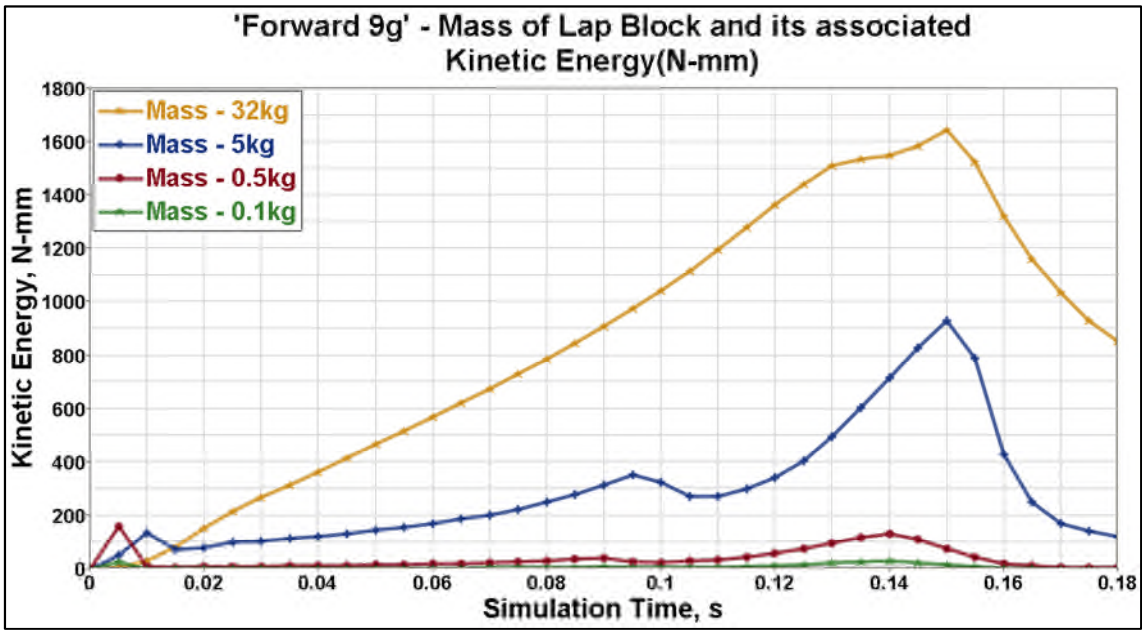

Figure 6-11 'Forward 9g' - Mass of Lap Block and its associated KE (N-mm). A lighter lap-block results in lower KE

However, as the block is pulled forward, its centre of gravity shifts, applying an additional bending moment to the front portion of the seat pan. The distance through which the block moves depends upon the stiffness of the pan and the connections used to attach it to the rest of the structure. It would be time consuming to exactly distribute the mass of the block over the seat-pan for each design modification. Therefore, the practice recommended by this research is to distribute the remaining mass (approximately 31.9kg) as a uniform pressure, with 2/3rd assigned to the front portion (equivalent to 21.3kg), and the remaining 1/3rd to the seat pan mid-portion (equivalent to 10.6kg) as shown in figure 6-12. This arrangement ensures the worst practical loading of a seat pan due to body block rotation in the forward 9g load case.

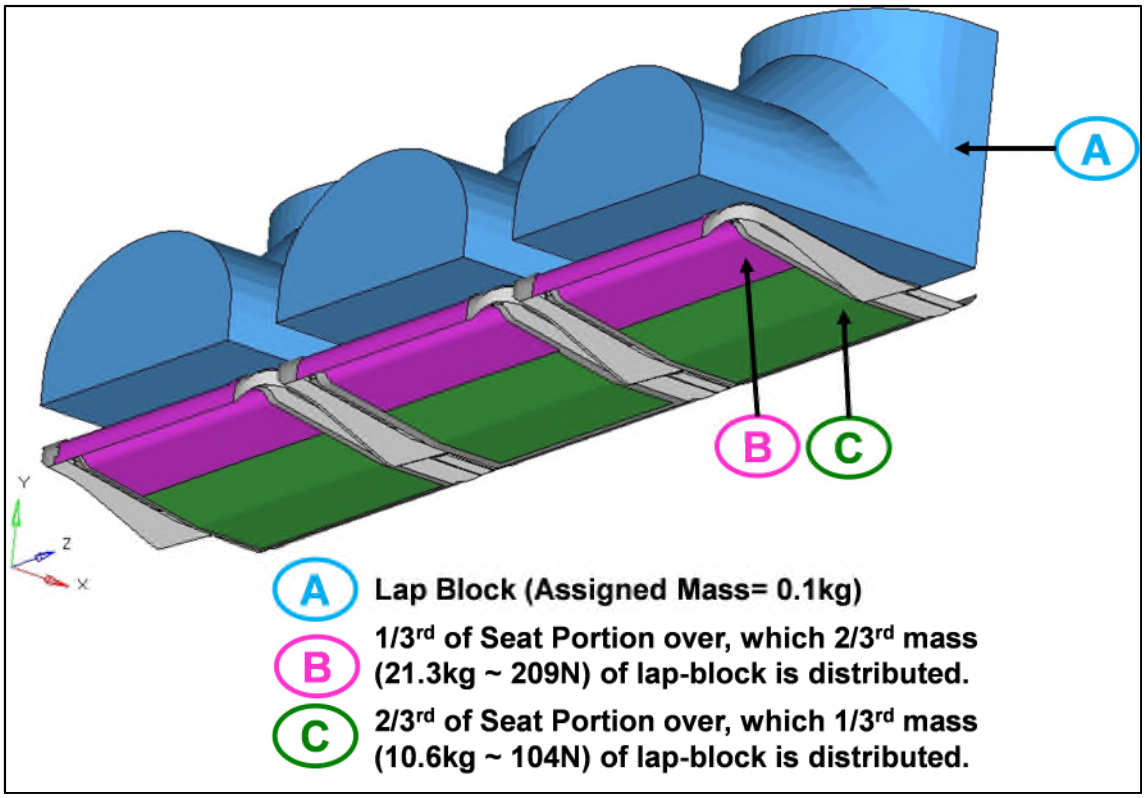

Figure 6-12 Distribution of mass of lap block over the Seat-Pan. In order to control the inertia effects due to lap-block, it has been assigned a mass of 1kg with rigid material properties. Loadcase – Forward 9g, Sideward 4g, Upward 3g

6.3.3 ELEMENT FORMULATION FOR SEAT-BELT

Element formulation 9 (membrane) and 16 (fully integrated shell) are the two different formulations available from LS-DYNA element library to model seat belt. Based on the reference [38], membrane elements were used to model the seat-belt as they exhibit better phenomenon of 'wrap-around the body block' than that observed with formulation 16, which has a high bending stiffness.

Using same procedure as described in Section 5.5.3, a total simulation time of 0.18s (0.15s to achieve 100% of load and 0.3s to hold the load constant) is chosen with a global damping factor of 350 units (as per flowchart, Figure 5-2). Simulation takes about five hours to complete and 5.6 gigabytes of memory with 16 processors. The results have been thoroughly checked as per the procedure developed in Section 5.6 and are quasi-static. Same technique has been used to simulate "Upward 3g" and "Sideward 4g".

6.4 VALIDATION OF FE METHODOLOGY

After performing FE checks, results were compared with those from experimental testing. Formation of plastic hinge at the aft section of the seat-leg ("A" in Figure 6-13) predicted by FEA results was observed during the experimental tests.

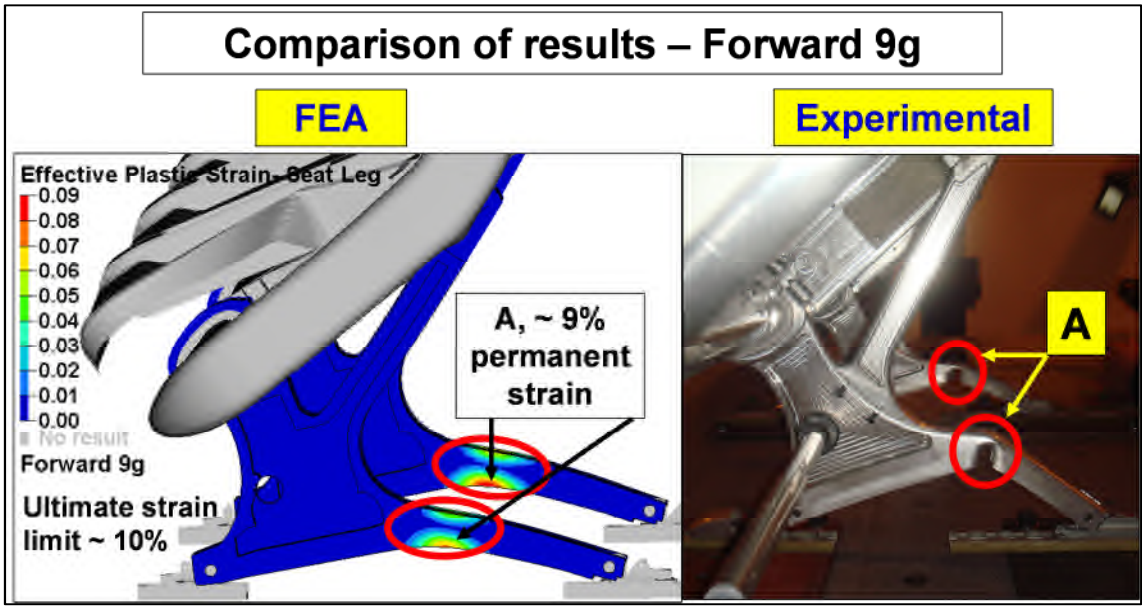

Figure 6-13 Formation of plastic hinge at the underside of the aft section of the leg (Region A) predicted by FEA was observed during experimental tests. Solver - LSDYNA

Methodology was then applied to simulate "Upward 3g" loadcase. FE model used for this exercise is same as that used in "Forward 9g" loadcase. The simulation takes about seven hours for completion with 8 processors. The behaviour of the seat-structure during load application, deformed shape and associated kinematic predicted by FE results are in agreement with those observed during the tests (Figure 6-14).

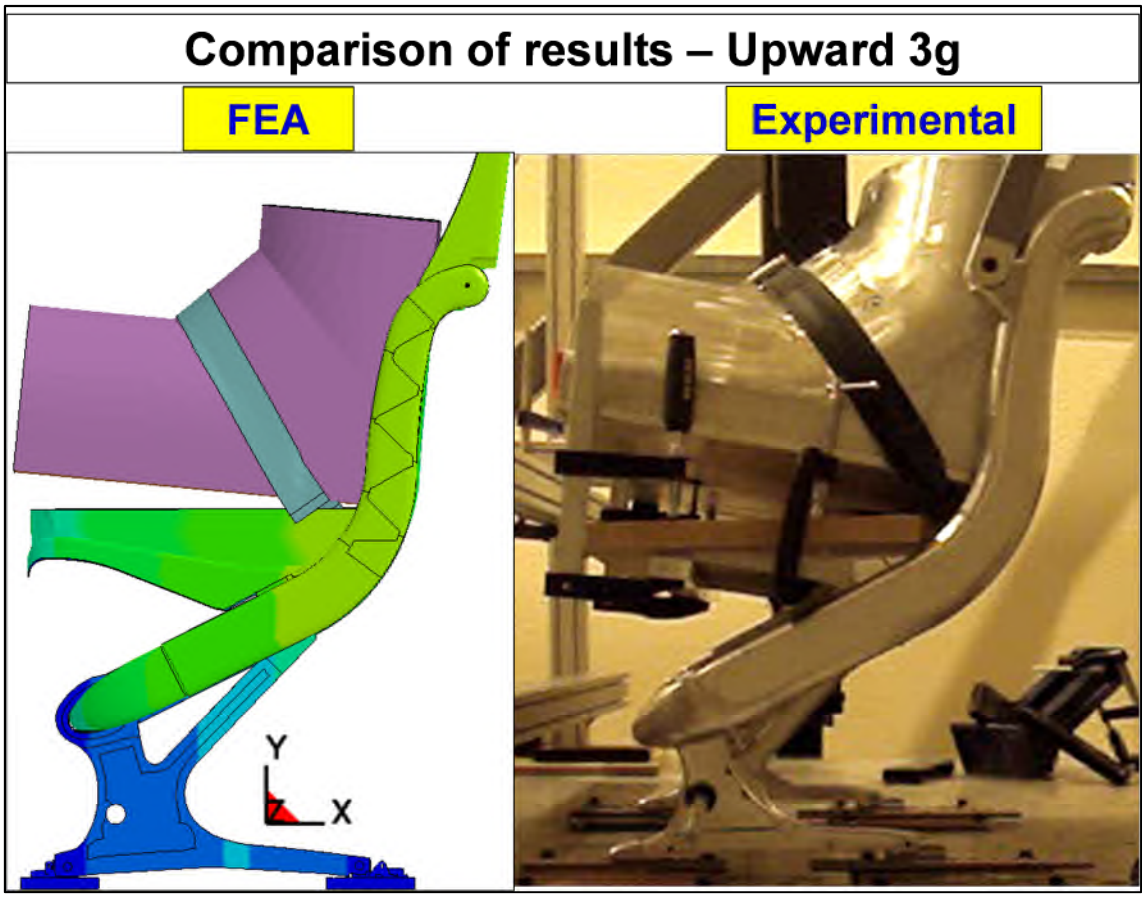

Figure 6-14 Good agreement in the kinematic behaviour of the seat-structure observed between FEA and experimental tests. Solver - LSDYNA

An acceptable agreement between FEA results and test results helped to validate the FE procedure developed in this research.

Conclusion – Chapter 6

A satisfactory solution i.e. converged with implicit formulation (Chapter 4) and quasi-static with explicit formulation (Chapter 5), was obtained for the case study of 'Downward 8.6g' applied to 'triple seat-structure'. In this chapter, these two solutions are compared against each other using parameters such as,

- Overall displacement and the deformed shape,
- VMS induced in the major load carrying members
- Cross-sectional forces
- Reaction forces
- Seat Interface loads and

- CPU time and disk-space required

To start with, an output matrix was developed to extract useful information (parameters defined above) from FE simulation. Results from both the formulations are found to be within reasonable tolerances. However, significant difference is observed in the CPU times (853s with implicit formulation i.e. LSDYNA with quasi-Newton solver and 7821s with LSDYNA / Explicit). The reason being

- FE model built considering the implicit algorithm (fine discretisation to avoid contact failures) was used for explicit simulation resulting in a very small stable time increment and very high CPU time. A further study can be undertaken to reduce the CPU time by coarsening the FE discretisation and/or mass scaling for explicit solution schemes.

After the self-verification of results obtained with two different schemes they were compared against experimental testing. Following observations were made,

- An acceptable correlation was observed in the kinematic behaviour predicted by FEA and recorded during the physical testing.
- Flattening of the lower aft section of the leg was observed in FEA results as well as in test results.
- Vertical downward displacement of the LHS end of the corner beam looking from behind predicted by ‘Implicit’ and ‘Explicit’ scheme is 7.2mm and 7.6mm respectively against 8.7mm observed in test.
- Vertical downward displacement of the RHS end of the corner beam looking from behind predicted by ‘Implicit’ and ‘Explicit’ scheme is 8.5mm and 8.8mm respectively against 9.4mm observed in test.

An acceptable agreement between FEA results (from two methods) and test results helped

- To validate the following assumptions made during FE model building

- To validate both FE procedures developed to use implicit formulation and explicit formulation for demonstrating the static compliance (CS25.561) of an aircraft seat.

Going further, FE approach to simulate the highly nonlinear loadcases in which load is introduced into structure through lap-blocks (such as 'Forward 9g' and 'Sideward 4g' as specified by CS25.561) was developed and following guidelines are proposed,

- A combination of 1D seat belt elements, slip-ring and a rigid support to hold the slip-ring should be used for applying the load to body blocks (also known as lap block). As this method can represent the socket and ball joint arrangement, it is consistent with the loading sequence
- Membrane element formulation should be used to model the seat-belt as they exhibit better phenomenon of 'wrap-around the body block'.
- Representation of actual mass of lap-block without a proper care may over-estimate the stiffness of seat-structure. Therefore, mass of lap block should be artificially reduced so as to transfer approximately the entire applied load to the seat-structure. Remaining mass of lap block can be distributed over seat-pan in terms of equivalent pressure.
- A good indicator of effect of mass of lap block is Kinetic Energy (KE) associated with it. As the mass of the lap block is reduced, their inertia reduces (simultaneously KE) stabilising the response

Proposed methodology was used to evaluate the behaviour of seat-structure under study for the applied "Forward 9g" and "Upward 3g" loads and results were compared with those from experimental testing. Deformed shape and associated kinematics (for both the loadcases) and buckling of the aft section of the seat-leg (in Forward "9g") predicted by FEA were corroborated by experimental tests.

Thus this research is successful in developing validated FE procedures, which can use three different solution methods (Abaqus (Research) 6.9-3, LSDYNA/Implicit and LSDYNA/Explicit) or two different formulations (i.e. Implicit

and Explicit) to assess structural performance of a seat-structure subjected to two categories of static inertia loads according to CS 25.561 i.e.

1. Loadcases in which load is directly applied to the seat-structure (Downward and Rearward loads), which can be solved either implicitly or explicitly.
2. Loadcases in which lap blocks are used for introducing the load in the seat-structure (Forward 9g, Sideward 4g and Upward 3g) and are solved using only explicit formulation.

Any of these methods can be used and tailored to suit the available software and hardware.

7 DAMAGED FLOOR CONDITION – FE SIMULATION AND DESIGN CONCEPTS

In earlier chapters, FE methodology to evaluate the complete seat structure subjected to static loads as specified in CS25.561 has been developed, evaluated and validated. Next step in seat certification is compliance against dynamic loads (CS25.562) known as ‘dynamic compliance’. Hence this research naturally propagates towards developing a robust FE methodology to evaluate the seat structure subjected to dynamic loads as specified in CS25.562.

CS 25.562 specifies two different deceleration pulses to be applied to the structure. A ‘16g’ pulse is applied in a combined longitudinal and lateral direction with ‘damaged floor condition’, whereas a ‘14g’ pulse is applied in a combined vertical and longitudinal direction. The details of these loading conditions and performance evaluation criteria are present in Section 2.1.3.2 of this report.

This chapter starts with a definition and purpose of ‘Damaged floor condition’ and a brief outline of the complex state of loading introduced in the primary load path (forward beam and seat-leg) due to these loads. Literature review presented shows that the ‘16g with damaged floor condition’ is the most challenging loading condition for an analyst to simulate using FEA and for a seat-designer to comply against structural requirements.

Earlier researchers have either failed or compromised on separating the two load cases. Four different methods developed during this research, to simulate damaged floor-condition, are presented next (which is one of the novelties of this research). Results from these different methods are compared against each other as a self-verification check.

The chapter ends with the evaluation of innovative design concepts developed to deal with ‘damaged floor condition’.

7.1 DEFINITION AND PURPOSE

It is the misalignment of the seat anchorages with respect to each other by 10 degrees vertically (i.e. out of parallel, PITCH) whilst the other leg is rolled through 10 degrees (Figure 7-1 LHS) [13]. Deformations are applied locally to the seat-anchorages. 'Damaged floor condition' is also popular as 'Seat-Track Pre-distortion', 'Floor Distortion' and 'Seat Pre-deformation'.

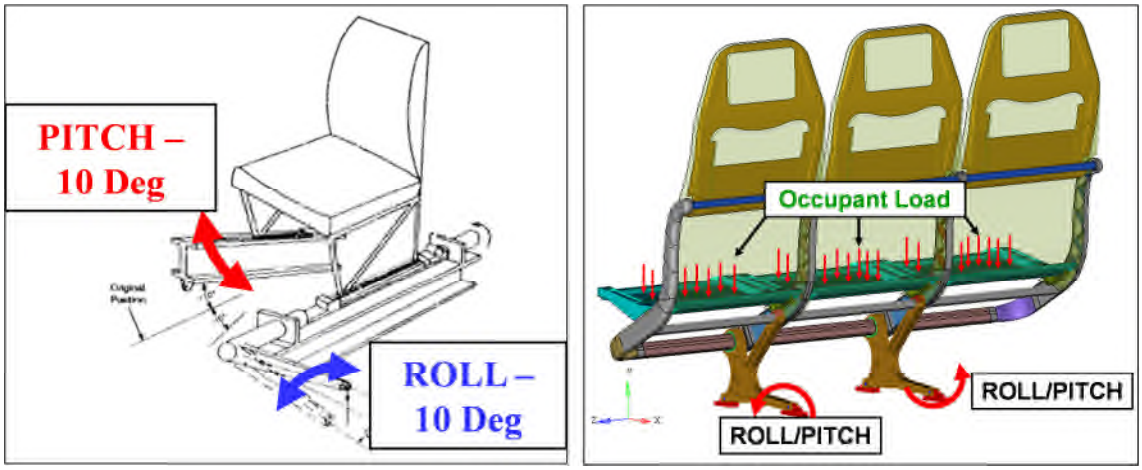

Figure 7-1 LHS - Definition of the Seat Pre-deformation (10 degree ROLL and 10 degree PITCH local enforced displacements creating the misalignment of the seat tracks) [13] RHS - Seat Pre-deformation loads applied to the globally yawed (by 10 degree) triple seat-structure.

Purpose of the initial floor-distortion is to demonstrate structural capacity of the seat structure to withstand the dynamic loads without disintegrating from the Airframe-floor, even when the floor is deformed by the forces associated with primary crash [5, 10, 13, 56]. It is achieved statically by applying the 'pre-deformation' loads to the seat structure that is globally yawed by '10 degree' with respect to the Aircraft Centreline. Actually, '10degree Yawed' orientation is a requirement of 'Dynamic 16g' loadcase. However, as the '16g' loads are applied to the deformed configuration (due to Pre-deformation) of the seat-structure, '10degree Yaw' should be applied to the seat structure prior to pre-deformation (another approach would be to perform the pre-deformation without '10degree Yaw' and to resolve the components of the '16g' loadcase in the corresponding 'Yawed' co-ordinate system).

AS8049 defines the ‘floor deformation’ procedure for various seat design families such as [11]

- Typical seats that use four seat-attachments and four attachments to the aircraft floor (‘Sleep Seat’ design falls under this category) and seats with three legs (one central leg in front or back of the seat, and one leg on each side of the seat)

  Pre-deformation loads are applied to the side legs while holding central leg in its un-deformed configuration.

- No ‘Pre-deformation’ loads are applied to the seats mounted solely to a bulkhead and to the seats that are cantilevered from one sidewall without connection to any other structure.
- Other cases - Seats that are attached to both floor and bulkhead, seats that are mounted between sidewalls or to the sidewall and floor, multiple occupant seat assemblies.

‘Floor-deformation’ Procedure for ‘Sleep Seat’

Triple seat assembly of ‘Sleep Seat’ considered for this exercise has been ‘Yawed ‘clockwise’ by 10 degree (to the aircraft centreline, when viewed from the above) so that the highest loaded leg (Leg-RHS, leg with the largest overhang) is the trailing leg for the test i.e. makes it more critical (Figure 7-2 LHS). Leg-RHS has been ‘Rolled’ counter-clockwise when viewed from behind, Leg-LHS has been ‘Pitched’ down by 10 degrees and Occupant mass of 77kg per seat has been uniformed distributed over the seat-pan.

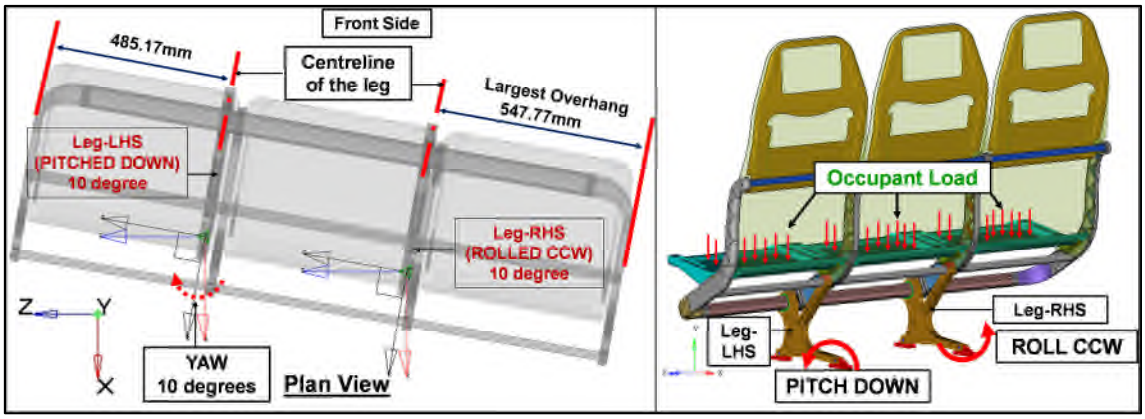

Figure 7-2 Definition of Seat Pre-deformation loads - 10 degree ROLL is applied in Counter Clockwise direction to the trailing leg (Leg-RHS, looking from the rear of the seat) constraining all degrees of freedom (dofs). 10 degree PITCH DOWN is applied to Leg-LHS. Occupant mass of 77kg is uniformly distributed over the Seat-pan.

Please note that the choice of 'YAW' orientation, selection of seat-leg for 'Pitch' and 'Roll' loads can be different for different designs of the 'Sleep Seat e.g. boundary conditions explained Appendix I are for another variant of the 'Triple Seat Assembly' in which, Leg-LHS has the largest overhang and hence it has been 'Rolled' counter-clockwise by 10 degrees. The main principle used for application of 'Pre-deformation' loads in this research is that the leg with the largest overhang should be a 'trailing' leg (achieved by YAW) and it should be 'Rolled counter-clockwise' while 'Pitching down' the other leg (agreed with BlueSky).

7.1.1 DETRIMENTAL EFFECTS ON THE STRUCTURAL CAPACITY OF SEAT – A LITERATURE REVIEW

Because of the Seat pre-deformation loads, seat structure experiences complex state of loading as explained in the following section.

'Rolled' leg experiences (Figure 7-3)

- Bending about longitudinal axis due to the applied 'Roll'. This may result in either complete failure or permanent strain in the weak area between the vertical web and the flange.

- Torsion about vertical axis as a consequence of forward motion of the other end of the Forward Beam as the front anchorage of the ‘pitched’ leg is pulled down.
- Bending about lateral axis induced by ‘pitching’ deformation and consequent Forward beam torsion
- Compression in the front flange and tension in the rear flange
- Out-of plane bending due to the Occupant loads

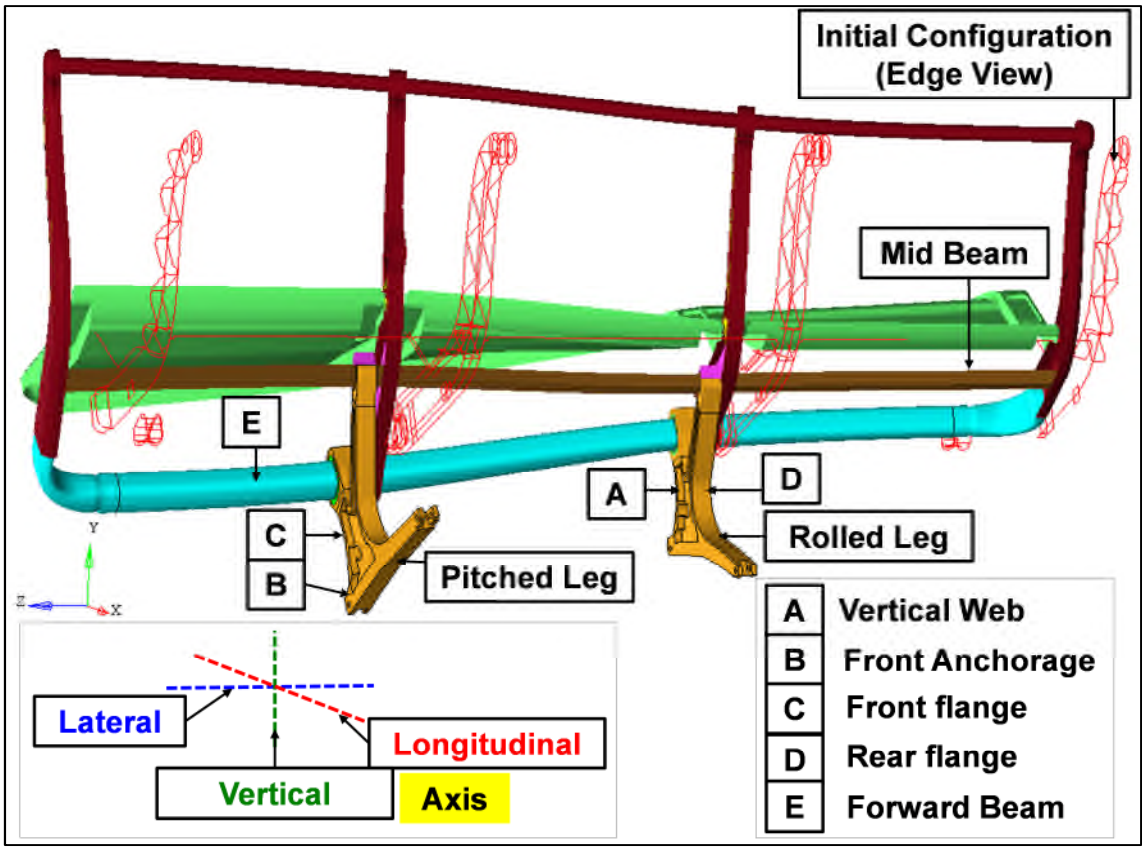

Figure 7-3 Seat Pre-deformation applied to the "Sleep Seat" considerably deforms the structure and induces high stress levels in the Seat-Legs and the Forward Beam. Deformed plot is scaled up by a factor of two for better visualisation.

‘Pitched’ leg experiences

- Tension in the vertical web due to the applied ‘Pitch’
- Bending about longitudinal axis because of the ‘Rolling’ deformation
- Failure of the front anchorage if the structure is ‘un-giving’ i.e. too stiff
- Out-of plane bending due to the Occupant loads

'Forward Beam' is subjected to

- Considerable torsion about lateral axis due to 'Pitching' deformation applied
- Bending about lateral axis of the Seat due to the 'Rolling' deformation applied
- Bending about vertical axis of the seat due to the 'Pitching'
- Bending due to the occupant loads

Boomerangs may show high permanent strain or may break depending on the stiffness of the secondary structure of the seat

Thus the entire seat structure experiences asymmetric complex loading due to pre-deformation loads. Such a state of stress may lead to a discontinuity in the load path even before the deceleration pulse is applied.

Stephens conducted a study of the crashworthiness of the civil aircraft seats, which comprised of a series of full scale dynamic tests on various commercial and prototype seat designs [65]. The author found many shortcomings in the design of the seats as a result of lack of a provision for the 'pitch release' and the 'roll release' in the floor-track fittings. Lack of 'Pitch' release resulted in either the permanent failure of the seat structure or failure of the seat anchorages detaching the seats from the floor. Lack of 'Roll' release ended in asymmetric loading of the seat anchorages and prying of the lips of the Seat-track.

The author concluded that a provision must be made in the seat structure to accommodate the pre-deformation without significant failure of the seat structure.

7.1.2 EARLIER ATTEMPTS TO INITIATE DAMAGED FLOOR CONDITION IN '16G' TEST – A LITERATURE REVIEW

Bhonge has applied pre-deformation loads, simultaneously with the '16g' pulse during the dynamic FE evaluation of a seat, for business jet [5]. The author has compared the interface loads acting on the most heavily-loaded legs (in tension and compression) established using FEA and experimental testing, for the

complete loading sequence of ‘16g’. Though the results agree in the later part of the loading i.e. after 16g pulse is applied; significant differences are observed during the initial loading. The author attributes these differences to the difference in the methods of applying Seat Pre-deformation in physical testing and his FEA methodology. During test, Seat Pre-deformation has been applied statically before application of the ‘16g’ pulse (as specified in the regulation FAR 25.562/ FAR 23.562) whereas in FEA it has been applied simultaneously with the ‘16g’ pulse.

Dhole has discussed the validation of the FE model of a typical transport category aircraft seat under Part 25.562 dynamic test conditions [23]. Seat pre-deformation has neither been considered in the FE simulations nor in the experimental testing. However, the author recommends validating the FE model for Pre-deformation for the future research.

Olschinka has discussed static and dynamic simulation of the passenger seats [22]. Out of three seats discussed, two have been analysed for ‘16g’ without applying ‘Seat Pre-deformation’. For the third ‘Business Class’ seat, the author attempted to include the seat pre-deformation in the dynamic simulation and tried to simulate the Pre-deformation loadcase with an Implicit solver (LS-DYNA) and Explicit solver (overlay of pre-deformation and 16g).

Since the Implicit code stuck in the convergence difficulties, the author chose to use solely explicit solution sequence to incorporate both the load cases. However it was quite challenging because pre-deformation must be applied in a small time-span to keep the explicit CPU time realistic at the same time, undesirable inertia effects should be avoided. In the paper presented, the author has not qualitatively investigated the FE results of the later method.

Further, the author has compared the experimental results and the results of the virtual simulations for the ‘Dynamic 16g Pulse’ applied to the ‘Foldable passenger Seat’. Seat Pre-deformation is considered during the experimental testing and not during the virtual simulations. Two major drawbacks of the seat-design i.e. rupture of the rear seat-leg and detaching of the ruptured leg from the seat-track highlighted by the experimental testing were not revealed by the

FEA results (only indication by FEA results was increase in the seat interface loads above the allowable limits). The author concludes that the most probable reason for these differences; is the absence of the pre-deformation of the seat structure during the FE simulation of the '16g' loadcase.

All these examples underline the need to develop a methodology to simulate and include the pre-deformation in a reasonable way in the dynamic simulation.

7.2 WHAT HAS BEEN ADDRESSED BY THIS RESEARCH?

It can be concluded that earlier attempts associated with Seat Pre-deformation have either failed in one or all of the following areas

Successful solution by FEA

- To obtain a converged solution by Implicit solution method
- To obtain a reliable or qualitatively verified solution by an Explicit solution algorithm
- To include the pre-deformation results in the 'Dynamic 16g' as specified in the CS25.562

Failure to accommodate the pre-deformation loads in the 'Dynamic 16g' simulation has resulted in significant discrepancies between the test results and the FEA results.

Satisfactory Design

- To obtain a seat design, which can sustain the pre-deformation loads; without significant structural damage or permanent failure

This research provides not only different verified FE approaches to perform the pre-deformation but also different design ideas to minimise the detrimental effects of the pre-deformation loads on the seat structure.

To start with, FEA solution techniques developed and verified against each other are presented. In the next phase, these simulation techniques have been applied to assess the suitability different designs concepts developed to deal with pre-deformation loads. In chapter 9, two different methods to initiate the

deformed configuration and stresses in the seat structure (due to pre-deformation loads) in a dynamic '16g' loadcase have been presented.

The FE model of the complete seat structure considered for following methods to simulate 'Seat Pre-deformation' loadcase consists of 187528 nodes and 196317 elements. Lower order reduced integration elements with appropriate hourglass control are used to build the FE model to be compatible with the dynamic simulations.

7.2.1 PRE-DEFORMATION USING ABAQUS (RESEARCH) 6.9-3 - METHOD A

The boundary conditions applied to the FE model of the 'Sleep Seat' to perform the pre-deformation are explained in detail in Appendix I. The main bottleneck in obtaining a satisfactory FE solution is 'Non-convergence'. All the guidelines outlined in the Section 4.3 of this thesis have been followed during model building. The methods those were particularly helpful are,

- Use of volume based stabilisation
  - The ratio of the stabilisation energy (ALLSD) to the IE (ALLIE) of the whole model is 1.4% and is below the allowable limit of 5% [33].
- Use of automatic smoothening of the contact segments
- Achieving the 100% load in small increments with automatic load increment
  - Initial load increment specified is 0.5% of the total load. Then the 'automatic time-step increment' of Abaqus (Research) 6.9-3, which adjusts the size of the load increment based on the convergence behaviour of the model, is used.
- During initial trial simulations, message file is thoroughly checked for any slave nodes missing corresponding master segment or for slave nodes those are not tied to the master segment because they fall out-of the 'position' tolerance.
- Soft springs attached to the parts held only by contact (Figure 7-4)

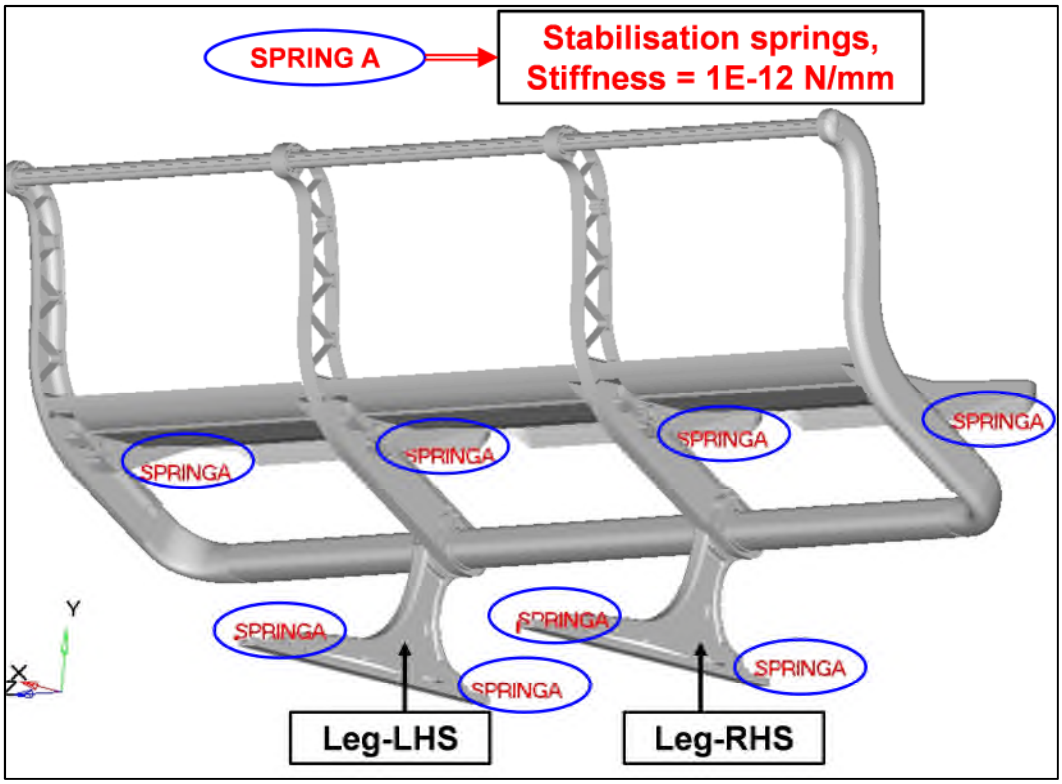

Figure 7-4 Stabilisation springs attached to the parts held only by contact (e.g. boomerang, tool-less fittings) and grounded at the other end. Negligible stiffness ensures no influence on the solution results. However, their presence avoids rigid body motion thereby initialising the solution process. Solver – Abaqus (Research) 6.9-3.

Careful execution of all these guidelines leads to a 'converged' FE solution of the 'Seat Pre-deformation' loadcase. Results are discussed in the Section 7.3 of this chapter.

7.2.2 PRE-DEFORMATION USING LS-DYNA (IMPLICIT) - METHOD B

The boundary conditions applied to the FE model of the 'Sleep Seat' to perform the pre-deformation using LS-DYNA 'Implicit' solver, 'Explicit' solver and the solver using 'Automatic switch between Implicit and Explicit' are same and are explained in detail in Appendix I.

Pre-deformation loadcase has been simulated in LS-DYNA (Implicit) by activating the 'Full Newton' by specifying ILIMIT equal to 1 on *CONTROL_IMPLICIT_SOLUTION [35]. Load increment is controlled by

‘Automatic Time stepping’ option of LS-DYNA. The guidelines specified in Section 4.2.5 and Section 4.3, have been collectively applied to obtain a converged solution.

7.2.3 PRE-DEFORMATION USING LS-DYNA (EXPLICIT) - METHOD C

The technique developed in Section 5.4 has been used to solve the pre-deformation loads applied to the FE model of the ‘Sleep Seat’. A very important point that should be taken care of is the restraints applied to the seat while estimating its first mode of frequency.

The restraints applied should be same as used for the ‘Pre-deformation’ load case (Figure 7-5 LHS) i.e.

- The point at which ‘Pitch’ is applied should be constrained for all the degrees-of- freedom except rotation corresponding to the ‘Pitch’ definition and
- The point at which ‘Roll’ is applied should be constrained for all the degrees-of- freedom except rotation corresponding to the ‘Roll’ definition

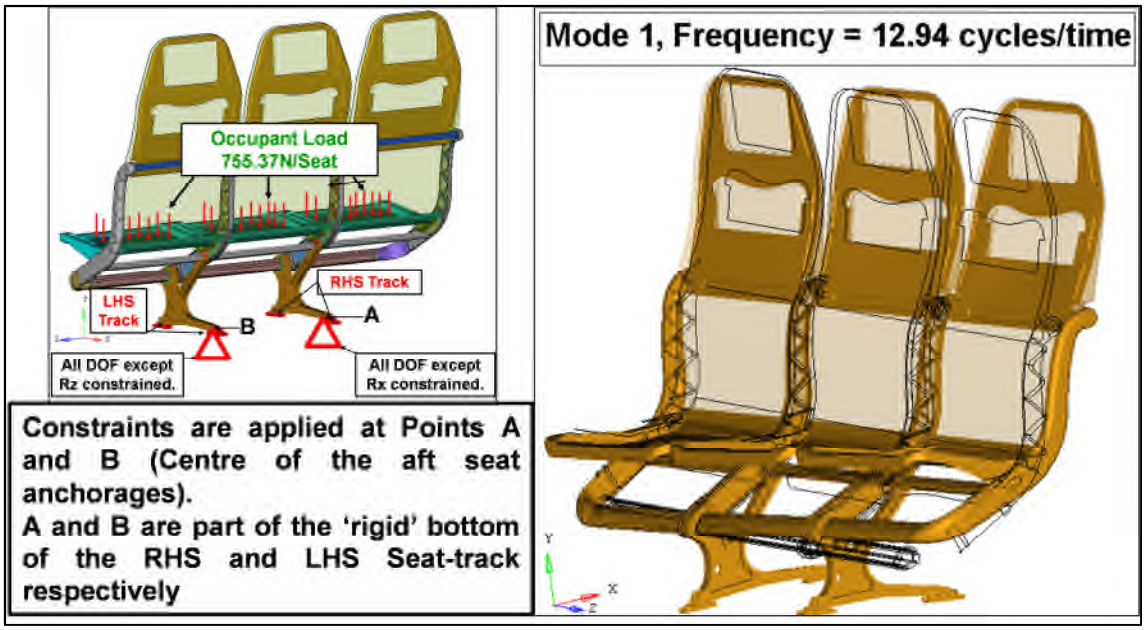

Figure 7-5 LHS -Constraints as applied during 'Seat Pre-deformation' for estimating the first mode frequency of seat structure. Points A and B are the centre of the aft seat anchorages where the pre-deformation loads are applied [10]. They have been attached with respective seat-tracks using *CONSTRAINED_EXTRA_NODE-RIGID definition of LSDYNA. Uniform mass scaling of 5 has been done. RHS – Frequency of first mode of vibration is ~13Hz.

Density of all the materials used for different components of the FE model of the triple seat-structure has been scaled up by '5' to achieve a uniform mass scaling of 5 to improve the minimum stable size of the time-step increment. The frequency of the first mode of vibration is 13 Hz. Thus the damping parameter VALDMP on *DAMPING_GLOBAL control card is set equal to 165 (calculated fusing Equation 5-3). The 100% of the prescribed 'Pitch' and 'Roll' displacements are obtained in 0.15s and thereafter held constant for 0.03s to stabilise the response (same time frame as used for 'Forward 9g' loadcase evaluated using explicit dynamic integration scheme). The resultant solution has been ensured to satisfy all the qualitative and quantitative checks discussed in Section 5.6 to guarantee an acceptable quasi-static solution. The maximum ratio of KE to IE is approximately 0.9% and 0.07% during load holding (i.e. from 0.15s to 0.18s) period ensuring a quasi-static solution. The results are discussed in Section 7.3.

7.2.4 PRE-DEFORMATION USING LS-DYNA IMPLICIT/EXPLICIT AUTOMATIC SWITCH - METHOD D

The FE model and the settings of the control cards used for the LS-DYNA environment with an 'automatic switching between an implicit solver and explicit solver with mandatory implicit finish' (hereafter called as Implicit/Explicit Switch) are same as that used for LS-DYNA Implicit except,

- Implicit/Explicit Switch method is activated by specifying IMFLAG equal to 5 on *CONTROL_IMPLICIT_GENERAL [35]
- DTEXP equal to 1E-4 on *CONTROL_IMPLICIT_AUTO. With 'Implicit/Explicit Switch', the solution algorithm begins as implicit. If it is stuck for convergence of equilibrium iterations, it automatically switches to the explicit time integration method for a time interval of DTEXP. A small value of DTEXP is suggested by the author of this report to avoid development of significant dynamic effects during the explicit phase so that in the succeeding implicit phase it is possible to recover the static equilibrium [35].

A uniform initial mass scaling of '5' has been achieved by scaling up the material densities. Care should be taken in case where much switching occurs between implicit solver and an explicit solver, which may develop unacceptably high inertia effects introduced during the explicit phase. The results are discussed in Section 7.3.

7.3 COMPARISON OF METHODS A, B, C AND D

The comparison has been made based on three important parameters

- Magnitude and the contour of the resultant overall displacement
- Magnitude and the contour of the von Mises stress, VMS for Forward beam and Seat-Leg (components of primary load path)
- Seat Interface loads

7.3.1 OVERALL RESULTANT DISPLACEMENT

Displacement plot of the FE model of the 'Sleep Seat' after the 'Seat Pre-deformation' loadcase simulated by method A, B, C and D leads to the following remarks (Figure 7-6),

- The contour of the overall displacement and the deformed shape of the structure are approximately same for all the methods.
- The magnitude of the maximum overall displacement shows a variation of +7.7% considering the 200.8 as base value (i.e. 200.8mm is the maximum displacement obtained with LS-DYNA Implicit, Method B).
- The solution with LS-DYNA 'Implicit/Explicit Switch' shows a small increment in the maximum overall displacement over that with LS-DYNA Implicit because of the inertia effects introduced in the system during explicit solution phase. An increment of approximately 1.2% over the implicit response shows that
    - The solution is Implicit for most of the time and
    - The Inertia effects are insignificant.
- The solution with LS-DYNA Explicit method (Method C) shows the highest maximum displacement among the other two solutions obtained with LSDYNA environment. This is natural as the quasi-static problem has been solved using an explicit time integration scheme. However, the difference between the results with Method B and D is 7.7% indicating that the inertia effects are not significant.
- The reason between the difference in the results obtained by Abaqus (Research) 6.9-3 and the LS-DYNA environment could be because of difference between the contact algorithms and the element formulations.

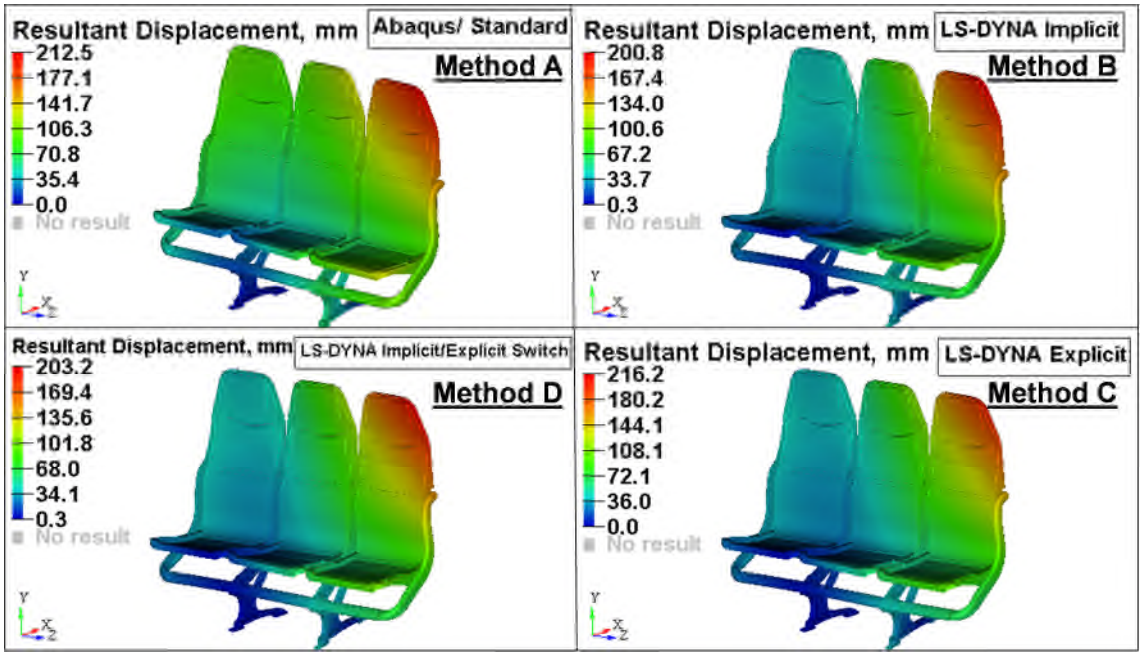

Figure 7-6 Magnitude and the contour of the resultant overall displacement for the 'Triple Seat Assembly' as a result of application of Pre-deformation loads, performed by Method A, B, C and D.

7.3.2 VMS FOR FORWARD BEAM AND SEAT-LEG

While comparing the methods A, B, C and D on the basis of stress levels induced, all the stress components for all the individual components of the 'Sleep Seat' have been considered and have been found to be within a reasonable tolerance. However, VMS contours of only 'Forward Beam' and 'Seat-leg' have been produced and compared in this report to keep it brief. Being the members of 'Primary Load Path', they experience severe loads due to the Seat Pre-deformation loads. The highly localised stresses (contact noise) if any, have been ignored and are not reported here.

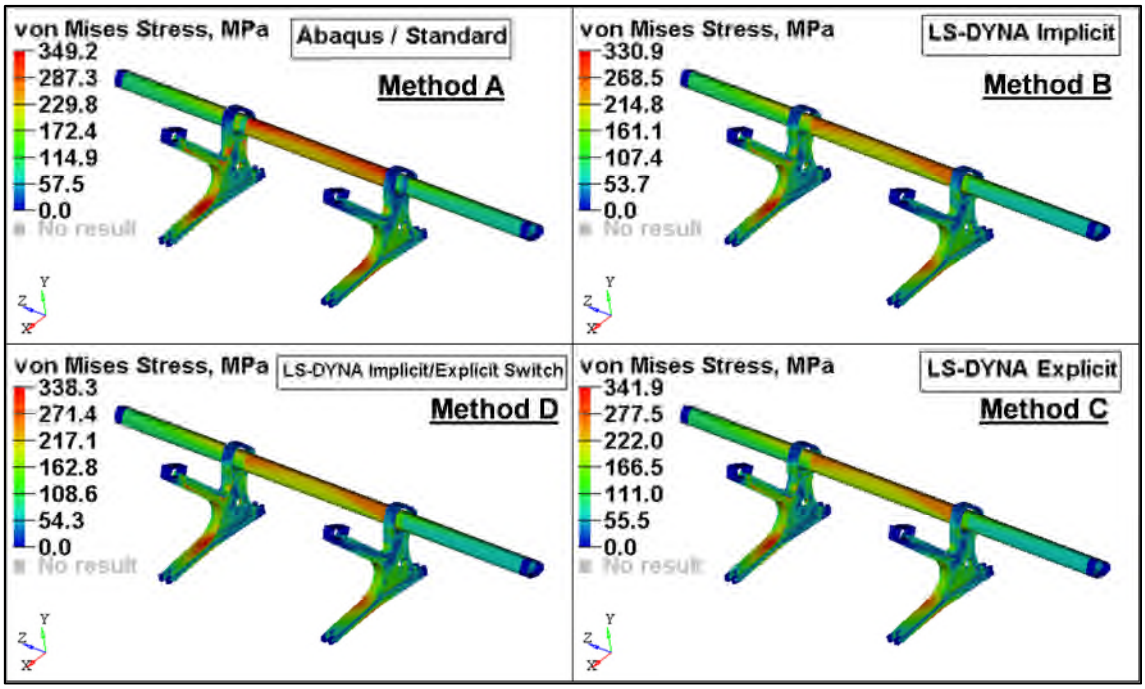

Figure 7-7 Magnitude and the contour of the VMS for Forward beam and Seat-Leg as a result of application of Pre-deformation loads, performed by Method A, B, C and D

The remarks on the VMS plots of the FE model of the 'Sleep Seat' after the 'Seat Pre-deformation' loadcase simulated by method A, B, C and D can be summarised as (Figure 7-7),

- The overall distribution of the VMS on the subassembly of the Forward beam and the Seat-leg is approximately same for all the methods.
- The magnitude of the maximum VMS shows a variation of +5.5% over the base value of 330.9 (The maximum VMS observed in Method B is the lowest among four methods and is 330.9MPa).
- The VMS observed with 'Method C' and 'Method D' is slightly higher than that with 'Method B' because of the inertia effects introduced in the system during explicit solution phase. However, the difference is within an acceptable limit.
- The reason between the difference in the results obtained by Abaqus (Research) 6.9-3 and the LS-DYNA environment could be because of difference between the contact algorithms and the element formulations.

7.3.3 SEAT INTERFACE LOADS

Seat Interface loads have been recovered for all the four methods using the procedures outlined in the Section D.4. The interface definitions chosen for the comparative study are, the interface between (Figure 7-8)

- RHS Front tool-less fitting (main body) and the seat-track
- RHS Rear tool-less fitting (main body) and the seat-track
- LHS Front tool-less fitting (main body) and the seat-track
- LHS Rear tool-less fitting (main body) and the seat-track

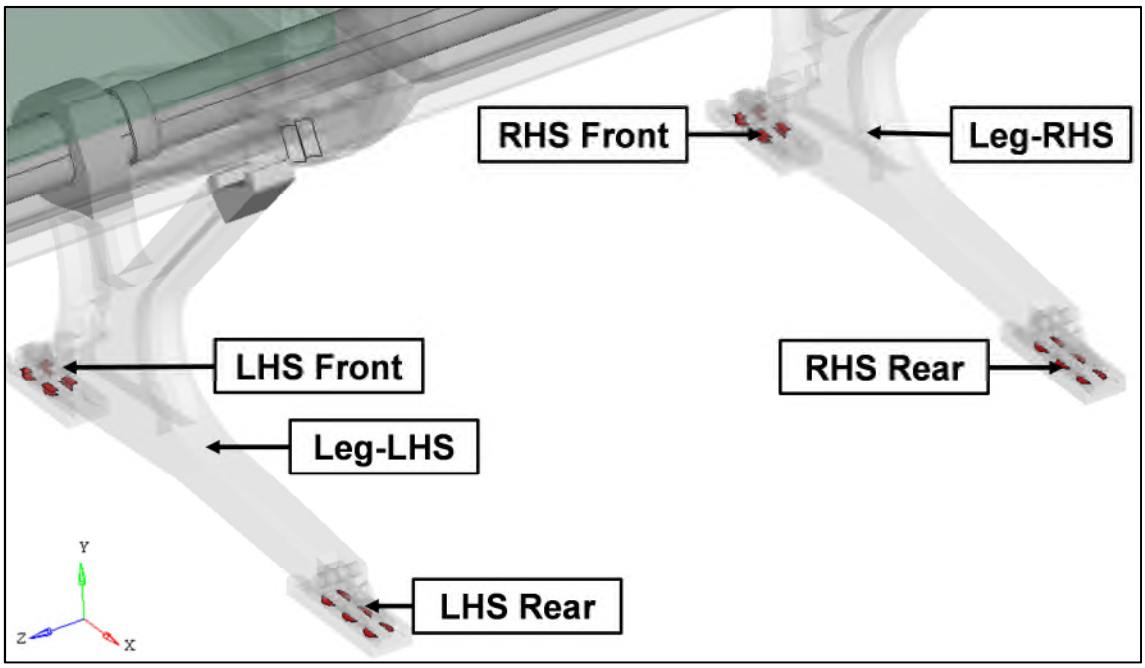

Figure 7-8 Nomenclature for Seat Interface Loads

It can be seen from Table Number 7-1 that

- The trend of the seat interface loads observed for the four methods is same.
- There are no significant differences between the X, Y and Z components of the seat interface loads.

Loadcase - Seat Pre-deformation												
	X, Y and Z Components of the Seat Interface Forces, N											
Interface Definition	Abaqus (Research) 6.9-3 (Method A)			LSDYNA-Implicit (Method B)			LS-DYNA- Explicit (Method C)			LSDYNA-Implicit/Explicit (Method D)		
	Fx	Fy	Fz	Fx	Fy	Fz	Fx	Fy	Fz	Fx	Fy	Fz
RHS Front	3434.0	-9264.4	-1516.4	3329.1	-9163.6	-1592.5	3513.6	-9414.2	-1627.2	3423.3	-9200.0	-1517.7
RHS Rear	-3080.8	9978.7	1609.9	-2988.8	9912.8	1588.9	-3179.8.	10215.6	1700.0	-3009.1	10107.1	1509.2
LHS Front	-5360.6	9015.3	-1159.4	-5189.5	8999.2	-1136.5	--5462.3	9251.3	-1207.2	-5214.8	9119.3	-1197.3
LHS Rear	5024.0	-9964.2	-39.7	5058.1	-9812.5	-34.9	5241.0	-10117.6	-47.5	5049.3	-9904.8	-31.9

Table 7-1 Comparison of the Components of the Interface forces acting on the interface definitions between various tool-less fittings and the seat-track (please refer Figure 7-8 for the nomenclature), calculated by different Solution Techniques. It can be observed that there a close co-relation between the interface loads. Loadcase – Seat Pre-deformation applied to 'Triple' structure of 'Sleep Seat'.

7.3.4 CONCLUDING REMARKS

- The objective of this exercise is to establish the solution procedures with two solution platforms: Abaqus (Research) 6.9-3 and LS-DYNA; which would provide an acceptable solution for the problem of the 'Seat Pre-deformation' loads applied to the FE model of the complete 'Sleep Seat'.
- The problem was attempted using four different methods A, B, C and D (explained in Section 7.2) based on two major solution environments: Implicit integration and dynamic explicit time integration.
- All the four methods yielded satisfactory solutions (from FE point of view e.g. a converged solution with implicit formulation and a quasi-static finish with explicit time integration).
- The methods are compared against each other based on three important parameters:
    - Overall displacement and the deformed shape,
    - Magnitude and the contour of the VMS for major load carrying members and
    - Seat Interface loads

  Based on these parameters the structural response of the 'Sleep Seat' subjected to the 'Seat Pre-deformation' loads; estimated by the four methods A, B, C and D is within acceptable tolerance.
- However, the four methods have not been compared for the CPU time and disc space and memory requirements. The reason being
    - The same FE model has been used for implicit and Explicit calculations. The model was basically built considering the implicit algorithm (fine discretisation to avoid contact failures) and hence resulted in a very small stable time increment for explicit algorithm (though the uniform mass scaling of '5' was used to increase the time-step) and hence very high CPU time.
    - A further study can be undertaken to reduce the CPU time by coarsening the FE discretisation and/or mass scaling for explicit solution schemes

To conclude, this research has developed four different methods to solve the 'Seat Pre-deformation' loadcase and any of these methods can be used and tailored to suit the available software and hardware.

7.4 NOVEL DESIGN SOLUTIONS TO MINIMISE THE DETRIMENTAL EFFECTS OF SEAT PRE-DEFORMATION

This section demonstrates application of FE procedures developed in Section 7.3 to evaluate the different designs of the 'Sleep Seat' and novel design concepts developed during present research.

7.4.1 DESIGN IDEAS TO DEAL WITH SEAT PREDEFORMATION – LITERATURE REVIEW

Pre-deformation is an 'enforced' displacement type of load and hence seat designers should re-act on this from a different angle than that used for force-type loads.

The common response of the seat-designers who encounter a failure of the seat-structure due to the 'Pre-deformation' loads is to strengthen the seat [4]. However, such a 'design-improvement (?)', produces even higher loads during 'Pre-deformation'. Hence better approach is to reduce the stiffness of the seat, which may also improve its energy absorbing characteristics.

'Aircraft Crash Survival Design Guide' emphasises on considering the possibility of a severe distortion of the floor-mounted seat (due to the floor distortion caused by impact forces) during design stage [3]. It states that the seat structure should withstand the floor deformation without separation of primary load path or deflections beyond stated limits. It suggests a possible design of a seat anchorage with a deliberate formation of the plastic hinge upon application of floor-deformation. It should also sustain the compressive, tensile and shear loads to retain the seat while yielding in bending during floor-deformation.

The rear legs of a crew-seat of US Army helicopters used to be attached to a base with castings. These castings failed repeatedly in accidents due to the combined effect of axial and bending stresses as the provision was not made for relative seat leg-to-floor rotation [3]. When the juncture between the rear-leg

and the track was changed from a fixed-to a pinned-end, the load carrying capacity of the seat was almost doubled [3]. This design guide also reports few additional methods to provide a torsional and moment release of the cross-members twisted during floor-deformation. Two of them are

- Slots in the end-fittings of a cross-member can provide a torsional release during floor-warping (Figure 7-9 LHS).
- A fully released joint can be designed to handle two torsional loads and a moment (Figure 7-9 RHS).

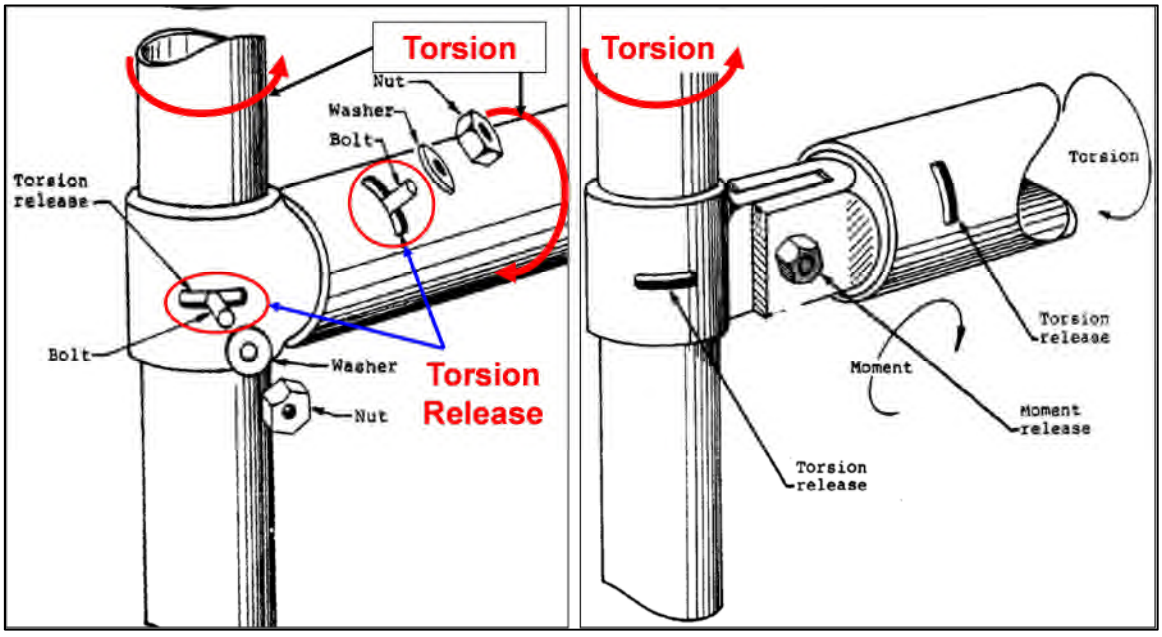

Figure 7-9 LHS - Slots to provide a tortional release, RHS - Slots and a pinned joint to provide a complete release against the bending moments produced due to floor-distortion [3]

The report also discusses the floor-deformation applied to the bulkhead-mounted seats, and combined sidewall-mounted and floor-mounted seats used in helicopters.

Ball and socket joint can be added in the design of seat anchorages to reduce the interface loads between the seat-structure and the floor due to damaged floor [4]. A combination of plastic hinge about one axis and rotation about a pin orientated along a perpendicular axis is also acceptable as long as the seat is not detached from the floor.

7.4.2 “STAY-OUT” ZONE

According to the “Airlines Specification”, a “Stay-out Zone” is incorporated in seat leg to eliminate direct loading of leg during floor deformation [57]. ‘Stay-Out Zone’ is the minimum vertical clearance between top of the seat track and any seat structure (in ‘Sleep Seat’ foot section of the leg) in the span from front connection to aft pivot. At mid span, the clearance should be 12.7mm (0.5 inches) with a gradual decrease to 2.5mm (0.1 inch) towards either end (Figure 7-10-B).

‘Stay-Out Zone’ can be provided by any of the two options:

- Maintain the clearance by initial design geometry or
- Achieve the clearance by applying a total up-load not exceeding 4448N (∼1000 lb) to the seat structure

In the design of the ‘Sleep Seat’, ‘Stay-Out’ Zone has been achieved by maintaining the specified clearances in the initial design geometry (Figure 7-10 A)

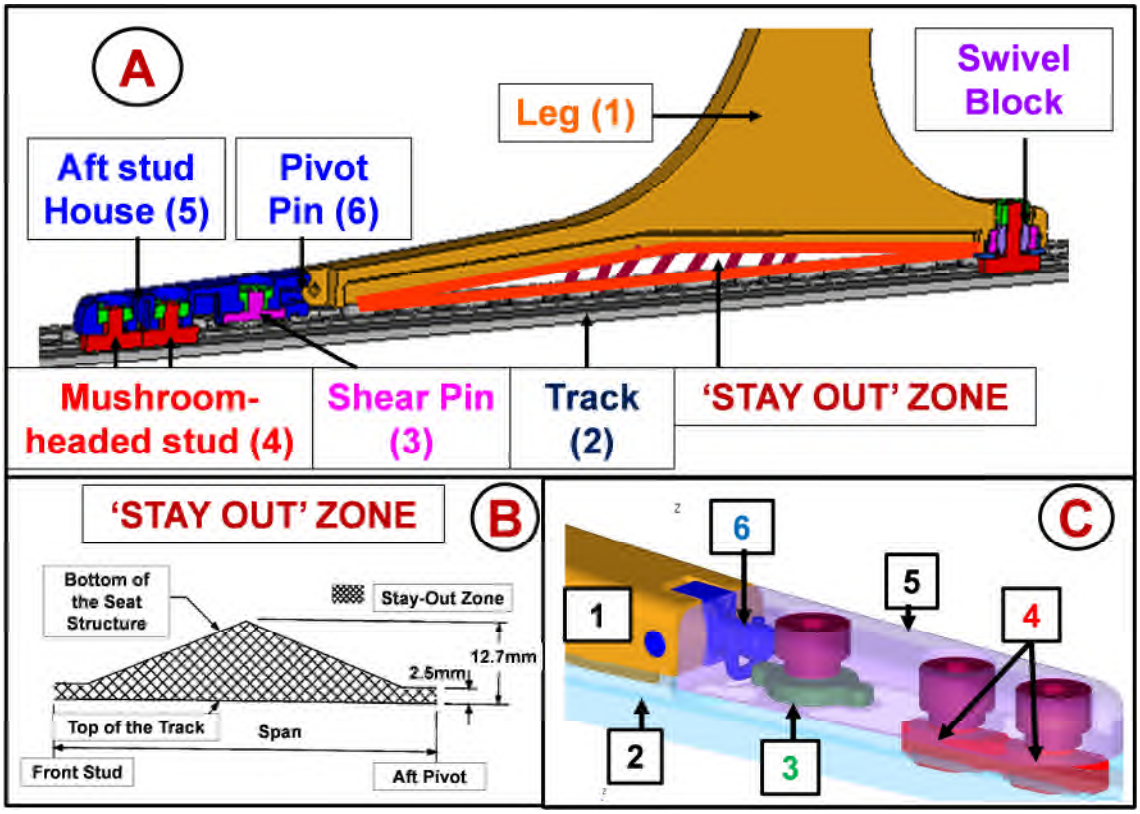

Figure 7-10 A. Cross-section of the Conventional "Aft Stud Housing" in the rear and "Swivel bearing" in the front, B. Definition of 'Stay-Out' Zone C. Aft Stud Housing (ASH) attached with leg through "Single Pivot Pin" and with track through mushroom-headed studs and shear pin [57]

Conventionally, "Aft Stud Housing" and the "Single Pivot pin" connections are used to fasten the seat structure to the seat track (Figure 7-10 A, C). However, shortcomings of such a joint are near-yield stresses induced in the leg, poor performance of the linkage during CS 25.561 and high initial assembly time (Details are present in Appendix A).

Therefore new means of anchorage were very much essential from safety aspect as well as to reduce the effort and time required to mount the seat on the aeroplane floor.

7.4.3 DESIGN SOLUTIONS TO NEGATE THE APPLIED 'ROLL'

Tool-less Fittings (TLF, explained in detail in Section 3.1.1) offered significant reduction in the time required for the initial assembly and switchover between the compartments, increased assistance while positioning the seat in the

aeroplane, prevented rattling and vibration caused due to aircraft operation [29, 30]. However, the problem of very high stress levels in the leg when subjected to the “Roll” of 10 degrees still persisted. Therefore, two modifications are suggested in the design of the TLF.

7.4.3.1 SPHERICAL TOOL-LESS FITTINGS

A ‘Spherical Joint” instead of the ‘Pinned Connection (Part 6 from Figure 7-10)’ at the Seat-leg and TLF interface (Figure 7-11 LHS) helped to completely alleviate the stresses induced due to the applied “ROLL” (Figure 7-11 RHS).

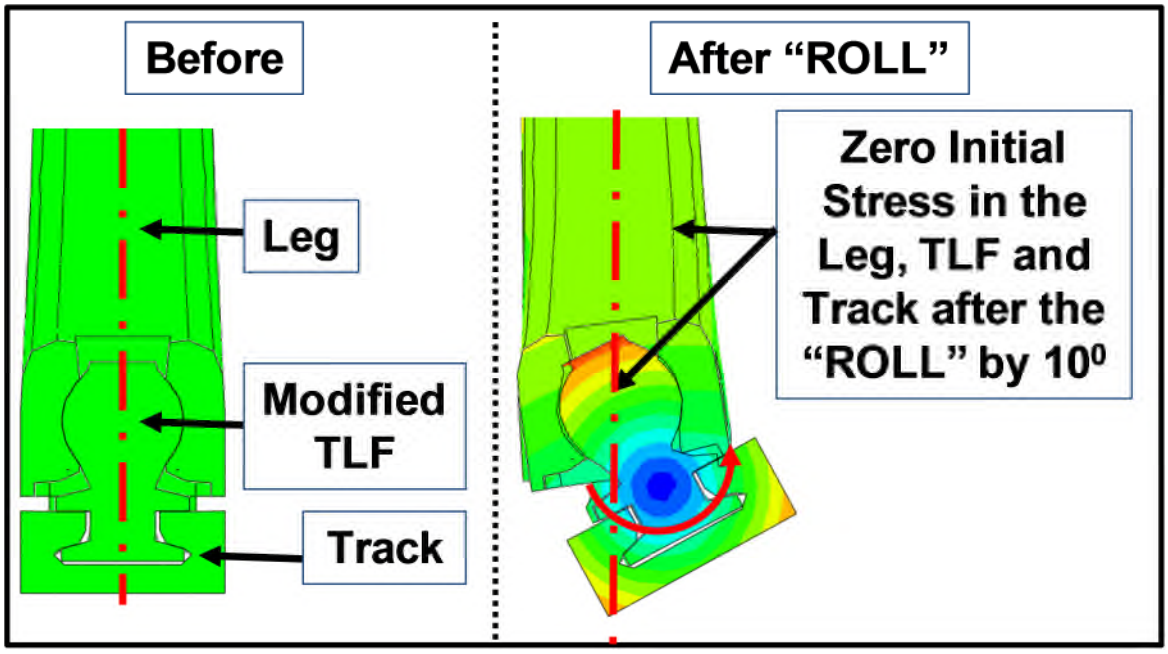

Figure 7-11 LHS-Cross-Section of the Seat-leg, Modified Tool-Less fittings (TLF) and the Seat-track before "ROLL" application, RHS – Un-deformed Seat-Leg and no stress initialisation in the seat structure "After Roll" due to the MODIFIED TLF

7.4.3.2 CONICAL TOOL-LESS FITTINGS

Alternatively, a conical recess can be provided in the TLF (Figure 7-12). If the design of the TLF cannot be changed then recess for 10 degree release can be provided in the Seat-leg (Figure 7-13).

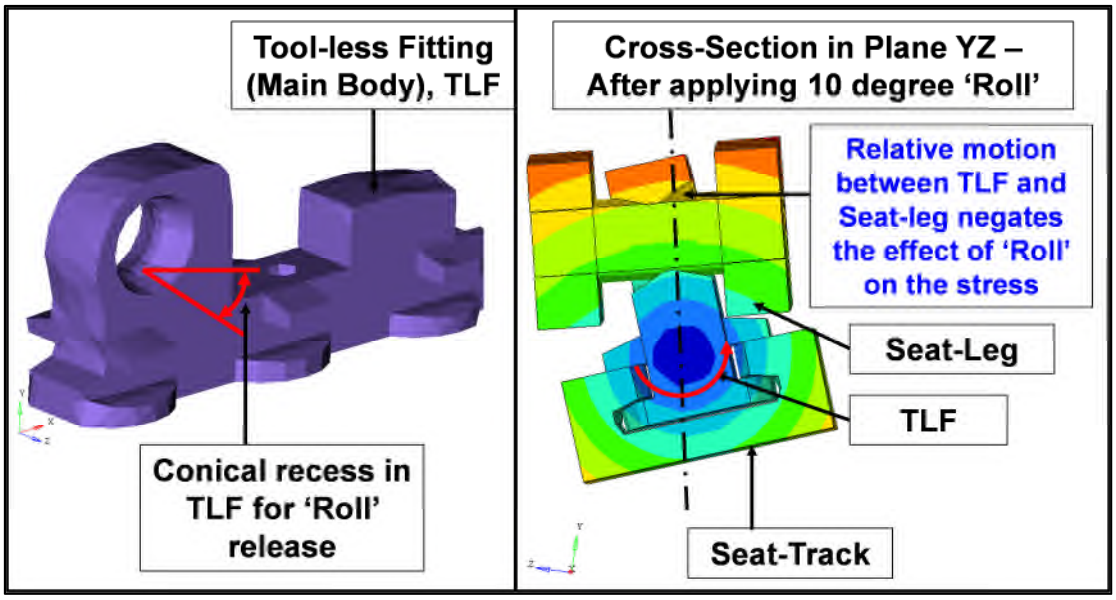

Figure 7-12 Conical recess provided in the main body of the tool-less fitting to allow relative movement between tool-less fitting and Seat-Leg. On RHS (Cross-Sectional View) - Relative displacement after application of '10 degree' roll.

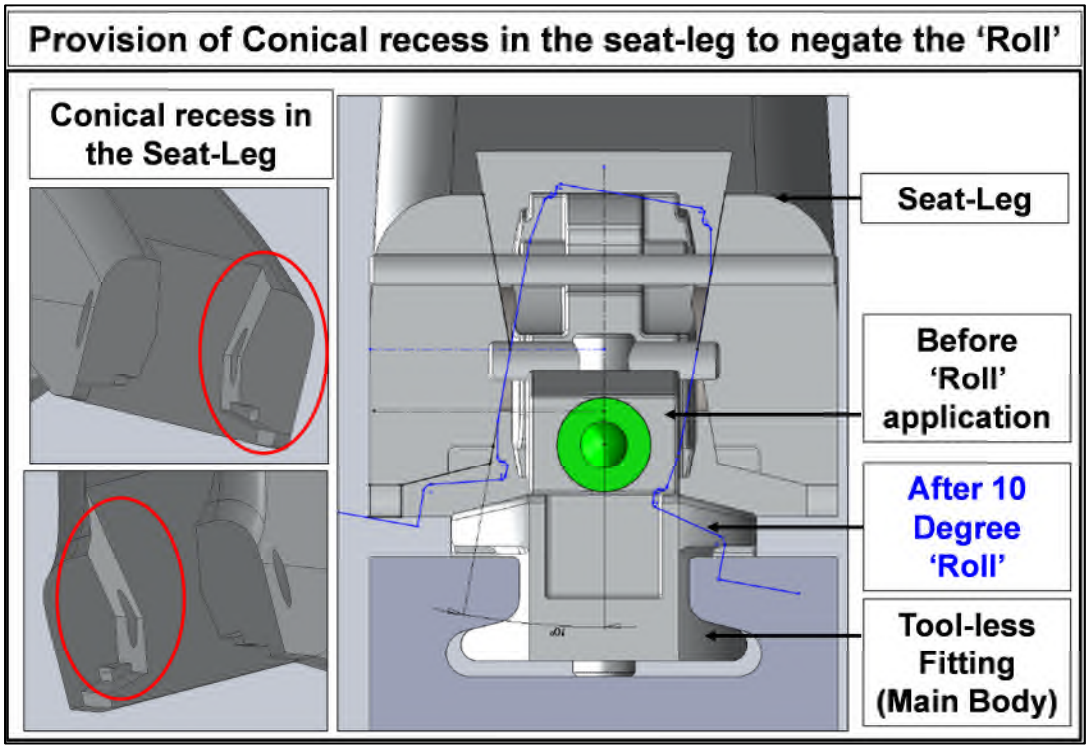

Figure 7-13 Conical recess provided in the Seat-Leg to allow relative movement between tool-less fitting and Seat-Leg. On RHS (Cross-Sectional View)- Relative displacement after application of '10 degree' roll.

Thus three different design modifications have been suggested to completely alleviate the detrimental effect on the seat structure due to the applied ‘Roll’. The presence of the ‘Spherical’ roll release or the ‘Conical’ Roll release (either in the Tool-less fitting or Seat-leg); provides a bending moment release and increases the compliance against the pre-deformation loads

During the design iterations of the ‘Sleep Seat’, these modifications have been used in combination with design solutions given for ‘Pitch’ relief and have been found to be satisfactory in terms of reducing the stress levels.

7.4.4 DESIGN SOLUTIONS TO REDUCE THE STRESSES DUE TO APPLIED ‘PITCH’

Design Philosophy - Design solutions provided in the Section 7.4.3 for ‘Roll release’ provide the relative motion between the Seat-anchorages and rest of the seat structure. Provision of the ‘Pitch release’ at these locations is not considered as it may weaken the seat anchorages or turn the seat into a mechanism leading to a catastrophic failure (due to single load path as shown in Figure 7-14) such as detachment of the seat from the seat-track when subjected to the ‘16g’ dynamic pulse applied as per CS25.562. Therefore, other regions of the seat should be considered for the ‘Pitch release’.

The “Sleep Seat” design is a unique “Single Forward beam design”, which leads to the single load path through the structure, which is from Seat track to the TLF to the seat leg and finally to the Forward beam (Figure 7-14). Considering this load path the only possible way to decouple the seat super-structure from the applied “Pitch” is to control the design of an insert (also called as Leg-Clamp) at the leg-Forward beam interface.

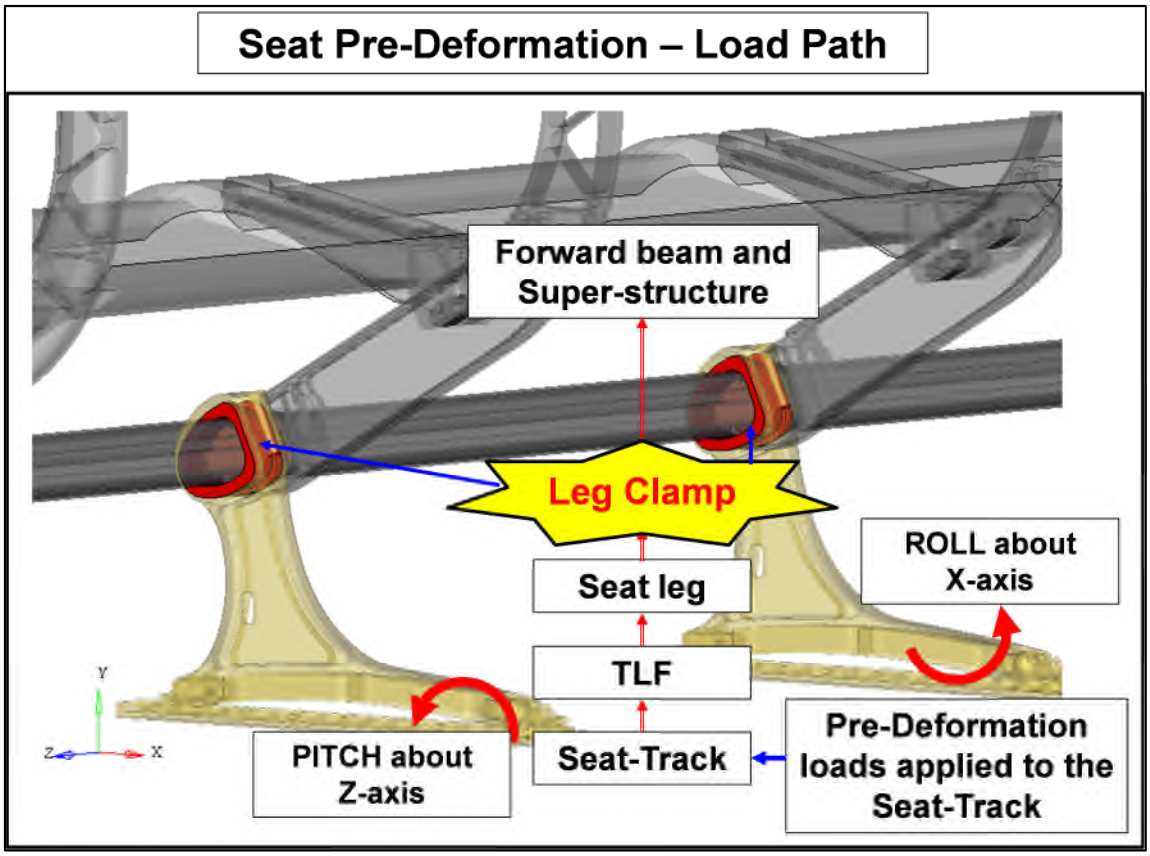

Figure 7-14 Logic behind provision of 'Pitch' release at the Leg-Clamp. The figure explains the load path for the 'Pre-deformation' loads applied at the Seat-Track. Being a 'Single' load-path, Leg-Clamp is an ideal location for 'Pitch' release

Once it was decided to design the leg-clamp to provide the ‘Pitch release’; the requirements of such a Leg-Clamp were outlined as it

- ✓ Should “Allow” the relative movement between the seat-superstructure and seat-substructure for the applied “Seat Pre-deformation” loads. This will ensure that the seat structure with damaged floor condition has the ability to sustain the dynamic loads without failure of the seat track.

- ✓ Should “Not Allow” relative movement between the seat-superstructure and seat-substructure for the applied static loads as per CS 25.561 and the dynamic loads as per CS 25.562. This will ensure the structure will not turn into a mechanism and will transfer the loads to energy absorbing components of the seat thereby reducing Occupant loads.

- ✓ As the ‘Roll release’ is present at the base of the structure, the joint between the Seat-leg and the Forward beam should ensure ‘positive’ engagement and should avoid the structure being a mechanism (Figure 7-15).
- ✓ Should be easy to manufacture and assemble
- ✓ Should be applicable to all the seat layouts with different track spacing, specific to the airlines.

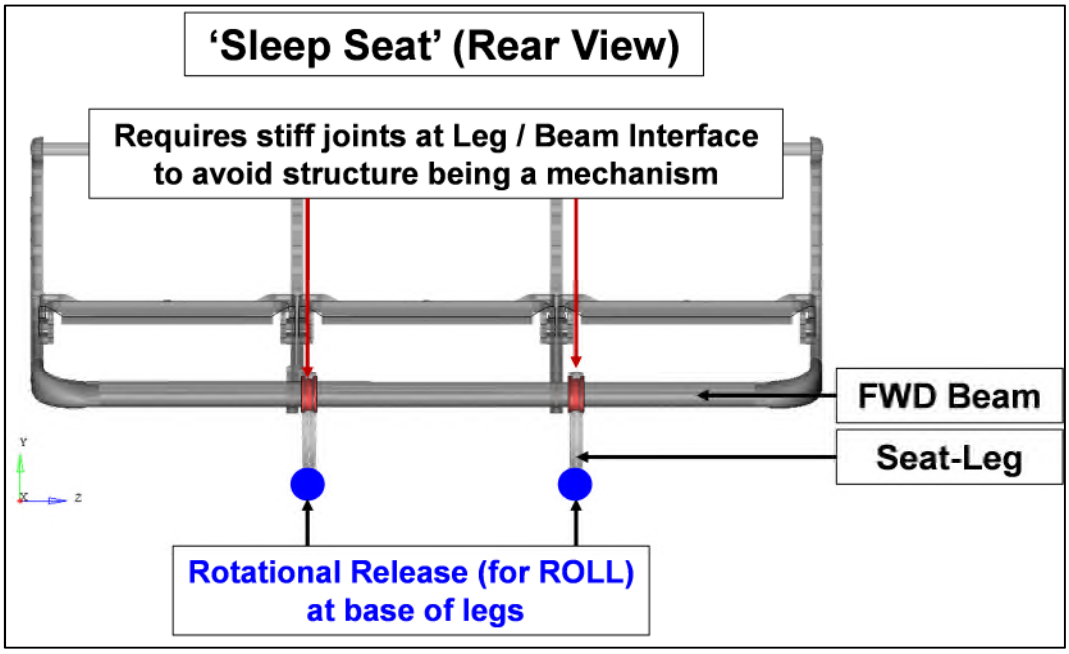

Figure 7-15 Provision of 'rotational' release for 'Roll' at the seat anchorages necessitates stiff or positive joint at the interaction of Seat-Superstructure and Seat-Substructure to avoid the structure turning into a mechanism.

Design Challenges were:

What should be the size the Leg-clamp?

The size of the Leg-Clamp is decided by the overall sizing of the ‘Sleep Seat’ i.e. Width is limited to 30mm as it should match the width of the leg (30mm) and the maximum thickness is constrained to 10mm by the gap between the Forward beam and the Seat-leg (Figure 7-16).

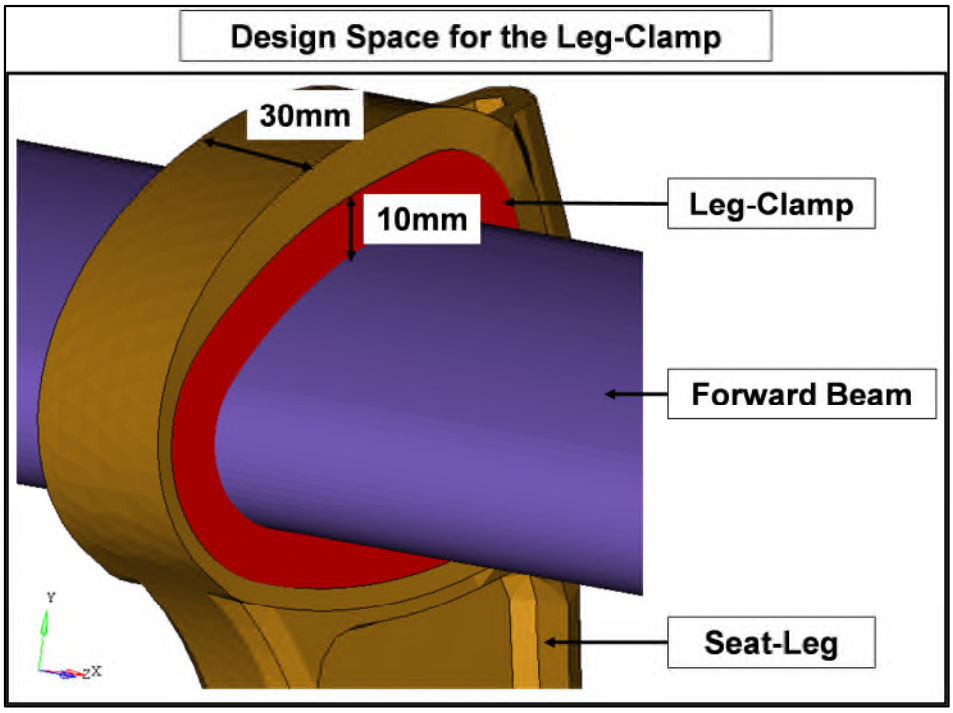

Figure 7-16 Restrictions on the Size of the Leg-Clamp mainly derived from aesthetics. Maximum width limited to 30mm to have a 'flush-finish' with the Seat-leg, Overall thickness must 'fill' the space between inner profile of the Seat-leg and corresponding outer pro

Since overall size of the Leg-Clamp could not be changed (or can be treated as an input); the entire success of the 'Pitch' release relied on the following parameters,

- Shape of the Leg-clamp and the
- Material of the Leg-clamp

A total of nine different designs of the Leg-Clamp are developed and studied in detail and finally two completely novel, practical and economical design solutions were provided, which were adopted by the BlueSky due to its simplicity, repeatability and reliability. The complete journey of designing of the Leg-Clamp has been described in the Appendix F and Appendix G. Following section provides the overview of the final design concept; to comply against 'Pitch' load; developed during this research.

7.4.5 ELASTOMERIC LEG-CLAMP – PROOF OF CONCEPT

A novel and practical solution to manufacture the Leg-Clamp from an elastomer; to alleviate the high stresses induced due to the applied 'Pitch'; was proposed.

7.4.5.1 IDENTIFICATION OF GRADE OF ELASTOMER

Following parameters are considered in the selection of type and the grade of elastomeric insert,

Properties - Service Conditions

- Maximum anticipated operating temperature – Ambient (in aircraft cabin)
- Anticipated service life - Seat structure should last 100,000 flying hours or 20 years. Elastomer is unlikely to have such a long life. Therefore, it should last for 7 years – a recommended term before replacement at a service interval (Input from BlueSky).
- Almost 100% of life its life the elastomeric insert will spend at the maximum working temperature.
- Minimum operating temperature- Ambient (in aircraft cabin).

Properties - Chemical/Environmental conditions

- Elastomeric insert is likely to have direct contact with the water or aircraft cleaning chemicals.
- It will not have any contact with oil or grease or any other lubricating fluid.
- A number of rubbers degrade when in contact with atmospheric levels of Ozone. However, elastomeric insert would be in a cabin environment and hence it is not supposed to be 'ozone resistant'.
- It should be strictly non-flammable.

Properties – Mechanical

Elastomeric insert should show continued airworthiness as it is the part of primary load path. Though the properties of visco-elastic materials change over time, the degradation should be minimal.

- It should have high fatigue resistance, high tear strength, insulating electrical properties and high wear resistance.
- It should have low compression set, which will ensure good recovery under compression.
- The colour of the elastomeric insert is insignificant but it should not have any odour or should not develop any, when in contact with the liquids used in airplane.

If an elastomeric material does not satisfy any one of the above stated requirements, it should be possible to improve its performance in that area by using appropriate additives in the formulation without adversely affecting other properties.

Considering all these aspects, Viton (a fluorocarbon elastomer, FCE) has been selected for preliminary proof of concept studies [58]. The Viton material verification is done as specified in WRL research report by Makino [59]. Details have been presented in the Appendix F.2.3.

7.4.5.2 PROOF OF CONCEPT STUDY

Two designs of the 'Sleep Seat' are studied for the applied 'Seat Pre-deformation' loads. The only difference in the design is the material used for the Leg-Clamp,

- Aluminium leg-clamp (Design A)
- Elastomeric (Viton) leg-clamp (Design B)

The rest of the parameters such as boundary conditions, FE models and interface definitions are same in both the models (Figure 7-17). The solver used for simulation is Abaqus /Standard. A double occupancy 'Sleep seat' structure; is used for this study to reduce the CPU time and FE model building efforts.

The secondary seat-structure (seat back) has not been considered because

- It does not play a major role in 'Seat Pre-deformation' loadcase
- It will increase the size of the FE model (secondary structure would approximately add another approximately 30000 nodes and elements to

the existing FE model) and hence the CPU time, which is not desirable for this conceptual study.

The pre-deformation loads are applied as specified in Section 7-1 (Figure 7-17). 'Spherical' design of the TLF (Section 7.4.3.1) has been used to anchor the seat to the track. 10 degree 'YAW' has not been considered as the simulation is not aimed to be continued for dynamic loadcase i.e. '16g'. The details of the boundary conditions are present in the Appendix I of this report.

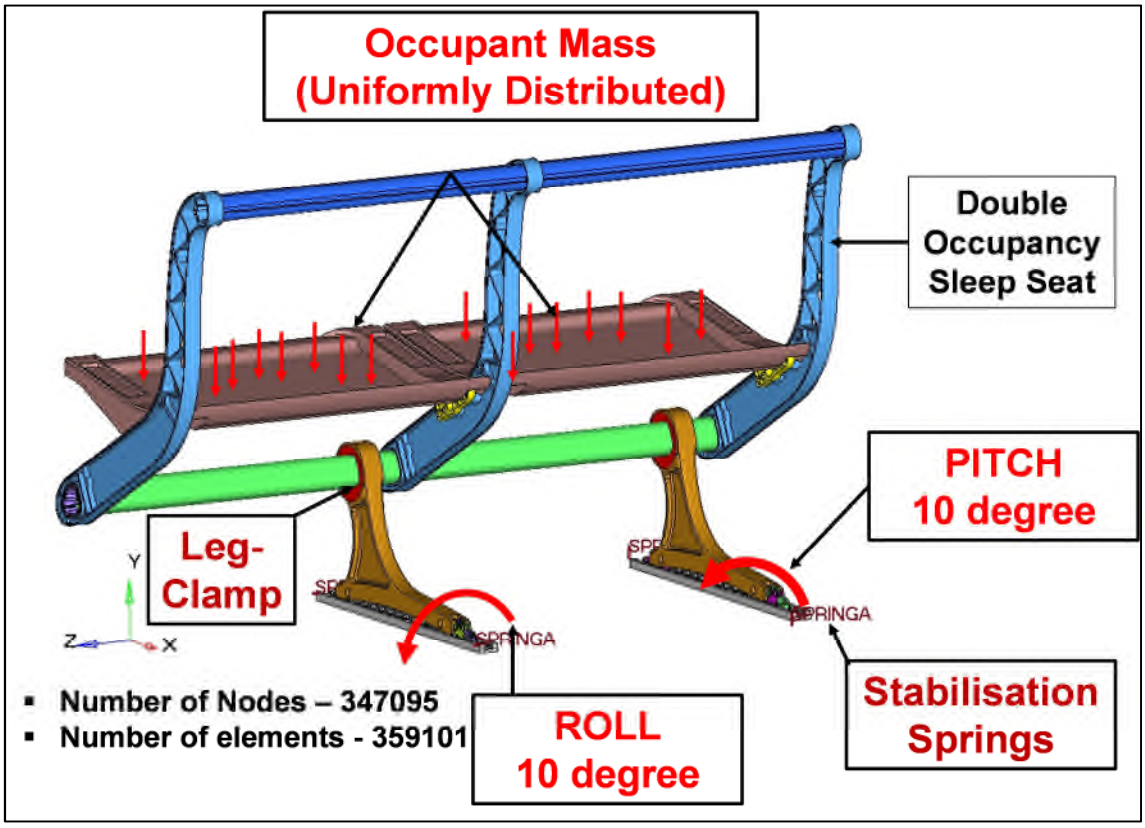

Figure 7-17 Definition of Seat Pre-deformation loads for a double occupancy version of 'Sleep Seat'- 10 degree ROLL, Rx(constraining all other dofs) is applied in Counter Clockwise direction (looking from the rear of the seat) to Leg-LHS, , which has more overhang seat-structure than Leg-RHS. 10 degree PITCH DOWN is applied to Leg-RHS. Occupant mass 77kg/seat uniformly distributed over seat-pan. Solver – Abaqus (Research) 6.9-3

Comparison of the 'Design A' and 'Design B'

Both the simulations are run of 16 processors on High Performance Computing facility at Cranfield University. Simulation time for the 'Design A' is 8145s while for 'Design B' is 10373s. Elastomeric clamp in 'Design B' is more flexible than the 'Aluminium' leg-clamp in 'Design A' and hence undergoes large geometric nonlinearity thereby increasing the solution time. No convergence difficulties are faced during the simulations as the guidelines for FE model building explained in Section 4.3 are followed and stabilisation springs with negligible stiffness 1E-12N/mm are attached to the parts held only by contact. FEA results with 'Design A' i.e. Aluminium leg-clamp are considered as the baseline results due to its presence in the original seat structure. von Mises stress (VMS) induced in the primary load path components i.e. the Forward Beam and Seat-Leg is considered for comparison as their strength is a critical factor in the successful design of 'Sleep Seat' against the '16g' dynamic load, applied after pre-deforming the seat-track. Following observations can be made from Figure 7-18.

- With the leg-insert made out of Viton, the overall VMS levels observed in the "Rolled leg (LHS leg)" have been reduced, when compared to the Baseline results.

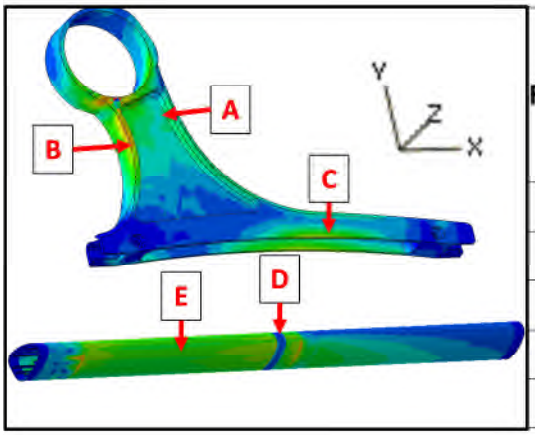

Region	Maximum von Mises Stress (MPa) after Seat Predeformation		Improvement (%)
	Design A (Aluminium)	Design B (Elastomer)	
A	200	50	75
B	340	117	66
C	362	87	76
D	360	107	70
E	220	103	53

Figure 7-18 Elastomer Leg-Clamp at the Seat-Leg and interface. RHS- Significant reduction in the VMS observed in the Seat-leg and Forward beam as compared to the seat with Aluminium Leg-clamp. This demonstrates usefulness of the elastomeric Leg-Clamp. Loadcase – Seat Predeformation

- Particularly at location C (foot-section of the leg, which was a matter of concern in earlier design), significant improvement can be seen as the VMS has reduced from 362MPa (near Yield limit of a general Aluminium alloy ≈375MPa) to 87MPa. Achieving this level of stress in the leg is desirable, before the dynamic loads are applied.

- With the leg-insert made out of Viton, the maximum VMS level observed in the Forward beam has reduced from 360MPa (Baseline result) to 107MPa, which is a significant improvement.

- FEA results indicate that a Viton leg-insert has a beneficial effect in reducing the stresses observed in both legs and Forward beam during pre-distortion. Stresses in the legs are reduced to approximately 30% of the yield stress of a general Aluminium alloy ($\sigma_y \approx$375MPa)

The exercise of concept demonstration concluded that the use of a flat elastomeric Leg-Clamp is extremely beneficial to reduce the stress levels observed in the components of the primary load path for the applied Predeformation loads. This simplified and passive insert proved to be an attractive solution and simplified the design and reduce the costs considerably.

7.4.6 SIZING OF ELASTOMERIC LEG-CLAMP

After the encouraging results obtained in a conceptual study of an elastomeric leg-clamp, the design was considered (Figure 7-20LHS) for the 'Triple Sleep seat' assembly. The challenging loadcases during designing are,

- *Seat Pre-deformation* – The motive behind an elastomeric insert is to mitigate the effect of the seat Pre-deformation (pitch) through its deformation relative to the rest of the structure. This deformation would allow the Forward beam to rotate / translate and then lock thereby enabling the primary load path of the seat structure to resist dynamic loading.

- *Downward 6g (CS 25.561)* – The response of the Leg-Clamp is critical for this load case, as the elastomer controls how the load is transferred

through the primary load path of the seat to the seat track. If too flexible, the seat will displace significantly in the vertical direction, which has implications on resulting unpleasant ride comfort and a potentially high impingement into the space for the occupant sitting behind, which could have serious implications on the brace position etc. Therefore, during the 'Downward 6g' load, the insert should lock after only a small deformation in order to minimise the downward motion of the occupant.

As can be seen, these two load cases pose contradicting requirements on the behaviour of the elastomeric insert, resulting in a trade-off in performance (in terms of shape, hardness, etc.), in order to satisfy both static and dynamic requirements. Initial study of the triple seat structure subjected to Pre-deformation loads and 'Downward 6g' loads with a design of 'elastomeric leg-clamp' 'carried-over' from conceptual study corroborates this observation (Figure 7.19).

The FE model of the complete seat considered has 187528 nodes and 196317 elements. The boundary conditions for 'Seat Pre-deformation' and 'Downward 6g' are same as explained in Section 7.1 and Section 4.4 respectively.

Please note that for 'Seat Pre-deformation' loadcase, VMS plot is provided only for the 'rolled' leg, which is critically loaded. Highly localised and unrealistic contact stresses have been ignored. For 'Downward 6g' only vertical displacement plot has been published because,

- The VMS induced in the individual components of the seat structure are well below the corresponding yield limits of the materials used.
- Estimation of the vertical downward displacement of the seat structure is the main objective of this simulation as it establishes a major link between the design of 'elastomeric' leg-clamp and evacuation procedure during emergency landing as well as ride comfort for a passenger.

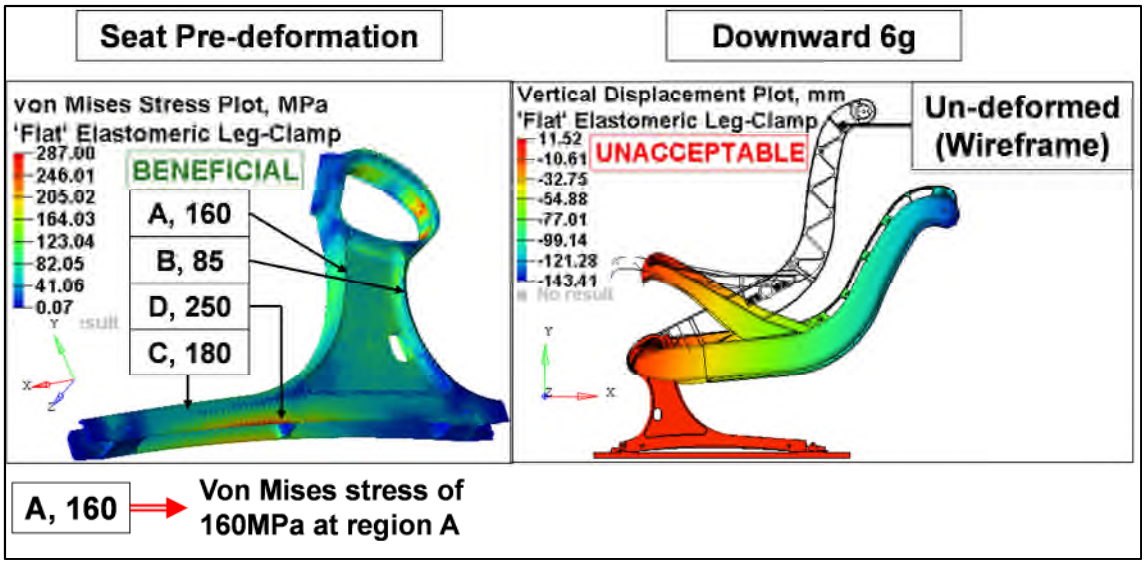

Figure 7-19 LHS - Seat Pre-deformation, VMS plot for 'Rolled' leg. Stresses are well below the Yield limit (Al7075, yield = 475MPa). Elastomeric Leg-clamp is beneficial. RHS - Downward 6g, Vertical Displacement plot. Unacceptable downward displacement of Seat-Pan, 82mm (Angle = 36 degree > Allowable, 35 degree [14])

Performance during 'Pre-deformation'

- The maximum VMS occurs at the lower foot section of the 'rolled' leg (location D, Figure 7-19LHS) and is 250MPa. As it is well below the yield limit of the material used for the leg (Al7075T6, Yield limit 475MPa), the elastomeric leg-clamp is beneficial. In a triple seat-structure, higher grade of aluminium Al7075T6 (than Al5082T6 for dual seat-structure) is used for seat-leg anticipating higher loads.
- The stress levels observed in all other components of the seat structure are within the respective yield limits of the material used and hence are not provided in this report.

Performance during 'Downward 6g' (Figure 7-19RHS)

The simulation stopped after 85% of the load due to convergence issues. High deflection of the seat-superstructure due to flexibility of leg-clamp resulted in contact chattering, many smaller load increments and finally negative volume in one of the elements used to model elastomeric leg-clamp. Due to poor

performance of the seat-structure (excessive downward displacement as explained in following section) for the 85% of load, no further attempts were made to take the corrective actions in the FE model so that response for 100% of load can be estimated. Instead efforts were focused on design improvement of the leg-clamp (as explained in coming sections). Interesting observations from the results are

- Present 'Un-Stepped' elastomeric Leg-Clamp suffers from the unacceptable vertical downward displacement of the Seat Pan (82mm). This displacement is caused by the high vertical flexibility of the insert.
- As the angle of rotation of Seat-Pan is 36degrees (allowable limit 35degrees), the seat does not comply with 'Downward 6g' load. This will impede the evacuation process in case of emergency landing and is therefore unacceptable.
- Further, during download tests, the inertia factor used by the airliner is approximately 8.6g (to represent heavy Occupants) against '6g' specified by CS25.561 (Input from BlueSky during experimental tests). For this increased load, seat-structure would collapse if 'flat' elastomeric leg-clamp is used.

Therefore, the next challenge is to "Size" the leg-clamp to get the expected behaviour in the download tests yet maintaining its current response for 'Seat Predeformation'. It is essential to use the insert with the variable stiffness. 'Spring rate (Stiffness)' of elastomer in shear, K_s (for Seat Pre-deformation) and in compression K_c (for Static - Downward 6g/ Dynamic – Downward 14g) are the key design parameters.

K_s mainly depends on,

- The load area (30mm, a limit imposed by the width of the leg-head) and
- Thickness of the elastomer (9mm, a limit imposed the contour of the leg-head and Forward beam and aesthetics).

As satisfactory behaviour of the seat structure is obtained with the current elastomeric leg-clamp, it was decided to use the same K_s for future

developments. However, an unacceptable vertical downward displacement of the Seat-Pan demanded significant improvements in K_c!

The logic used behind the “Sizing” of the Elastomeric Leg-Clamp is

- Introduction of rigid/stiffer material into the elastomeric section increases compression spring rate while maintaining the same shear spring rate [60].
- A thin pad of an elastomer offers great resistance to the compression.

Thus variation in the stiffness of the elastomeric insert can be achieved by designing the “Insert with variable thickness” i.e. with stepped variation in the thickness. The logic behind such an insert is,

- The portion of the insert with lower thickness would transfer the static loads (CS 25.561) to the Forward beam without any relative movement between the seat-superstructure and the seat-legs. This “Locking” of the insert would prevent the “Rigid body motion” of the seat-superstructure and hence the high vertical downward displacement of the seat-pan.
- The portion with higher thickness will absorb the “Seat Predeformation” loads by deforming in radial direction as well as in the lateral direction thereby alleviating the high stresses induced by damaged floor condition.

This meets the requirements as,

- It increases the “Compression Spring Rate (K_c)” thereby reducing the vertical downward displacement of the Seat-pan during download tests yet
- Maintains the same “Shear Spring Rate (K_s)” ensuring ‘expected’ flexibility during “Seat Predeformation”
- As the overall size and thickness of the leg-clamp is maintained same as the earlier, design would be still aesthetic.

Therefore, the “Stepped” Elastomeric Leg-Clamp design (Figure 7-20 RHS) was proposed in which

- Leg is extended by 3mm into the space of leg-clamp over a centrally symmetric width of 15mm. Leg (made of Aluminium) acts as a rigid/stiffer material (comparing the modulus of elasticity of Aluminium and Elastomer).
- Over this 15mm central width, thickness of the leg-clamp is 4mm, which automatically results in a thin pad offering greater resistance during download tests.
- Over each side of 15mm portion i.e. a width of 7.5mm on each side; thickness of the leg-clamp is 7mm.

This design of elastomeric leg-clamp is termed as a '4/7mm Stepped insert (based on its thickness)' in this report. The detailed study on its sizing is present in Appendix G of this report.

'Seat Predeformation' and 'Downward 6g' loadcases were once again simulated with '4/7mm stepped' insert and results are compared with original 'flat' insert (Table 7.2).

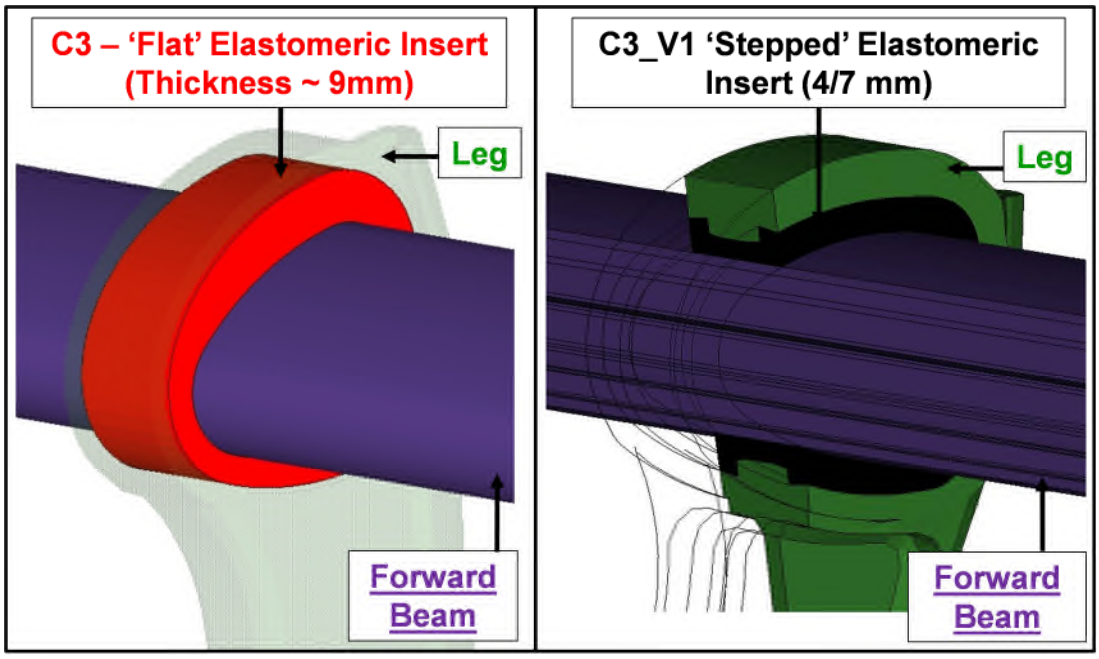

Figure 7-20 LHS - Design of original 'Flat' elastomeric Leg-Clamp. RHS - Design of 'Stepped' elastomeric Leg-Clamp (4/7mm)

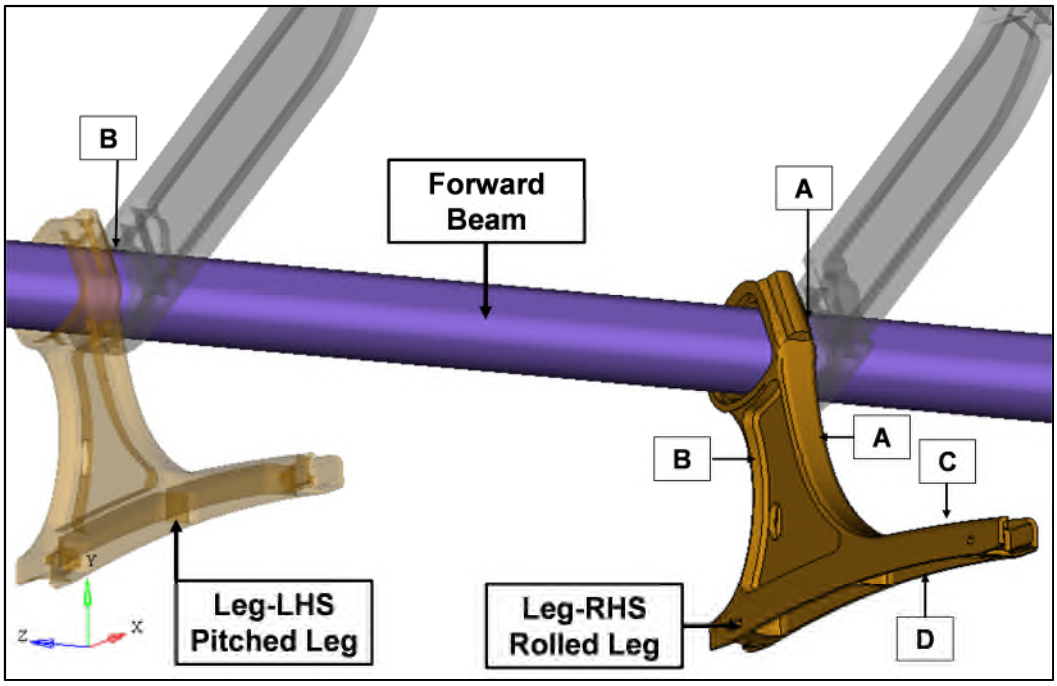

Figure 7-21 Nomenclature for the high-stress locations in Forward beam and Seat-leg when subjected to Seat Pre-deformation loads

Loadcase	Seat Pre-Deformation					Downward ‘6g’
Parameter for comparison		VMS, MPa				Vertical Downward Displacement of Seat-Pan, mm
High Stress Locations	Component	A	B	C	D	
‘Flat’ Elastomeric Leg-Clamp	‘Rolled’ leg	160	85	180	250	82
	‘Pitched’ Leg	185	100	120	200	
	Forward Beam	240	190			
4/7 ‘stepped’ Elastomeric Leg-Clamp	‘Rolled’ leg	220	140	240	295	28
	‘Pitched’ Leg	210	140	165	230	
	Forward Beam	165	135			

Table 7-2 Comparison of the structural performance of the two 'triple' Sleep seat-structures only differing in the design of Leg-Clamp: C3_‘Flat’_9mm thick Leg-Clamp and 4/7mm ‘Stepped’ Leg-Clamp, Loadcase1: Seat Pre-deformation- VMSes induced at the high stress locations in in the Forward Beam and Seat-leg are compared (please refer figure 6-17 for the nomenclature of the high-stress locations). Loadcase 2 – ‘Downward 6g’, Vertical downward displacement of the Seat-Pan has been compared. Conclusion – 4/7mm ‘stepped’ Leg-clamp is beneficial as it offers less downward displacement of Seat-Pan (28mm) yet maintains the VMSes during Pre-deformation below the yield.

From Table 7-2, following remakes can be made,

The parameters chosen for comparing two designs of the 'elastomeric' Leg-Clamp are: VMS for pre-deformation loads and the vertical downward displacement for 'Downward 6g'. Nomenclature for the high stress locations in the Forward beam and Seat-leg during 'Seat Pre-deformation' is provided in Figure 7-21.

- With the 'Flat' elastomeric Leg-clamp, the VMS induced in both the legs i.e. 'Pitched' leg (maximum VMS of 200MPa at rear foot section, location D) and 'Rolled' leg (maximum VMS of 250MPa at rear foot section, location D) are well within the yield limit of the material used for leg (Al7075, Yield limit = 475MPa). Though the VMS observed for seat-legs with '4/7mm' insert have increased (at all the high stress locations; maximum VMS of 230MPa in 'Pitched' leg and maximum VMS of 295MPa in 'Rolled' leg) over those with 'flat' leg-clamp design, they are still within the yield limit.
- In the seat-structure with 'flat' elastomeric leg-clamp, because of the high degree of flexibility in the vertical direction (due to the thicker elastomer along the top and bottom surfaces), the RHS and LHS sides of the Forward beam are subjected to the different displacements. This misalignment places the beam under additional bending, resulting in higher stresses being induced in the Forward beam (maximum VMS of 240MPa at the section between Leg-RHS and boomerang, location A on Forward beam in Figure 7-21) than observed with 'stepped' elastomeric leg-clamp (maximum VMS of 165MPa at location A on Forward beam in Figure 6-21). However, the VMS levels in the Forward beam are within the yield limit (Al6082T6, Yield limit=250MPa) for both the designs.
- The major shortcoming of the 'flat' elastomeric insert is excessive downward displacement of the 'Seat-Pan' 82mm, observed for the applied 'Downward 6g' load (simulation stops after 85% of the load due to highly distorted elements). This results in an unacceptable angle of rotation, 36degrees (allowable angle of rotation from Reference 14 is

35degrees). With ‘Stepped’ elastomeric insert ‘Downward 6g’ produces 28mm of vertical downward displacement of Seat-pan (for 100% of load), which is ~14degree of angle of rotation and hence within limit.

Therefore, considering a “Trade-Off” between the structural response of the seat for the applied “Seat Pre-deformation” loads and “Downward 6g” loads; ‘Stepped 4/7mm’ insert design is chosen for the Leg-clamp, placed between ‘Forward beam’ and ‘Seat-leg’.

Conclusion - Chapter 7

Seat Pre-deformation also known as or ‘floor distortion’ or ‘damaged floor condition’ is a pre-requisite (initial configuration) for dynamic ‘16g’ loadcase and is conducted statically. It is the misalignment of the seat anchorages with respect to each other by 10 degrees vertically (i.e. out of parallel, PITCH) whilst the other leg is rolled through 10 degrees. Its purpose is to demonstrate structural capacity of the seat structure to withstand the dynamic loads without disintegrating from the Airframe-floor, even when the floor is deformed by the forces associated with primary crash

Literature review showed that earlier attempts (by various researchers) have failed either to simulate the pre-deformation using FEA codes or to initialise the stresses due to pre-deformation in a dynamic ‘16g’ loadcase. The problem with implicit solution technique was of solution-convergence and with explicit solution technique was quasi-static solution.

The problem is attempted by four different schemes in this research e.g. Abaqus (Research) 6.9-3, LSDYNA/Implicit, LSDYNA/Explicit and LSDYNA-Implicit/Explicit Switch. A satisfactory and an acceptable solution was obtained from each of these methods, when the guidelines for FE model building derived in Chapter 4 and Chapter 5 were followed. The results from these different methods are compared based on parameters like VMS in individual components, overall displacement of the seat structure and the seat interface loads. A close agreement between the results served as a self-verification check for these four different FE approaches to simulate the Seat Pre-

deformation. Following guidelines are proposed by this research for choosing a particular method for an analyst,

Implicit Time Integration	Explicit Time Integration	Implicit/Explicit Integration
▪ Considerable efforts for a Converged solution ▪ High memory Requirements ▪ Satisfies test requirement ▪ Recommended during detailed design and sizing cycle	▪ Considerable efforts for a Quasi-static solution ▪ Low memory Requirements ▪ Damping to achieve a quasi-static solution ▪ Recommended during – 'Complete 16g' evaluations	▪ Dynamic Effects should be monitored ▪ Reduces efforts on FE modelling ▪ No Convergence issues ▪ Recommended during feasibility studies for inexperienced analysts

Going forward, novel design concepts to minimise the loads introduced by pre-deformation loads in the seat structure are developed, evaluated and compared. For 'Roll' release, modifications are suggested in the seat anchorages (tool-less fittings) while an innovative elastomeric leg-clamp is designed at the Forward beam and Seat-leg interface to deal with the applied 'Pitch'.

Thus this chapter discusses two novelties of this research: Four different FE methodologies to simulate pre-deformation loadcase using FEA and different design concepts to minimise the detrimental effects of pre-deformation loads on the seat structure.

8 TOPOLOGY OPTIMISATION OF SEAT-LEG

During MSc by research of the author of this report, design of the Forward beam of double occupancy seat (a '9g compatible' seat) was developed through analytical calculations considering mainly "Forward 9g" and "Downward 6g" loadcases [9]. An elliptical cross-section with a wall thickness of 2mm was chosen for the Forward Beam. Design of the seat leg was developed considering that the leg was dominated by bending and torsion and using 'Free Shape Optimisation' technique (as there was a keen interest to retain the shape of the leg for aesthetic purpose).

Though the aim of this research is to develop FE methodologies, this chapter takes an overview of the design procedures developed simultaneously during the process. For the triple seat-structure ('16g Compatible' seat), design of the Forward beam (from double Occupancy seat) was modified with localised inserts and stiffening ribs. However, it was required to design a seat leg considering static as well as dynamic loads.

First phase of this chapter describes the importance of seat-leg design followed by the procedure adopted, in this research, for its design. Later part of this chapter demonstrates compliance of the triple seat-structure against static certification loads (CS25.561).

8.1 IMPORTANCE OF SEAT-LEG DESIGN – LITERATURE REVIEW

Design of Seat-leg plays a major role in

- Transferring the loads to aircraft floor
- Offering a rigid support for the Occupant during normal flight operating loads
- Absorbing crash energy thereby reducing the loads transferred to the occupants,

Seat-legs have been employed in the design of the several successful energy absorbing seat by exploiting their potential for developing plastic deformations thereby increasing the stroking distance and absorbing the energy [4].

Lankarani has shown that a properly designed seat-leg could reduce the lumbar loads by 40% [2].

Hooper has discussed an example of designing an energy-absorbing seat-leg by considering two important parameters: Initial stiffness of the leg and the strain to failure (i.e. strength of the member) [4]. The authors have presented the effect of seat-leg strength on the lumbar loads by combining: different leg designs exhibiting different elastic-plastic behaviour, and the nonlinear DRI (Dynamic Response Index) model, which contains the nonlinear springs representing the dynamic compliance of the seat cushions and the seat pans. The authors conclude,

- Lumbar loads are directly proportional to the leg strength and hence leg strength and leg deflection are powerful design variables in controlling the lumbar loads.
- Seat-leg design is bounded from below by the necessity that the seat should be adequately strong so as to sustain the limit loads and bounded from above by the lumbar injury criteria.

8.2 REVIEW OF SEAT-LEG DESIGN TRIPLE SEAT-STRUCTURE

As a start-up, seat-leg design from double Occupancy variant of 'Sleep Seat' was used for the triple seat (Figure 8-1 A). However, due to mass of an extra occupant, unacceptable downward displacement of the Seat-Pan was observed for the applied 'Downward 8.6g' loads. This leg design could have resulted in

- Unpleasant ride comfort for the passengers due to excessive downward displacement even during normal flight loads
- Severe deformation of the seat-structure during '14g' dynamic loads (approximately 45^0 > allowable limit 35^0), which would have created difficulties for the passengers while evacuating the damaged plane resulting in casualties due to fire and
- Additional bending loads on the Forward beam

Therefore, a supporting member was added to this design, which would lie approximately below the centre of gravity of Occupant thereby cancelling the bending moment applied (Figure 8-1 B). Supporting member was bolted to the existing leg design and to the midbeam (spanning laterally across the side boomerangs). Since this was a simple design change, experimental tests were performed for the 'Forward 9g' loadcase. A bucking of the aft portion of the leg was

observed during tests (Figure 8-1 B). FE procedure developed during this research was able to reproduce this test (Figure 6-13).

In the third conceptual design of the seat-leg, web of the leg was approximately placed below the centre of gravity of Occupant. However, severe rotation of the seat-pan was observed for the applied 'Forward 9g' loads. Mass of the Occupants applied bending loads to the front portion of the seat-pan, which in turn rotated around its rear attachment point with the boomerang. This excessive rotation and subsequent buckling of the Seat-pan was because being unsupported from the bottom.

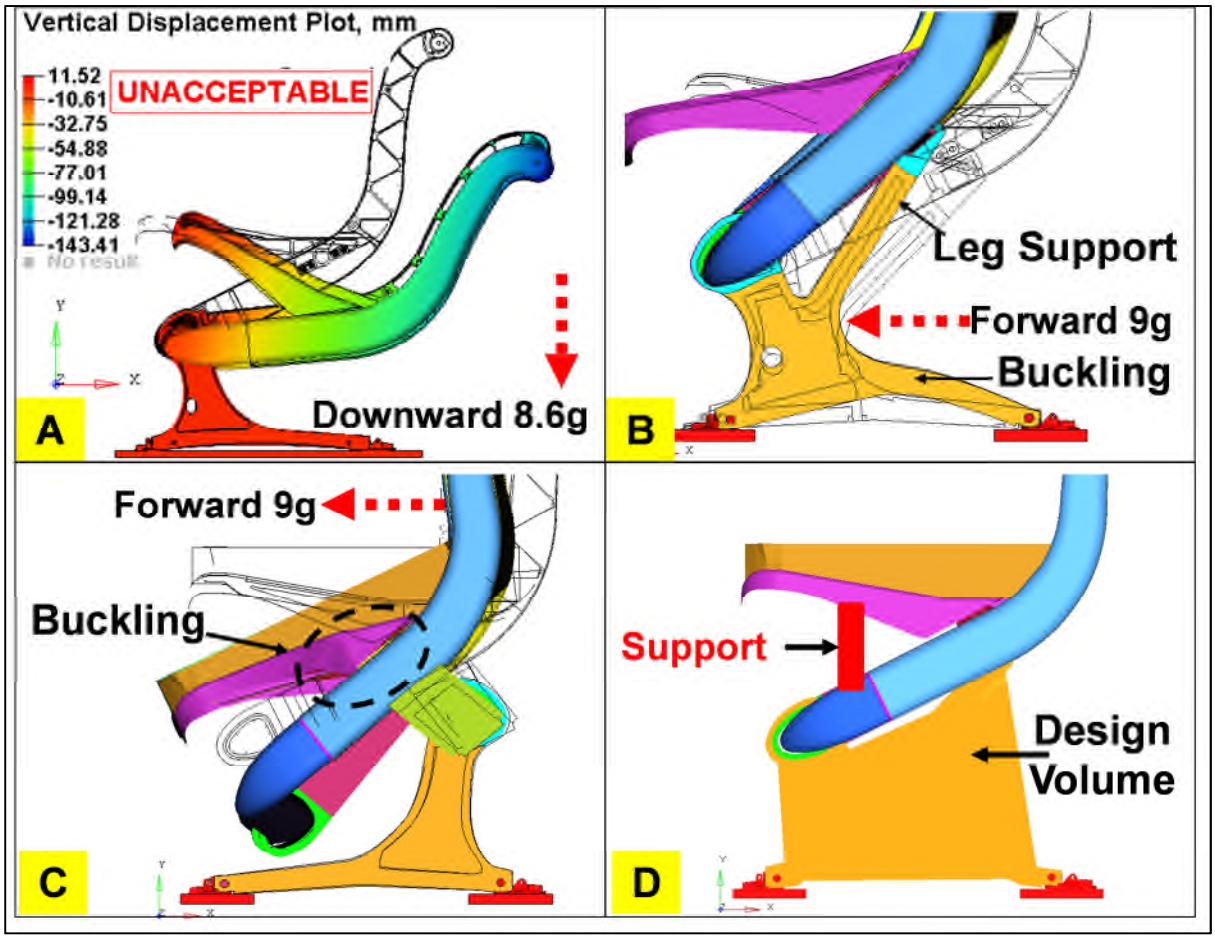

Figure 8-1 Behaviour of different leg designs (used in triple occupancy seat-structure) for the applied CS25.561 loads, A – With the leg-design 'carried forward' from double occupancy seat, unacceptable downward displacement of seat-pan i.e. rotation of seat pan by approximately 45^0 (allowable limit 35^0), is observed. B – When the leg support is added to 'Design A', aft foot section of leg buckles for the applied 'Forward 9g' loads, C – For the 'reverse' leg design i.e. leg head placed below passenger centre of gravity, excessive rotation of seat pan and subsequent buckling of aft section is

observed for applied 'Forward 9g' loads, D – Design space for the leg and support added to the front portion of seat-pan for preventing excessive rotation during 'Forward9g' loads.

From three different conceptual designs of the seat-leg following conclusions were drawn.

- A supporting member should be added at the front side of the Seat-pan connecting it with the boomerang (Figure 8-1 D). This would prevent the bending of the seat-pan about its aft connection with boomerang, due to Occupant loads.
- 'Forward 9g' and 'Downward 8.6g' loadcases are critical for the seat-leg design.
  - ✓ Due to Static '9g' loads, leg experiences severe bending loads, which may result in the rupture of the leg at its weakest cross-section (as seen in leg design B). Hence, leg must be strong enough so as not be drastically deform.
  - ✓ '16g' dynamic load is applied, approximately in the direction of 'Forward 9g' loads. Success against this loadcase demands that the leg should withstand the pulse (without developing any discontinuity in the load path) yet should plastically deform thereby absorbing crash energy.
  - ✓ Seat leg should be designed in such a way that it does not deform resulting in an unpleasant ride comfort even during normal downward loads.
- Seat leg should connect front beam of the seat-structure (Forward beam) as well as lower aft beam (Mid beam, which lies below the centre of gravity of Occupants). This yielded a design space for the seat-leg (Figure 8-1 D)

It was decided to use Optistruct, a commercial design optimisation developed by Altair Hyperworks; to derive the design of the seat-leg through topology optimisation. Its advantages during conceptual design phase are [61, 62],

- Powerful optimisation techniques help to generate innovative yet significantly lighter designs.
- As response from multiple loadcases (e.g. two major loads from CS25.251, Forward 9g and Downward 8.6g) can be simultaneously considered during

optimisation, number of design iterations drastically reduces thereby accelerating the design process.

- Manufacturing constraints such as symmetry and draw directions enable to achieve a realistic design.
- Optistruct offers an easy-to-use graphical interface and is tightly integrated into other Hyperwork products such as HyperMesh for model set-up and HyperView for post-processing.

B/E Aerospace used Optistruct during the early stages of development of 'Spectrum Seat line' [62]. They could accelerate the development process by achieving 30% reduction in weight and 60% savings in physical testing.

8.3 DERIVING SEAT-LEG DESIGN – TOPOLOGY OPTIMISATION

Input required by Optistruct is FE model of design space, boundary conditions, an objective function and design constraints [61]. FE model of the leg considered for the optimisation has 23690 nodes and 19629 hexagonal elements with Al7075T6 material assigned. Objective of optimisation is to minimise weighted compliance (of the 'Forward 9g', 'Downward 8.6g', and 'Sideward 4g' loadcases) with a constraint on volume (an upper bond of 50% of original volume). A weighing factor of 'Two' has been considered for the 'Forward 9g' loadcase, being the most critical while other two loadcases have a weighing factor of 'Unity' for the calculation of total compliance. Interface forces between leg-clamp and leg are recovered for 'Forward 9g','Downward 8.6g', and 'Sideward 4g' loadcases and are applied at the centre point of front and rear bore-holes (to accommodate forward beam and mid-beam respectively) as shown in Figure 8-2. Summary of forces and moments applied to the leg is as follows (Table 8-1).

Loadcase	Application Region	Force, N (Direction)	Moment, N-mm (About axis)
Forward 9g	Front	7779.2 (-X)	6425010.3(+Z), 2200186.1 (+Y)
	Rear	15558.1 (-X)	4714600.2 (+Z), 2200186.7 (+Y)
Downward 8.6g	Front	5240.3 (-Y)	2622095.3 (+X)
	Rear	10700.9 (-Y)	2622095.3 (+X)
Sideward 4g	Front	2619.3 (+Z)	2619270.4 (+X), 890550.0 (+Y)
	Rear	2619.3 (+Z)	2304957.6 (+X), 314312.1 (-Y)

Table 8-1 Summary of loadcases considered for topology optimisation of seat-leg. Loads have been applied at the centre point of the front and rear attachments of the leg with Forward beam and Mid beam respectively (Refer Figure 8.2 RHS for co-ordinate directions).

Optistruct algorithm alters material density of the design space in order to satisfy user defined objective and constraints. Design space has been developed considering (Figure 8-2)

- A curvature in the front would enable collapse of the front portion of the leg during '16g'. This would enable lowering of the centre of gravity of the entire seat structure thereby reducing the seat interface loads. In addition, it would put rear portion of the leg under tension, which would then absorb crash energy. Mass of the design space is approximately 3.3kg.
- A curvature in the rear may offer an easy access or egress to the occupants.

The design of the areas, for the assembly purpose, mating surfaces and fastening joints cannot be altered so those regions become the non-design region. Portions of

the leg near its attachment with the seat tie-down connections, forward beam and mid-beam are declared as ‘Non-Design’ space.

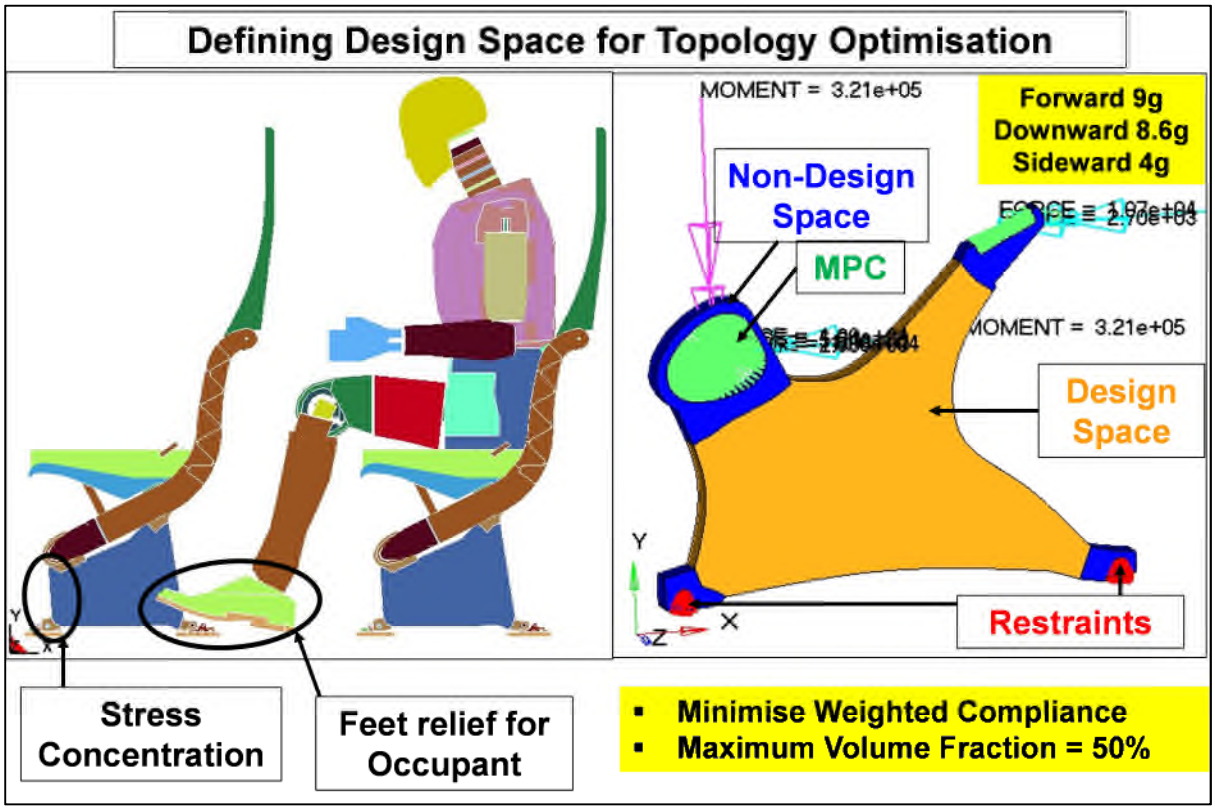

Figure 8-2 LHS - Development of design space for the Seat-leg. A curvature in the front would enable collapse of the front portion of the leg during ‘16g’. RHS - Definition of the optimisation problem.

Seat-leg will be produced by machining process. It would be easier for programming the path of machine tools if the design is symmetrical. Symmetry constraint is applied through two nodes (anchor node and first node); on the vertical web such that the vector from anchor node to the first node is perpendicular to the plane of symmetry XY (Figure 8-3).

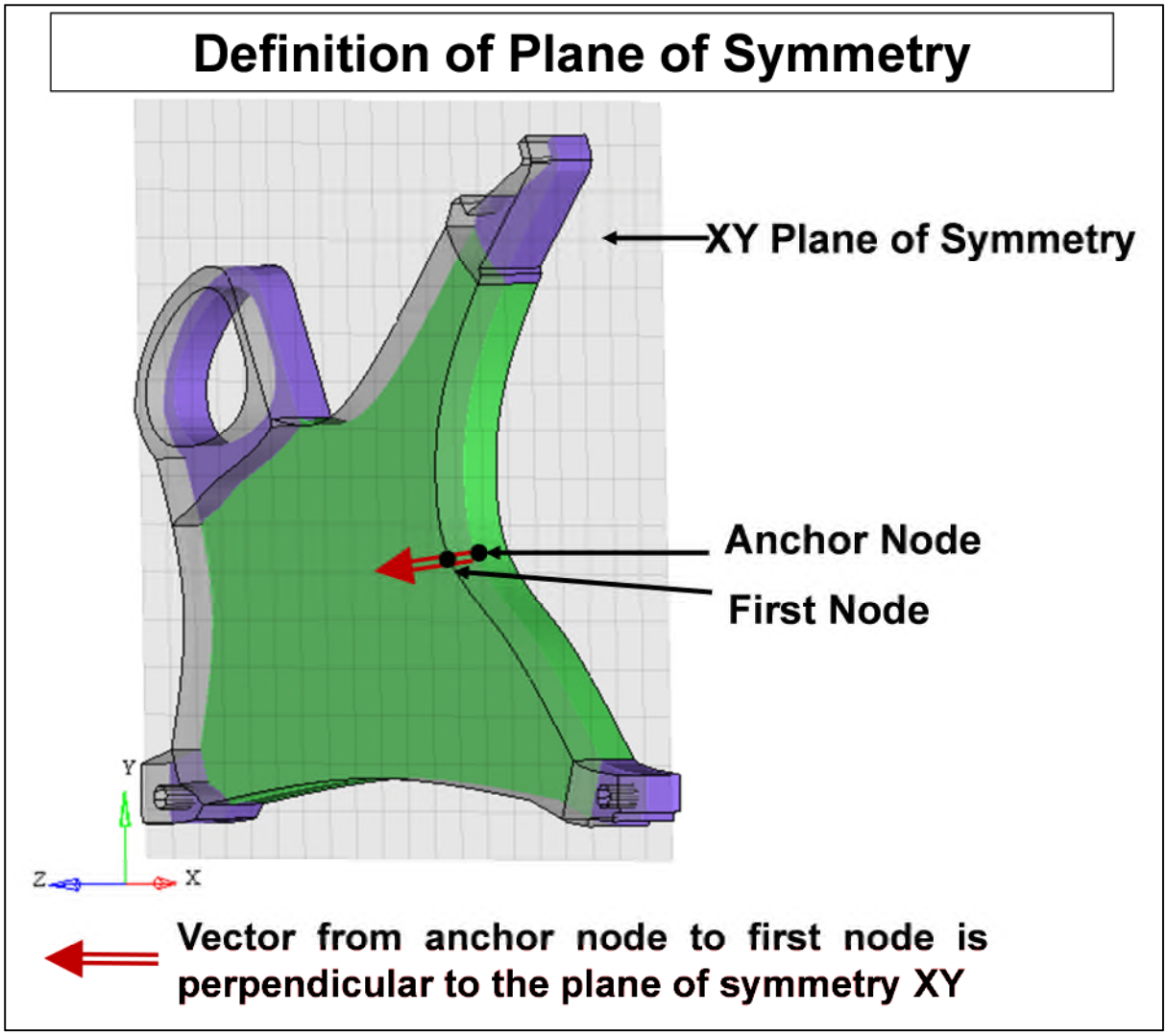

Figure 8-3 Symmetry constraint is applied about a vertical plane to the Seat-leg in topology optimisation problem

Manufacturing constraints play a major role in arriving at a feasible design concept i.e. design that can be easily manufactured during mass production. In the absence of appropriate constraints, internal voids are present in the design suggested by optimisation (Figure 8-4).

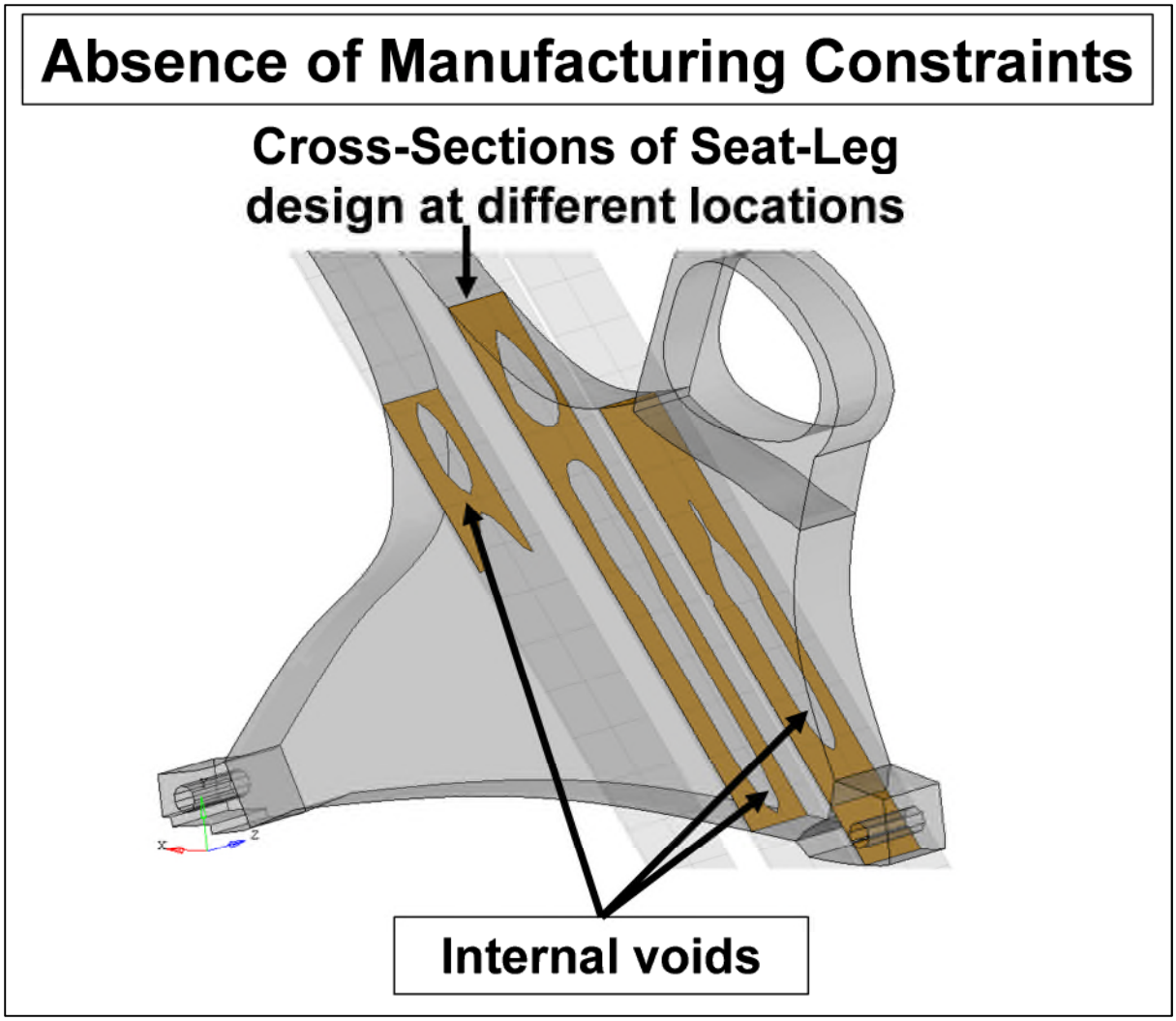

Figure 8-4 In the absence of appropriate manufacturing constraints, internal voids are present in the design of Seat-leg, suggested by Topology Optimisation. The design is impractical for machining during mass production.

In order to avoid, a concept with internal voids, “Draw direction” constraints have been applied (Figure 8-5). “Split” draw direction is used to be able to machine seat-leg from both the sides. Non-design parts are considered as obstacles during splitting.

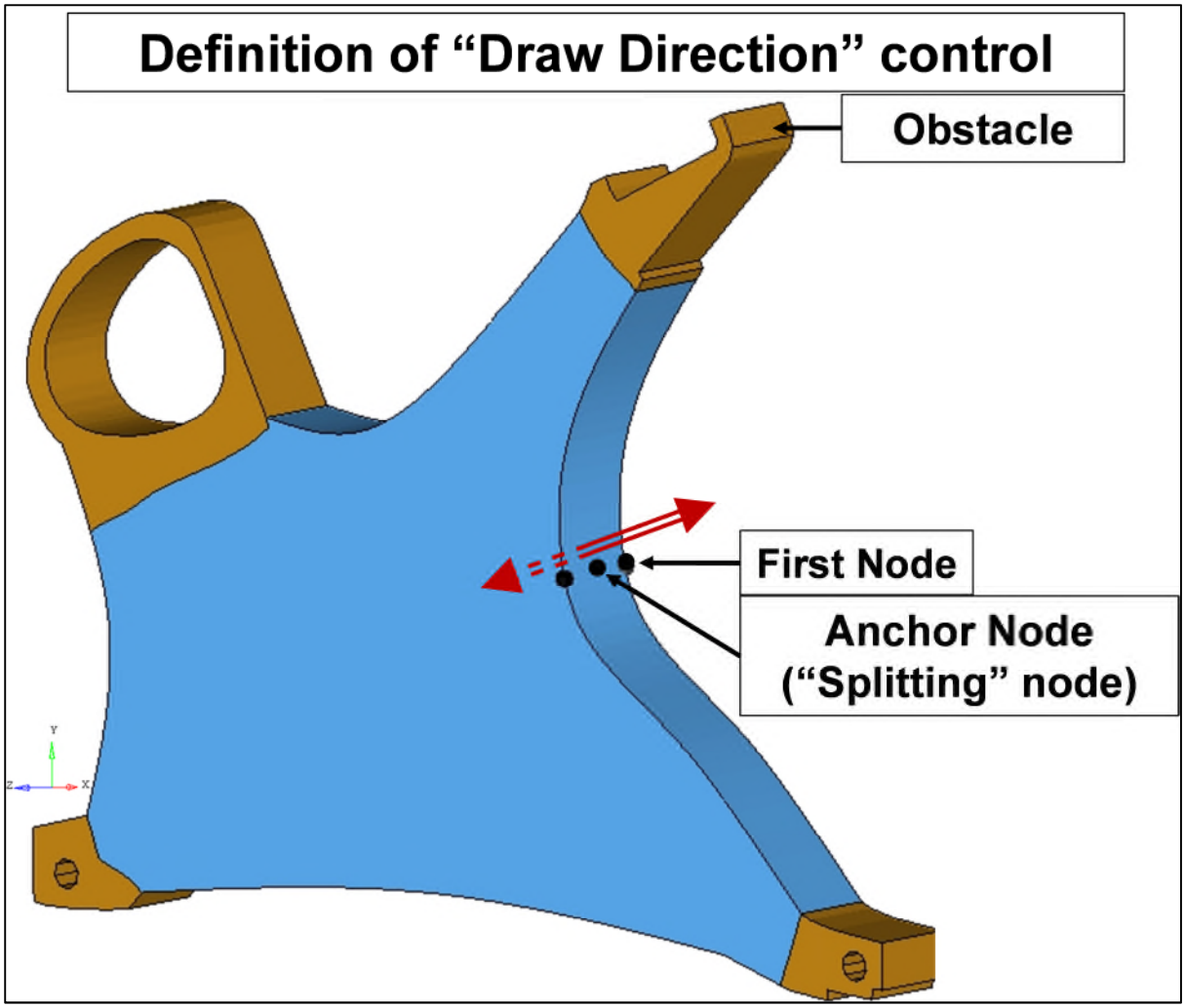

Figure 8-5 "Split" draw direction control has been applied to the topology optimisation problem defined for "Seat leg".

After 50 iterations, Optistruct reports convergence i.e. changes in the objective function for two successive iterations; is within 5%. *Filename.out* file contains the useful information on file set-up, definition of optimisation problem, memory and disk space requirements and CPU time required [61]. Total weighted Compliance reduced by 62percent from design iteration 1st to 50th iteration (Figure 8-6).

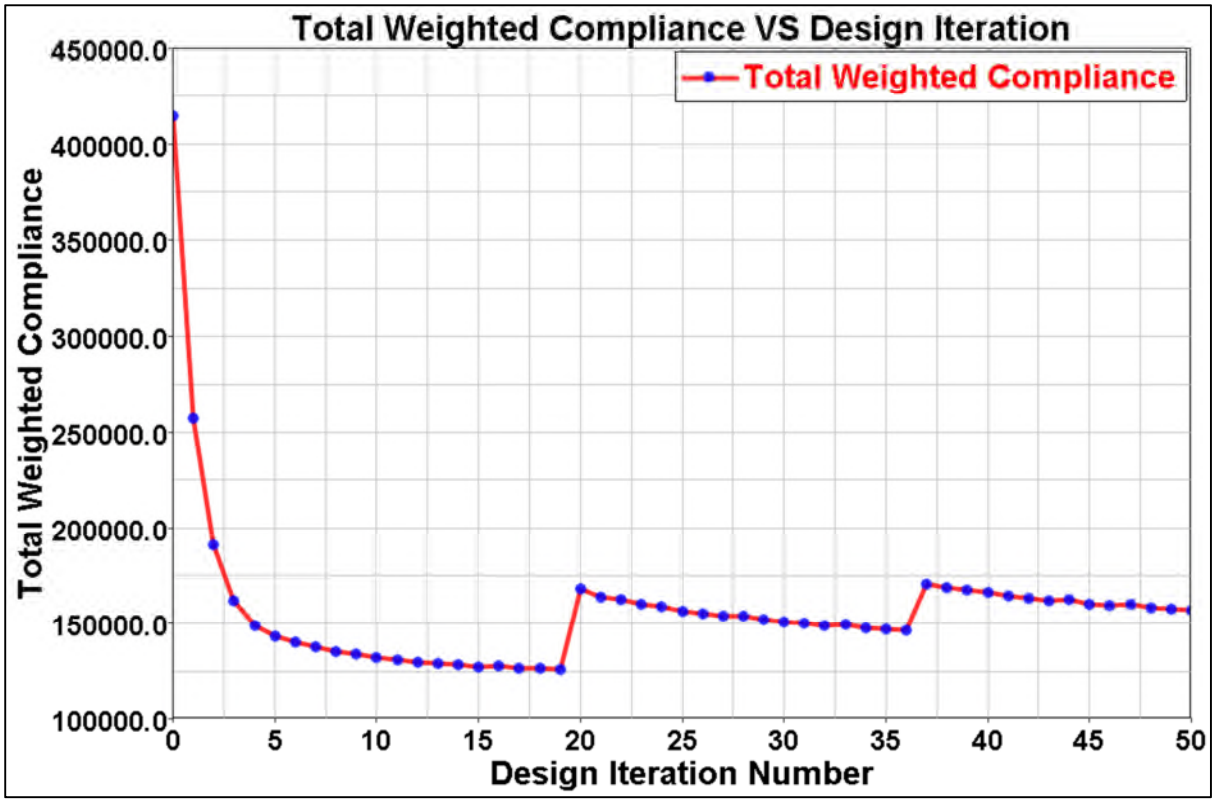

Figure 8-6 62% reduction in "Total Weighted Compliance" achieved by topology optimisation of Seat-leg. Loadcases considered – "Forward 9g", "Downward 8.6g" and "Sideward 4g". Solver – Altair/ Optistruct.

The CPU time is two hours and thirty minutes on a four processor Intel 660 machine. Memory required is approximately 86MB while the disk space required is approximately 554MB.

Via element density plot (density varying from 0 to 1), optimal material distribution plot can be obtained (Figure 8-7).

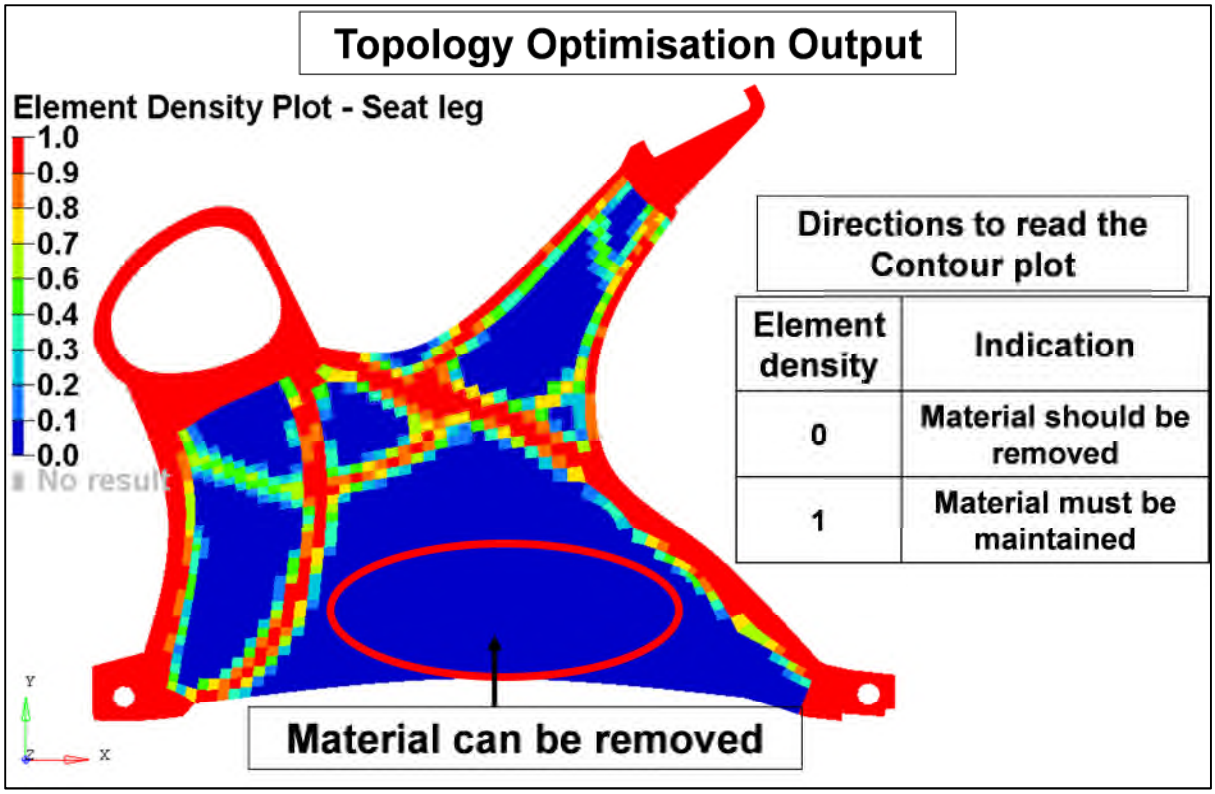

Figure 8-7 Element Density plot for Seat-leg, obtained as a result of topology optimisation. Solver - Altair / Optistruct

Shape suggested by Optistruct (Figure 8-8) was also useful during dynamic '16g' loads as

- During 'Dynamic 16g' load, front portion of the Seat-leg is supposed to deform such that rear portion of the leg is subjected to tension and there-after absorbing crash-energy through extension (plastic strain). Web in the 'I-Section' can be used for energy-absorption purpose (Figure 8-9).

CAD geometry for the FE design concept can be recovered by port processing the results using 'OSSmooth', software embedded in Altair Hypermesh [61]. It can generate iso-surfaces for the elements above the specified element density threshold. Mass of the design concept for Seat-Leg suggested by topology optimisation exercise is approximately 1.3kg (mass of design space 3.3kg).

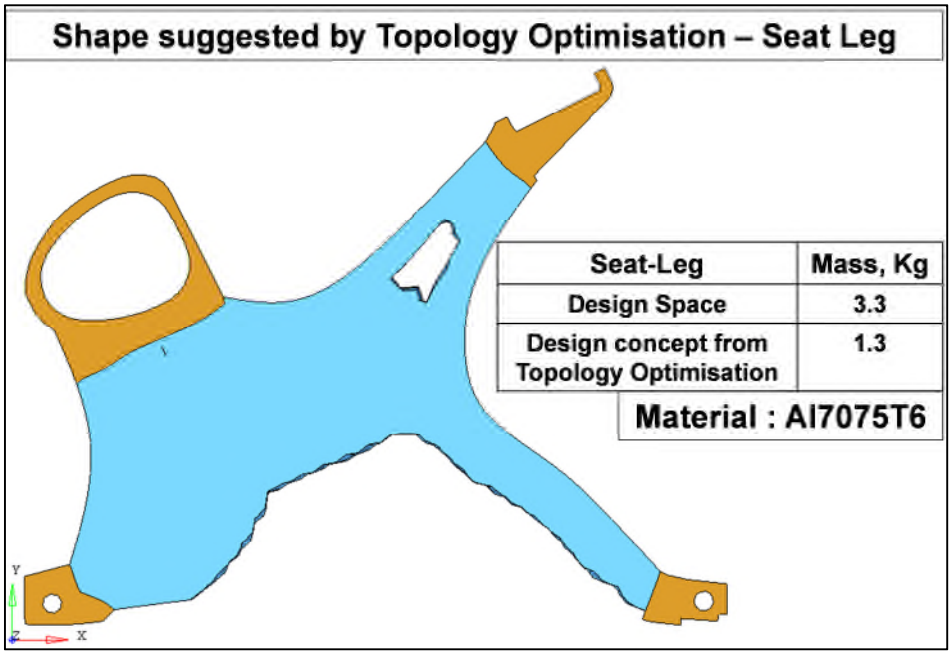

Figure 8-8 Shape suggested by topology optimisation for the design of Seat-leg. Solver - Altair / Optistruct

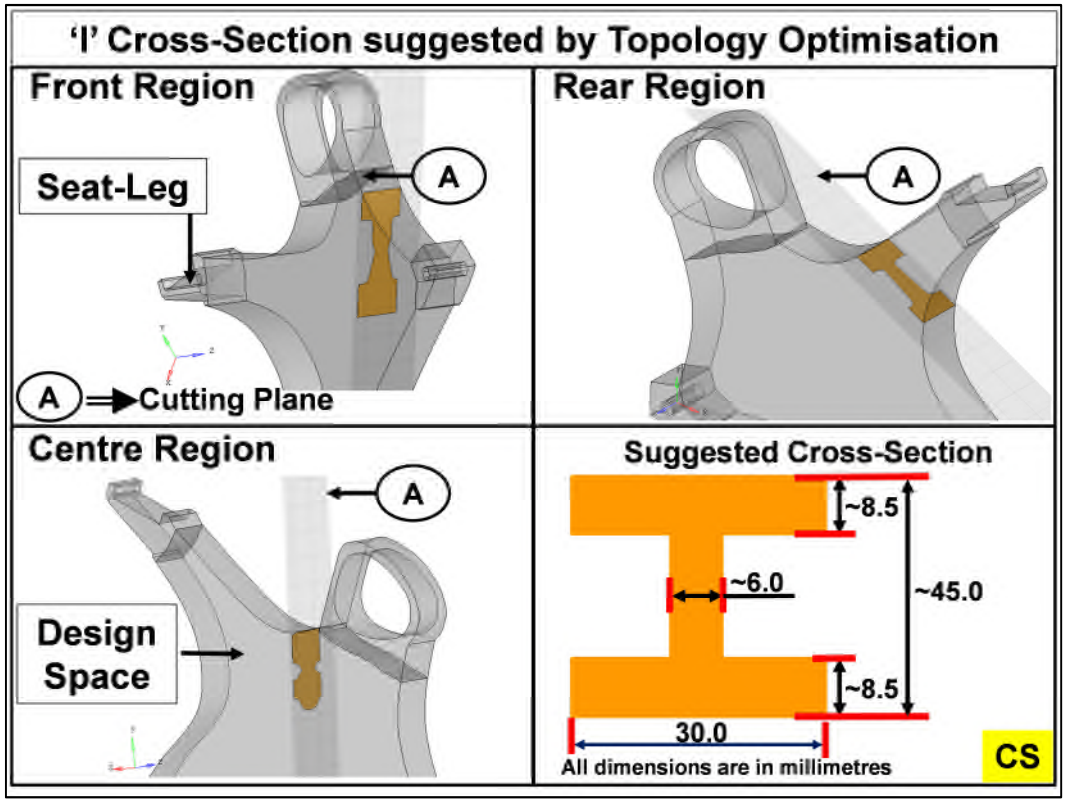

Figure 8-9 "I" Cross-section suggested by topology optimisation for Seat-leg. It would be beneficial for dynamic "16g" loadcase so that the web can be used for absorbing crash energy. Solver - Altair / Optistruct

A concept can be then created using design direction suggested by optimisation process (CAD geometry output from OSSmooth), concepts of design for manufacturability, stress concentrations, aesthetics and expected performance during dynamic loadcases (Figure 8-10 and 8-11). Leg variant VX1 developed by this process has a mass of 1.25kg.

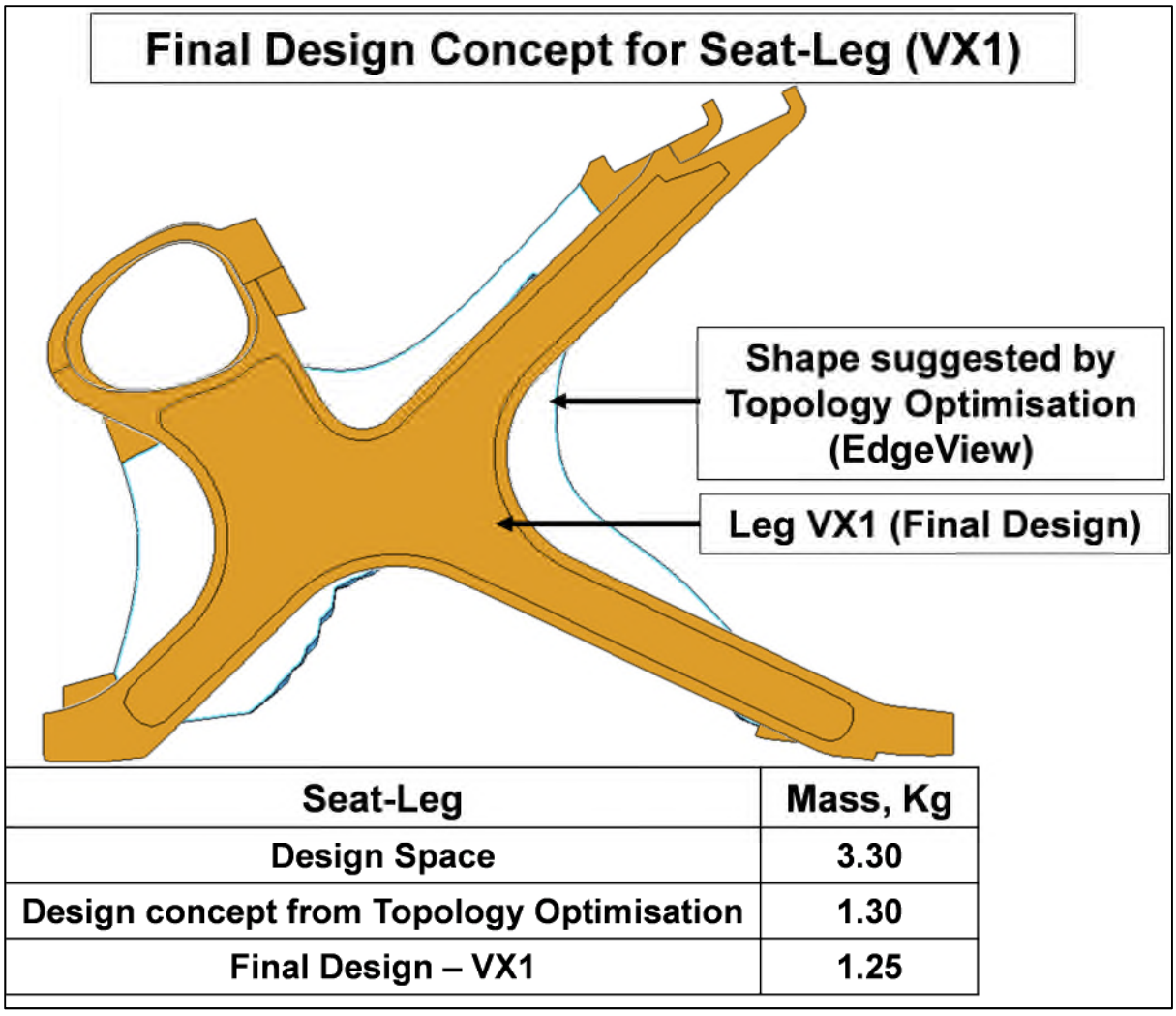

Seat-Leg	Mass, Kg
Design Space	3.30
Design concept from Topology Optimisation	1.30
Final Design – VX1	1.25

Figure 8-10 Final rendered design concept for Seat-leg (VX1) of triple seat-structure, generated using topology optimisation results and concepts for design for manufacturibility. CAD modelling software – SolidWorks.

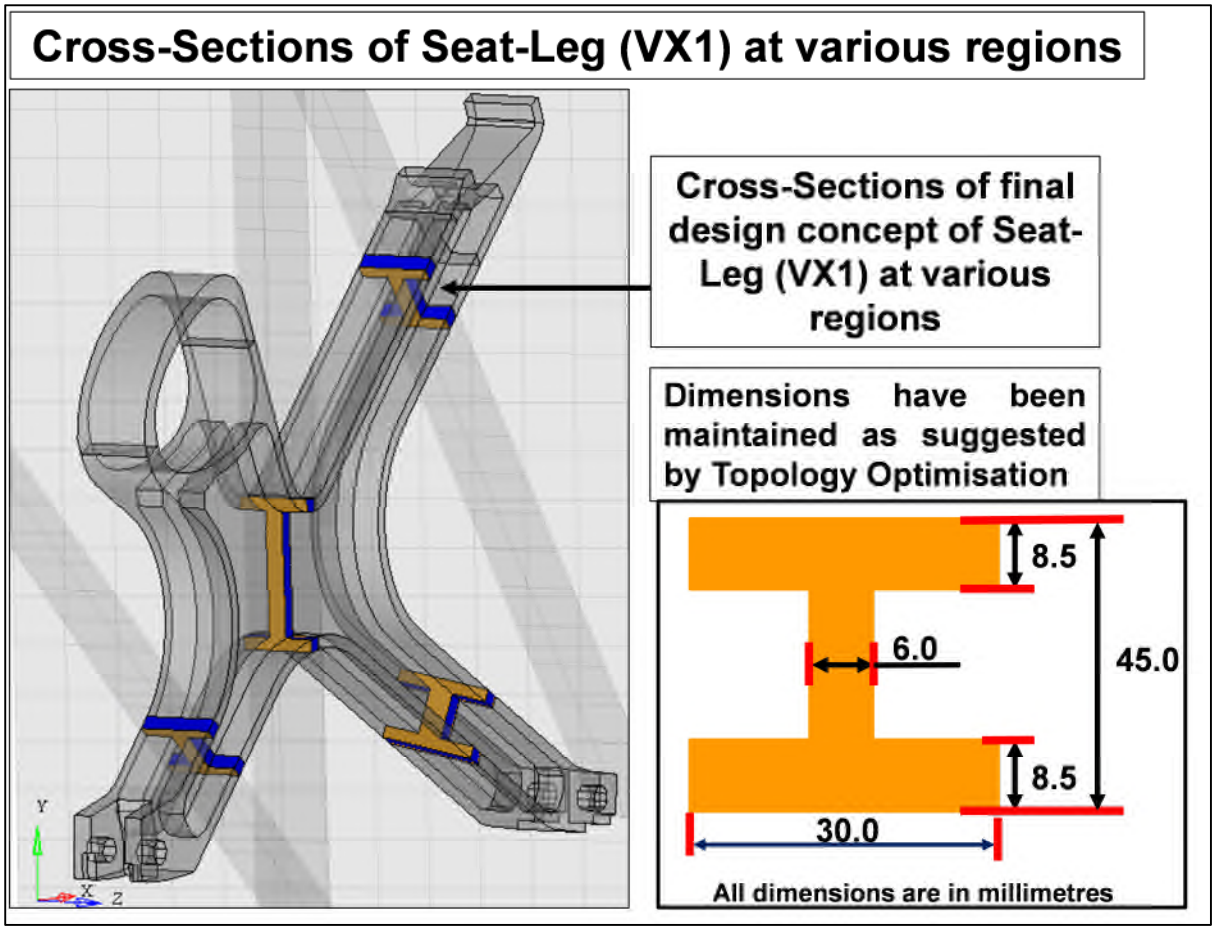

Figure 8-11 Cross-section of Seat-Leg VX1 at various regions

Next task is to build and incorporate FE model of "Leg VX1" into the triple seat-structure and assess its performance when subjected to static certification loads according to CS25.251 using validated FE methodologies (developed during this research – Chapter 4, 5 and 6).

8.4 STATIC COMPLIANCE OF THE TRIPLE SEAT STRUCTURE

FE model of 'triple' seat-structure with LegVX1 consists of 194644 nodes and 199052 elements. The maximum aspect ratio of 4.69 is observed for seven elements located in the aft upper quadrant of the Forward beam. 99% of the elements have warpage less than 5^0, while the maximum warpage of 19^0 is observed in the Seat-pan [61]. Figure 8-12 shows FE set-up for simulations performed to demonstrate static compliance. Bottom surface of the seat-track is constrained for all degrees of freedom for all the simulations and CS25.561 loads are applied as per the procedure discussed in Section 2.1.3.1 of this report. In order to be consistent with

experimental testing, factor of “8.6g” has been used for the download test. Load application point is defined according to ARP5526 [10]. Interaction definitions between different components are present in Appendix M.3. Bill of materials (BOM) containing mass of each component, material used and thickness of components (wherever applicable) are provided in Appendix M.2. Material stress-strain curves are present in Appendix K. Table number 8-2 summarises simulation history.

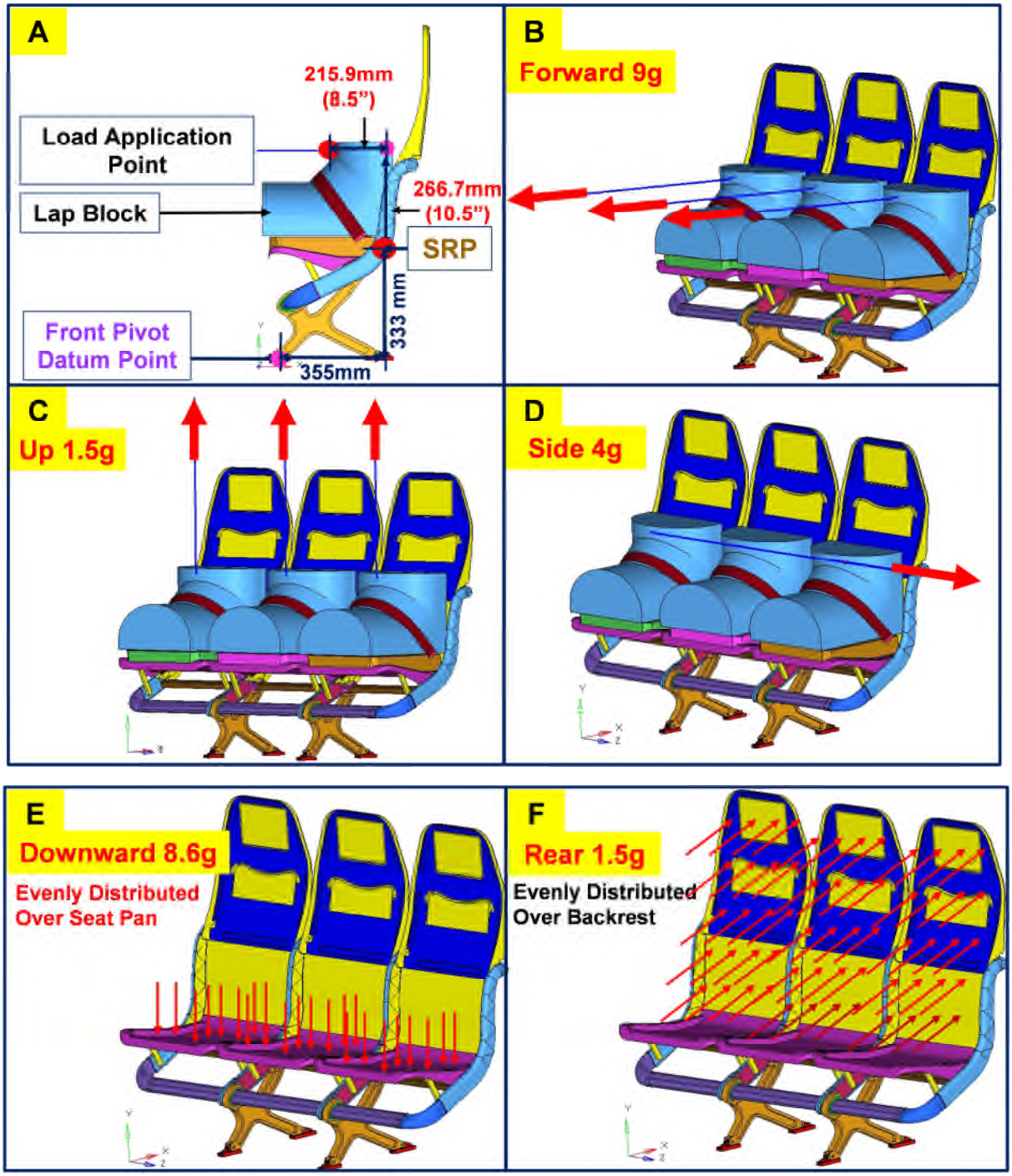

Figure 8-12 A- Definition of the Load Application Point for CS 25.561 inertia loads (in accordance with ARP5526 [10, 13]. B to F – CS25.561 loads applied to the triple seat-structure with leg variant VX1

Loadcase	Code Used	Simulation Summary	CPU time, (Hour. minute)
Forward 9g 7857.81N per seat	Explicit with quasi-static finish (LSDYNA / Explicit)	100% of load achieved in 0.15s and held constant for 0.03s. Minimum Stable time-step = 7.08E-7 , Memory required = 9.8GB	7.52 with 8 processors
Downward 8.6g, 9339.12N per Seat	LSDYNA / Implicit	8 load increments, Memory required = 5.2GB	0.49 with 8 processors
Sideward 4g, 3492.36N per seat	Explicit with quasi-static finish (LSDYNA / Explicit)	100% of load achieved in 0.15s and held constant for 0.03s. Minimum Stable time-step = 7.08E-7, Memory required = 9.4GB	7.57 with 8 processors
Upward 3g, 2619.27N per seat	Explicit with quasi-static finish (LSDYNA / Explicit)	100% of load achieved in 0.09s and held constant for 0.03s. Minimum Stable time-step = 7.08E-7, Memory required = 8.7GB	7.20 with 8 processors
Rear 1.5g, 1309.64N per seat	LSDYNA / Implicit	9 load increments, Memory required = 5.1GB	0.43 with 8 processors

Table 8-2 Summary of solver used, load application time and CPU time for CS25.561 loads applied to triple seat-structure to demonstrate static (9g) compliance.

8.4.1 DISCUSSION OF RESULTS

Please note that

- All the six components of stress are investigated for CS25.561 loadcases simulations. However, in order to keep this report brief, plots are provided only for distribution of von mises stress (VMS).
- In this section, results have been discussed only for “Forward 9g” loadcase being the most critical loadcase.
- VMS contours for remaining loadcases have not been provided in this report as seat-structure does not experience severe stresses or any plastic strains for all these loadcases.
- A summary of maximum deformations of the seat-structure observed for remaining loadcases has been provided in Table 8-3 and contour plots are present in Appendix N.

LOADCASE - “FORWARD 9G”

- Maximum displacement observed at the upper portion of backrest (Figure 8-13) is approximately 53.9mm, which is below the allowable limit of 75mm [14].

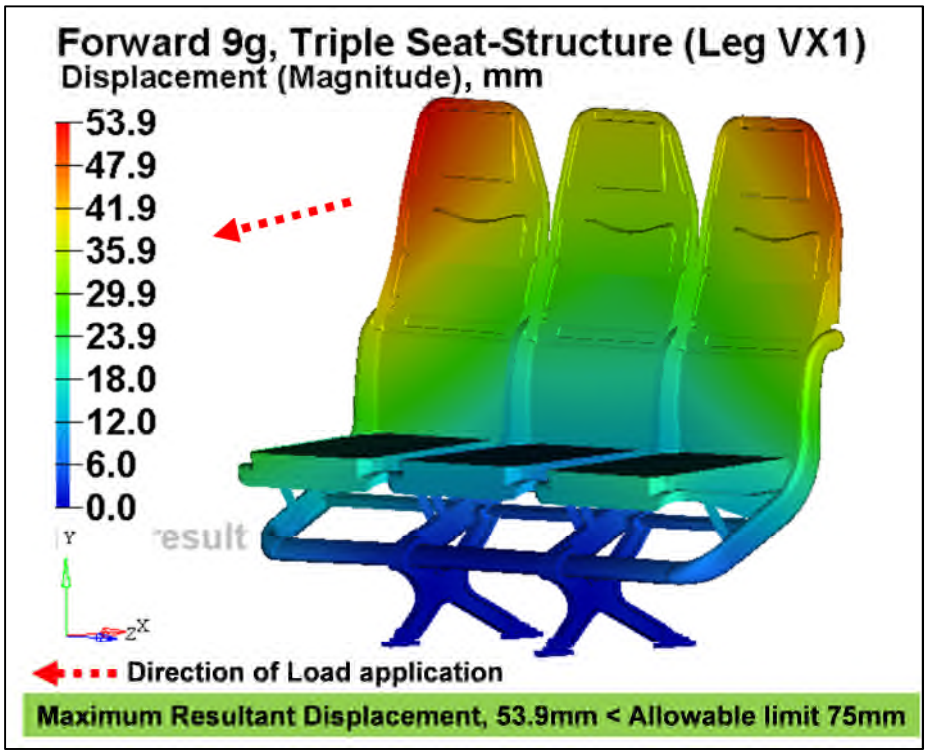

Figure 8-13 Overall displacement plot for triple seat-structure subjected to 'Forward 9g'. Lap blocks and loading mechanism is not shown.

- Higher stresses are induced in the RHS-Leg compared to that in LHS-Leg because of the overhang of seat-structure (in terms of Occupancy) on RHS side (Figure 8-14).
- Maximum VMS of 365MPa is observed (Figure 8-14 additional view) in the rear aft portion of the RHS seat-leg (Yield limit ~ 475MPa).
- A maximum VMS observed in the upper forward quadrant of Forward beam is approximately 150MPa (Yield limit ~260MPa). It occurs in the region where beam is connected with the leg.

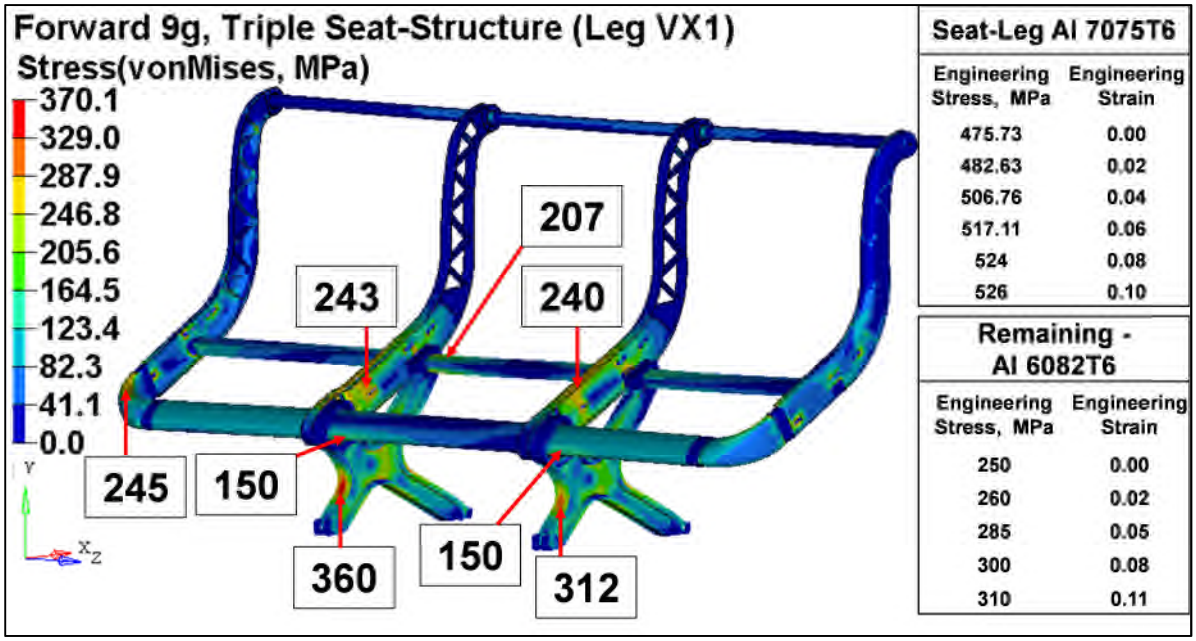

Figure 8-14 VMS plot for triple seat-structure subjected to 'Forward 9g'. Seat-structure can withstand the load without disintegrating form the track or deforming excessively, which may hamper evacuation process

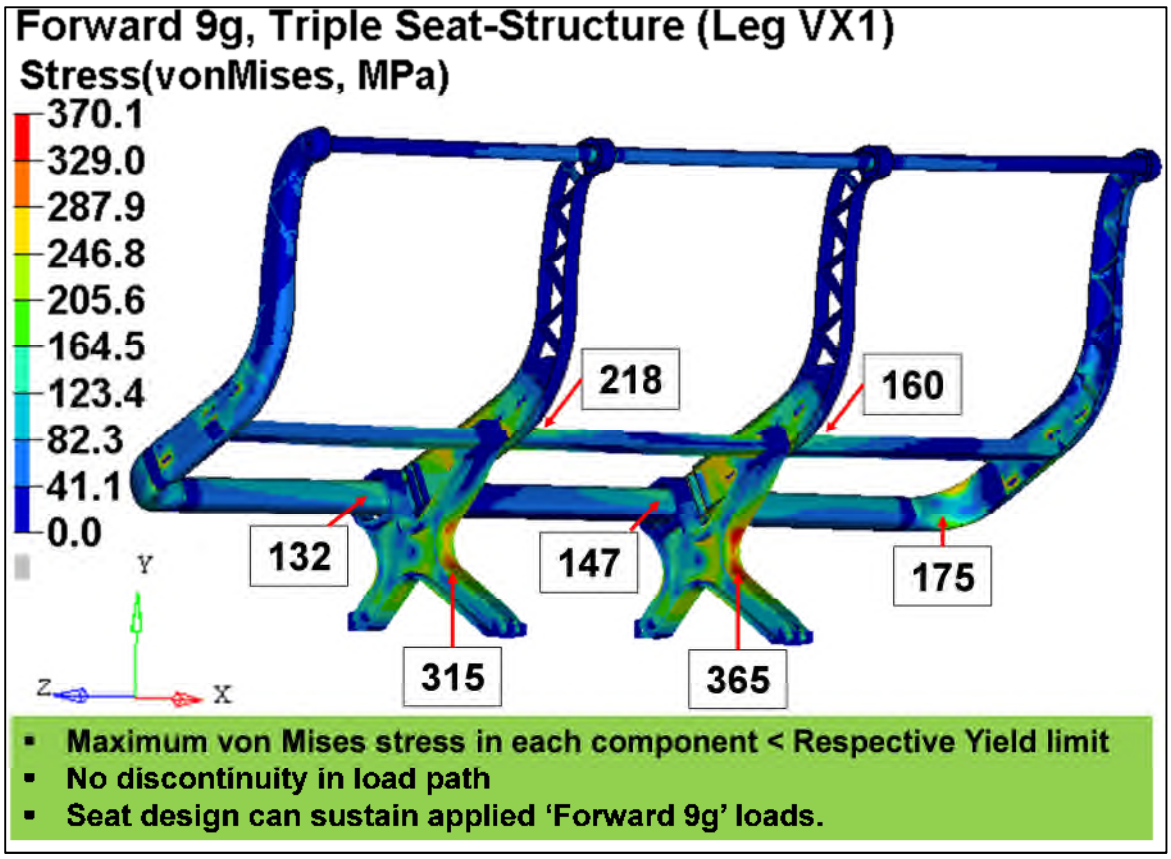

VMS plot for triple seat-structure subjected to 'Forward 9g' (Additional View)

- Seat interface loads (SIL) are provided in the Figure 8-15. Maximum tension loads of approximately 13.3KN and 20.2KN are observed in rear tool-less fitting and front tool–less fitting respectively. As there is no specific guideline available on the floor capability (i.e. maximum limit on SIL) of a particular aircraft, a specific remark cannot be made regarding SIL.
- The seat-structure functions in the elastic-strain region for the applied 'Forward 9g' loads.
- No discontinuity in the load path or separation of seat from seat-track is observed.

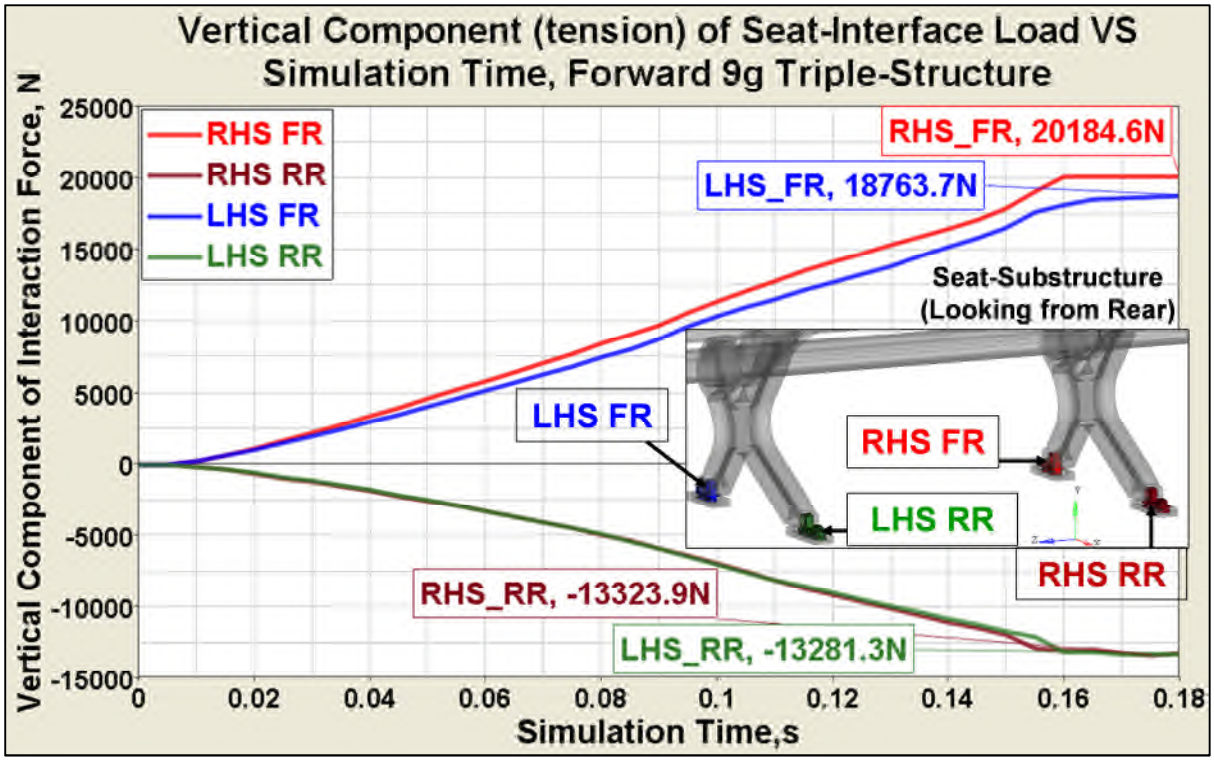

Figure 8-15 Tensile load (vertical component of Seat Interface Load) induced in the main body of tool-less fitting. Loadcase - Forward 9g' applied to triple seat-structure

Table 8-3 summarises the maximum deformations of the seat-structure predicted by FEA and compares against evaluation criteria defined by Advisory Circular 25.562-1B [14]. It can be observed that the maximum deformation of the seat-structure in each of the loadcases is within the allowable limit. It does not dis-integrate from the floor. Therefore, compliance of 'triple' seat-structure against static certification loads (CS25.561) is demonstrated by virtual simulations using validated FE methodologies developed during this research.

The drawbacks of previous leg designs such as buckling of the underside of the aft-foot section ("Forward 9g") or excessive rotation of the seat-pan ("Downward 8.6g") are not observed with leg variant VX1. Hence it was decided to maintain its design for subsequent dynamic simulations (Chapter 9).

CS25.561 Load	Allowable displacement, mm	Observed Displacement (FEA), mm	Other Observations	Remark
Forward 9g	75	53.9	▪ VMS in all the components below the respective yield limits, ▪ No discontinuity in the load path, ▪ Seat-Structure remains integral with Seat-track	**As the 'triple' seat structure meets all the design requirements specified by AC 25.562-1B, 'static compliance' is demonstrated using validated FE procedures developed during this research.**
Downward 8.6g	Maximum Angle of Seat-Pan rotation < 35^0	2.4^0		
Sideward 4g	38 (till 635mm above floor), 50 (above 635mm)	17.9 (till 635mm) 28.3 (above 635mm)		
Upward 3g	38	4.3		
Rear 1.5g	75	57.4		

Table 8-3 Summary of FEA results for structural evaluation of triple seat-structure subjected to static certification loads (CS25.561). It can be observed that as the seat design satisfies all the regulatory requirements it is '9g' compatible.

Conclusion – Chapter 8

Though aim of this research is to develop FE methodologies for evaluating seat-structures subjected to crash scenario; design of major load carrying members i.e. Forward beam and seat-leg; happened simultaneously. A spreadsheet based on analytical calculations developed during the first phase of the research, was helpful in preliminary sizing of the Forward beam.

Being a single load path seat-structure, it was quite challenging to design a seat-leg. Initial leg designs suffered from drawbacks such as,

- Buckling of the lower aft section due to significant bending loads applied by the “Forward 9g” loads
- Excessive deformations of the seat-pan in downward direction creating unpleasant ride comfort for the Occupants due to bending load applied by their mass.

Excessive rotation of the seat-pan about its rear attachment point to the boomerang was observed during “Forward 9g” loadcase. Such a rotation significantly changed the direction of applied loads leading to a severe failure of the leg. It would have also resulted in excessive permanent deformation of the seat pan during dynamic loads thereby impeding Occupant evacuation. Rotation of the seat-pan was a result of forward shift in centre of gravity of occupant during ‘Forward 9g” and seat-pan being unsupported at the front. Therefore, a supporting bracket was used to connect seat-pan with boomerang in the front. This modification helped to nullify the bending moment applied by mass of the occupant and hence rotation of the seat-pan.

Optistruct, an optimisation algorithm developed by Altair/ Hyperworks; was used to derive the leg design. The objective of optimisation was to minimise weighted compliance of “Forward 9g”, “Downward 8.6g” and “Sideward 4g” loadcases with a constraint on volume. Symmetry constrains and ‘Split Draw direction control (manufacturing constrains) were defined. Mass of the design space was approximately 3.3kg. 62% reduction in total weighted compliance

was achieved with 60% reduction in mass. Final design concept for leg (called “VX1”) was developed using a CAD geometry recovered from Optistruct (using OSSmooth, a semi-automated design software embedded in Hypermesh) and applying concepts of ‘Design for Manufacturability’ and had a mass of 1.25kg.

Next task was to evaluate the structural performance of the triple seat-structure (with leg variant “VX1”) against static certification loads (CS25.561) using the validated FE methodologies developed in this research. Loads were applied as defined in “Advisory Circular 25.562-1B” and the maximum deformation limits specified by “Technical Standard order TSO C-39a” were used for assessment.

The maximum deformation of the seat-structure in each of the loadcases was found to be within the respective allowable limit. Seat-structure neither did dis-integrate from the floor nor developed any discontinuity in the load path. Therefore, compliance of ‘triple’ seat-structure against static certification loads (CS25.561) is demonstrated by virtual simulations.

The drawbacks of previous leg designs such as buckling of the underside of the aft-foot section (“Forward 9g”) or excessive rotation of the seat-pan (“Downward 8.6g”) were not observed with leg variant “VX1”. Hence it was decided to maintain its design for subsequent dynamic simulations (Chapter 9).

9 ‘16G COMPATIBILITY’ OF THE SEAT

In the first phase of the chapter, elements related to the application of explicit dynamic time integration scheme for solving a transient problem have been discussed namely stability conditions, element technology, contact stiffness and suitable algorithms for tied interfaces.

Literature review (Section 7.1.2) showed that attempts by various researchers to initiate damaged floor condition in a ‘16g’ simulation have either failed or compromised on separating the two loadcases. In the next phase of this chapter, two methods to accomplish it have been developed and demonstrated.

In the last phase of the chapter, procedures to simulate dynamic loads applied to the seat-structure according to CS25.562 (‘16g’ and ‘14g’) are discussed and demonstrated for a triple seat-structure. It is then followed by interpretation of the FE results.

9.1 EXPLICIT DIRECT INTEGRATION

In direct integration, the governing equilibrium equations are integrated using a numerical step-by-step procedure [31, 32]. Prior to numerical integration, equations are not transformed into a different form (as necessary in modal methods). Instead discretisation in time is accomplished by “directly” using finite difference approximations of time derivative. It has two characteristics,

- Governing equilibrium equation is satisfied only at discrete time intervals Δt apart i.e. the static equilibrium including the effects of inertia and damping forces is sought at Δt within the interval of the solution.
- The variation of displacement, velocity and acceleration within each Δt is assumed, which in turn determines the accuracy, stability and cost of the solution procedure adopted.

Methods of direct integration calculate conditions at time step ‘$t+\Delta t$’ from the equation of motion, a difference expression and known conditions at one or more preceding time steps [32]. Depending upon the difference equation used direct integration algorithms can be classified as Explicit or Implicit.

An explicit algorithm uses a difference expression of general form [32],

$\{D\}_{t+\Delta t} = f(\{D\}_t, \{\dot{D}\}_t, \{\ddot{D}\}_t, \{D\}_{t-\Delta t}, \ldots)$ **Equation 9-1**

Where, D, $\dot{D}$, $\ddot{D}$ are the displacement, velocity and acceleration at corresponding time-step respectively, which is historical in nature. The difference expression is then combined with the equation of motion at time step 't'.

An implicit algorithm uses a difference expression of general form,

$\{D\}_{t+\Delta t} = f(\{D\}_{t+\Delta t}, \{\dot{D}\}_{t+\Delta t}, \{D\}_t, \{\dot{D}\}_t, \ldots)$ **Equation 9-2**

Equation 9-2 is combined with the equation of motion at time step't+Δt'

The Central Difference Method is a two-step explicit method as the right hand side of equation contains information dating back to time step't' and 't-Δt' [31, 32]. Using conventional central difference formula, with Δt timestep, velocity and acceleration at time t can be approximated as [32]

$\{\dot{D}\}_t = \frac{1}{2*\Delta t}(\{D\}_{t+\Delta t} - \{D\}_{t-\Delta t})$ or **Equation 9-3**

$\{\ddot{D}\}_t = \frac{1}{\Delta t*\Delta t}(\{D\}_{t+\Delta t} - 2\{D\}_t + \{D\}_{t-\Delta t})$ **Equation 9-4**

It can be seen from Equations 9-3 to 9-4 that the terms that contain Δt to powers higher than second are omitted. The primary error term is therefore proportional to Δt^2 and {D} has second-order accuracy. In practice, adequate accuracy is provided by the small Δt essential for computational stability.

9.1.1 STABILITY OF EXPLICIT TIME INTEGRATION

The aim of the numerical integration of the FE equilibrium equations is to predict the dynamic response of the structure accurately. Therefore, it is of utmost important to evaluate the time increment (Δt), which ensures the stability of the integration scheme. Stability of an integration scheme means for arbitrary initial

conditions at time t, error in displacements, velocities and accelerations if any, which may be due to round-off in the computer, does not grow without any bound [32]. Time increment of explicit algorithm should be less than a critical value for stability purpose and hence explicit algorithms are “Conditionally Stable”. Critical time-step Δt without considering damping is given by [32]

$\Delta t_{cr} < (2/\omega_{max})$ **Equation 9-5**

Therefore it becomes necessary to determine ω_{max} or to accurately control it. Calculation of the exact ω_{max} of a structure is practically impossible considering the considerable FE modelling efforts required and significant memory requirements. Another way to bound ω_{max} is the fact that it must be less than the largest ω_{max} of any assembled and unsupported element of the FE mesh. Considering an unsupported two node bar element with lumped masses, the highest frequency is calculated by

$\omega_{max = 2 * } \sqrt{(AE/mL)}$ **Equation 9-6**

Where,

A – Cross-Sectional area

E – Modulus of elasticity

m - Mass per unit length, pAL **Equation 9-7**

p – Density of the material of the bar

L – Length of the bar

Speed of sound in the material, c = $\sqrt{(E/\rho)}$ **Equation 9-8**

Substituting Equations 9-13 to 9-15 in Equation 9-12, the minimum stable time step (critical time step) for an undamoed material is given by

$\Delta t_{cr} \leq (\frac{L}{c})$ **Equation 9-9**

This is called as CFL condition after Courant, Friedrichs and Lewy [31, 32]. The physical interpretation of “Critical Time Step (Δt_{cr})” is that the time increment (Δt) of the direct explicit numerical integration must be smaller than the Δt_{cr} so that the information such as stress wave does not propagate more than the distance between the adjacent nodes during a single time step [32].

9.1.2 REDUCED INTEGRATION ELEMENTS FOR EXPLICIT ANALYSIS

Full integration is a quadrature rule of sufficient accuracy to exactly integrate all coefficients of stiffness matrix (K_{ij}) of an undistorted element [32]. As a general rule, a polynomial of degree (2n-1) is integrated exactly by n-point Gauss quadrature [31, 32]. Use of an integration rule less than full order is called "Underintegration" or "Reduced Integration". For large-scale three-dimensional calculations, lower order under-integrated elements are preferred over full-integrated due to

- In a complex nonlinear problem involving large deformations, element distortion is a vexing drawback of higher-order fully integrated elements. Performance and convergence of these elements significantly degrades due to distortions and solution may fail due to negative Jacobian determinant at one of the quadrature points.
- Fully integrated lower order (linear) elements suffer from excessive shear stiffness (known as shear locking) when subjected to bending loads so the overall deflections are unrealistically small [32].
- Lower order under-integrated elements offer a very attractive savings in the computational cost by an order of 6 to 8 [31]. e.g.
- For non-linear problems, internal forces at any time n, $\{R^{int}\}_n$ are generated in element-by-element fashion, by summing element contributions [31],

$$\{R^{int}\}_n = \sum_{i=0}^{n} (\{r\}_n^{int})_i \qquad \textbf{Equation 9-10}$$

Where,

$$\{r\}_n^{int} = \int [B]^T \{\sigma\}_n \, dV \qquad \textbf{Equation 9-11}$$

Evaluation of this integral requires the same order of quadrature as the element stiffness matrix. Calculation of $\{R^{int}\}$ consumes large portion of the per-time-step cost of explicit integration. Reduced integration (one

quadrature point per element) rather than full integration (four one quadrature points per element), quarters the computational cost.

However, under-integration inherits instabilities in the displacement field, which leads to one or more deformation modes that exist without any elastic resistance. This phenomenon is known by various names: hourglassing, keystoning, kinematic modes, spurious zero-energy modes, singular mode, instability mechanism, and chickenwiring. Consistent control of these modes does not decrease the rate of convergence, so generally for large-scale applications, one-pint quadrature with hourglass control is very effective.

Single point integration brick element (Element formulation 1 in LSDYNA) with Puso assumed strain stiffness form (Hourglass control type 9 in LSDYNA), which can combine coarse mesh accuracy and computational robustness and efficiency for large-scale nonlinear problems has been used to model the seat leg VX1 [35, 63]. Its characteristics are [63]

- It is indifferent to orientation of frame and the scheme used for node numbering.
- It is well suited for bending dominated problems (e.g. seat leg is subjected to bending loads due to the applied “Forward 9g” loads, which is the most critical load case) and eliminates volumetric locking.
- Only four hourglass stabilisation forces are required to be stored for small strain applications exploiting the orthogonally of the hourglass strain fields. In conventional stabilisation algorithms, thirty-six stabilisation forces need to be stored.
- Since the Jacobian matrix, which maps the isoparametric domain on to the physical domain is evaluated at the centroid of the element, the element performance is insensitive to the distortion.

Effect of element distortions on FEA results

Computed results are less accurate, when element shapes are distorted. Distortion refers to initial element shapes, before displacements are generated by loads. The cause of loss of predictive capability is due to the loss of

element's capability to represent the same order of polynomial in the physical co-ordinate (say x, y, z) after geometric distortion as they could without distortion [31]. Therefore analyst should build a FE model with regular shaped elements ensuring smooth transitions between different mesh densities.

9.1.3 EXPLICIT CONTACT

The robust treatment of sliding and impact along the interfaces is one of the important capabilities in LSDYNA [63]. Penalty method, used to handle surface interactions consists of placing normal interface springs between the penetrating node and the corresponding contact surface. With the exception of the spring stiffness matrix, which must be assembled into the global stiffness matrix, the implicit and explicit treatments are same [63]. Characteristics of the penalty method are,

- Due to the symmetry approach used, the solution excites little if any mesh hourglassing.
- Momentum is exactly conserved without imposing the impact and release conditions.
- No special treatment of the intersecting surfaces (e.g. slave surface should be finer than the master surface) is necessary greatly simplifying the FE model building process.

LSDYNA has three implementations of the penalty algorithm [63]

I. Standard Penalty Formulation
II. Soft constraint Penalty Formulation
III. Segment-based Penalty Formulation

In standard penalty formulation, the interface stiffness is approximately the same order of magnitude of the underlying element normal to the interface. For a large interface pressure, unacceptable penetration can be controlled by scaling up the stiffness and scaling down the time step size. However, this results in increased number of time steps and consequently increased cost of computation. Therefore, this formulation with "sliding only" option is used for treating explosive-structure interaction problem thereby avoiding use of penalty

approach. “Sliding only formulation” is a specialisation of distributed parameter method.

In LSDYNA penalty stiffness or interface stiffness can be chosen from

- Minimum of the stiffness of the master segment and slave node stiffness (default)
- Use stiffness of the master segment
- Use slave node value, area or mass weighted
- Use slave node value that is inversely proportional to the shell thickness

Different options for selecting the penalty stiffness are necessary to tackle the peculiar problems such as materials in contact having drastically different bulk moduli or high velocity impact. The master segment stiffness K_i for a brick element is calculated as

$K_i = (f_{si}\, k_i\, A^2_i / V_i)$ [63] **Equation 9-12**

Where,

f_{si} is a scale factor for the interface stiffness (default 0.1).

k_i is the bulk modulus

V_i is the volume of the brick element

A_i is the face area of the element that contains the master segment

Soft Constraint Penalty Formulation

Very soft materials (e.g. foam) have very low stiffness values, which lower the contact stiffness undesirably causing excessive penetrations. When these soft materials come in contact with the stiffer materials (e.g. contact between foam and aluminium seat pan in “Sleep Seat”), contact instabilities may initiate. To treat such problems, ‘Soft Constraint Penalty Formulation”, which uses a different formulation for the contact stiffness to eliminate excessive penetrations, is used.

In addition to the master and slave contact stiffness, an additional stiffness called as “Stability Contact Stiffness, K_{cs} is calculated based on the stability (Courant’s limit for minimum stable time increment) of the local system comprising of masses of the slave and master segments connected by a spring.

K_{cs} (t) = 0.5*SOFSCL.m*.($1/\Delta t_{cs}$ * (t)) **Equation 9-13**

Where

SOFSCL is the scale factor for the Soft Constraint Penalty Formulation

m* is a function of the mass of the master nodes and slave nodes

Δt_{cs} is set to the current time step to prevent instabilities

The maximum of stiffness calculated by traditional penalty formulation (K_i from Equation 9-19) and that by soft constraint approach (K_{cs}) is taken as the contact or interface stiffness.

Segment-based Penalty Formulation (Surface based formulation)

Segment-based interface definition is a general purpose shell and solid element penalty contact algorithm. In this formulation, segment masses are used instead of nodal masses that are used with “Soft constraint” approach. Penalty stiffness at time t for segment-based penalty formulation, K_{sg} is calculated as

K_{sg} (t) = 0.5*SLSFAC.(($M_S * M_M/(M_S + M_M)$).($1/\Delta t_c * (t)$)^2 **Equation 9-14**

Where,

SLSFAC is the scale factor sliding interface penalties (either of a master segment or slave segment)

Δt_c is set equal to the initial solution time step. Δt_c is updated only if the solution time step grows more than 5%.

M_S and M_M are the mass of slave segment and master segment respectively.

For shell segments, entire mass of elements that define the interface is taken into account. For the interfaces containing solid elements, half of the mass of the corresponding element is considered for calculating the penalty stiffness.

*CONTACT_AUTOMATIC_SINGLE_SURFACE, the most commonly used contact algorithm in impact simulations, has been used for the dynamic simulation performed during this research, to ensure contact compatibility [35, 63]. It accounts for shell thickness and has no particular segment-based orientation i.e. it looks for contact in both the directions. Thus while modelling the interface containing shell element appropriate gap must be considered for shell thickness.

9.1.4 INITIAL INTERPENETRATIONS AND STATEGIES TO AVOID IT

The orthogonal distance between a slave node and its closest master segment is computed by projecting the slave node coordinates on to the master segment using a local coordinate system embedded in the master segment [33, 63]. A positive projected distance depicts no penetration condition while a negative projected distance indicates the penetration. Depending on penetrated distance, a force is applied to remove it.

A problem arises when a slave node or slave segment penetrates its closest master segment during the initialisation of the problem (at time t=0). Such a penetration is called as “Initial Penetration” or “initial Interpenetration”.

Where undetected initial penetrations occur

- Apart from other cases of undetected initial interpretations due to a coarse discretisation of the mating surfaces, a common case of edge of a shell element penetrating the surface of a solid element at the intersection is observed in the geometries like aircraft seat. This occurs as the shell edges are rounded with a radius equal to one-half of the shell thickness to maintain the surface continuity by default (alternately shell edge shapes can be assumed to be square using SHLEDG option under *CONTROL_CONTACT [35]). However, when the FE model is

rendered in a conventional manner (i.e. line display for beam elements and planer display for shell elements), the interpenetrations cannot be detected.

- If a node in used in two different contact definitions, modification of the co-ordinates to remove its penetration from one contact definition may introduce a new penetration for the second contact definition (known as a residual penetration).

Adverse effects of unintended initial interpenetrations

LSDYNA attempts to remove any initial penetrations at the first cycle of simulation by applying forces to the nodes involved [63]. These large initial forces in the beginning of the solution,

- Lead to severe numerical problems destroying the stability of the solution.
- Can produce non-physical localised initial stresses and strains.
- 'Residual penetrations' tend to produce a "negative energy" thereby lowering the numerical accuracy of the simulations.

Ways to detect initial interpenetration

- A list of nodes interpenetrating the respective master segments and their new modified positions (to remove the penetrations) is reported by LS-DYNA in the D3HSP file [35]. These geometry modifications should be thoroughly checked for as they are performed based on numerical reasons. In reality, it may move the problem elsewhere producing unrealistic or non-manufacturable geometries.
- Negative growth of contact energy at early stages of the simulation is one of the signs that initial interpenetrations exist.

In case of "Sleep Seat", which has a large number of contact interface definitions, it is cumbersome to track these adjusted nodes from these files by their node numbers and then to adjust their positions in FE model. An easy way proposed by this research to visualise initial penetrations in a particular region using LS-PREPOST is:

- Load a binary D3PLOT file with LS-PREPOST.
- From Page 1, click on Vector (Time =0)
- From the Drop-down menu under the vector plot, select ‘Displacement’ and click ‘Apply’
- A contour of displacements in X, Y, Z directions; with the magnitude, by which the nodes are moved and arrows pointing in the direction of movement; is plotted. These displacements at time zero are ‘Initial penetrations’. Such a visualisation makes it easier for the analyst to modify the FE model to remove the ‘Initial penetrations’.

To avoid undesired structural response due to initial interpenetrations, author suggests following tips from various strategies developed during FE model building of ‘Sleep Seat”

- If the shell thicknesses are considered while defining an interface between two shells, adjacent surfaces must be offset by at least a distance equal to the sum of one-half of the thicknesses of each shell unless contact thickness is not scaled down using *PART_CONTACT [35].
- Using *Part_CONTACT, a smaller contact thickness can be used for interpenetrating shells. This does not affect the stiffness or mass of the shell element. Very small contact thickness may be result in a contact failure or unacceptable penetrations as the solution propagates [35, 63].
- Adjacent parts with significant curvatures should have consistently refined meshes. In concave regions, a slave node may have its isoparametric co-ordinates [$\pm$1] that lie outside of all master segments, yet still have penetrated the surface. Definition of master surface is extended so that they overlap by small amount. However, even this procedure may fail in case of a very sharp concave corner discretised with coarse elements.
- In order to connect the two parts with a mid-surface representation, spot weld should be used instead of using coincident nodes to maintain the require shell offset.

To conclude, instead of using automatic modifications; sufficient efforts to build the FE model without initial interpenetrations; is recommended by the author of this report.

9.1.5 TACKLING CONTACT NOISE

The problems involving impact e.g. an aircraft seat subjected to a dynamic pulse of 16g or 14g may suffer from high frequency noise in the contact force. Viscous Damping Coefficient (VDC) should be added in the contact definition to damp out oscillations normal to the contact surface [63]. VDC is input in terms of the percentage of critical damping, ξ_{WD} (usually 20% of ξ_{WD}).

Contact damping coefficient, $\xi = (0.01*VDC)\ \xi_{WD}$

VDC is usually 20

$\xi_{WD} = 2m\omega$ **Equation 9-15**

m = minimum of $\{m_{slave}, m_{master}\}$

Natural frequency, $\omega = \sqrt{k}\ (m_{slave} + m_{master})/ m_{slave} * m_{master})$

Where,

k is the interface stiffness

m_{master} is the mass interpolated from the master nodes of the segment containing the slave node, using the interpolation function evaluated at the contact point of the slave node

m_{slave} is the total mass of the slave nodes.

In a seat structure, lot of curved surfaces undergo relative motion e.g. interface between tool-less fittings and restrained track; generating oscillations in the force. In such cases, VDC helps to damp the high frequency content in the contact reaction force.

9.1.6 TIED INTERFACES

Sudden transitions in zoning and strong bolted or riveted connections can be easily represented with tied interfaces. This feature is quite useful while building the FE model as, it drastically reduces the amount of effort required to match the nodes across the interfaces of merged parts. Useful tips (from the author of this report) for modelling tied connections in a seat-structure are,

- For the default tied contact option, LSDYNA automatically projects the tied slave nodes (within the default tolerance) to the master surface to avoid the problems of rotational constraints [63]. Such a projection alters the geometry and may further distort the poor shaped elements if any.
- Nodes that lie outside of the default tolerance-distance are discarded from definition with a warning message. In some cases, this may discard the nodes, which are actually required to be tied.
- The built-in tolerance can be increased by a parameter known as “SST” on ‘*CONTACT’ card; to involve all the required slave nodes in a tied contact definition [63]. However, this may considerably modify the geometry. At the high-stress locations (e.g. a reinforcing insert is attached to the Forward beam, which is then attached to the boomerang) automatic modification of the geometry would a produce a dent in one of the components, which may result in unphysical stress concentration.
- Tied surface interfaces must be excluded from automatic contact definitions with thickness offset.

For the structures like ‘Sleep Seat”, where most of the components are discretised using shell elements, it becomes necessary to use the options, which can tie both translational and rotational degrees of freedom.

Therefore a tied contact ‘with constrained offset’, which can tie translational and rotational degrees-of-freedom and retain a physical gap between tied surfaces is used while defining shell-to-shell tied interfaces in “Sleep Seat” [63]. The forces and moments developed due to physical gap are transferred in a beam-

like manner. The mass of the slave nodes is redistributed to the master surface but in doing so the rotary inertia of the slave nodes is also transformed.

9.2 INITIALISING DAMAGED FLOOR CONDITION IN '16G'

Damaged floor condition (floor distortion) can be initiated in a '16g' dynamic simulation by two solution strategies,

9.2.1 STRATEGY I - SINGLE SWITCH ANALYSIS

Using a single input deck where floor distortion is simulated first and then seamlessly continued for '16g' pulse. Both the simulations can be performed either by using explicit formulation or switching between implicit (for floor distortion) and explicit (16g). Switching can be activated by setting IMFLAG to a curve on *CONTROL_IMPLICIT_GENERAL card [35]. The abscissa of the curve is time and the ordinate is set to 1.0 for implicit and to 0.0 for explicit (curve is a step function).

Single input deck strategy was not used in this research due to

- Incompatible elements types e.g. seat belt elements are not implemented for implicit calculations.
- Inclusion of dummies and seat belts (using *MAT_ELASTIC for implicit part of the simulation), trolley or sled and switch between contact definitions and boundary conditions would have required significant amount of FE modelling efforts and time, which was not desirable during this conceptual design phase.

9.2.2 STRATEGY II - TWO SEPARATE SIMULATIONS

Simulate floor distortion loadcase using implicit or explicit formulation and then include deformed geometry, stresses and strain in the input deck for '16g'. This strategy is adopted in this research as it helps

- To reduce the FE modelling efforts as dummies, seat belts and trolley are not required to be included in the input deck for floor distortion.

- Better handling of the input deck as deformed geometry, stresses, strains, dummies, seat belts and trolley can be stored in the separate files and can be included in the main deck using '*INCLUDE' command [35]. These individual files are easier to edit than a single file containing the entire database.

Depending on the package used to simulate floor distortion, two separate approaches to perform a 'Complete 16g' simulation developed during this research are,

- *Approach A* - Simulate floor distortion loadcase using Abaqus (Research) 6.9-3 and then include deformed geometry, stresses and strain in LSDYNA input deck for '16g'
- *Approach B* -Simulate floor distortion loadcase using LSDYNA (Implicit or Explicit) and then include deformed geometry, stresses and strain in LSDYNA input deck for '16g'

A particular approach should be selected based on available commercial package and experience of analysts in using a particular solver.

The logic behind 'Approach A' is explained with a flowchart (Figure 9-1).

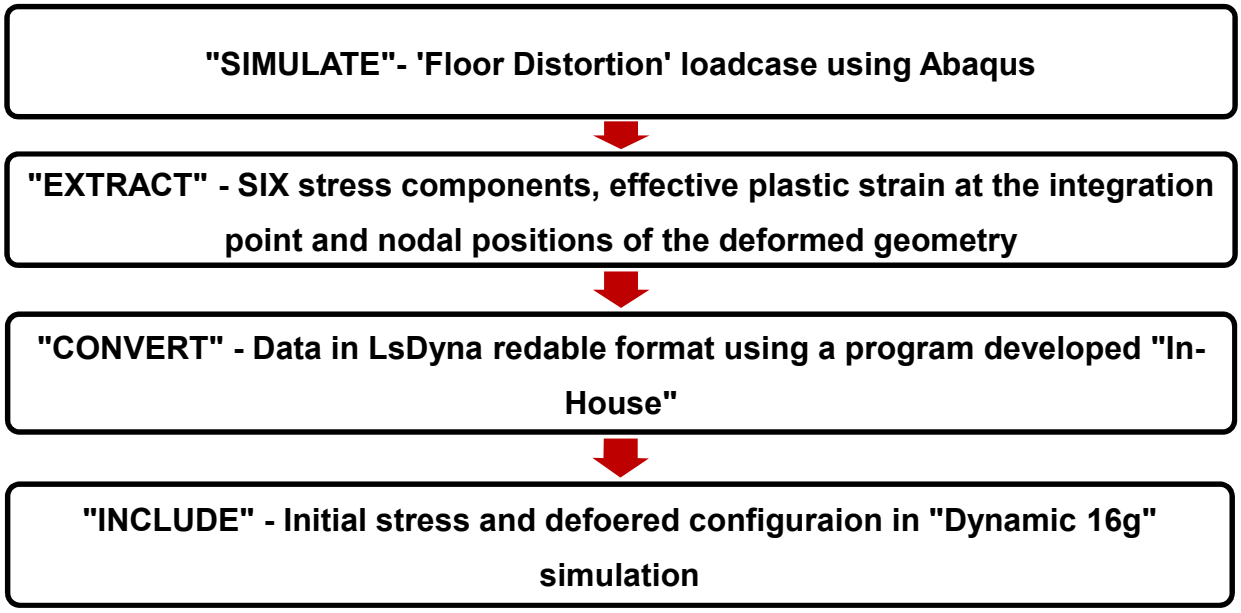

Figure 9-1 Flowchart for converting the stress and strain outputs from Abaqus (Research) 6.9-3 to LSDYNA to initialise the stress and strain (due to Floor Distortion) in the seat structure subjected to "16g" pulse (CS 25.562).

A program is written using “FoxPlus” to convert the stress components and equivalent plastic strain from Abaqus (Research) 6.9-3 into the format required by LSDYNA. The details are present in Appendix J.2. The method has been tested and it initialises the stresses and strain in the deformed seat structure as per the requirement (Appendix J.1).

The logic behind ‘Approach B’ is explained with a flowchart (Figure 9-2). Floor distortion can be simulated using either LSDYNA/Implicit or LSDYNA/Explicit formulation e.g. FE model of the triple seat structure containing 193689 nodes and 200443 elements is solved using LSDYNA/ Implicit using 8 processors (Figure 9-3). CPU time required is 3396s.

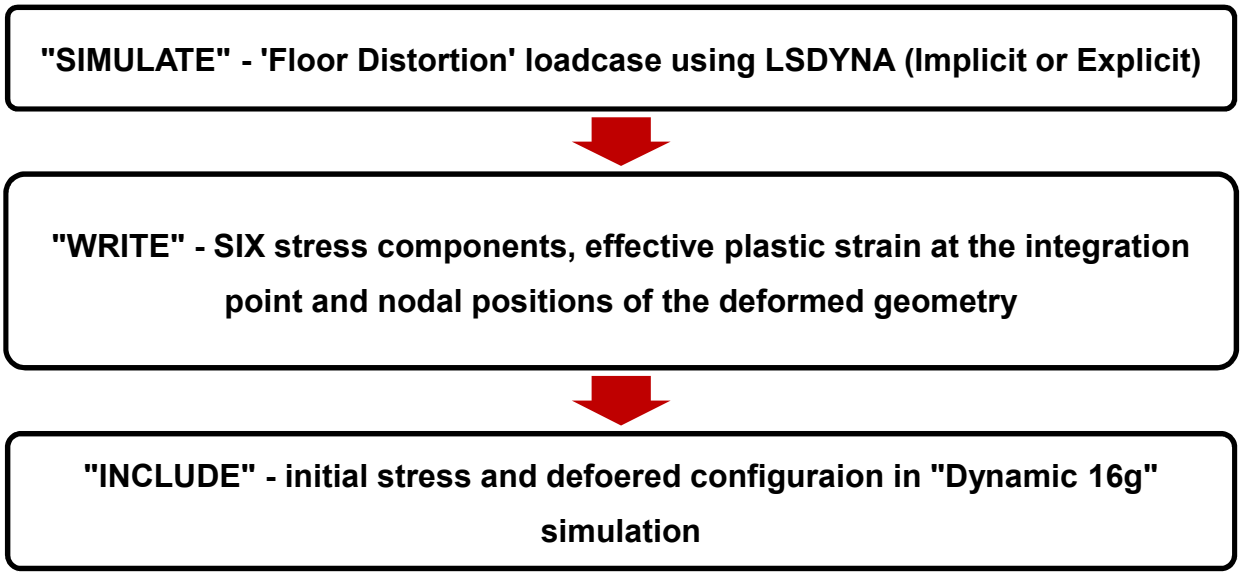

Figure 9-2 Flowchart for initialising the stress and strain (due to Floor Distortion) in the seat structure subjected to "16g" pulse (CS 25.562).

A 'DYNAIN' file containing the deformed geometry (in terms of nodal coordinates), stresses and plastic strains can be written by two ways either [35]

- By defining *INTERFACE_SPRINGBACK_LSDYNA keyword in the input deck of floor deformation or
- Extracting the data from 'D3PLOT' database using Ls-PrePost

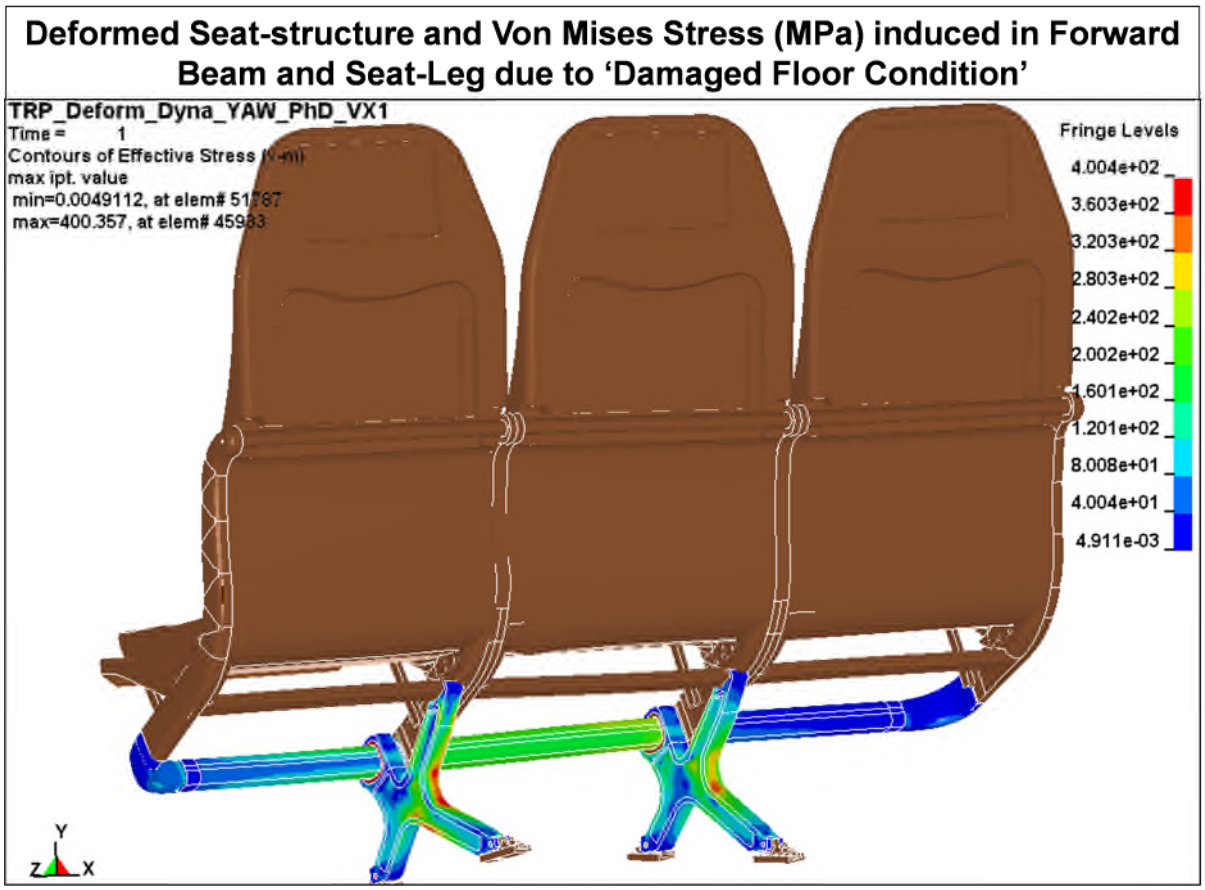

Figure 9-3 Deformed triple seat-Structure due to the damaged floor condition (Seat Predeformation). VMS (MPa) induced in the primary load path components i.e. 'Forward beam' and 'Seat-Leg', will be initiated for the '16g' dynamic simulation.

'DYNAIN' file can be then then merged into the input deck for '16g' dynamic simulation through *INCLUDE filename command, which would initiate stresses and strains due to floor deformation (Figure 9-4). For the present simulation, stresses and strains induced only in Forward beam and seat leg are initiated in '16g' simulation because,

- They are major load carrying members i.e. components of primary load path.
- The elastomeric leg-clamp designed at the interface of forward beam and seat-leg provides a relative movement between seat-superstructure (seat-pan, seat backrest and aft tube) and seat-substructure (forward beam, and seat-leg) when the floor deformation loads are applied.

Therefore, components of seat super-structure are not subjected to severe loads thereby experiencing low stress levels.

- Consideration of stresses and strains induced in the seat-superstructure generates a FE model, which struggles to initiate solution phase due to insufficient memory or scratch space available, on high performance computing facility available at Cranfield University.

After initialising stresses, strains and deformed geometry due to floor deformation loads, next task is to position the 50 percentile Hybrid III Anthropometric Dummy (ATD) in each place of occupancy (three in present case), model seat belts and define contact between seat belts and dummies.

9.3 "16G" WITH DAMAGED FLOOR CONDITION

Following section discusses various elements such as dummy positioning, modelling dummy and seatbelt interaction, FE representation of experimental set-up and considering gravity load, associated with simulation of dynamic '16' loadcase with damaged floor.

9.3.1 POSITIONING OF THE 50%ILE ATD

'Dummy positioning' and 'Seatbelt positioning' panels from the LS-PrePost have been used for positioning the dummy and modelling the seat belt for each occupancy respectively [35]. ATD has been positioned in accordance with the AS8049 [11]. Seatbelt is modelled with linear triangular shell elements with a thickness of 2mm and *MAT_SEATBELT has been assigned [66]. Seatbelt has been routed around the pelvic of the ATD with zero gap to represent tightened belt as would be during normal use.

*CONTACT_AUTOMATIC_SINGLE_SURFACE with soft constraint Penalty formulation is used to define contact between the dummy and seatbelt and rest of the seat-structure [35, 66].

9.3.2 FE REPRESENTATION OF EXPERIMENTAL SET-UP

During experimental tests, set-up for applying floor deformation is mounted on a trolley, which is accelerated to attend a speed of 13400 mm/s and then is decelerated to achieve 16g in 0.09s. To represent test sequence in FE model, deformed geometry of the seat-structure is attached to the trolley by maintaining coincident nodes between bottom surface of seat-track and top surface of the trolley. General steel properties have been assigned to the trolley, which weighs approximately 1.2 tonne so as not to deform under dynamic loading. FE model of the complete seat structure, trolley and three ATDs contains 254661 nodes and 250868 elements.

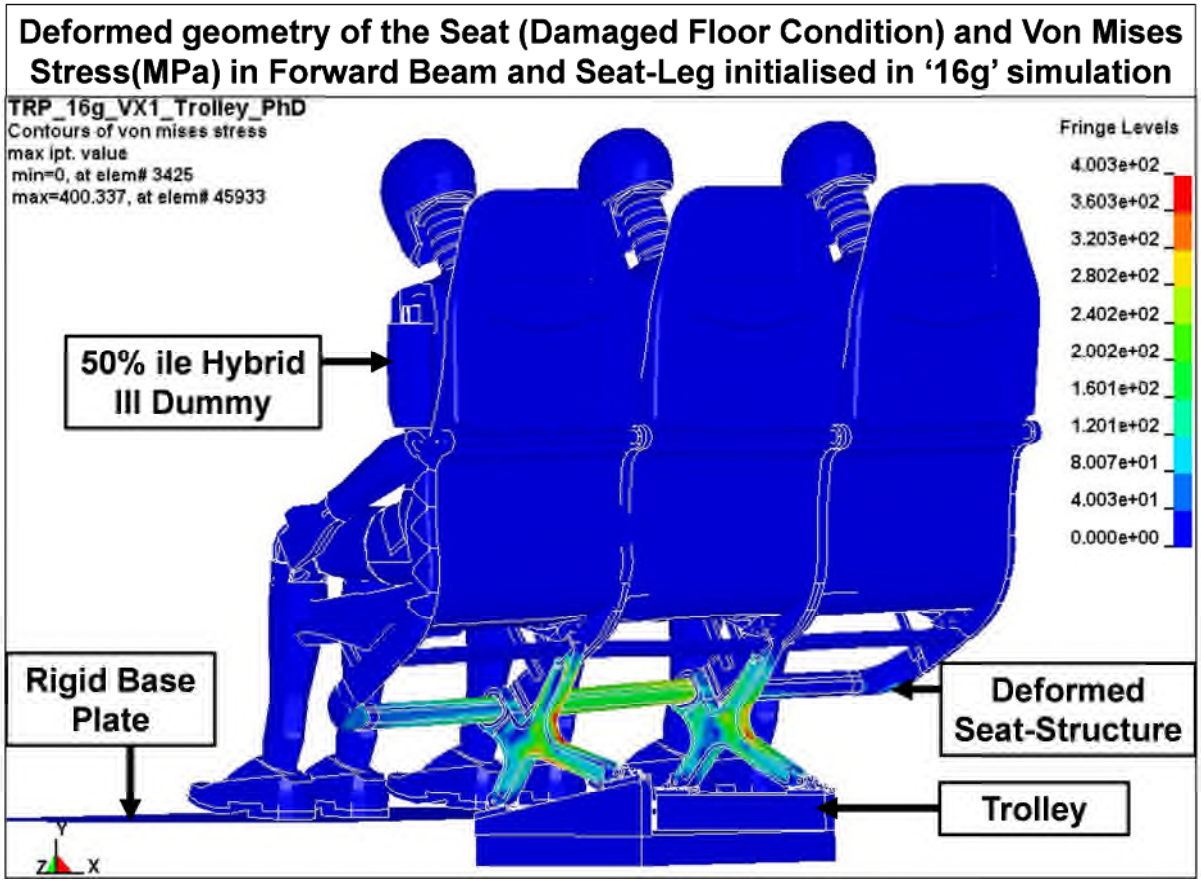

Figure 9-4 Deformed geometry of the seat-structure (damaged floor condition) initiated in the '16g' simulation. VMS (MPa) in the primary load path components (i.e. Forward Beam and Seat leg) and corresponding strains are also initiated. Seat is mounted on a trolley, which is decelerated with a pulse of '16g' according to CS25.562.

9.3.3 GRAVITY LOAD

Before commencing '16g' simulation, it is essential to introduce gravity load into the structure and attend a stabilised seat-structure. Gravity load has been applied using *LOAD_BODY_Y (as the Y-axis is vertical) and defining two curves of acceleration verses time [35]. In first curve, gravity has been linearly ramped from zero to a constant (9810 mm/s^2) value over 0.01s and then held constant. Stress initialisation by dynamic relaxation has been invoked for this curve, by setting SIDR parameter equal to '1' in *DEFINE_CURVE. It preloads the structure with gravity however does not hold the load during transient phase (i.e. 16g pulse). This curve is input in 'LCIDDR' field of *LOAD_BODY.

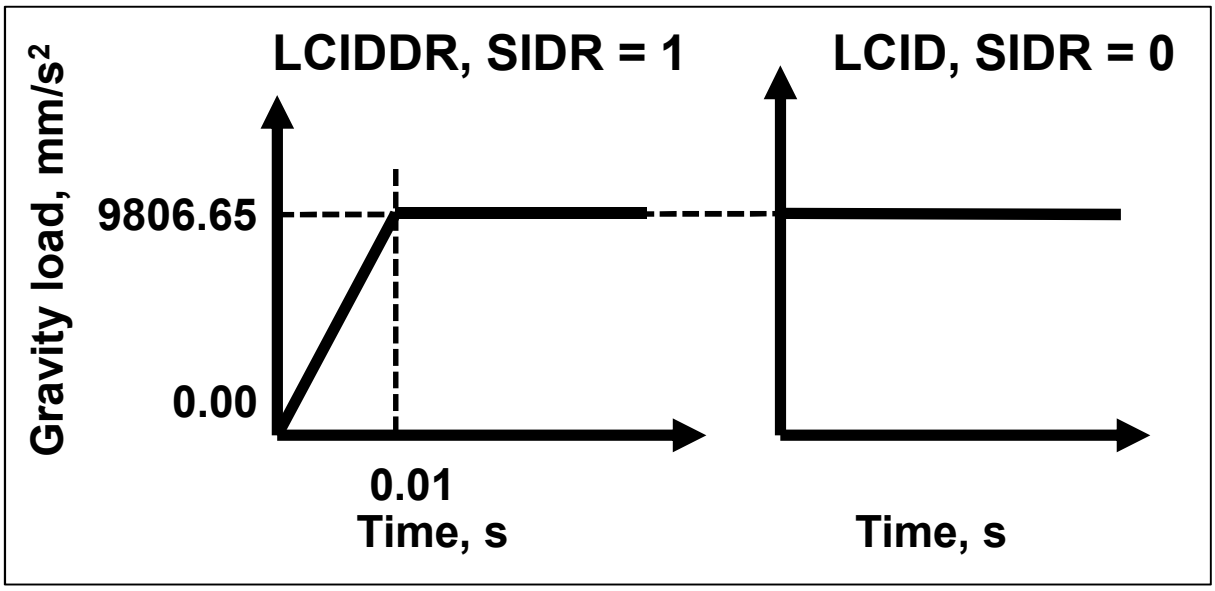

Figure 9-5 LHS - Curve to preload the structure due to gravity by dynamic relaxation, RHS - Curve to hold the preloaded structure during transient phase i.e. 16g pulse

To maintain the gravity load during transient phase, second curve has been defined with SIDR equal to '0' and prescribing a constant acceleration verse time. This curve is input in 'LCID' field of *LOAD_BODY [35].

9.3.4 '16G' PULSE

At the end of dynamic relaxation phase problem time is set to zero for the transient analysis. An initial velocity of 13400 mm/s is applied in a global

longitudinal direction to the deformed seat structure(which is in initial '10 Degree Yaw' orientation to as to receive dynamic loads in a combined longitudinal and lateral direction) with the damaged floor condition. Bottom surface of the trolley is connected to the rigid base plate to which a deceleration pulse rising from 0 to 16g (156960 mm/s^2) in 0.09s and reducing again to 0 at 0.18s is applied in accordance with AS8049 [11].

The simulation takes approximately 58hours 11minutes with 8 processors with a time-step of 2.79E-7s. It requires approximately 17.8 gigabytes of memory to perform the calculations. Simulation stops at 0.13s due to negative volume of the element situated in the shoulder of the left hand side dummy (looking the seat structure from behind).

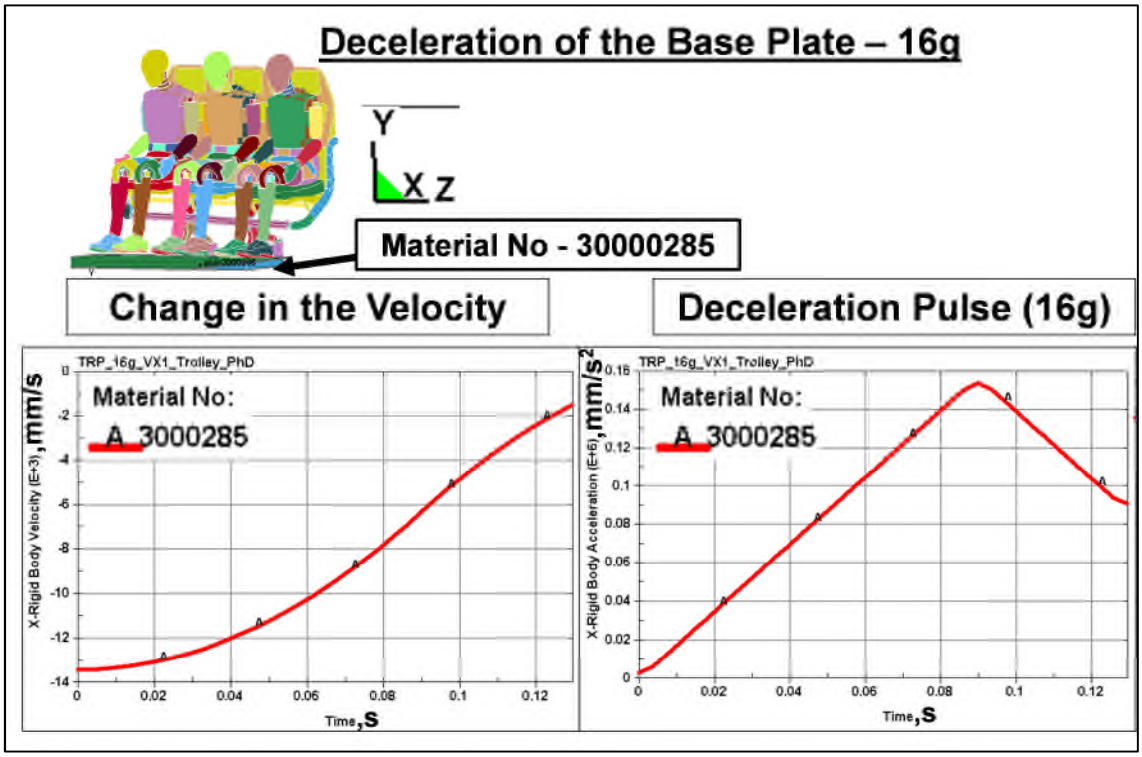

Figure 9-6 Triple Seat-Structure with damaged floor condition (Seat Predeformation) and three 50 percentile Hybrid III numerical dummies, subjected to '16g' dynamic pulse (as specified in CS 25.562). Results demonstrate the change in the forward velocity of the base plate (Material Number – 3000285) from 13400 mm/s to 1488mm/s achieved in 0.13s with a maximum deceleration of '16g (156960 mm/s^2)' occurring at 0.09s

Though the simulation does not reach its normal termination time of 0.18s, the results are still acceptable as the maximum deceleration of 16g is reached at 0.09s, which is consistent with the CS25.562 [13].

9.3.5 DISCUSSION OF RESULTS – '16G' WITH FLOOR DISTORTION

Please note that objective for this PhD thesis is to establish a FE modelling procedure to evaluate the structural capability of a seat-structure subjected to CS25.562 loads (i.e. compliance against '16g Compatible' requirements, which does not comment of loads transferred to the Occupants). Hence, no attempt has been made to evaluate the Occupant loads such as Head Injury Criteria (HIC) or pelvic loads.

Interpretation of the results shows that

- No visible discontinuities have been observed in the load path. Therefore, structural integrity is maintained (Figure 9-7 LHS).
- Seat structure remains attached with the floor.
- The maximum forward movement of the front edge of the seat pan is approximately 31mm, as occurred at the node 22051 at 0.1s (Figure 9-7 RHS). Allowable limit is 3inch = 76.2mm [14]. As the maximum deformation of the front portion of the seat-structure is within the limit, seat would not severely deform, which would otherwise hammer the rapid evacuation process. Seat starts unloading after 0.1s (peak deceleration is applied at 0.09s).

Time history plots for movement of the seat-structure and ATDs are provided in Appendix P.

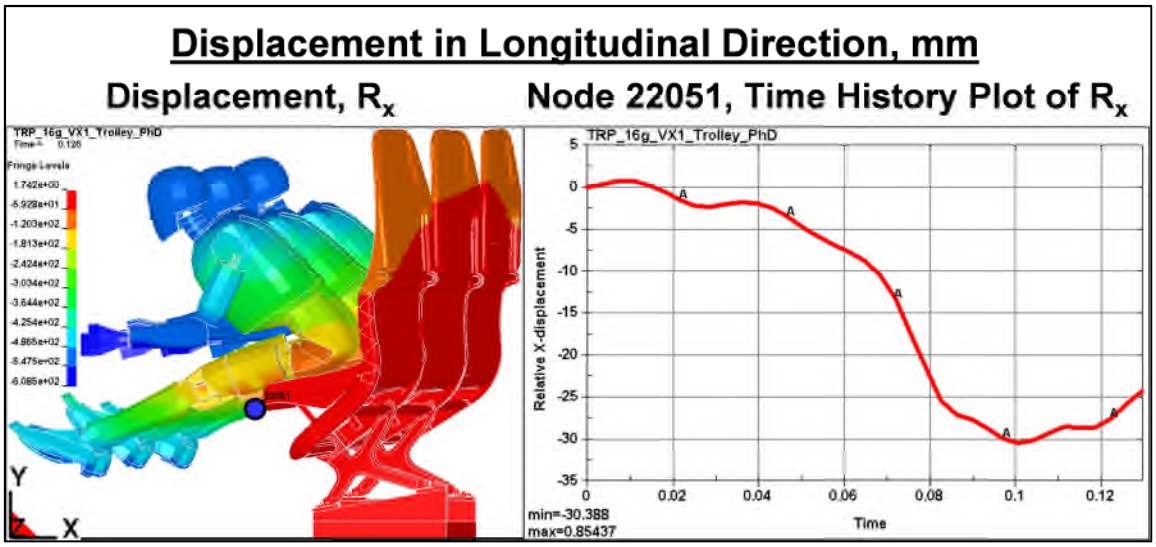

Figure 9-7 LHS – Displacement in longitudinal direction (R_X), of the structure at 0.13s RHS – Time history plot of R_X for node 22051, which is on the front edge of the LHS seat pan. It moves forward by approximately 31mm (allowable limit 3" = 76.2 mm [14]). Seat unloads after 0.1ms (peak deceleration is applied at 0.09s). Hence the maximum deformation of the front portion of the seat-structure is within the limit.

- The maximum equivalent permanent strains observed in the RHS and LHS seat-leg, forward beam, boomerangs and mid beam are under respective rupture strains (Table 9-1). Please note that the von mises stress (VMS) contours for these components are provided in Appendix O.1. All the other components of stress (e.g. normal and shear) have been carefully studied. However, they have not been produced in this report so as to keep it brief.
- Therefore with the damaged floor condition, triple Seat-Structure can withstand the 16g deceleration pulse applied according to CS25.562.

Component	Maximum VMS, MPa (Equivalent Plastic Strain %)	Material Used, Ultimate Stress, MPa (Rupture Strain %)
RHS Seat Leg	496 (2.0)	Al7075T6, 526 (10)
LHS Seat Leg	450 (0.0)	Al7075T6, 526 (10)
Forward Beam	265 (2.4)	Al6082T6, 310 (11)
Offset Boomerang	500 (2.4)	Al7075T6, 526 (10)
Centre Boomerang	450 (0.0)	Al7075T6, 526 (10)
Side Boomerang	270 (0.0)	Al7075T6, 526 (10)
Mid Beam	255 (1.5)	Al6082T6, 310 (11)

Table 9-1 Summary of maximum VMS (MPa) and equivalent plastic stain induced in the major components of triple seat-structure due to the applied '16g' pulse. It can be observed that the structure can withstand the '16g' loads.

9.4 SIMULATION OF LUMBAR TEST "14G"

For "Downward 14g Dynamic" simulation, it is not required to initialise the damaged floor condition [10]. Parts considered, interface definitions, material and section properties are exactly same as those used in "16g' simulation. Therefore the same FE model as used for "16g' simulation is used (without '10 degree YAW' and trolley) to simulate the "14g" pulse. FE model consists of 218109 nodes and 215881 elements. Loading is as follows,

Gravity load has been applied as explained in Section 9.3.3 of this Chapter. To replicate the experimental test scenario, the seat structure has been rotated clockwise by 60 degrees with respect to the aeroplane floor (i.e. the horizontal

axis). This is consistent with the requirement posted in the CS 25.562 i.e. seat structure should experience dynamic '14g' pulse in a combined downward and horizontal direction i.e. aeroplane's longitudinal axis is tilted downwards 30 degrees with respect to the horizontal plane of the seat-structure [10].

An initial velocity of 10700 mm/s (in Negative X direction, Figure 9-8) is applied for the entire FE model and a deceleration pulse rising from 0 to 14g (137340 mm/s^2) in 0.08s and reducing again to 0 at 0.16s is applied to the seat-track, which represents rigid floor used in physical tests. Rigid material properties have been assigned to seat-track.

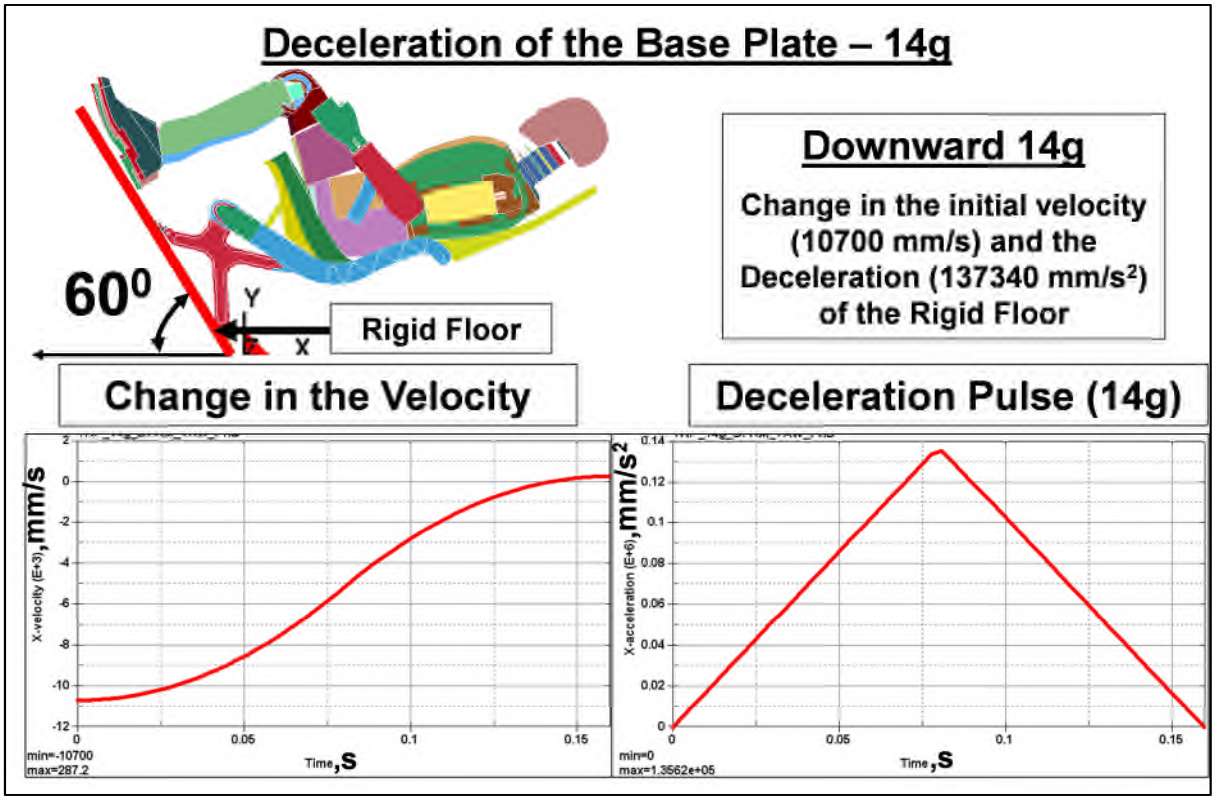

Figure 9-8 Triple Seat-Structure with three 50 percentile Hybrid III numerical dummies, subjected to '14g' dynamic pulse (as specified in CS 25.562). Results demonstrate that there is a minimum change in velocity of 10700 m/s and a minimum peak deceleration of 14g (137340 mm/s^2) is reached at 0.08s

The simulation takes approximately 23hours with 16 processors with a time-step of 5.7E-7s. It requires approximately 6.3gigabytes of memory to perform the calculations.

9.4.1 "14G" – RESULTS DISCUSSION

- No visible discontinuities have been observed in the load path. Therefore, structural integrity is maintained (Figure 9-9).
- Seat structure remains attached with the floor.

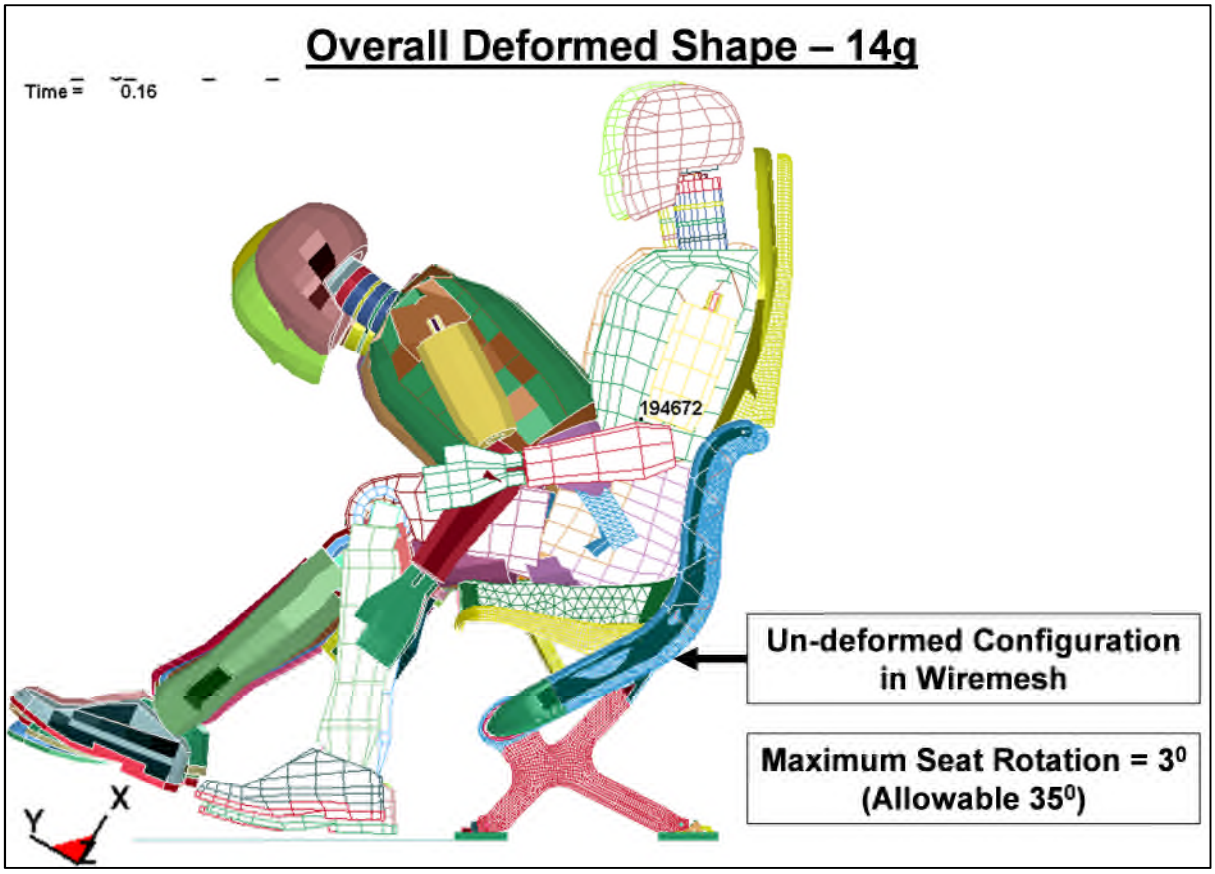

Figure 9-9 Deformed configuration of the seat after dynamic '14g' simulation using LSDYNA. No discontinuity in the load path is observed and structure remains essentialy static.

- The maximum VMS induced in the major load carrying members of the seat (Table 9-2) due to the applied '14g' pulse is below the respective yield stress limit indicating that the structure is in the elastic strain region. The VMS contours for these components are provided in Appendix O.2.

All the other components of stress (e.g. normal and shear) have been carefully studied. However, they have not been produced in this report so as to keep it brief.

Component	Maximum VMS, MPa	Material Used, Ultimate Stress, MPa (Rupture Strain %)
RHS Seat Leg	140	Al7075T6, 526 (10)
LHS Seat Leg	110	Al7075T6, 526 (10)
Forward Beam	120	Al6082T6, 310 (11)
Offset Boomerang	210	Al7075T6, 526 (10)
Centre Boomerang	100	Al7075T6, 526 (10)
Side Boomerang	120	Al7075T6, 526 (10)
Mid Beam	40	Al6082T6, 310 (11)
Corner Piece	105	Al6082T6, 310 (11)

Table 9-2 Summary of maximum VMS (MPa) induced in the major components of triple seat-structure due to the applied '14g' pulse. It can be observed that the structure can withstand the '14g' loads.

- The maximum seat-pan rotation is around 3 degree (Figure 9-9). As the structure is in the elastic regime, it resumes back to the original shape at the end of the '14g' pulse. Therefore there is no permanent seat rotation. Therefore, seat would not severely deform in any manner when subjected to '14g' dynamic load (according to CS25.562), which would hammer the evacuation procedure. This also indicates that the pelvic

loads for Occupants may be severe as the seat-structure does not absorb any of the crash energy by deforming plastically.

To conclude, present design of the triple seat-structure can withstand '14g' dynamic loads without dis-integrating from the seat-track. As the entire seat-structure is in the elastic strain regime, loads on the Occupant may be severe.

Conclusion – Chapter 9

General guidelines to be followed during evaluation of the structural performance of an aircraft seat subjected to CS25.562 dynamic loads can be summarised as follows,

- For the stability of the explicit codes, time increment (Δt) must be smaller than the critical time step, which depends on characteristic length of the element and speed of sound in the material assigned to it.
- Single point integration brick element with Puso assumed strain stiffness form, which can combine coarse mesh accuracy and computational robustness and efficiency for large-scale nonlinear problems has been chosen to build the FE model the of seat leg.
- Unintended initial interpenetrations can lead to non-physical localised initial stresses and strains or can destroy the stability of the solution. Their presence can be detected either through D3HSP file (LSDYNA code) or growth of negative contact energy. They can be visualised by plotting displacements in LS-PrePost.
- For the contact between soft and stiff materials (e.g. contact between foam and seat-pan) 'Soft Constraint Penalty Formulation, which calculates 'Stability Contact Stiffness' based on the stability conditions should be used.
- In order to damp contact oscillations, 'Viscous Damping Coefficient (VDC)' should be added in the contact definition.
- A tied contact algorithm with 'with constrained offset', which can tie translational and rotational degrees-of-freedom and retain a physical gap

between tied surfaces, should be used while defining shell-to-shell tied interfaces in the seat-structure.

Next challenge was to simulate the combined “Seat Predeformation and 16g pulse”, as specified in CS 25.562. Literature review (Section 7.1.2) showed that earlier attempts have either failed or compromised on separating the two load cases. **Two procedures developed to introduce damaged floor condition (i.e. floor distortion) in the input deck for ‘16g’ simulation become one of the novelties of this research.** Both the procedures are discussed and demonstrated for the triple seat-structure.

Seat structure with damaged floor condition is mounted on a trolley, base of which is accelerated to attend a speed of 13400 mm/s and then is decelerated to achieve ‘16g’ in 0.09s according to CS25.562. It is also evaluated against ‘14g’ dynamic loads.

Interpretation of the results show that the seat structure can withstand both the dynamic loads without: disintegrating from the load path, excessive plastic deformation of the components, damaging the seat track and exceeding the allowable deformation limits. **This demonstrates the compliance against ‘16g Compatible’ requirements** i.e. a seat should structurally withstand both the dynamic loads according to CS25.562. Thus the last aim of this research is achieved i.e.

Develop a dynamic FE solution procedure to obtain reliable and acceptable numerical results – CS25.562

As the compliance of triple seat-structure (with leg “VX1”) against static (CS25.561) and dynamic (CS25.562 – 16g compatible) certification regulations has been demonstrated using validated FE methodologies developed by this research, the aim of this research has been achieved i.e.

Build a framework for analysis led design of a novel seat structure to demonstrate compliance against Crash Safety Certification Specifications (CS 25.561 and CS 25.562) – 16g compatibility

10 CONCLUSION

The aim of this research was to develop a practical finite element methodology, which would help seat (aircraft or automobile) designers to estimate the structural performance of the seat against static and dynamic crashworthy requirements (16g compatibility) and to provide conceptual design solutions thereby accelerating the seat design and certification process.

Aerospace Recommended Practice ARP5526 is the most important document to be used during seat certification, as it involves findings from the most relevant regulations such as Certification Specifications CS25.561 and CS25.562 (specifies static and dynamic loads that a seat-structure has to withstand respectively) Aerospace Standard AS8049 (which defines static and dynamic load application procedures), and Advisory Circular AC25.562-1B (evaluation criteria for certification).

- CS25.561 specifics six static inertial loads to be applied separately in six different co-ordinate directions.
- CS25.562 specifies two dynamic loads (16g with damaged floor condition and 14g).

The performance requirements are

- Seat-structure should withstand both the static and dynamic certification loads without disintegrating from the load path or deforming excessively, which would hinder passenger egress in the event of an emergency landing.
- Maximum limits on permanent deformation of seat-structure and Occupant loads should be within the limits specified in AC25.562-1B (shown in Figure 2-1 and Figure 2-2).

The evaluation of structural performance of a complete seat against Certification Specifications (CS 25.561 and CS 25.562) is a classic example of complex nonlinear FEA involving large defamation and strain (geometric and material nonlinearity), changing boundary conditions (contact nonlinearity) and

high computational time. Three critical loadcases were chosen in order to develop different solution strategies to address these issues. Each load case has different numerical and technical challenges and represents different stages in the design process to achieve ‘16’ compatibility.

I. Compliance against static CS25.561 loads (“9g Compliance”)

The objective of this stage was to identify the problems encountered while simulating static loadcases (CS 25.561) using implicit and explicit FE schemes and offer solutions.

It was observed that implicit schemes suffer from solution non-convergence due to rigid body motion (initial clearances) and high unrealistic stresses due to initial unintended interpenetrations. Guidelines were developed to avoid initial penetrations and clearances during structural idealisation phase so that the surfaces in contact are in ‘Just touching’ position at the start of the simulation. Comparative studies between different solution techniques supported the recommendations that the quasi-Newton method based on rank two updates of stiffness matrix offers significant reduction in computational time. Checks such as force equilibrium, ratios of artificial strain energy and contact damping energy to internal energy and distribution of contact pressure were proposed for assessing the quality of FE results achieved using the implicit scheme.

Presence of unwanted vibrations (inertia effects) represents a major bottleneck when using an explicit scheme to simulate quasi-static loadcase. Mass proportional global damping was used to eliminate these strong geometric excitations for achieving a quasi-static solution. A methodology based on mass and time scaling was developed to reduce the high computational time associated with explicit schemes based on stability considerations. Ratio of Kinetic Energy to Internal Energy was used as a main parameter to assess the quasi-static nature of the solution obtained with explicit scheme.

Both the implicit and explicit methodologies were validated against experimental tests conducted for the static downward loadcase, which helped to boost confidence in FEA results.

The proposed methodology was extended to the topology optimisation of seat-leg, which considers the weighted responses of three critical loadcases (Forward 9g, Downward 8.6g and Sideward 4g) and appropriate manufacturing constraints. Final design was 60% lighter and 62% stiffer than the original design space.

Section 10.1 summarises the major findings of the studies performed to demonstrate the compliance of a seat-structure against static certification (9g) loads.

II. Compliance against damaged floor condition, a pre-requisite for '16g'

The objective of this step was to extend the methodology developed for demonstrating '9g Compliance' to simulate the highly non-linear 'Damaged floor condition (DFC)' loadcase.

Use of soft stabilisation springs to prevent rigid body motion of the parts held together only through contact and stabilisation schemes based on contact and volume to arrest local instabilities developed during simulations, proved to be beneficial in terms of achieving a satisfactory solution. DFC was successfully analysed by three different schemes and two commercial codes i.e. Abaqus (Implicit code), LSDYNA/Implicit, LSDYNA/Explicit and LSDYNA-Implicit/Explicit Automatic switching. The results from these different methods were compared in terms of overall displacements, stresses induced in the individual components and seat interface loads. A close agreement between the results served as a self-verification check for these FE approaches and provided confidence with proposed methodology.

Section 10.2 summarises the major findings of the methodologies and guidelines proposed for using a particular methodology based on the experience of the CAE analyst as well as the design phase.

III. Compliance against dynamic CS25.562 loads - 16g compatible

'16g compatible' means that the seat-structure can sustain CS25.562 loads (structural metric only) and does not take into account occupant loading or assessment of injury severity. The objective of this step was to develop a

methodology to initiate DFC in a forward sled test (‘16g’) and develop guidelines for assessing the seat-structure against dynamic loads (CS 25.562).
In the first approach, Abaqus (implicit code) was used to simulate the DFC and LSDYNA/ Explicit for ‘16g’. Deformed configuration due to DFC and initial stresses and strains were initiated in the ‘16g’ simulation through a programme developed in-house.
In the second approach, LSDYNA/ Explicit (using global damping) was used to simulate the DFC and simulation was continued (after removing global damping) for ‘16g’ loadcase. A particular approach should be chosen based on the available packages and experience of the user. For the ‘16g’ simulation, LSPRE-POST was used for positioning the dummies and guidelines are provided on modelling of seat belts and seat cushions. Major findings during each of these approaches are summarised in Section 10.3.

Compliance of a triple seat-structure against static (CS25.561) and dynamic (CS25.562 – 16g Compatible) safety regulations was demonstrated using the FE methodologies developed during this research, thus achieving the objective of this research. Going further, this research will be a milestone and a future guideline for “Certification By Analysis (CBA)”, a programme undertaken by Federal Aviation Authorities (FAA) to replace the physical testing by ‘Computer Modelling Techniques’.

10.1 LOADCASE 1 - STATIC (9G) COMPLIANCE

CS25.561 inertia loads can be roughly classified into two categories depending on method used in FEA to introduce load into the structure,

- Category 1 - Loads that are applied directly to the seat-structure - Downward and rearward; i.e. loadcases with moderate nonlinearities such as nonlinear contact and finite strains
- Category 2- Loads that are applied over lap-block - Loads such as ‘Forward 9g’, ‘Sideward 4g’ and ‘Upward 3g’ are introduced into the seat-structure using lap-blocks. It requires FE modelling of lap-block, seat belt and their interaction with each other and with the seat-structure, which is

quite challenging to simulate due to contact between unexpected regions of the structure, severe geometric nonlinearities and configuration dependent loading direction.

Implicit time integration and Explicit Dynamic Integration are the two FEA techniques that can be used to evaluate the performance of the seat-structure subjected to static loads.

Implicit formulation has advantages such as unconditionally stability of the algorithm and strength to model the physics of static loading accurately. However, as the size and complexity of nonlinear problem increases, it requires significant amount of efforts to build the FE model (particularly at the contact interfaces so that they are in initial contact before the solution begins) and in many cases offers non-convergent solutions. Therefore it was decided to use implicit formulation to solve the moderately nonlinear loadcases (Category 1). “Downward 8.6g” load applied to the triple seat-structure was taken as a case-study because experimental test was planned for it.

Following guidelines are proposed by this research to successfully deal with issue of ‘Solution Non-Convergence’,

- Initial Clearance and significant dissimilar mesh densities along contact interfaces should be avoided.
- A refined mesh ensuring adequate discretisation on the contact pair should be used. Contact pairs with abrupt geometry changes or sharp concave or convex contours should be thoroughly checked for initial penetrations.
- Springs with very small amount of stiffness (usually one thousandth of lowest stiffness in the model) should be attached to ‘ground’ the parts held only by contact. Due to very low stiffness assigned, their effect on the results is negligible.
- Adaptive automatic stabilisation scheme should be employed to arrest the local unphysical instabilities.

- Non-linear variation of the penalty method should be used to ensure contact compatibility.

To assess the quality of the solutions, following guidelines are recommended by this research

- Reaction force should approximately balance the applied force.
- Energy dissipated by viscous damping (artificial stabilisation strain energy) should be less than 5% of the total strain energy.
- Distribution of the contact pressure should be uniform without any peaks and valleys ensures.
- The ratio of contact damping pressure to the contact pressure should be low.

It was observed that the FE methodology developed for applying implicit formulation to simulate the loads that are directly applied to the seat-structure was successful in offering an acceptable solution to the 'Downward 8.6g' loadcse. Two commercial codes that were used in the process are: Abaqus (Research) 6.9-3 and LSDYNA / Implicit. Going further, a study was conducted to reduce the computational time required for implicit calculations. The findings are as follows,

- Initial load increment should be adjusted based on convergence history.
- 'Quasi-Newton with BFGS updates' solver should be used to minimise calculations of stiffness matrix and hence computational time.
- Balanced memory settings (e.g. in LSDYNA) should be used to accelerate computations during linear algebra phase.

The explicit formulation, which can handle large FE models with all the non-linearities and does not face convergence problems, is an attractive option for simulating complex loadcases (Category 2). Applying explicit formulation for simulating complex quasi-static processes is a challenge in itself as the core objective of explicit algorithm is to simulate dynamic loadcases in which inertia plays an important role. The challenges faced were

- Unrealistic computational (CPU) time due to conditional stability of code and large FE model of the complete seat and loading mechanism
- Significant influences of unwanted inertia effects on the solution accuracy
- Representation of experimental loading procedure in FEA, which utilises ball and socket joint, ensuring a consistent pull in a given loading direction (e.g. horizontal pull during Forward 9g) irrespective of the deformation of seat-structure.
- Representation of mass of body block as explicit algorithm satisfies dynamic equilibrium.
- How to ensure quasi-static nature of the FEA solution?

Initially the Explicit methodology was developed for re-evaluate the "Downward 8.6g" loadcase (Category 1) as, a verified implicit solution was available and experimental test was planned.

The methodology proposed by this research utilises 'Mass scaling (artificial increase of material density, which improves the minimum stable time increment) and 'Time Scaling (artificial reduction in simulation time)' to reduce the CPU time. Due to sudden acceleration of the event, lower eigen modes are excited. Mass proportional damping along with a progressive loading sequence (i.e. linearly ramp the load from 0 to 100% and hold it constant thereafter to stabilise the response) has been effectively used to critically damp out the vibrations i.e. the unwanted inertia effects.

A matrix to assess quasi-static nature of the FEA results, includes following guidelines,

- Energy ratio, the ratio of the 'Total energy' to the sum of 'Initial Total Energy' and 'External Work done'; should be unity.
- Maximum ratio of Kinetic Energy to Internal Energy should be within 5%.
- Maximum ratio of Hourglass Energy to Internal Energy should be within 5%.
- Variation of Kinetic Energy and Internal Energy should reflect the loading sequence

- If the FE model contains the interface definitions with friction, the 'Interface Sliding Energy' must be positive

Explicit methodology is successfully in reducing the CPU time required for 'Downward 8.6g' loadcase, from 62hours (natural time scale) to approximately over 2hours yet offering a quasi-static solution.

After the self-verification of FEA results for the "Downward 8.6g" loadcase offered by implicit and explicit methodologies, they were compared against those from experimental testing. An acceptable correlation observed between the results in the areas such as kinematic behaviour of the seat-structure, deformed shape of leg, and vertical downward displacements of the ends of the corner beam helped to validate both FE procedures developed to use implicit formulation and explicit formulation for demonstrating the static compliance (CS25.561) of an aircraft seat.

Going further, methodology was extended for 'Category 2' loadcases. A series of simulations varying in mass of the lap-block were performed and following guidelines are proposed,

- Combination of one dimensional seat-belt element, slipring and rigid support to hold the slipring should be used to represent the ball and socket joint used during experimental testing (in LSDYNA/ Explicit)
- Membrane element should be used for FE modelling of seat-belt as they have better wrap around capability,
- Lighter lap-block should be used so as to transfer approximately the entire applied load to the seat. Remaining mass of lap-block should be distributed over the seat-pan in terms of equivalent pressure. Kinetic Energy of the lap- block is an useful indicator of inertia introduced by lap-block

Proposed methodology was used to evaluate the behaviour of seat-structure under study for the applied "Forward 9g" and "Upward 3g" loads. Deformed shape and associated kinematics (for both the loadcases) and buckling of the

aft section of the seat-leg (in Forward “9g”) predicted by FEA were corroborated by experimental tests.

Another method, which can automatically switch between Implicit and Explicit algorithms based on convergence behaviour of the model, was also studied during this research. The method is recommended during conceptual development to reduce the FE model building efforts.

Thus this research is successful in developing validated FE procedures, which can use three different solution methods (Abaqus, LSDYNA/Implicit and LSDYNA/Explicit) or two different formulations (i.e. Implicit and Explicit) to assess structural performance of a seat-structure subjected to static certification loads according to CS25.561. The characteristics of each of these formulations are summarised below along with the guidelines for their selection for a particular loadcase.

Comparative assessment of Implicit and Explicit Schemes applied for Seat-Certification (CS25.561 and CS25.562)

	Implicit Formulation	Explicit Formulation	Implicit/ Explicit Formulation
Challenges	▪ Rigid Body Motion ▪ Converged solution ▪ Significant FE modelling effort ▪ High memory Requirements	▪ Conditional stability ▪ Unrealistic computational time ▪ Unwanted inertia effects ▪ CPU time - smallest element	▪ Dynamic effects may destroy the solution ▪ High inertia may make implicit convergence difficult
Solutions	▪ Similar mesh density along contact interface ▪ Adaptive stabilisation ▪ Contact stabilisation	▪ Time Scaling ▪ Mass Scaling ▪ Mass proportional critically damped system	▪ Definition of ‘switch time’ between implicit and explicit ▪ Mass Scaling to improve stable time-step (explicit phase)
Checks	▪ Reaction Force Equilibrium ▪ Artificial Strain Energy < 5% of total strain energy ▪ Uniform contact pressure	▪ KE / IE < 5% ▪ Damping inactive during rigid body modes ▪ Variation of KE and IE	▪ KE / IE < 5% ▪ Shorter explicit phase ▪ Variation of KE and IE ▪ Residual forces
Recommendations	▪ Though ideally suitable for CS25.561, recommended only for loadcases without lap-blocks e.g. download tests ▪ Recommended during detailed design and sizing phase	▪ Strongly Recommended for CS25.561 loads applied with lap-blocks e.g. forward load tests ▪ Recommended during evaluation of ‘Complete 16g’ and for experienced analysts	▪ Recommended for CS25.561 loads applied without lap-blocks e.g. download tests ▪ Recommended during feasibility, proof of concept studies and to inexperienced analysts

After studying the results from FEA and those from experimental tests, design of the Seat-leg was identified as a potential area for failure. Hence, it was necessary to strengthen the leg design.

Optistruct, an optimisation algorithm developed by Altair/ Hyperworks; was used to derive the leg design. The objective of optimisation was to minimise weighted compliance of “Forward 9g”, “Downward 8.6g” and “Sideward 4g” loadcases with a constraint on volume. Symmetry constrains and ‘Split Draw direction control (manufacturing constrains) were defined. Mass of the design space was approximately 3.3kg. 62% reduction in total weighted compliance was achieved with 60% reduction in mass. Final design concept for leg was 60% lighter than the design space with 62% reduction in the total weighted compliance.

Next task was to evaluate the structural performance of the triple seat-structure against static certification loads (CS25.561) using the validated FE methodologies developed in this research. The maximum deformation of the seat-structure in each of the loadcases was found to be within the respective allowable limit (defined by Advisory Circular 25.562-1B). Seat-structure neither did dis-integrate from the floor nor developed any discontinuity in the load path. Therefore, compliance of ‘triple’ seat-structure against static certification loads (CS25.561) is demonstrated by virtual simulations.

The drawbacks of previous leg designs such as buckling of the underside of the aft-foot section (“Forward 9g”) or excessive rotation of the seat-pan (“Downward 8.6g”) were not observed with new leg design.

10.2 LOADCASE 2 – COMPLIANCE AGAINST ‘DAMAGED FLOOR CONDITION’

‘Damaged Floor Condition also known as ‘Seat Pre-deformation’, or ‘Floor Distortion’ is a pre-requisite (initial configuration) for dynamic ‘16g’ loadcase. It is the misalignment of the seat anchorages with respect to each other by 10^0 vertically (i.e. out of parallel, PITCH) whilst the other leg is rolled through 10^0. Its purpose is to demonstrate structural capacity of the seat structure to withstand

the dynamic loads without disintegrating from the Airframe-floor, even when the floor is deformed by the forces associated with primary crash.

Literature review showed that earlier attempts (by various researchers) have failed either to simulate the pre-deformation using FEA codes or to initialise the stresses due to pre-deformation in a dynamic '16g' loadcase. The problem with implicit solution technique was of solution non-convergence and that with explicit solution technique was obtaining a quasi-static solution.

Seat Predeformation was successfully solved by four different schemes (using the guidelines developed during 'Milestone 1') e.g. Abaqus, LSDYNA/Implicit, LSDYNA/Explicit and LSDYNA-Implicit/Explicit Switch. The results from these different methods are compared based on parameters like VMS in individual components, overall displacement of the seat structure and the seat interface loads. A close agreement between the results served as a self-verification check for these FE approaches to simulate the Seat Pre-deformation.

Going forward, novel design concepts to minimise the loads introduced by pre-deformation loads in the seat structure are developed to demonstrate compliance against 'Damaged Floor Condition', achieving the target set for "Milestone 2'. Spherical globe added to the seat anchorages (tool-less fittings) completely negated the effect of applied 'ROLL'. An innovative elastomeric leg-clamp designed at the Forward beam and Seat-leg interface, offered a relative motion between seat-superstructure and substructure reducing the effect of applied 'PITCH'.

10.3 LOADCASE 3 – COMPLIANCE AGAINST DYNAMIC (16G COMPATIBLE) LOADS

General guidelines proposed by this research during evaluation of the structural performance of an aircraft seat subjected to CS25.562 dynamic loads (using LSDYNA) can be summarised as follows,

- Single point integration brick element with assumed strain stiffness form, which can combine coarse mesh accuracy and computational robustness

and efficiency for large-scale nonlinear problems should be used to build the FE model the of seat leg.

- For the contact between soft and stiff materials (e.g. contact between foam and seat-pan) 'Soft Constraint Penalty Formulation, which calculates 'Stability Contact Stiffness' based on the stability conditions should be used.
- A tied contact algorithm, which can tie translational and rotational degrees-of-freedom and retain a physical gap between tied surfaces, should be used while defining shell-to-shell tied interfaces in the seat-structure.

Two procedures were developed to introduce damaged floor condition in '16g' simulation. Seat structure was then evaluated against '16g' and '14g' dynamic loads (CS25.562). Interpretation of the results showed that the seat structure can withstand both the dynamic loads without: disintegrating from the load path, excessive plastic deformation of the components, damaging the seat track and exceeding the allowable deformation limits. This demonstrates compliance of the triple seat-structure against '16g Compatible' requirements.

10.4 RECOMMENDATIONS FOR FURTHER WORK

Based on the conclusions of this work, a list of potential areas for further research can be provided as follows,

- *Evaluation of Occupant Injuries*

  Present methodology can be easily extended to estimate Occupant loads such as Head Injury Criteria (HIC), femur and pelvic loads. As minimum deformations of the seat-structure were observed during dynamic load simulations, the Occupant loads may be higher than the corresponding limits [14]. Hence the framework presented in this report should be extended to consider reducing occupant loads under the human tolerance limit through

  - Energy Absorbing Mechanisms,
  - Redesign of foam to reduce Spinal Loads,

- Use of other materials.

- *Material Characterisation*

  In present research, mechanical material properties used for different components of the seat structures, are taken from the handbooks and reliable open source literature. However, a further research should be performed on characterising the material models used (especially for the elastomers and seat cushions). Uniaxial tension, bi-axial tension (compression) and shear tests should be performed in order to extract the elastomeric material constants. For seat cushion, compression tests should be aimed to provide the static and dynamic force-deflection data.

  In addition, influence of the variation in material properties (minimum and maximum values) on structural performance should be studied.

- *FE representation of joints*

  In present research, connections between two components have been modelled either through classic spider-beam or 3D bolts or tied contacts. Present methodology can be extended to model different joints such as spherical or revolute and interference fits and to study their effect on computational time.

- *Non-linear topology optimisation/ Multi-Disciplinary optimisation*

  Guidelines developed in the present research for the topology optimisation of the seat-leg, are valid for the linear material properties. It should be extended to include the nonlinear material properties, interaction with the other components (e.g. seat-leg attachment with the forward beam), statistical variation in the material properties, variations in the manufacturing process, design variables such as Occupant loads e.g. pelvic load experienced by an Occupant during downward '14g' dynamic test and dynamic loads (CS 25.562).

One of the drawbacks of the current numerical dummies is that they do not have human-like response or weight patterns. In automotive sector, more advanced dummies (e.g. THOR advanced crash test dummy) with significantly improved bio-fidelity and greatly expanded injury assessment capabilities in all

body regions, are being developed. Present methodology should be extended to incorporate such advanced human-like dummies in dynamic loadcases. It would also require working with dummy model developers to identify if these human surrogates could be modified to take into account large variations in survivability tolerances across a broader population.

REFERENCES

1. European Transport Safety Council (December 1996), “Increasing the Survival rate in aircraft accidents - Impact protection, fire survivability and evacuation” , ISBN: 90-801936-8-2 http://www.etsc.eu/documents/copy_of_Increasing_survival_rate_in_aircraft_accidents.pdf (accessed 27th September 2013)
2. Lankarani, H.M., and Hooper, S.J. (1999), “Application of Computer-Aided Analysis Tools for Aircraft Occupant and Seat Crashworthiness” , *International Journal of Crashworthiness*, Vol. 4, No. 4, p.433-448, available at DOI:10.1533/cras.1999.0117 (accessed 27th September 2013)
3. Desjardins, S.P. and Laananen, D.H. (June 1980), *Aircraft Design Survivable Guide Volume IV – AIRCRAFT SEATS, RESTRAINTS, LITTERS, AND PADDING*, report number USARTL TR-79-22D.
4. Hooper, S.J. and Ellis, D.R. (1996), “Aviation safety and crashworthy seat design”, *International Journal of Crashworthiness,* Vol. 2, Issue 1, p 39-54, available at DOI:10.1533/cras.1997.0034 (accessed 27th September 2013)
5. Bhonge, P. (December 2008), *A methodology for aircraft seat certification by dynamic FEA*, PhD thesis, Wichita State University.
6. Department of Transportation, Federal Aviation Administration (October 2002), *Improved Seats in Air Carrier Transport Category Airplanes*, Proposed Rule 67 FR 62294), Docket No. FAA-2002-13464, Notice No. 02-17, RIN 2120-AC84, p 62294.
7. Cherry, R., Warren, K. and Chan, A. (April 2000), *Benefit Analysis for Aircraft 16-g Dynamic Seats*, report number DOT/FAA/AR-00/13.
8. Department of Transportation, Federal Aviation Administration (September 2005), *Improved Seats in Air Carrier Transport Category Airplanes*, Final Rule 67 FR 62294, Docket No. FAA-2002-13464-2; Amendment No. 121-315, Notice No. 02-17, RIN 2120-AC84, p 56542

9. Gulavani, O. (2011), *Non-linear FEA led design of a Novel Aircraft Seat against Certification Specifications (CS 25.561),* Master of Science by research thesis, Cranfield University.
10. Aircraft Seat Committee (May 2011), *Aircraft Seat Design Guidance and Clarifications*, report number - Aerospace Recommended Practice ARP5526, rev. C.
11. Aircraft Seat Committee (July 1990), *Performance Standard for Seats in Civil Rotorcraft, Transport Aircraft, and General Aviation Aircraft*, Product Code AS8049.
12. Homepage for the European Aviation Safety Agency http://www.easa.europa.eu/home.php (accessed 27th September 2013)
13. European Aviation Safety Agency (August 2010), *Certification Specifications (CS) for Large Aeroplanes CS25 Amendment 9*, http://www.easa.eu.int/agency-measures/docs/certification-specifications/CS-25%20Amendment%209.pdf (accessed 27th September 2013).
14. Advisory Circular 25.562-1B by Federal Aviation Administration (October 2006), *Dynamic Evaluation of Seat Restraint Systems and Occupant Protection on Transport Airplanes* https://www.faa.gov/regulations_policies/advisory_circulars/index.cfm/go/document.information/documentID/22657 (accessed 27th September 2013).
15. Department of Transportation, Federal Aviation Administration Aircraft Certification Service (February 1972), *Technical Standard Order TSO-C39a AIRCRAFT SEATS AND BERTHS*, http://rgl.faa.gov/Regulatory_and_Guidance_Library/rgtso.nsf/0/0FAEF96A8A3C339C86256E8C005C62A6?OpenDocument (accessed 27th September 2013).
16. Boeing Specifications (1993), *D6 36238 Passenger Seat Structural Design and Interface Criteria Rev C.*

17. Department of Transportation, Federal Aviation Administration (February 1973), *A Summary of Crashworthiness Information of Small Airplanes*, report number FS-70-592-120A http://www.dtic.mil/cgi-bin/GetTRDoc?AD=AD0756811 (accessed 27th September 2013).
18. Greer, D.L., Breeden, J.S., and Heid, T.L. (September 1964), *Federal Aviation Administration, Technical Report ADS – 24* http://www.dtic.mil/dtic/tr/fulltext/u2/623575.pdf (accessed 27th September 2013).
19. Federal Aviation Administration (May 2003), *Advisory Circular 20-146 Methodology for Dynamic Seat Certification by Analysis for Use in Part 23, 25, 27, and 29 Airplanes and Rotorcraft*, http://rgl.faa.gov/Regulatory_and_Guidance_Library/rgAdvisoryCircular.nsf/list/AC%2020-146/$FILE/ac20-146.pdf (accessed 27th September 2013).
20. Olivares, G., Acosta, J.F. and Yadav, V. (May 2010), *CERTIFICATION BY ANALYSIS I and II*, Computational Mechanics Laboratory National Institute for Aviation Research, WSU Wichita. http://depts.washington.edu/amtas/events/jams_10/pap16-Olivares.pdf (accessed 27th September 2013).
21. Ayyar, A. and Laananen, DH. (2001), "Prediction of head and neck injury in transport aircraft seats as a function of occupant size and seat configuration", *International Journal of Crashworthiness*, Vol. 6, Issue 2 available at DOI: 10.1533/cras.2001.0177 (accessed 27th September 2013)
22. Olschinka, C. and Schumacher, A. (2006), "Dynamic Simulation of Flight Passenger Seats", 5th *LS-Dyna Anwenderforum*, p J-II-41 to J-II-58.
23. Dhole, N. (2010), *Development and validation of a FE model of a transport aircraft seat under Part 25.562 dynamic test conditions*, Master of Science thesis, Wichita State University.

24. Shanahan, D. (2004), RTO HFM Lecture Series *on Pathological Aspects and Associated Biodynamic in Aircraft Accident Investigation*, Madrid, 28-29 October 2004, Königsbrück, 2-3 November 2004, and published in RTO-EN-HFM-113.

25. Barth, T. (2009), *Aircraft Crash survivability from viscous injury in vertical impacts,* PhD thesis, Cranfield University. https://dspace.lib.cranfield.ac.uk/bitstream/1826/4002/1/T_Barth_Thesis_2009.pdf (accessed 27th September 2013).

26. Cailleteau, J. (2009), *Airline Seat Testing Soars to new heights*, Concept to Reality Spring/Summer Iss. 2009, http://www.altair.com/(S(h1znvn45cqzjy355r42b3555))/Magazine09SpringSummer.aspx (accessed 27th September 2013).

27. Department of Transportation, Federal Aviation Administration (July 2002), *Technical Standard Order, TSO-C100b,* http://www.caa.gov.tw/BIG5/download/fsd/C100b.pdf (accessed 27th September 2013).

28. Robinson, D. (2012), *BlueSky Designers Ltd*., Guildford, UK, http://www.blueskydesigners.com/ (accessed 24th June 2012)

29. Vanderwolk, J. (2010), *Tool-less Track Fastener Patent Application number 20100096502*, Assignees are BE Aerospace, Inc., http://www.freepatentsonline.com/y2010/0096502.html (accessed 27th September 2013).

30. Ancra International Lic, *Rear Tool-Less Seat Fitting Part Number 49623-10, Boeing SCD S441W001-250*, http://www.ancra.com/images%5Cpdfs%5CLiterature_402B.pdf (accessed 27th September 2013).

31. Bathe, K-J. (1982), *Finite Element Procedures in Engineering Analysis* (1st ed), Prentice-Hall, ISBN-10: 0133173054.

32. Cook, R.D., Malkus, D.S., Plesha, M.E. and Witt, R.J. (2001), *Concepts and applications of Finite Element Analysis* (4th ed.), Wiley, ISBN 9814-12-683-7.

33. Abaqus (2012), *6.9.3 Online Documentation*, http://abaqus.civil.uwa.edu.au:2080/v6.9/books/usb/default.htm (accessed 27th September 2013).
34. Ansys Inc. (2004), *Theory Reference (Release 9.0),* http://www1.ansys.com/customer/content/documentation/90/ansys/a_thry90.pdf (accessed 27th September 2013).
35. Livemore Software Technology Corporation (2007), *LsDyna Keyword's User Manual 971*, Vol. 1, ISBN – 0-9778540-2-7.
36. Suri, B., *LS-DYNA and d3VIEW Blog from* http://blog2.d3view.com/identifying-problem-areas-for-poorly-converging-implicit-solutions/ (accessed 27th September 2013).
37. Grimes, R. (2012), "A tutorial on how to use Implicit LSDYN", *12th International LS-DYNA users conference*, Detroit, p1-8, http://www.dynalook.com/international-conf-012/computingtechnologies14-d.pdf (accessed 27th September 2013).
38. Yang, D.Y., Shim, H.B. and Chung, W.J. (1990), "Comparative investigation of sheet metal forming processes by the elastic-plastic FE method with emphasis on the effect of bending", *Engineering Computations*, Vol. 7, Iss.4, p 274-283, DOI http://dx.doi.org/10.1108/eb023814 (accessed 27th September 2013).
39. Reddy, R., Reddy, M. and Prasad, R. (2012), "A Review on FE Simulations in Metal Forming", *International Journal of Modern Engineering Research*, Vol. 2, Iss. 4, p 2326-2330, ISSN 2249-6645.
40. Mattiasson, K., Bernspång, L. and Samuelsson, A. (1996), "Solution of quasi-static, force-driven problems by means of a dynamic-explicit approach and an adaptive loading procedure", *Engineering Computations*, Vol. 13 Iss. 2/3/4, p 172 – 189, ISSN - 0264-4401, DOIs - http://dx.doi.org/10.1108/02644409610114521 (accessed 27th September 2013).

41. Yu, H., Burgess, I.W., Davison, J.B. and Plank, R.J. (2008), "Numerical simulation of bolted steel connections in fire using explicit dynamic analysis", *Journal of Constructional Steel Research*, Vol. 64, Iss. 5, p 515–525
DOI - http://dx.doi.org/10.1016/j.jcsr.2007.10.009 (accessed 27th September 2013).

42. Xu, F., Chowdhury, P., Sambamoorthy, B. and Halder, T. (2002), "Correlation of the Federal Motor Vehicle Safety Standard 225 (FMVSS225) Requirement of an Automotive Seat System Using LS-DYNA", *7th International LS-DYNA Users Conference*, 19-21 May 2002, Dearborn, USA, p 9-1 to 9-8.

43. Wang, M., Yang, H., Sun, Z. C., Guo, L.G. and Ou, X.Z. (2006), "Dynamic explicit FE modelling of hot ring rolling process", *Transactions of Nonferrous Metals Society of China (English edition),* Vol. 16, Iss. 6, p 1274–1280, DOI http://dx.doi.org/10.1016/S1003-6326(07)60006-5 (accessed 27th September 2013).

44. Kim, J., Kang, Y.H., Choi, H.H., Hwang, S.M. and Kang, B.S. (2002), "Comparison of implicit and explicit finite-element methods for the hydroforming process of an automobile lower arm", *The International Journal of Advanced Manufacturing Technology*, Vol. 20, no. 6, p 407-413, DOI 10.1007/s001700200170 (accessed 27th September 2013).

45. Pan, F., Zhu, J., Helminen, A. and Vatanparast, R. (2006), "Three point bending analysis of a mobile phone using LS-DYNA explicit integration method", *9th International LS-DYNA Users Conference*, 4-6 June 2006, Dearborn, USA, Vol. 9, p 1-12.

46. Patwardhan, V., Halder, T., Xu, F. and Sambamoorthy, B. (2002), "Simulation and Validation of FMVSS 207/210 Using LS-DYNA", *7th International LS-DYNA Users Conference*, 19-21 May 2002, Dearborn, USA, p 9-9 to 9-16.

47. Hessenberger, K. (2003), “Strength Analysis of Seat Belt Anchorage According to ECE R14 and FMVSS”, *4th European LS-DYNA Users Conference*, 22-23 May, 2003, Ulm, p B-II-15 to B-II-20.
48. Prior, A.M. (1994), “Applications of implicit and explicit FE techniques to metal forming”, *Journal of Materials Processing Technology*, Vol. 45, Iss. 1–4, p 649–656, DOI: http://dx.doi.org/10.1016/0924-0136(94)90413-8 (accessed 27th September 2013).
49. Lars, O. L., Simonsson, K. and Unosson, M. (2005), “Selective mass scaling for explicit FE analyses”, *International Journal for Numerical methods in engineering*, Vol. 63, Iss. 10, p 1436–1445, DOI: 10.1002/nme.1293
50. LS-DYNA online support, http://www.dynasupport.com/howtos/general/mass-scaling (accessed 27th September 2013).
51. Maker, B.N. and Zhu, X. (2000), “Input Parameters for Metal Forming Simulation using LS-DYNA”, http://www.dynalook.com/Personally/forming_parameters_maker_zhu.pdf (accessed 27th September 2013).
52. Suri, B. (Livermore Software Technology Corporation), *LS-DYNA and d3VIEW Blog,* http://blog2.d3view.com/overview-of-mass-scaling/ (accessed 27th September 2013).
53. LS-DYNA online support, *Energy Data*, http://www.dynasupport.com/tutorial/ls-dyna-users-guide/energy-data (accessed 27th September 2013).
54. LS-DYNA online support, *Total Energy*, http://www.dynasupport.com/howtos/general/total-energy (accessed 27th September 2013).
55. *Official website ‘ImageJ’*, http://rsb.info.nih.gov/ij/ (accessed 27th September 2013).

56. Stephens, V.M. (1992), *Crashworthiness of Composite seats for Civil aircraft*, PhD thesis, College of Aeronautics, Cranfield Institute of Technology.
57. Boeing Specifications (1993), *D6 36238 Passenger Seat Structural Design and Interface Criteria Rev C.*
58. DuPont Dow Elastomers (1999), *Viton® - Excelling in Modern Automotive Fuel Systems*, http://www.biofuels.coop/archive/viton.pdf (accessed 27th September 2013).
59. Makino, A., Hamburgen, W. and Fitch, J. (1993), *Fluoroelastomer Pressure Pad Design for Microelectronic Applications*, WRL Research Report 93/7. http://www.hpl.hp.com/techreports/Compaq-DEC/WRL-93-7.pdf (accessed 27th September 2013).
60. Gent, A.N. (2001), *Engineering with Rubber - How to Design Rubber Components* (2nd ed.), Hanser, ISBN - 978-3-446-21403-3.
61. Altair Hyperworks 11.0 Documentation (2012), http://www.altairhyperworks.com/ClientCenterHWLoginForm.aspx?from_page=ClientCenterHWTutorialDownload.aspx (accessed 27th September 2013).
62. Yancey, B. (2012), *Aircraft Seating Design, Analysis, and optimisation*, Altair Engineering Inc.
63. Hallquist, J.O. (2006), *LS-DYNA Theory Manual*, Livermore Software Technology Corporation. ISBN – 0-9778540-0-0.
64. Shigley, J. E. and Mischke, C.R. (1996), *Standard Handbook of Machine Design* (2nd ed.), McGraw-Hill, ISBN 0-07-056958-4.
65. Department of Defence Handbook (2003), *Metallic Materials and Elements for Aerospace Vehicle Structures*, MIL-HDBK-5J http://www.grantadesign.com/userarea/mil/mil5.htm (accessed 27th September 2013).

66. Allegheny Ludlum Technologies, *Technical Data Blue Sheet – Stainless Steel AL 17-4 TK Precipitation Hardening Alloy*, UNS Designation S17400, http://www.specialtysteelsupply.com/17-4ph-stainless-steel.php (accessed 27th September 2013).

67. Lewell, A. (2011), *Evaluation of Occupant loading under the CS 25.562 (14g) dynamic emergency landing conditions*, Master of Science thesis, Cranfield University.

APPENDICES

Appendix A DRAWBACKS OF THE CONVENTIONAL ANCHORAGES

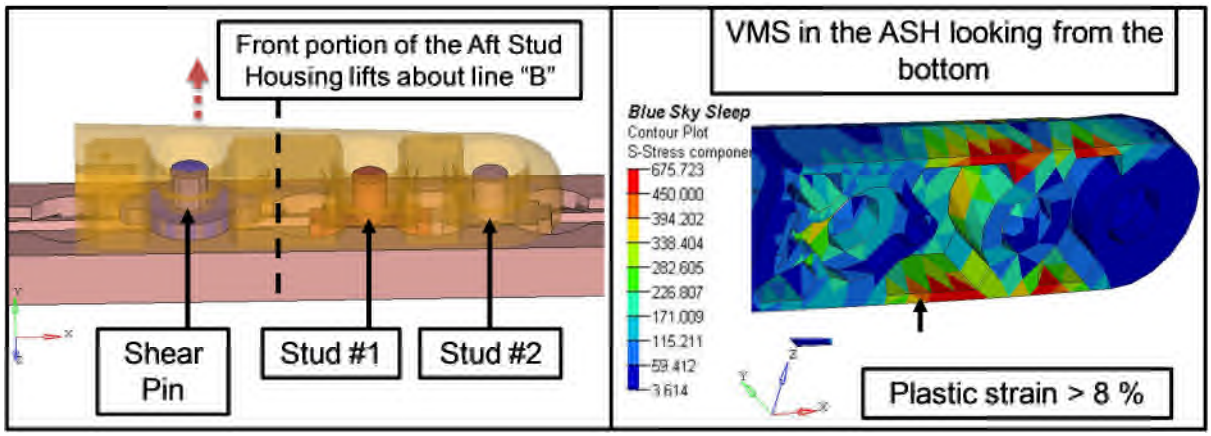

Figure Ap A-1 "Forward 9g" loadcase inducing excessive plastic stain (>8%, rupture strain). Therefore, design of ASH is UNSAFE.

- Shear pin offers the resistance only in longitudinal and lateral direction (Figure A-1 LHS). Therefore, it is disengaged from the Seat-track for the applied "Forward 9g" loads. Front portion of 'Aft stud housing (ASH)' lifts up about B as it is unrestrained in +GY direction; whereas behind "B", sudden restriction in +GY is offered by stud #1. This generates very high stresses in ASH resulting in excessive plastic strain >8 %(Figure Ap A-1 RHS).

- The pin joint is not effective, due to immediate butting of surfaces of leg with those of ASH.

- Since the design relied upon the single pivot pin to transfer the load from the seat structure to the anchorage points, the pin is subjected to very high load (25KN in tension) along with considerable twisting and bending during "Floor-distortion". Being the only load path from the leg to the seat track there was a potential hazard of discontinuity in the load path.

Appendix B IMPORTANT CONTROL CARDS TO ACCOMPLISH AN IMPLICIT SIMULATION USING LSDYNA

**CONTROL_IMPLICIT_AUTO* card can be used to control automatic time stepping during implicit analysis [35].

IAUTO is used to activate either automatic adjustment (by LS-DYNA) of the size of the time-step or to maintain constant user-defined size of the time-step. For nonlinear complex large –scale FE simulations, automatic adjustment of the size of the time-step is recommended by the author of this report. Thus IAUTO should be set equal to 1.

ITEOPT and ITEWIN define number of equilibrium iterations allowed per time-step and tolerance on number of equilibrium iterations to 'automatically' adjust the time-step, respectively. If the number of equilibrium iterations required for the convergence, $N_{EQIT,}$ of a particular load increment, is greater than (ITEOPT+ITEWIN), time step is reduced and is N_{EQIT} is less than (ITEOPT-ITEWIN), time-step is increased. For "Sleep Seat", 'aggressive' time-step control mechanism is used over the default one as

- With the default values of ITEOPT and ITEWIN (11 and 5 respectively), time-step is decreased if more than 16 equilibrium iterations are required.
- For "Sleep Seat" simulations, initially a large number of equilibrium iterations are required.
- Thus default settings often lead to a decrease in size of the time-step even after a successful convergence.

Under 'aggressive' time-step control strategy,

- ITEOPT has been set equal to 100 with default ITEWIN.
- DTMAX, the size of the maximum allowable time-step and is set equal to 0.3 (as an initial guess)

- Thus step-size is always increased if the convergence is achieved and aggressively pushed toward DTMAX thereby reducing the total load increments and CPU time.
- The ‘divergence’ of the solution decreases the time-step as ‘automatic’ time-step control is activated by IAUTO=1.

**CONTROL_IMPLICIT_SOLUTION* an optional card that is used to choose different nonlinear solvers and set limits on number of reformulations of stiffness matrix and convergence tolerances [35].

NSOLVR activates the solution method for implicit analysis with the chosen algorithm. For “Sleep Seat” simulations, the default solver i.e. ‘Nonlinear with BFGS updates’; is used.

ILIMIT specifies the number of equilibrium iterations after which the global stiffness matrix is reformulated (for the default BFGS method). Otherwise, an inexpensive stiffness update of rank two is performed. If ILIMIT is set equal to 1 then the full Newton-Raphson method with line search algorithm is used for solving the given nonlinear FE problem. If a very large value is used for ILIMIT, it may reduce the number of reformations and factorisations of the stiffness matrix, which may significantly save the computational cost but will cause substantial increase in the storage requirements. For the present research, ILIMIT has been set equal to 20 by a trial and error method. However, further research can be undertaken to derive the optimum value.

MAXREF specifies the number of reformulations of the global stiffness matrix. Divergence of the solution after MAXREF will force the ‘automatic’ time-step control scheme to decrease the load increment. If ‘Automatic’ time-step option (on *CONTROL_IMPLICIT_AUTO) is not used then solution would be abandoned with a non-convergence error. For present research, MAXREF has been set equal to 9 by a trial and error method. However, further research can be undertaken to derive the optimum value.

D3ITCTL is a very useful flag to identify the problematic regions of the FE model exhibiting poor convergence. When activated, D3ITCTL writes a binary file D3ITER, which contains the model information (search directions for the solution) at each iterative step. By scaling-up the nodal displacements, problematic regions of un-converged solution can be easily found using LS-PREPOST. D3ITCTL should be set equal to 1 so that the D3ITER file is reset after every time-step.

This is a very powerful technique for debugging the model and has been used frequently during “Sleep Seat” simulations. However, once the method to obtain a converged solution has been identified, this flag should not be used as it consumes a lot of disc space.

**CONTROL_IMPLICIT_SOLVER* can be effectively used to check the memory requirements for inversion of global stiffness matrix by setting LPRINT to 2 or 3 [35].

Appendix C LIST OF GENERAL CONTROL CARDS IN LSDYNA [35, 63]

*CONTROL_CONTACT

This is a very important control card and is often visited by an analyst to change the default values. Important entries in this card that were modified or used during this research are,

SLSFAC is the scale factor for the penalty stiffness for sliding interfaces. Default value is 0.1 of the calculated interface stiffness. SLSFAC is used to scale the default penalty stiffness for the interior contact as well (generally interior contact is defined for a foam material subjected to a high compressive load).

ISLCHK is the flag to set up a check for initial penetrations. The author of this report recommends a full check of initial penetration by setting this flag equal to 2. If it is not possible to remove the initial penetration, a contact birth time (on *CONTACT) should be specified so that the contact is not active at time zero. The deflections of the model should be carefully reviewed with a pilot run and contact should be activated once the surfaces with ‘initial penetration’ become ‘Non-Penetrating’ due to the deflections. However, such a practice is not recommended by author of this report during design iterations as the pilot runs are time-consuming and penalise user’s account on the shared computing resources.

SHLTHK parameter deals with the consideration of shell thickness in node-to-surface or surface-to-surface contacts. Shell thickness of deformable bodies or rigid bodies can either be included in the analysis or excluded.

PENOPT option can be used to choose different values for the penalty stiffness.

ORIEN should be set equal to 2 to activate the automatic orientation of the contact interface segments.

*CONTROL_BULK_VISCOCITY

A smooth initial data can lead to shock discontinuities destroying the solution. *CONTROL_BULK_VISCOCITY should be added to the input data which automatically detects the shock and adds a pressure term to treat it [63]. The pressure term *q,* containing the quadratic and linear terms of bulk viscosity, is given by

If $\dot{\varepsilon}_{KK} < 0$, $q = \rho\, l\, (Q_1 l \dot{\varepsilon}^2_{KK} - Q_2\, a\, \dot{\varepsilon}_{KK})$

If $\dot{\varepsilon}_{KK} > 0$, $q = 0$

Where,

$\dot{\varepsilon}_{KK}$ is the trace of strain rate tensor. $\dot{\varepsilon}_{KK}$ is computed by LS-DYNA at every cycle. If it is negative, which indicates divergence of velocity field in multi-dimensional problems; LSDYNA automatically adds a pressure term, while a positive trace is ignored.

ρ is the material density

l is the characteristic length; In 2D, square toot of area, In 3D, cubic root of the volume.

a is the local sound speed

The terms Q_1 and Q_2 are input by the user and are dimensionless constants. Q_1 is called as ‘Quadratic’ term and it prevents the element from collapsing when the particle velocity exceeds the speed of sound for the corresponding material. Q_2 is called as ‘Linear’ term and it damps out the oscillations known as ‘ringing’. In this research their default values defined by LSDYNA i.e. Q_1 = 1.5 and Q_2 =0.06, have been used [35]. By default these are active for solid elements.

By setting TYPE on card 3 equal to '-2', the bulk-viscosity pressure can be activated for shell elements to avoid negative Internal Energy (IE) in shell elements [35].

*CONTROL_SHELL

This control card helps to adjust the settings for shell elements [35]. The important parameters for a crash analysis are

WRPANG is the warpage angle of the shell element in degrees. If the warpage greater than specified here is found, a warning message is printed either in MESSAGE file or in D3HSP file. The default value of 20 is used for "Sleep Seat" simulations.

ESORT should be set equal to 2 to activate complete sorting of triangular shell elements (from a mixture of triangular and quadratic shell elements e.g. seat pan) to treat them as DKT shells. If this option is not activated, triangular shell elements are treated as the collapsed Belytschko-Tsay formulation, which is not recommended. DKT shells are discrete Kirchhoff triangular shell elements with three integration points in the plane and have better bending behaviour than the traditional C_0 triangular element. Hence they are recommended for crash analysis.

ISTUPD is the shell-thickness change option for deformable shell elements. If shell thickness change is required during a crash analysis, this option should be set to '4' (elastic strains are neglected for thickness update), as recommended by LS-DYNA for improving energy conservation and stability. For present research, the default option '0' i.e. no thickness change; has been used.

NFAIL4 can be set to '2' (if required), to delete the highly-distorted fully-integrated shell element and to print the message for post-processing.

*CONTROL_SOLID provides the controls for solid element response [35].

ESORT should be set equal to 1. This automatically prevents the default treatment of ‘degenerated solid element’ applied to tetrahedron and pentahedron elements. More stable element forms i.e. one point tetrahedron (type 10) and 2 point pentahedron (type 15); are applied to the respective elements.

*CONTROL_TIMESTEP has different options to control the structural time-step size [35].

TSSFAC is the scale factor for the computed time step. The default scale factor of 0.9 has been used.

ISDO option can be used to change the basis of time-step calculation for linear triangular and quadrilateral shell elements.

DT2MS Negative value of desired time-step size is specified using this option, if mass-scaling needs to be activated. The time-step size is then equal to TSSFAC*IDT2MSI.If the input for DT2MS is negative then mass is added only to those elements whose time-step is less than IDT2MSI. GLSTAT and MATSUM files can be used to plot the time history added mass for the complete model or for individual parts respectively.

MS1ST can be used to decide whether mass should be added only once during initialisation (MS1ST = 1) or can be added anytime during the course of simulation to maintain the desired time-step of IDT2MSI (MS1ST = 0).

IMSCL parameter gives the option of ‘Selective Mass Scaling (SMS)’. The options such as SMS for all the parts or SMS for a part set can be specified using this parameter. In SMS, mass of the rigid body is kept constant and it is memory and CPU intensive. For this option to function, mass scaling should be active i.e. DT2MS must be defined.

C.1 Ways to terminate or stop the simulation [35]

*CONTROL_TERMINATION can be used to define the termination time of the simulation using ENDTIM, which is a mandatory card.

ENDMAS can be used to terminate the analysis based on percentage change in the total mass due to mass scaling.

*TERMINATION is an alternative way of terminating an analysis before the ENDTIM is reached. Using this card an analysis can be terminated when

- Component of the displacement in a particular co-ordinate axis (X, Y or Z) or the resultant displacement, of the centre of mass of rigid body exceeds either the maximum or minimum limit.
- The magnitude of resultant interface force from any of the interface definitions is zero, for specific time duration.
- The specific number of elements have been deleted from a part or group of parts

Appendix D DEFINITION OF OUTPUT MATRIX – LSDYNA

The information required from FEA of an aircraft seat is integrity of the seat structure. This can be visually checked by animating the results. In addition, KE plot for the duration of entire analysis can be verified for any high and monotonous increment in KE indicating separation.

If element deletion after reaching the rupture strain for the material used, is not been modelled, a counter of permanent strain helps to identify the maximum plastic stain in the component, which can be compared against the rupture strain of the material.

A care should be taken to ensure that all the contacts modelled in the structure are functioning appropriately. A failure of the contact may falsely indicate the discontinuity in the load path.

Before in depth interpretation of the FEA results, following points should be considered,

- Overall deflection contour should be checked first. It should be scaled up with different scale factors for easy visualisation. The displacement contours should be thoroughly checked for the displacements in unexpected directions or at unexpected regions, or surprisingly small or large e.g. in one of the FEA results of the “16g” dynamic simulations of the ‘Sleep Seat”, unexpected downward displacement of the seat pan was observed with the plausible interpretation of weaker seat pan. However, the error was in the incorrect material density used for the foam.
- Then the displacement plot should be animated with different scale factors and with different frame rates for all the time frames of the analysis. This helps to check for any failure in the contact mechanism for the interior parts of the structure and hour-glassing. This immediately reveals the load increment at which a particular contact fails (if any).

If nothing is obviously wrong with these visual checks then the analyst should proceed to more detailed and quantitative checks and results interpretation.

D.1 Procedure to extract reaction forces from the simulation

The overall sum of the reaction forces and moments should be then checked against the applied loads. Reaction forces should approximately balance the applied loads (in case of nonlinear analysis some energy is used for automatic stabilisation or controlling hourglass). A due care should be taken to refer the same co-ordinate system for the applied loads and reaction forces and moments.

*DATABASE_SPCFORC should be defined to generate the time history plot for x, y, z forces and corresponding moments experienced by the nodes restrained by the analyst e.g. bottom surface of the seat-track has been restrained in all the degrees-of-freedom for the static evaluation of “Sleep Seat” subjected to loads specified in CS25.561 [35]. A heading should be defined for a particular *BOUNDARY_SPC card so that it the reaction forces written in ASCII file contain the same heading and data can be easily identified.

D.2 Procedure to extract different energies from the simulation

In case of static nonlinear problems, ratio of stabilisation energy to the total strain energy should be within acceptable limits. In addition, the ratio of hourglass energy to the total strain energy should be within the tolerance defined by the particular analysis.

For dynamic analysis, check for the energy balance should include Kinetic Energy (KE), Hourglass energy, Internal Energy (IE), contact energy, and the total energy. For a quasi-static analysis performed using direct integration, ratio of the KE to IE should ensure the static response of the structure. In an assembly, individual material energies should also be monitored for any occurrence of dynamic effects.

*DATABASE_GLSTAT command should be included in the input database to extract the time history of global statistical data, which contains the outputs of all the energies, ratio of the total to initial energy, information about time-steps and the x, y, z components of the global velocity [35]. Some of the important energies that are reported in GLSTAT are: KE, IE, hourglass energy, sliding interface energy, total energy, external work and spring and damper energy. It is a very useful file and must be generated at regular intervals (time interval is input for its definition) to monitor the performance of FE model.

The energy associated with the mass-scaling is reported in the GLSTAT. KE reported is computed from nodal velocities.

In *CONTROL_ENERGY option, all the cards should be assigned as value of 2 to include hourglass energy, stonewall energy, sliding interface energy and damping energy; in GLSTAT file [35].

*DATABASE_MATSUM reports the material energies (KE, IE and hourglass energy), x, y, z momentum, x, y, z rigid body velocities, eroded energies and added mass [35]. This file must be requested in the database file.

KE reported is computed from element midpoint velocities. Since, energy is computed by an element-by-element approach for the deformable materials, KE of the nodes of the deformable bodies coincident with the rigid body, is accounted twice i.e. for the deformable body as well as in the rigid body total.

*DATABASE_SLEOUT command can be included in the input deck to extract all the contact interface energies in ASCII output file [35]. If the global statistic file (GLSTAT) indicates problematic contact behaviour e.g. large negative contact energy, SLEOUT file can be used to isolate the problematic contact interface.

In order to check the contact stress distribution in the normal and tangential direction in the form of fringe plots; a binary interface file, *DATABASE_BINARY_INTFOR needs to be requested in the input deck [35]. Either SPR or MPR on card 1 from the corresponding interface definition should

be set equal to 1. The option s=*'Intended filename'* should be present on the LS-DYNA execution line. *Intended filename* is the name of the binary database; defined by the analyst; to be post-processed using LS-POST.

*DATABASE_BINARY_D3PLOT card must be defined; to get the complete output states containing all the components of the deflections, stresses, strains and the deformed geometry; at the desired intervals [35]. If this card is absent from the keyword deck then a complete output state is written for every time-step, requiring a substantial amount of disc space.

D.3 Procedure to extract forces and moments acting at a cross-section

During the design iterations, it becomes necessary to estimate the forces and moments acting at various cross-sections of a component. It helps designers to choose different cross-sections depending on the strength requirements, intended buckling or collapse of a sacrificial member at a pre-determined load-level, and pre-defined collapse of the entire seat structure for energy absorption.

*DATABASE_CROSS_SECTION card should be included in the input data to extract the forces and moments acting at the cross-section [35]. A definition of the cross-section includes the nodes, which define the cutting plane and the deformable elements (shell or brick) to 'one side of' and 'touching to' these nodes.*DATABASE_SECFORC should be included as well to define the output interval for the cross-section forces and moments. The output can be written either in the Global-Coordinate system (default option) or in the Local-coordinate system.

If a PLANE option is selected to define the cross-section (*DATABASE_CROSS_SECTION_PLANE), LSDYNA makes a list of nodes and the elements cut by the plane [35]. This set of nodes and elements is reported in the D3HSP file under the heading 'interface definition'; for the information of the analyst.

Alternatively, in LSPREPOST, SPLANE can be defined to gather the forces and moments at a cross-section, which is fixed in space [35]. This is an interesting option in which the cutting plane does not follow the deforming material and the contribution to forces and moments come only from the displayed parts.

If a 'certified' component has been declared as a rigid body in the analysis (to save the CPU time), duplicate elements should be defined at the desired cross-section; with elastic material properties and the *DATABASE_CROSS_SECTION card should be defined with these elements and corresponding nodes. This technique has been successfully used to obtain the cross-sectional forces at the mid-plane of the pin, which connects the Seat-leg to the main body of the tool-less fittings.

D.4 Procedure to extract contact forces / Seat Interface loads

Contact forces acting at various locations are required in situations like

- To account for the loads applied by the pelvis restraint, to the Occupant.
- To account for the loads applied by seat-pan cushion and back-cushion, to the Occupant.
- For the structural components sandwiched between two parts, it is important to account for the loads acting on them when the seat structure is evaluated for its structural performance against CS 25.561 and CS 25.562 loads. For example, to estimate the grade, size and hardness of the elastomer used at the Seat-leg and Forward beam joint, it is essential to extract the forces transferred across any one of the interfaces either an interface between the elastomer and the Seat-leg or an interface between the elastomer and Forward beam.

*DATABASE_RCFORC command should be included in the input deck to produce the resultant interface data at specified regular intervals [35]. RCFORC is an ASCII file containing the resultant X, Y, Z components of the contact force acting on the slave and master side of each of the contact interface. The forces are written in the Global-Coordinate system. Due to the nature of the contact-impact interactions, the interface output is very noisy

and scattered. To eliminate the inherent noise in the contact force output, the magnitudes of the forces are averaged over the preceding output interval.

While the RCFORC gives resultant forces acting on the slave or master segments, *DATABASE_NCFORC can be defined in the input deck to produce an ASCII file containing X, Y, Z contact force at each of nodes involved in the interface [35]. To include the nodes on the slave side of an interface definition in *DATABASE_NCFORC file, SPR on card 1 should be set to 1, in the *CONTACT definition of that particular interface. Similarly, to include the master side MPR on card 1 in *CONTACT definition should be set equal to 1.

Calculation of the forces exerted by the seat structure on the aircraft floor (called as seat interface loads) is essential; so as to ensure that the interface loads are within the floor's structural capability. Since, the material defined for the tool-less fittings and the seat track is rigid (*MAT_20 in LSDYNA) and single surface contact algorithm has been used for contact compatibility, a special technique is employed to extract the seat interface loads.

By default, RCFORC file is not written for the single surface contact as absence of master side definition in this interface definition results in zero net contact force. To obtain the interface force data (i.e. RCFORC file) for a single surface interface, force transducer should be added via the *CONTACT_FORCE_TRANSDUCER_PENALTY command in the input deck [35]. A force transducer measures the contact forces produced by other contact interfaces defined in the input deck. It does not produce any contact force and thus the interface behaviour is unaffected by its presence. In its definition, no master side is required (default option). Only subset of parts, which has been defined in the corresponding single-surface definition, should be defined as the slave side in the definition of a force transducer. Then, RCFORC file contains the total contact forces applied by all contacts for the defined segment.

However, during design iterations, interaction response between two particular surfaces is required e.g. though the seat-leg, tool-less fittings and seat track are

included in the single-surface definition, interface forces between main forged body of the tool-less fitting and seat track are required to estimate 'Seat Interface Loads'. In such cases, a master side should be defined in the FORCE_TRANSDUCER_PENALTY command so as to obtain the contact forces applied between the slave and master sides. This option works only with 'AUTOMATIC_SINGLE_SURFACE' contact type [35].

D.5 Displacement, Velocity and Acceleration at a node

It is of utmost importance to extract the nodal history data in following conditions,

- There can be considerable round-off errors due to the numerical precision used i.e. single precision or double precision. Therefore, to ensure an accurate consideration of the input data by the software, the plot of applied deceleration and initial velocity should be generated from the output.
- The displacement, velocity and acceleration of various parts of ATD e.g. head and neck; are required to evaluate the response of the Occupant when subjected to dynamic loads. A node can be defined at the centre-of-gravity of the required part of ATD and its motion can be monitored throughout the course of the analysis.

D.6 Procedure to extract Nodal history data

*DATABASE_HISTORY_NODE_SET should be defined to generate the time histories such as both translational and rotational displacements, velocities and accelerations for the nodes of interest [35]. *DATABASE_NODOUT defines the time interval at which the data is written to ASCII file.

Using IACCOP on CARD 4 of *CONTROL_OUTOUT, the nodal accelerations can be averaged or reported as it is or can be filtered using built-in filters of LS-DYNA.

*DATABASE_BINARY_D3DHDT can be used to obtain the time-history data for element sets defined by *DATABASE_HISTORY.

D.7 Forces induced in the pelvis restraint

Axial tensile forces induced in the pelvis restraint i.e. seat belt are required to account for the load introduction in the seat as well as to choose the appropriate webbing.

D.8 Procedure to extract the forces induced in the seat belt

*DATABASE_SBTOUT should be defined to extract the axial force in the one-dimensional seatbelts [35]. The input for this card is the time interval at which the data should be written to ASCII file.

As a standard practice, unique headings should be defined for all the database cards, associated node sets and element sets, so that the data can be easily identified during post-processing of ASCII files.

*DATABASE_BINARY_D3DUMP card must be defined to generate the restart files at a regular frequency [35]. *DATABASE_BINARY_RUNRSF file can also be requested after certain intervals. For RUNRSF option same file is ‘overwritten’ after specified intervals or a series of files can be ‘overwritten’ in a cyclic order. Whereas for D3DUMP file, a ‘new’ restart file is written, after specified intervals.

Dynamic simulation of the large scale models such as ‘Sleep Seat” may take 30-35 hours on ‘high performance computing’. In the event of server break-down or power-failure, if the restart files are not defined then the entire simulation needs to be performed from time zero! However, files like D3DUMP and RUNRSF create complete database necessary for restarts.

When the mass-scaling is used to obtain the desired CPU time, STSSZ should be set equal to ‘3’ in *DATABASE_EXTENT_BINARY to produce the fringe plots of added mass in parts comprised of shell elements [35].

Appendix E PROCEDURE TO CALIBRATE ‘ImageJ’

A Java-based, public domain image processing program; ‘Image J’ is developed at the National Institutes of Health [55]. It can be downloaded on any computer with a Java5 or later virtual machine. It can read many image formats such as PNG, BMP, JPEG and TIFF and can measure distance and angles. The steps to measure the distance using ‘Image J’ are very simple and user-friendly,

E.1 Set the Scale

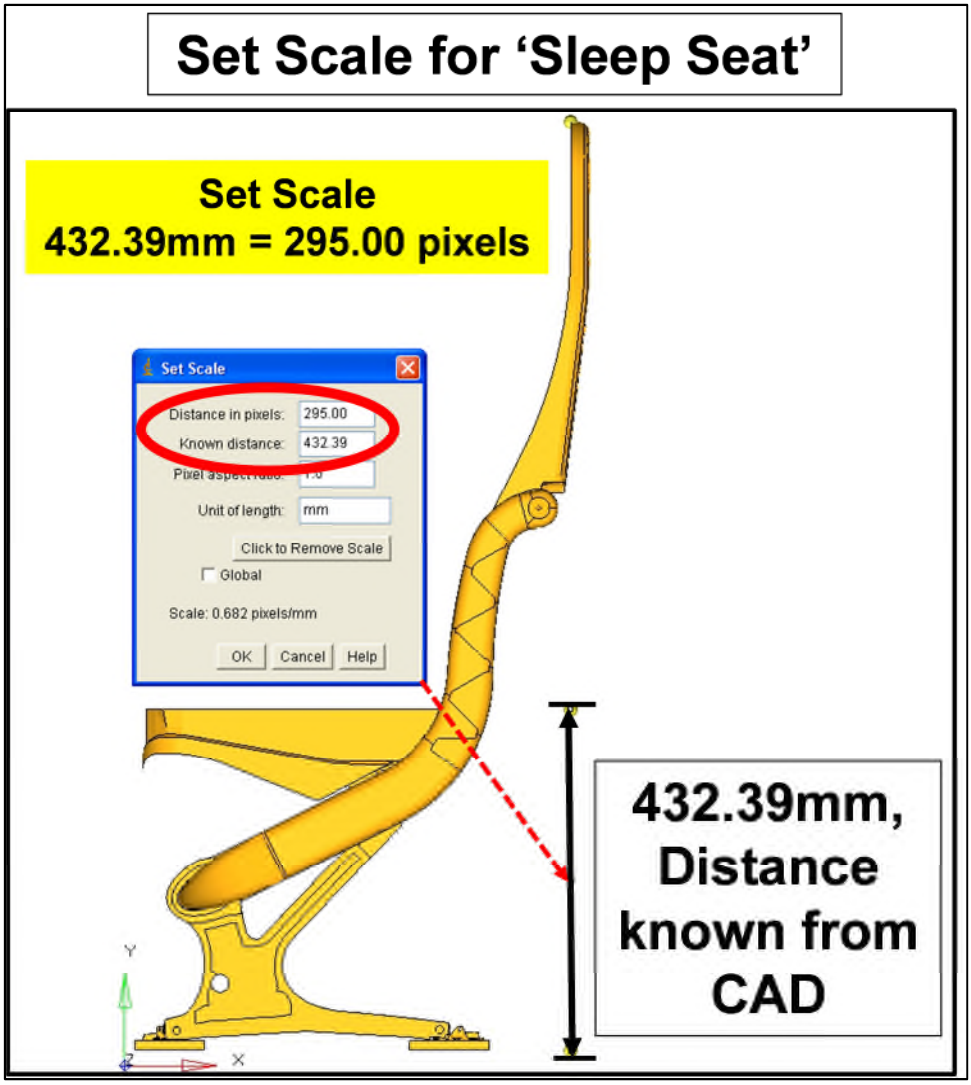

Figure Ap E-1 A known distance of 432.39mm (from CAD geometry) is recorded as equivalent 295.00 pixels in ‘ImageJ’

A known distance e.g. a distance on the ruler should be set in terms of equivalent ‘distance in pixels’ (Figure Ap E-1).

Calibrate, Once the ‘scale’ is set, a known distance should be measured using ‘Image J’ for verification. Height of the seat (HS) is measured using ‘Image J’. ‘HS’ is known from CAD model and is 1177.266mm. The HS measured by ‘Image J’ is 1177.152 mm (Figure Ap E-2). This calibrates the scale.

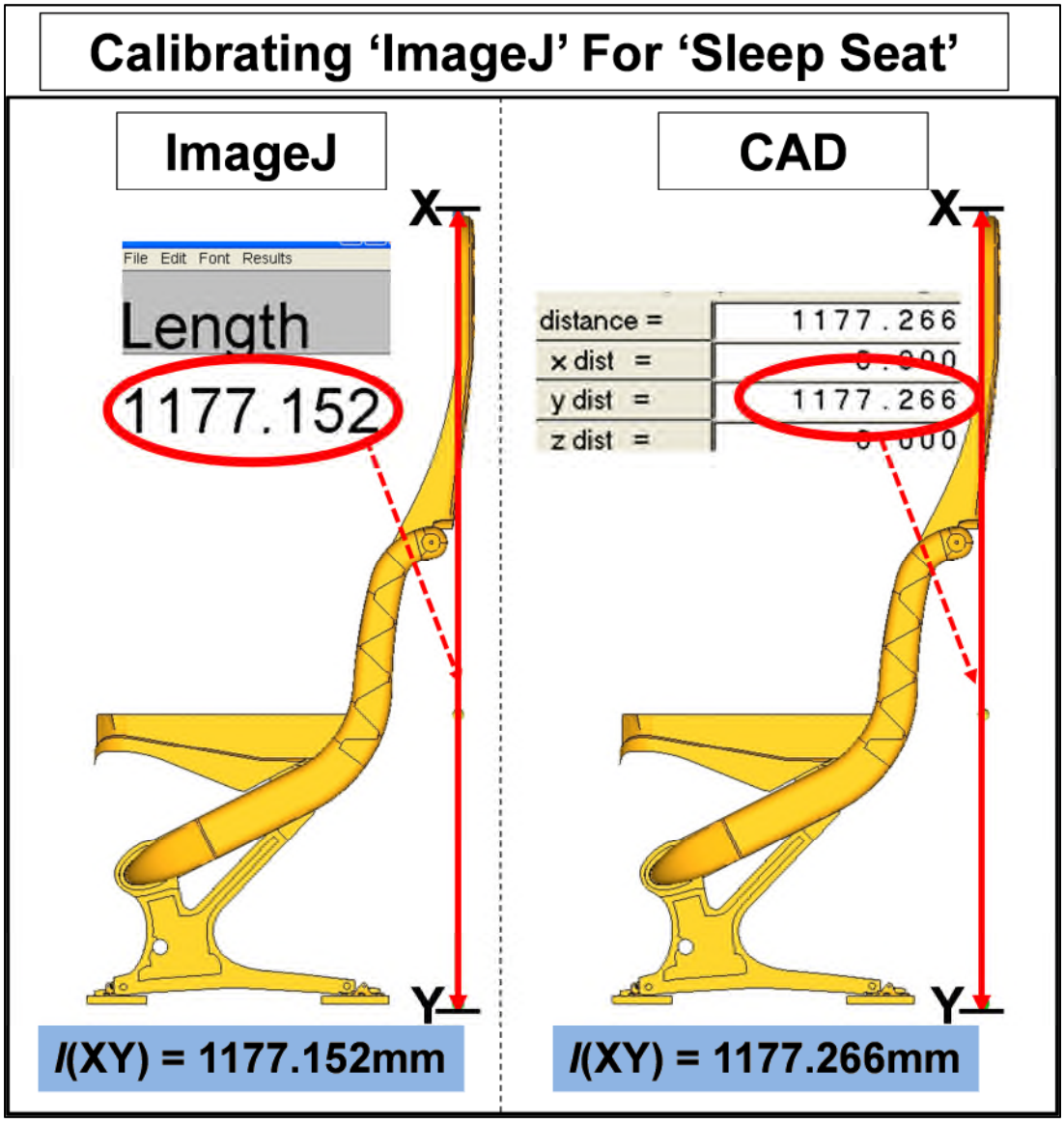

Figure Ap E-2 Figure Ap E-1 scale is set in equivalent pixels. Using this scale, height of the seat (HS) is measured using ‘Image J’. ‘HS’ is known from CAD model and is 1177.266mm against 1177.152 output from ‘ImageJ’

E.2 Measure the distance

A line (either straight, or segmented or free-drawing) can be drawn between any two points and using ‘Measure’ tab under ‘Analyze’ toolbar, the magnitude of the distance can be obtained [55].

Appendix F STUDY OF DIFFERENT DESIGNS OF THE LEG-CLAMPS

After the careful study of the load path, three design solutions were provided and studied in detail.

I. Metallic Spherical Insert
II. An elastomeric insert
III. Stack of O-rings and a Nylon cover

F.1 Logic behind 'Spherical' metallic Leg-Clamp

Initially "Floor-distortion" was simulated for the "Sleep Seat" with "C" shaped leg-clamps (Figure Ap F-1). A considerable yielding in the forward beam and seat legs was observed. However FE model helped to identify the key contact areas, precautions and measures to be taken for the solution convergence and potential failure areas in the leg. A further post-processing of the FEA results helped to identify the deflections of the "Forward Beam" at the cross-sections taken at the regular intervals.

As shown in the Figure Ap F-1 (LHS), LHS of Forward beam moves in forward direction (-X) by 34 mm and in RHS moves backward (+X) by 18 mm. Considering the vertical displacements, LHS moves down by 30 mm and RHS moves upwards by about 26mm (Figure Ap F-1, RHS).

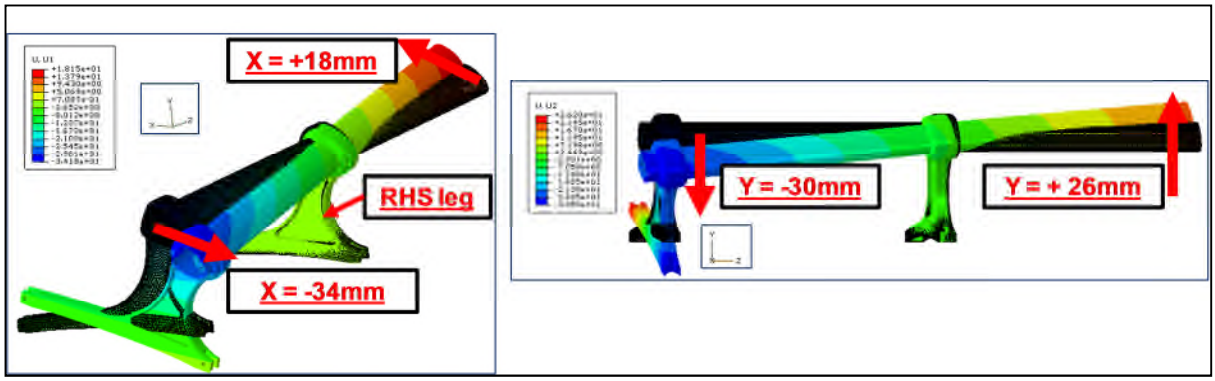

Figure Ap F-1 Displacement of the Forward beam due to floor-distortion loads is recorded and then used shape spherical metallic Leg-Clamp at the Beam-Leg interface.

Considering global displacements, a study was undertaken to check the displacement of cross-sections of Forward beam taken at regular intervals starting from the RHS leg. Based on this study, spherical clamp was designed in such a way that it can give a YAW release of 6 degrees and ROLL release of 3 degrees (Figure Ap F-2). Further aspects of the spherical clamp design are,

- It should not provide any relative motion between the leg and the forward beam when the seat structure is subjected to the static loads as per CS 25.561, preventing the rigid body motion of the seat superstructure. The “Elliptical” shape of the clamp, which is in the firm contact with the forward beam and the variation of the thickness along the contour prevents the activation of YAW and ROLL release during CS 25.561.
- It should operate only during the “Floor-distortion” providing the relative motion between the seat superstructure and the seat sub-structure. The YAW release provided by the contour of the “Spherical Clamp” and the ROLL release provided by the lug movement in the corresponding recess of leg permits the relative motion thereby alleviating the high stress levels generated during “Floor-distortion”.
- However, it should not provide any relative motion between the leg and the forward beam during dynamic loads i.e. CS 25.562. The lugs provided on the front and rear side of the clamp hit their limits after the “Floor-distortion” and come in contact with the ends of the respective recess provided in the leg. The combination of flat surface at the top and the spherical counter at the bottom helps to “POSITIVELY LOCK” the clamp in the leg thereby avoiding any further relative movement.

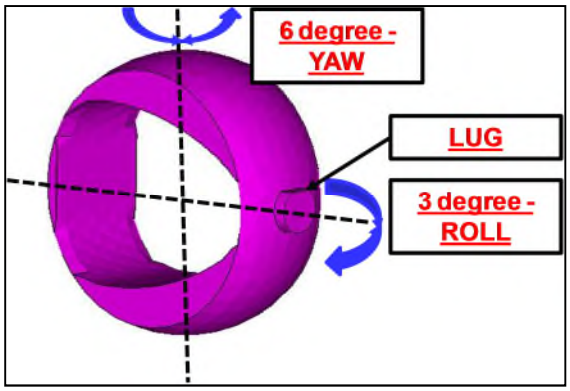

Figure Ap F-2 Spherical Metallic (Al6068T6) Leg-Clamp at the Forward Beam and leg interface designed by considering the displacements of the Forward beam to provide a relative motion between Seat-superstructure and Seat-leg during "Floor Distortion".

Beneficial effect of such a spherical insert can be clearly seen from the Figure Ap F-3. The YAW release provided by the outer-surface of Spherical clamp and the ROLL release provided by the lug movement in the corresponding recess in the leg, helps the “Pitched leg” to slide relative to the clamp which is in the firm contact with the forward beam. This results in alleviating the high stresses observed in the seat leg.

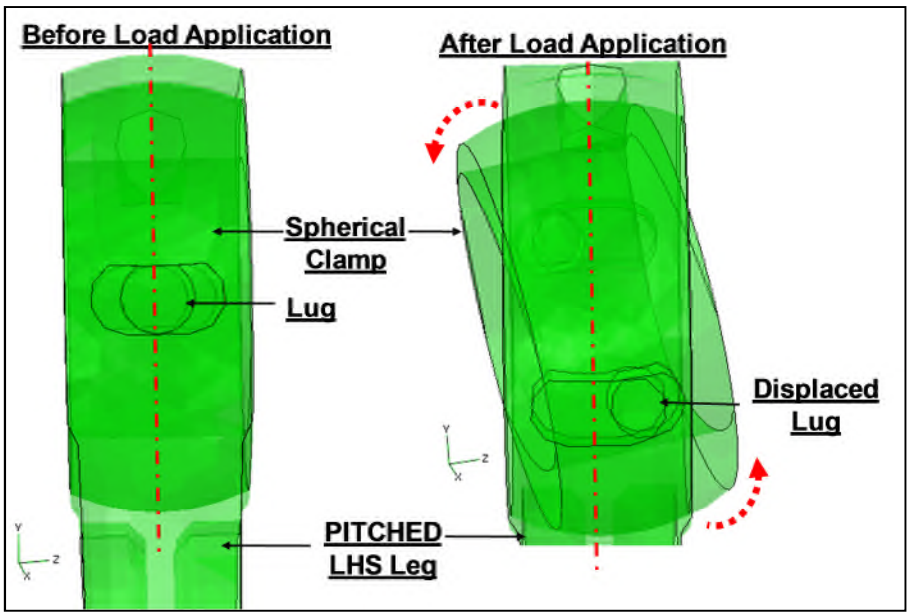

Figure Ap F-3 Spherical Metallic Insert provides the necessary relative motion between Forward Beam and Seat-leg thereby alleviating the high stresses induced due to the applied “PITCH” during “Floor-distortion” loadcase.

F.1.1 Results Discussion - Spherical metallic Leg-Clamp

The effect of this “Spherical Clamp” on the stress levels experienced by the Forward beam and the leg when subjected to “Seat Pre-deformation” loads is investigated and the results are compared to those observed with the original “C” Leg-Clamp. In this simulation, the interface between “Seat leg” and “Spherical Clamp” is modelled with “Zero Coefficient of friction” i.e. Frictionless, a desired ideal condition!

The significant achievements with the “Spherical leg-clamp” are,

- The maximum VMS observed at the front upper throat of the “ROLLED leg” is reduced by approximately 51% (Figure Ap F-6). Note – Nomenclature of the Seat-leg based on high stress regions is given in the Appendix L**.**
- The maximum VMS observed at the front upper throat of the “PITCHED leg” is reduced by approximately 50%, while at front lower throat by 37% (Figure Ap F-5).
- The well distributed (i.e. avoiding the spurious stresses due to contact) VMS observed in the forward beam is reduced by approximately 20%, (Figure Ap F-4).
- All the VMS levels observed are within the yield limit of the Al 6082T6 used for the leg.
- In addition, mass of the “Spherical Clamp” is around 124g, whereas that of “C-Clamp” is around 182g. Hence, approximately 32 % saving in mass per clamp is achieved with the help of “Spherical Clamp**”.**

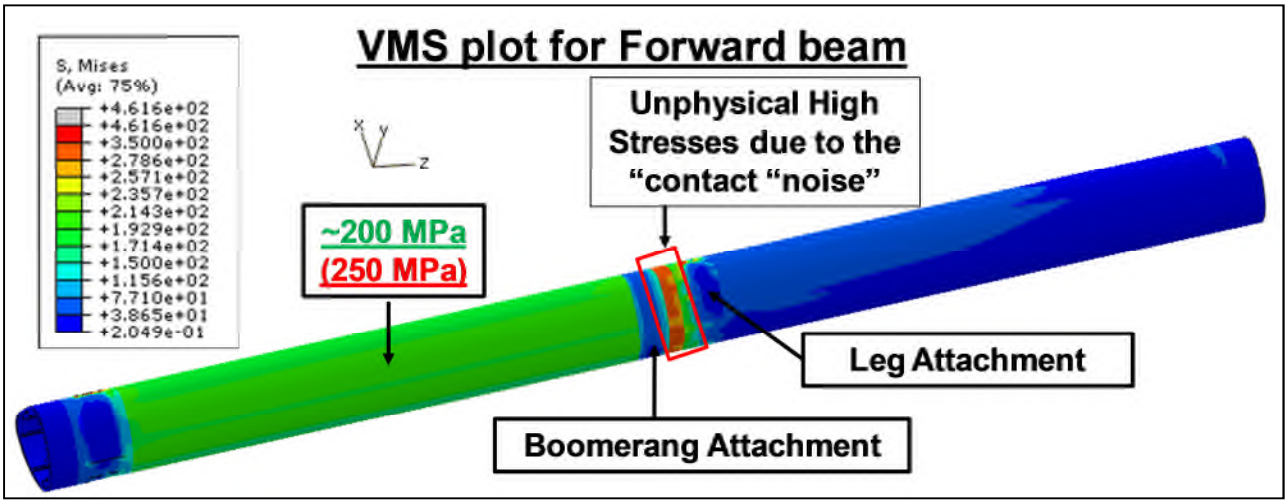

Figure Ap F-4 VMS distributed over a considerable area has reduced from 250 MPa (observed with C Leg-Clamp) to 200 MPa (with the help of Spherical Leg–Clamp). The unrealistic stress at the region between the boomerang and leg attachment can be ignored. Loadcase simulated – Seat Predeformation

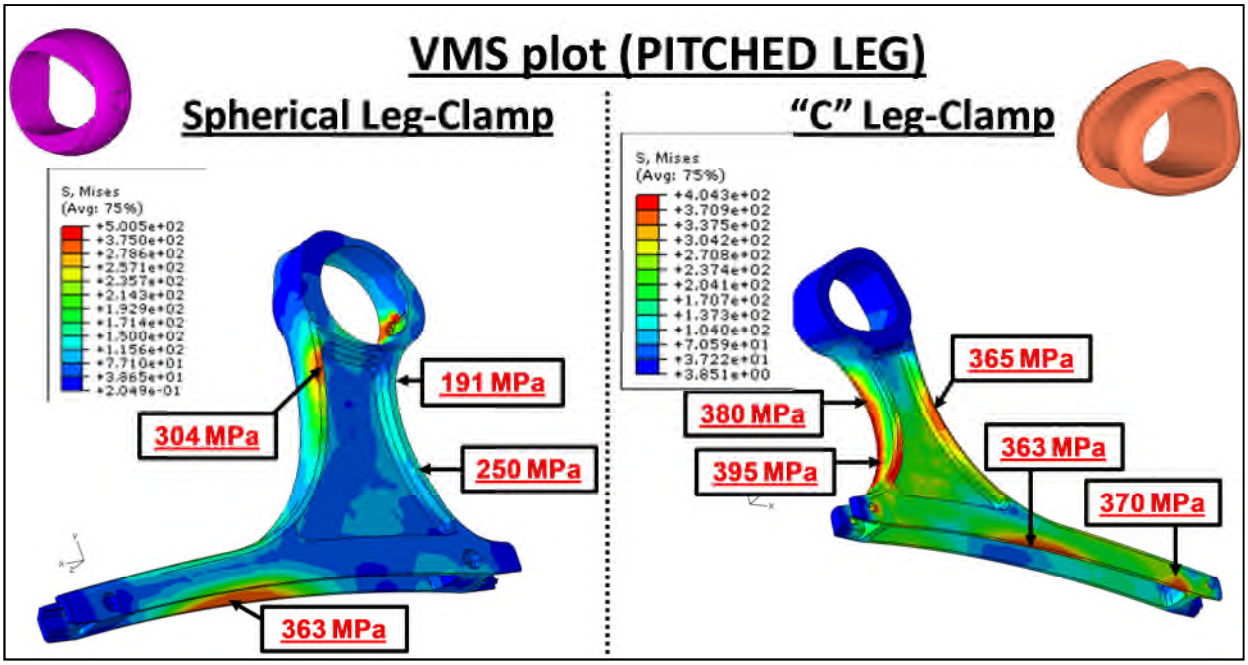

Figure Ap F-5 A VMS observed at the front upper throat and front lower throat of the "PITCHED leg" is reduced(with the help of Spherical Leg–Clamp) to 191MPa and 250 MPa from 380 MPa and 395 MPa (observed with C Leg-Clamp) respectively. Therefore the dynamic load carrying capacity of the leg has increased. Loadcase simulated – Seat Predeformation

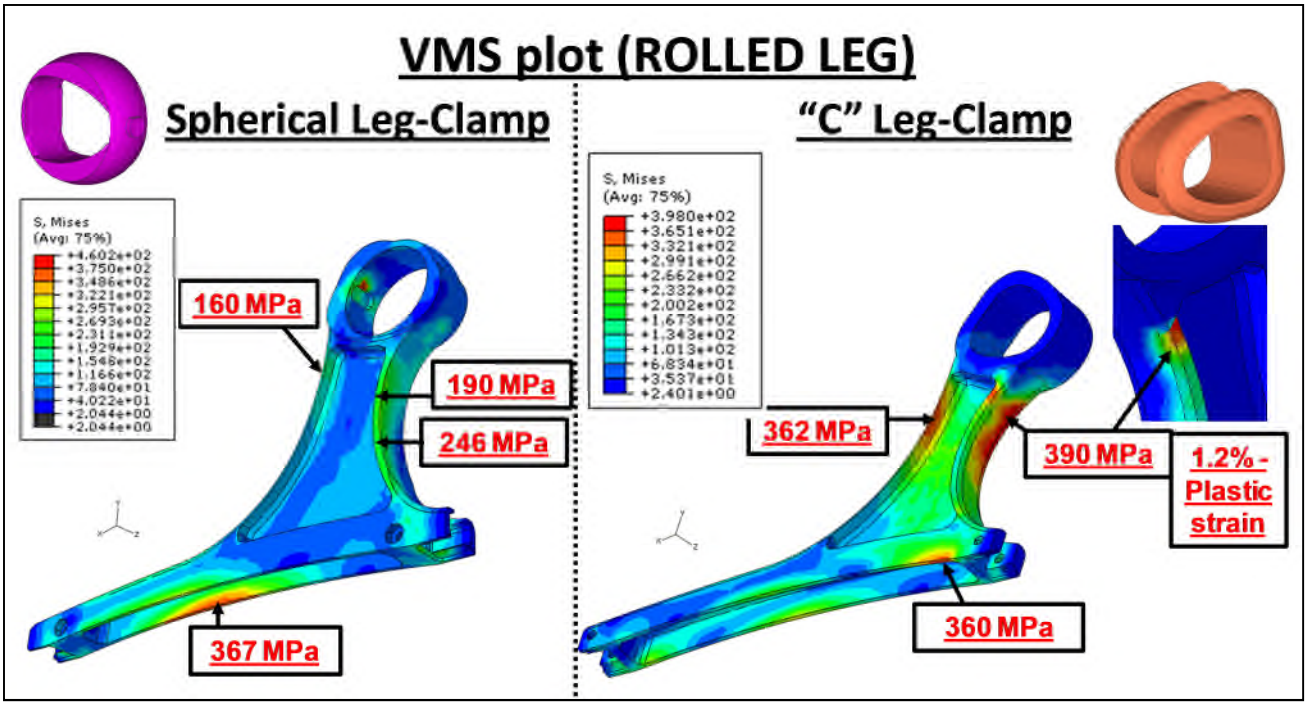

Figure Ap F-6 A VMS observed at the front upper throat region of the "ROLLED leg" is reduced to 190 MPa with the help of Spherical Leg-Clamp (Yield limit for a general Aluminium alloy 350 MPa). The existing "C Clamp" design results in a plastic stain of 1.2% at the same location. Loadcase simulated – Seat Predeformation

F.1.2 Shortcomings of Spherical metallic Leg-Clamp

Even though the “Spherical Leg-Clamp” offered significant reduction in the VMS levels observed in the “Forward Beam” and in the “Seat leg”, following reservations were recorded with the proposed concept:

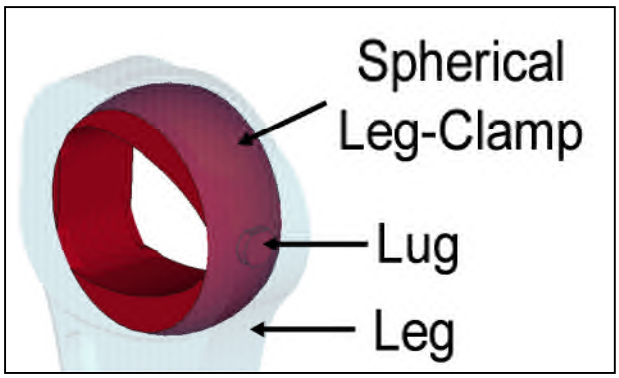

Figure Ap F-7 Location of the Spherical clamp in the Leg (transparent)

I. The ability of the concept to work is heavily controlled by the coefficient of friction (μ) between insert and leg.

   To investigate the effect of friction (at the leg and spherical leg-clamp interface) on the stress levels experienced by the forward beam and leg when subjected to “Seat Pre-deformation”, four different cases were studied based on different values for “μ (0.0, 0.1, 0.2 and 0.3)” and keeping all the other parameters constant. It was observed that the maximum VMS levels in the seat leg increase by approximately 50% even when μ= 0.1 thereby completely offsetting the benefits offered by the “Spherical leg-clamp” (Due to the restriction on the size of this report, details are not provided here. However, a detailed report has been shared with the BlueSky).

II. Therefore, for “Spherical Leg-Clamp” concept to work, the interface had to be frictionless, which increases complexity concerning,

   ✓ Cost / Complexity of manufacture, together with any manufacturing tolerances would result in the design being nowhere near “frictionless”

in operation, and any one of these parts could result in the insert / lugs becoming “jammed”.

- ✓ Concerns over repeatability of manufacture and the reliability of operation of the “Existing Ball Design” between one seat and another.

III. The “Spherical Leg-Clamp” (Figure Ap F-7) consists of the aft and forward lugs that engage with shaped profiles within a leg recess. As the lugs (nipples) transfer the entire load to the seat legs, they are subjected to the stresses above the yield (Figure Ap F-8). High grade of Aluminium or steel is required to be used for them, which adds to the cost and manufacturing difficulties (Fusion of “Soft” grade of Spherical ball and a “Hard” lug. Wearing of the recess provided in the leg (Soft grade of Aluminium) due to the movement of the “Hard” lug.

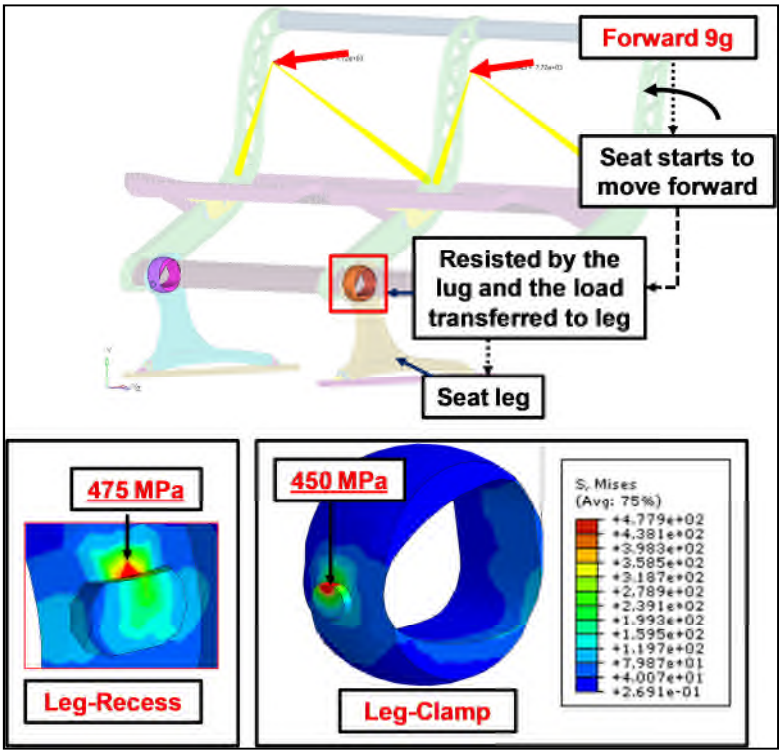

Figure Ap F-8 Lug in the Spherical Leg-Clamp is subjected to the heavy loads (for the applied CS 25.561 loads). The example demonstrates stresses above the yield developed at the lug and corresponding recesses the leg due to small contact area; when the seat is subjected to the “Forward 9g” loads

Due to these shortcomings of the Spherical Leg-Clamp, it was discarded and any further development on it was stopped.

F.2 Development of Elastomeric Leg Clamp

An alternate option to “Spherical Leg-Clamp (metallic)” was proposed to design the Leg-Clamp out of an elastomer, which would be “fixed” in the normal use, but would allow some degree of flexibility under the Predeformation case to alleviate the stresses in the legs. The displacements of Forward beam in each of the Cartesian axes were recovered (near the leg-inserts) from the baseline results (as explained in the Appendix F.1). The idea is to size the elastomer to accommodate the beam displacements by deforming it to 50% or less of its original thickness.

F.2.1 Key Design Issues – Elastomeric Leg-Clamp

- **Size of the insert UNKNOWN** – Need to be sized to provide enough deformation to accommodate the movement of the beam under seat-predeformation, whilst remaining “firm” under normal flight loads.
- **Hardness of the Insert UNKNOWN** – To assess the feasibility of concept, three different grades will be considered based on the hardness (Section F.2.2).
- **Shape of the insert UNKNOWN** – Depending upon grade, cut-outs / notches may be required to weaken the elastomer so that it can deform under predeformation, but appear “firm” under normal flight loads.
- **Ensure no rigid body motion of forward beam**– The insert could be shaped so that it is pre-stressed during assembly to provide a secure grip on the forward beam. Have to ensure that the beam is held under CS25.561 (particularly ‘Sideward 4g’) loads.
- **Minimum Deviation of the Seat leg** - Complete absorption of the movements of the Forward beam by leg-insert before it starts transmitting the load to the seat; is constrained by the aesthetics of the leg design. Seat leg design is almost finalised based on the structural performance.

Therefore, new leg-insert should offer minimum deviation of the seat leg from its current configuration (Figure Ap F-9).

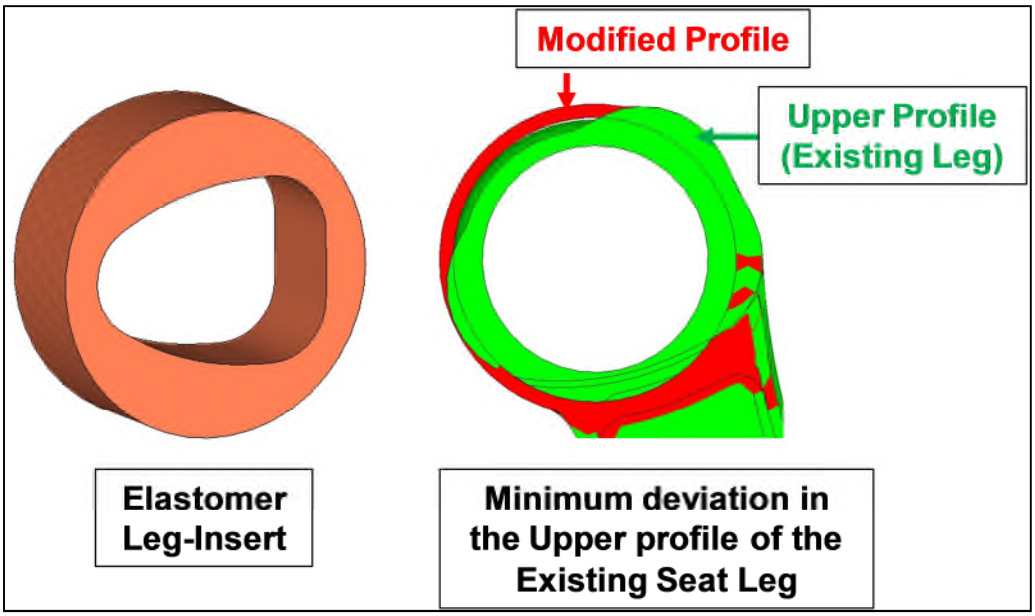

Figure Ap F-9 Elastomeric Leg-Clamp designed to minimise the deviation of the contour of upper profile of the Seat-leg thereby satisfying the aesthetic requirement posed by the Industry

Therefore size of the "Elastomeric Leg-Clamp" is fixed by the corresponding mating contours of the forward beam and leg. Next task is to investigate its effect on the stress levels experienced by the forward beam and leg when subjected to the "Seat Pre-deformation" loads and to compare the results with those from the "Spherical leg-insert" with μ between leg and the insert of 0.1. Results with μ = 0.1 are considered as base-line results since the minimum practical value that can be achieved (using a typical "Teflon to Teflon" coating at the interface) is 0.1.

F.2.2 Selection of Material Grade for Elastomeric Leg-Clamp

A study to identify the adequate stiffness (modulus of elasticity) of the "Elastomeric Leg-Clamp" was conducted. Elastic material model was used for this 'Proof of Concept' exercise. Three different values of modulus of elastic were used [60].

Material Model	Durometer Shore Hardness (A)	Modulus of Elasticity, E (MPa) till 50% compression
Viton FluroElastomer	75	7
Neoprene Rubber	90	15
Processed Hard Rubber	95	30

Table Ap F-1 Suitable material grades and their Young's moduli identified for the 'Elastomeric' Leg-Clamp.

The reasons to choose these materials are [58-60],

- Suitable for Crashworthiness
- High resistance to damage
- Long Service life
- Low lifetime-cost components
- Designed assembly and service connection
- Resistance to oil, all fuels and fuel mixtures
- Wide service temperature range (-40^0C to $+225^0$C)

It was found that Viton Elastomer with Shore Hardness 75A gives the satisfactory results compared to other two materials and hence was chosen for the Leg-Clamp (Due to the restriction of the size of this report, details are not provided here. However, a detailed report has been shared with the BlueSky).

F.2.3 Verification of the material model

The Viton material verification is done as specified in WRL research report by Makino [59]. The test sample is 15*15*0.86 mm with a central hole of diameter 47mm. A force of 890N is applied using MPC with the boundary conditions as specified in the WRL report. The FE model consists of 9081 nodes and 7633 elements. The element type used is a linear hexahedral element with a reduced integration and hybrid formulation (C3D8RH) [33]. The solver used is Abaqus/ Standard.

The displacements of nodes at the centre and at the corner are compared with the reference values obtained from the WRL research report. It can be seen that there is a good agreement between the values (Figure Ap F-10).

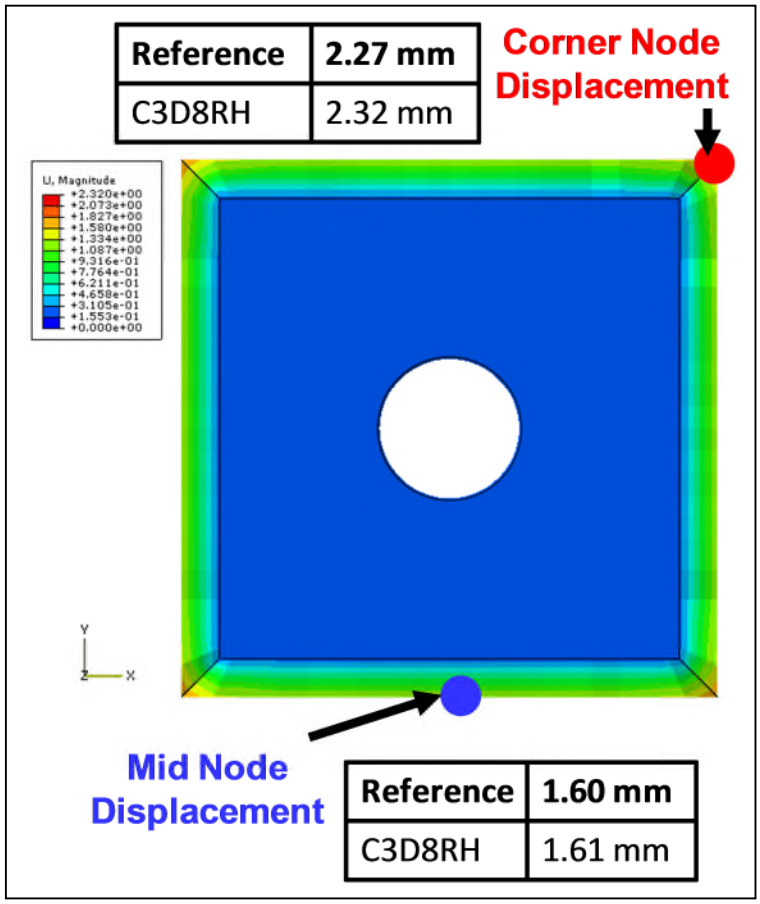

Figure Ap F-10 FEA results for the Verification of Elastomer (Viton 75A) material model. Displacements at the corner node and mid node are compared with the reference values [59]. Mooney-Rivlin material parameters are A – 1.194 and B – 0.163.

F.3 COMPARISION BETWEEN "SPHERICAL" AND "ELASTOMERIC" LEG-CLAMP

During the post-processing of FEA results of "Seat Pre-deformation", it was observed that high stress locations in the legs are comparable across the two different insert designs (only magnitude of VMS changes). Therefore, for both

the seat legs and for Forward beam, VMS levels induced at these locations are given in a tabular format, which allows direct comparison between the “Elastomeric” and the “Spherical (Aluminium)” Leg-Clamp.

F.3.1 VMS Induced in the ‘ROLLED’ Leg

- With the leg-clamp made out of Elastomer, the overall VMS levels observed in the “Rolled leg (LHS leg)” have been reduced when compared with the Baseline results (Figure Ap F-11).
- Particularly at location D (foot-section of the leg, which was a matter of concern in the baseline design), significant improvement can be seen as the VMS has reduced from 340MPa (near Yield limit of a general Aluminium alloy ~ 375MPa) to 140MPa.
- The maximum VMS in the leg for the applied predeformation loads should be approximately 50% of the yield strength of the material used for the leg (general Aluminium Alloy ~350MPa). Achieving this level of stress in the leg is desirable, before the dynamic loads are applied.

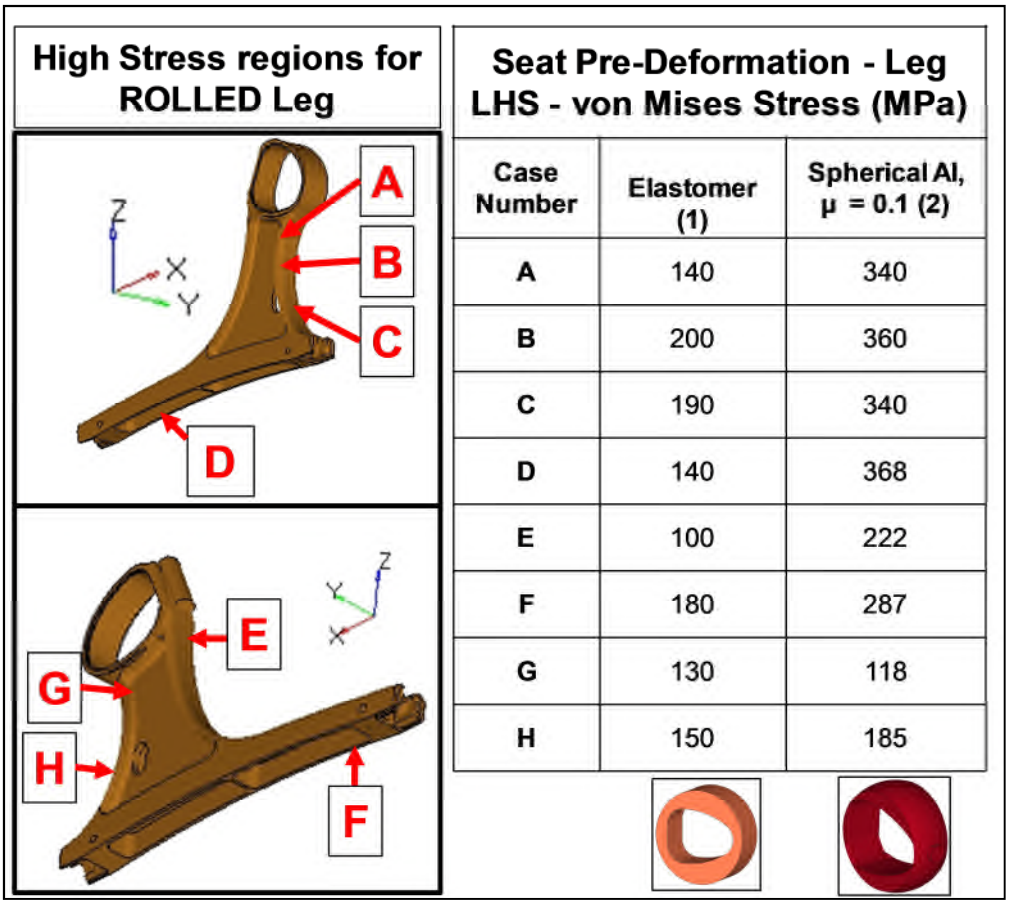

Seat Pre-Deformation - Leg LHS - von Mises Stress (MPa)

Case Number	Elastomer (1)	Spherical Al, μ = 0.1 (2)
A	140	340
B	200	360
C	190	340
D	140	368
E	100	222
F	180	287
G	130	118
H	150	185

Figure Ap F-11 VMS levels in the High stress regions of the 'Rolled' leg are compared for the two cases: Case 1 - "Elastomeric Leg-Clamp" and Case 2 - "Spherical Leg-Clamp" with a 0.1 coefficient of friction modelled between the leg-clamp and corresponding mating surface of the leg. Elastomer leg-clamp has certainly an edge over the spherical metallic leg-clamp. Load Case – Seat Predeformation

F.3.2 VMS Induced in the "PITCHED" Leg

- With the leg-insert made out of an Elastomer, the overall VMS levels observed in the "Pitch leg (RHS leg)" have been reduced when compared to the baseline (Figure Ap F-12).

- Particularly at location C and E (which was a matter of concern in earlier design), significant improvement can be seen as the VMS has reduced from 364MPa (at 'C') / 219MPa (at 'D') to 87MPa / 75MPa respectively.

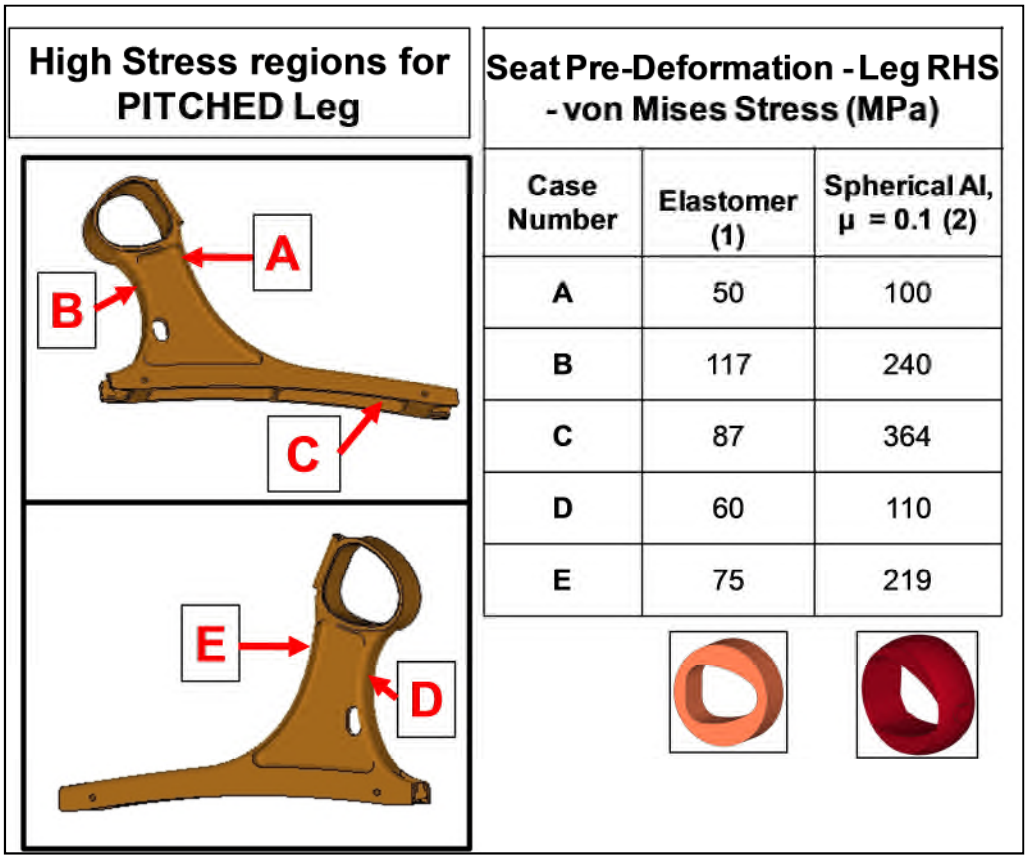

Seat Pre-Deformation - Leg RHS - von Mises Stress (MPa)

Case Number	Elastomer (1)	Spherical Al, μ = 0.1 (2)
A	50	100
B	117	240
C	87	364
D	60	110
E	75	219

Figure Ap F-12 VMS levels in the High stress regions of the 'Pitched' leg are compared for the two cases: Case 1 - "Elastomer Leg-Clamp" and Case 2 - "Spherical Leg-Clamp" with a 0.1 coefficient of friction modelled between the leg-clamp and corresponding mating surface of the leg. Significant reduction in the VMS is achieved due to the use of elastomer leg-clamp, which will increase the load carrying capacity of the leg. Load Case – Seat Predeformation

F.3.3 VMS Induced in the 'Forward Beam'

With the leg-insert made out of an Elastomer, the overall VMS level observed in the Forward beam has reduced from 341MPa (Baseline result) to 10MPa, which is a significant improvement (Figure Ap F-13).

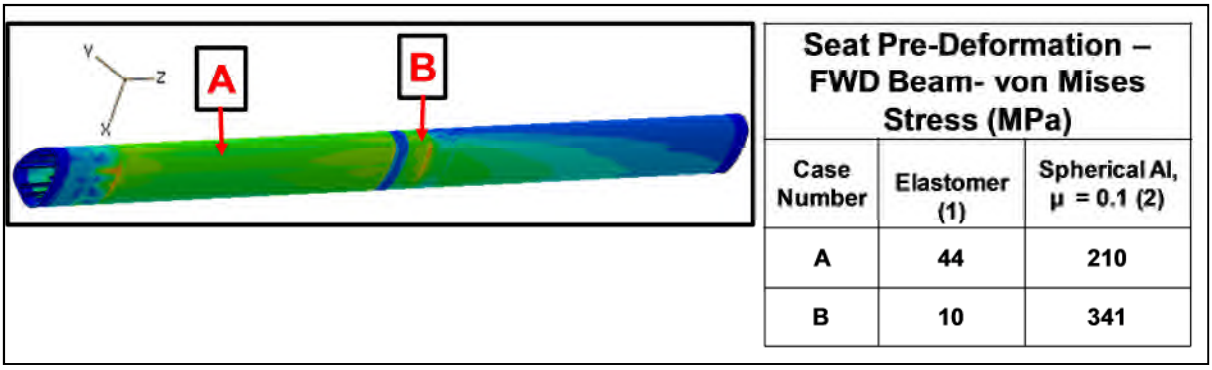

Seat Pre-Deformation – FWD Beam- von Mises Stress (MPa)		
Case Number	Elastomer (1)	Spherical Al, μ = 0.1 (2)
A	44	210
B	10	341

Figure Ap F-13 The highest benefit of the Elastomeric Leg-Clamp is observed in the Forward Beam where the maximum VMS (observed with the Spherical Leg-Clamp) has dropped by 97%

F.4 Elastomeric Leg-Clamp, Concluding Remarks

- FEA results for the “Floor-distortion” indicate that “Elastomeric Leg-Clamp” has a beneficial effect in reducing the stresses observed in both of the legs and the Forward beam (Primary Load Path, PLP). Stresses in the legs are reduced to approximately 50% of the yield stress of a general Aluminium alloy (~ 375MPa).
- Even for the other load cases i.e. “Forward 9g”, “Downward 6g” and “Side 4g”, the maximum VMS values observed in the PLP are within the yield limit (Results are available in the internal delivery and have been shared with BlueSky).
- The maximum deformation of the Elastomer insert is limited to approximately 1.5mm under the “Forward 9g” Load case, which indicates that the seat would appear “firm” under normal in-flight loads preventing “bouncy” feeling for the Occupant.
- Elastomeric insert (at its smallest dimension) is deformed up to the 30% of its original thickness, which demonstrates that the proposed size of the insert is sufficient.

Therefore, it was decided to use the “Elastomeric Leg-Clamp” and direct the further design activities towards finalising the size and shape of it.

Appendix G EVALUATION OF SIZE OF THE ELSTOMERIC LEG-CLAMP

The first step in the elastomeric leg-clamp design is to select the material grade to be used, which has been accomplished in the Section F.2.2. The next important task is to derive its the “SIZE”.

G.1 Design Activities

The formulas used for spring rate (compression and shear) calculations are taken from reference 60. As the elastomeric leg-clamp satisfies the following conditions (which are essential for their use)

- The operation (Downward 6g) remains in the linear range of the elastomer modulus i.e. the less than 30% strain for compression (In present case, the maximum compressive strain observed is 11/12 % for the applied “Downward 6g” load).
- The elastomer between the Seat-leg and the Forward beam is a classic case of the “Flat rubber plate sandwiched in the metal casings”.

List of the assumptions made for the analytical calculations,

- Though the thickness of the leg-clamp (C3, 9mm) is not uniform (due to the different contours of the leg-head and Forward beam), it has been assumed to be uniform for calculation purpose (as the deviation observed in the thickness from a base thickness of 9mm is within ±5%).
- Though the actual “stepped” Leg-clamp has two steps of 6mm and 9mm; for the calculation purpose; 50% of the original thickness (i.e. 50% of 9mm – 4.5mm) is used.
- A representative load area of 30mm length and 15mm width has been used from the upper section of the elastomeric leg-clamp.

Shear Spring Rate, $K_s = (A*G)/t$

Compression Spring Rate, $K_c = (A*E_c)/t$ – for the elastomer with uniform thickness

Compression Spring Rate, K_{cs} = $(A*E_c)/ (t*N)$ – for the "stepped" elastomer thickness

Effective compression Modulus, $E_c = E_0*(1+2*\Phi*S^2)$ – for elastomeric blocks

Bulk Correction factor, $C_b = (1+ (E_0/E_b))-1$

Where,

A – Load area, (length (30)* width (15)) mm^2

G- Shear Moduli, 1.689 N/mm^2

t- Thickness of the undeformed elastomer – 9mm (Case 1) and 4.5mm (Case2)

N – Number of identical elastomer layers, 2

Φ – Elastomer compression coefficient, 0.53

Shape factor, S = (Load area)/ (Bulge area)

For the rectangular block considered in present calculations,

S = (length*width)/ (2*t (length+ width))

E_0 – Elastic modulus, 7.170 N/mm^2

E_b – Bulk Modulus, 1241 N/mm^2

Case 1 - For the original design of elastomeric leg-clamp (C3, 9mm),

K_s = 84.45 N/mm, S= 0.67, E_c= 10.58 N/mm^2, K_c = 529 N/mm

$(K_c/ K_s)_{CASE1} = 6.26$

Case 2 – For the "Stepped" design of elastomeric leg-clamp (C3_V1, 6/9mm)

K_s = 84.45 N/mm, unchanged as the load area and total thickness same as original

S= 1.11, E_c= 16.55 N/mm^2, K_{cs} = 827.65 N/mm, **$(K_{cs}/ K_s)_{CASE2} = 9.8$**

In Case 2, the ratio of K_c to K_s has increased by 56.5% while maintaining the same K_s as that in Case 1, which is the design requirement. As the deflection is inversely proportional to the stiffness, increment in the “Compression Spring Rate” (i.e. increment in the spring rate in the vertical direction as applicable to the “Sleep Seat Design”) by 56.5% should result in reducing the vertical downward displacement by 56.5 % (for the applied vertically “Downward 6g” load).

Therefore, by analytical calculations the vertical downward displacement of the Seat-pan for the applied “Downward 6g” should reduce from 82 mm (C3, 9mm Leg-Clamp Figure Ap G-2) to 52.4mm (C3_V1, 6/9 mm Stepped Leg-clamp). FEA results show that the displacement is 56mm.

As the FEA results are within ±7% of the analytical calculations, excellent co-relation has been observed (considering the assumptions made during analytical calculations) establishing the confidence in the FE models.

A total of SIX different design variants for the “Elastomeric Leg-Clamp” were studied (Figure Ap G-1) based on manufacturing constraints, aesthetic requirements, cost, design simplicity and performance when subjected to the loads as per CS 25.561 and Floor-distortion.

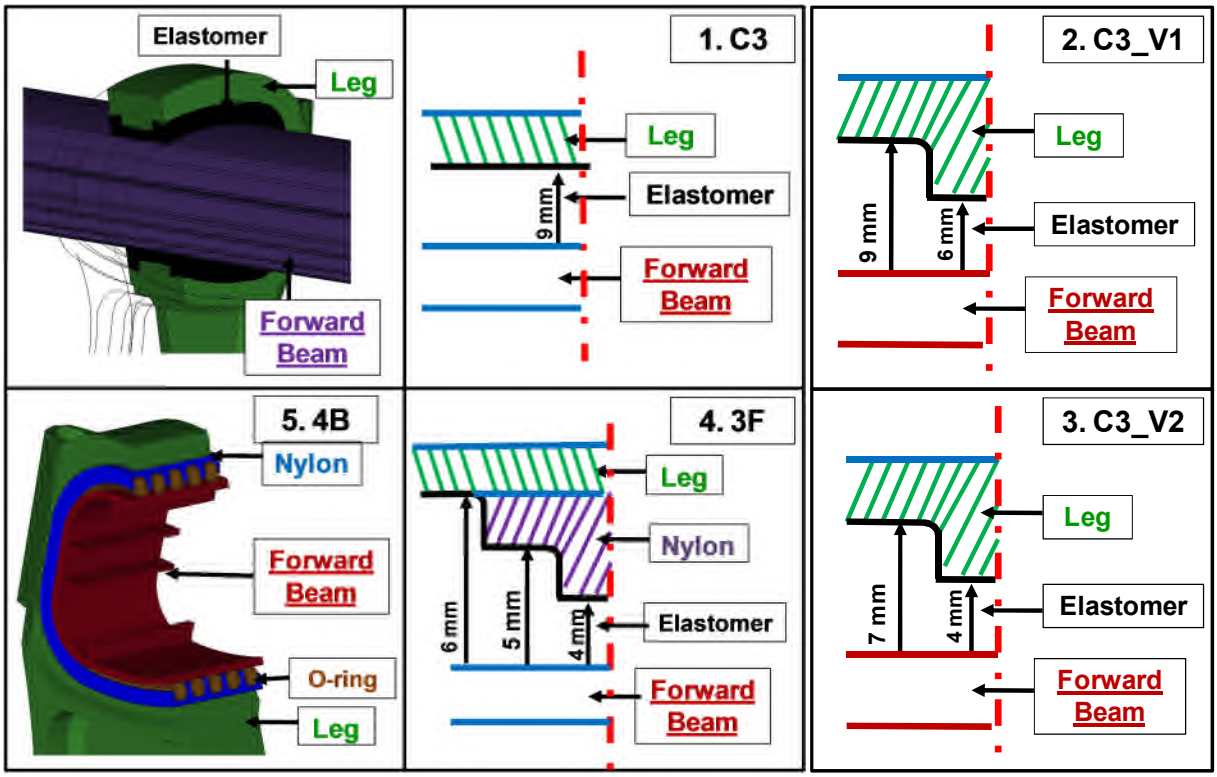

Figure Ap G-1 Cross-Section of the elastomeric leg-clamp at the Forward beam and leg interface is shown. Version 1 (C3) – Thickness of the elastomer insert = 9 mm around the elliptical Forward beam. S Stepped Elastomer Leg-Clamp for versions 2, 3 and 4 (C3_V1, C3_V2 and 3F). Version 5 (4B) contains FIVE O-rings held together by a nylon casing. Nylon casing then matches with the inner profile of the leg-head, while O-rings rest on Forward beam. Seat Variant– Triple seat structure

Merits and demerits of each one of them are discussed in the next session with reference to the Figure Ap G-2 (Detailed reports for the individual variant have been delivered to the BlueSky).

- Leg-Clamp C3 suffered from the unacceptable vertical downward displacement of the Seat Pan (82mm). This displacement is caused by the high vertical flexibility of the insert and therefore it was essential to use the insert with the variable stiffness.

Serial Number, Leg-Clamp		Load Case	Seat Predeformation				Downward 6g					Sideward 4g					Forward 9g			
			von Mises Stress, MPa				von Mises Stress, MPa				Def, mm	von Mises Stress, MPa				Def, mm	von Mises Stress, MPa			
		Location	A	B	C	D	A	B	C	D		A	B	C	D		A	B	C	D
1	C3 (9mm)	Leg - LHS	210	80	180	385	200	179	260	450	82						299	115	173	106
		Leg - RHS	240	100	120	230	175	210	255	475							290	80	173	107
		Beam	190	256			216	300									72	90		
2	C3_V1 (6/9mm)	Leg - LHS	210	110	235	410	185	100	210	460	56	230	210	160	130	45.7	190	140	250	424
		Leg - RHS	215	110	130	285														
		Beam	120	150			220	230				200	220				80	78		
3	C3_V2 (4/7mm)	Leg - LHS	270	150	270	476	250	200	200	420	28	477	477	425	376	27	155	140	160	272
		Leg - RHS	308	150	185	403														
		Beam	135	165			215	240				255	255				192	205		
4	3F (4/5/6mm)	Leg - LHS	275	160	280	475	160	145	150	380	40	355	280	230	190	38.7	130	105	210	355
		Leg - RHS	330	160	150	315														
		Beam	130	145			190	222				200	200				82	88		
5	4B (O Ring)	Leg - LHS	195	90	200	300	150	115	145	320	100						150	115	220	386
		Leg - RHS	200	120	100	280														
		Beam	220	260			350	325									255	256		
6	Mixed EI+AI	Leg - LHS	438	200	210	476	99.8	240	300	480	22(EI) 48(AI)									
		Leg - RHS	220	100	150	290	90	90	130	225										
		Beam	156	270			290	245												

Figure Ap G-2 VMS in the seat-leg and in the Forward beam along with the deformations observed in the structure for "Forward 9g", "Downward 6g", "Sideward 4g" and "Seat Predeformation" are documented and compared for the SIX different designs of the Elastomeric Leg-Clamp. As the overall performance of the C3_V2 (4/7 mm_ Leg-Clamp is satisfactory, it is carried forward for further use and simulations.

Due to the Unsymmetrical nature of the seat-structure in terms of Occupant spacing and the high degree of flexibility in the vertical direction due to the thicker elastomer along the top and bottom surfaces, the RHS and LHS sides of the Forward beam are subjected to the different displacements. This misalignment places the beam under additional bending, resulting in higher stresses being induced in the Forward beam.

- Leg-Clamp C3_V1 (6/9 mm) resulted in the excessive (56 mm) vertical downward displacement of the Seat-pan for “Downward 6g” loads (when compared with that observed with Insert “C3_V2”) and 45.7mm of lateral

displacement (into the longitudinal aisle space), which is well above the limit (38mm, Reference 14) for the applied “Sideward 4g” loads.

- Leg-Clamp 3F (4/5/6 mm) resulted in the increased vertical downward displacement of the seat-pan for “Downward 6g” loads (when compared with that observed with Insert “C3_V2” and 38.7mm of lateral displacement (into the longitudinal aisle space), which is over the limit (38mm, Reference 14) for the applied “Sideward 4g” loads.

- Leg-Clamp 4B (O-Ring) resulted in the unacceptable (100 mm) vertical downward displacement of the seat-pan for “Downward 6g” loads and highly stresses Forward beam when subjected to the “Forward 9g” loads due to the contact between Nylon Cover and the beam.
- Combination of Elastomeric insert in the “PITCHED” leg and Aluminium Insert in the “ROLLED leg” did not have any practical merit and hence was discarded.

Overall satisfactory performance of the Seat Structure when subjected to static loads as per CS 25.561 and “Floor-distortion” as per CS25.562 was observed with the “Elastomeric Leg-Clamp C3_V1 (4/7 mm). Though comparatively (with C3_V1 (6/9 mm)) high von mises stresses were observed in the leg during “Floor-distortion”, they are below the yield limit. The major advantage was the lowest (28 mm) vertical downward displacement of the seat-pan for “Downward 6g” loads and lateral displacement of 27mm when subjected to the “Sideward 4g” loads. Therefore, there was a “Trade-Off” between the structural response of the seat for the applied “Floor-distortion” loads and “Downward 6g” and “Sideward 4g” loads.

Appendix H CONTACT PRESSURE DISTRIBUTION ON MODIFIED TLF

The Tool-Less Fittings (TLF) were modified with addition of a spherical globe to the forged (main) body. This decoupled the Seat-leg (and hence rest of the seat structure) from the Seat-track for the applied “10 degree ROLL” during “Floor-distortion” and thereby completely negating its detrimental effect (Figure Ap H-1 - RHS).

H.1 Radius for the ‘Spherical’ TLF

While deciding the radius for the spherical globe of the TLF, following factors were considered,

- Minimum wall thickness of the leg was fixed to 5mm based on the required second moment of area to sustain the applied static inertia loads (CS 25.561)
- The housing used to accommodate the main body of the TLF, is made of Aluminium. For Aluminium components used for long service life, the minimum wall thickness should be 4mm for the stability (to avoid buckling or twisting). Therefore, maximum possible radius of 7mm (to spread the load) was used for the spherical globe of the TLF.
- The overall profile of the interaction between main body of TLF and the housing was engineered in such a way that there will be a relative motion between the two for the applied “Roll” but the joint will not disengage during other load cases i.e. Static loads as per CS 25.561 and dynamic loads as per CS 25.562.

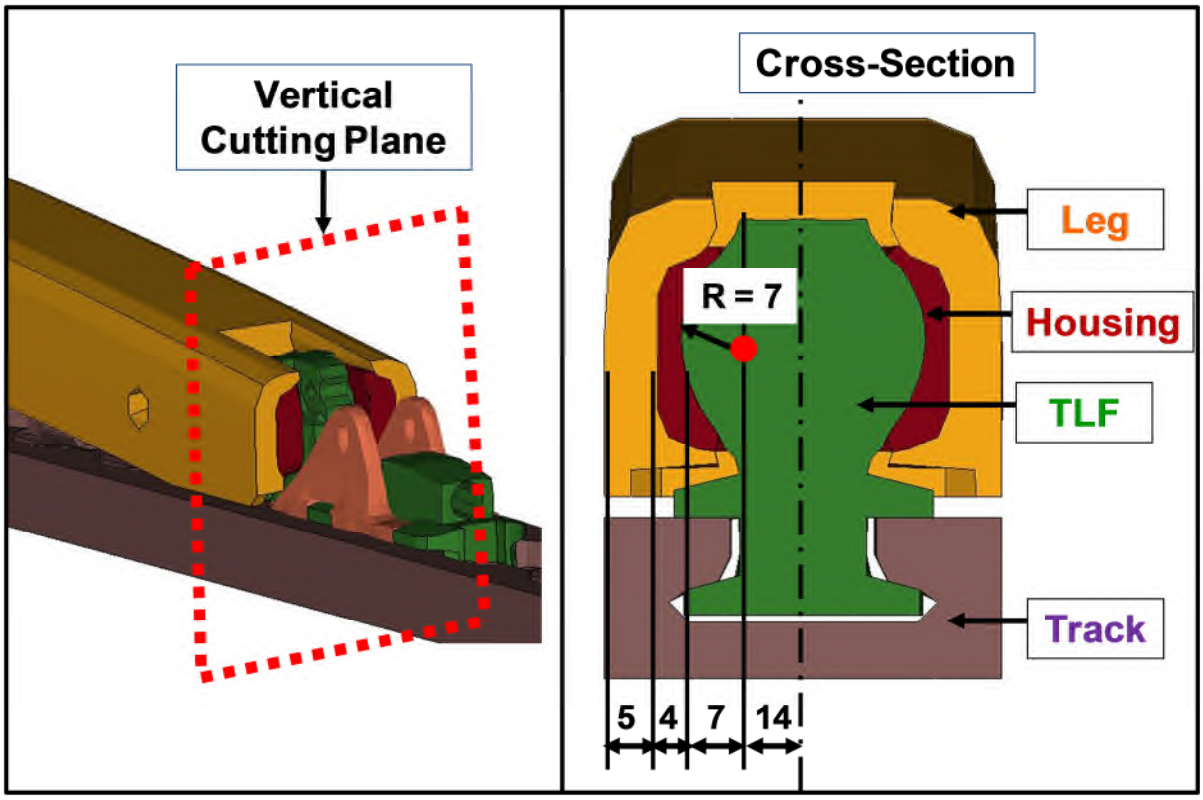

Figure Ap H-1 LHS Definition of the cross-section plane. RHS - Cross-section of the rear anchorage along with the wall thickness for each of the components (All dimensions are in millimetres). 7mm radius of the spherical globe of the TLF

H.2 Contact pressure at Seat-Leg and TLF interface

The maximum contact force exerted on the Forged Body of the Tool-Less Fittings is 8006N as observed in the “Forward 9g” loadcase. The radius of the contact surface between the external spherical surface of the main (forged) body of the TLF and internal spherical surface of the TLF-Housing is can be calculated by [64],

$$a= ((3*F/8)*((1-v_1^2)/E1 + (1-v_2^2)/E2)/ ((1/D_1)-(1/D_2)))^{1/3}$$ **Equation H-1**

Where,

F- Applied force, 8006NTherefore, Radius of contact, a = 3.7mm

Property	TLF Housing (Al)	TLF - Main Body (Cres 17-4 PH)
Poissons' Ratio	$\nu_1 = 0.34$	$\nu_2 = 0.29$
Modulus of elasticity, MPa	$E_1 = 71000$	$E_2 = 196000$
Diameter of the Sphere, mm	$D_1 = 14.2$	$D_2 = 14$

Figure Ap H-2 Mechanical Properties for toll-less fittings

The maximum pressure at the contacting point, $P_{max} = (3*F)/ (2*\prod*a^2)$

This gives, $\mathbf{P_{max} = 279\ MPa}$

Whereas the “Contact Pressure” distributed over a reasonable area form FEA results is around 263MPa (Figure Ap H-3). As it can be seen that the FEA results are within ±7% of the analytical calculations, the FE representation of the most important joint i.e. between the anchorage (TLF-Main body) and the Seat-leg (TLF-Housing) is reliable.

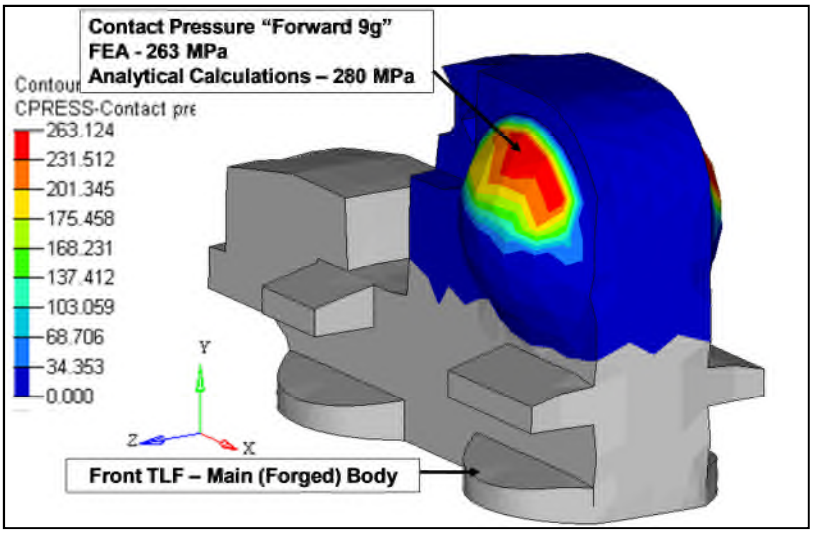

Figure Ap H-3 Distribution of the Contact Pressure for the Front Tool-less Fitting Main Body for the applied "Forward 9g" load. Results from FEA and those from analytical calculations are in good agreement.

Appendix I BOUNDARY CONDITIONS FOR FLOOR-DISTORTION

As per the CS 25.562, the seat tracks must be misaligned with respect to each other by 10 degrees vertically (PITCH) with one of the seat tracks rolled 10 degrees [10]. According to the Airline specifications (for A320), the highest loaded leg should be rolled 10 degrees Counter Clock Wise (CCW), looking from behind) and the other leg should be “Pitched Down” 10 degrees so as to test the worst loading scenario. In “Sleep Seat”, the LHS-Leg will be rolled and RHS-Leg will be pitched as the LHS-Leg is,

- With the largest overhang. In the economy seat configuration, LHS-Leg is at the outboard position and due to the restriction of the aircraft side wall, outboard position is the one with largest overhang (Figure Ap I-1).
- The trailing leg. According to the airline specifications, the leg with the largest overhang (in present case LHS-leg) should be yawed 10° CC) to Aircraft Centreline (when viewed from above), which makes it the trailing leg for the test, i.e. makes it more critical.

The “Roll” and “Pitch” application point is the pivot point of the aft fitting (in “Sleep Seat” is the centre point of the spherical globe of Tool-Less fittings) projected in the Seat Track-Crown plane, Point A (Figure Ap I-2).

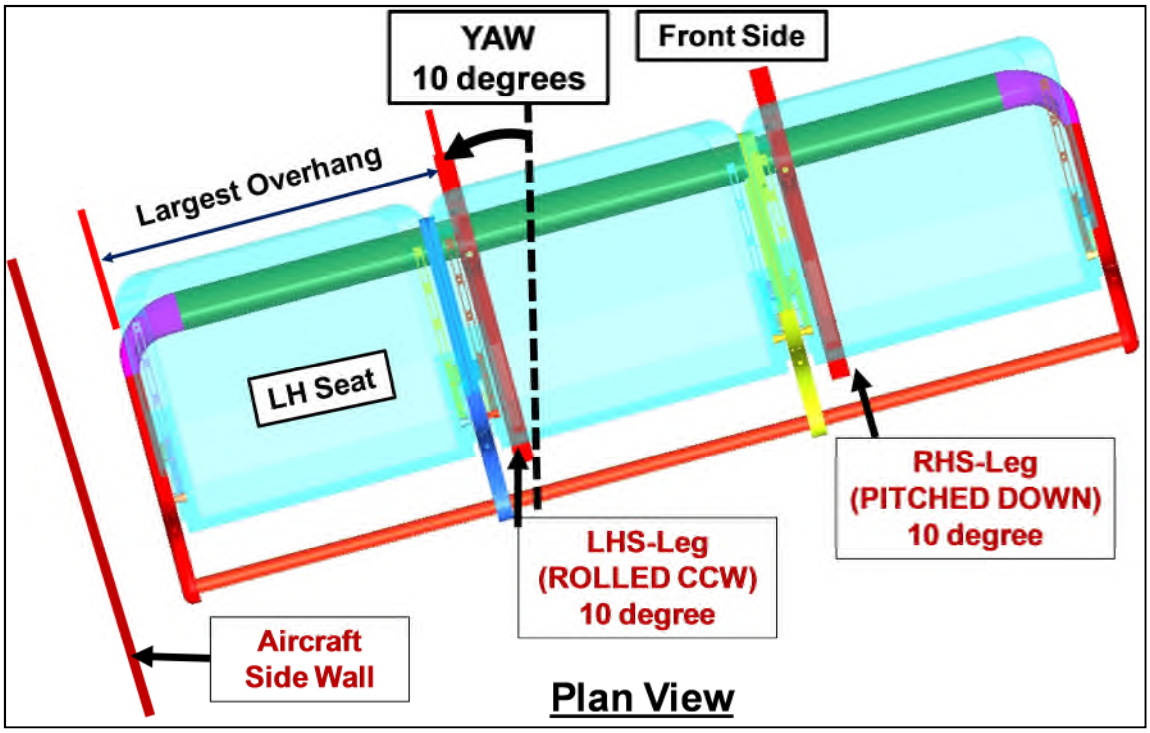

Figure Ap I-1 "Sleep Seat" yawed at 10 degrees. Leg-LHS with the largest overhang (trailing due to the yawing) to be ROLLED by 10 degrees and other leg (RHS) to be PITCHED by 10 degrees

I.1 Procedure to apply Floor-Distortion in Abaqus (Research) 6.9-3

Bottom Section of the track is connected by multi point constraints (MPC) to Point A (Figure Ap I-2). Support conditions and enforcement displacements are applied to the independent node, which is “Point A”. The point at which “Pitch Down” is applied is constrained for all degrees of freedom (dofs) except rotation corresponding to “Pitch Down”. The point at which “ROLL CCW” is applied is constrained for all dofs except rotation corresponding to “ROLL” (Figure Ap I-2).

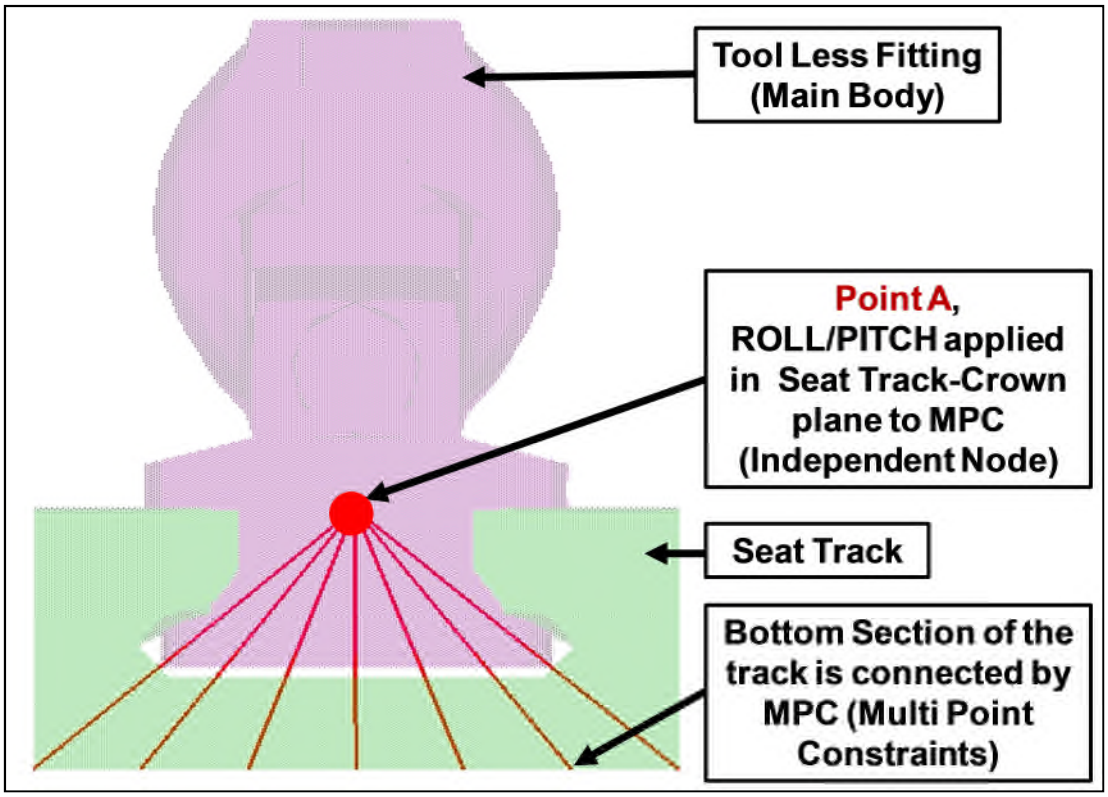

Figure Ap I-2 Floor-distortion loads are to be applied at the pivot point of the aft fitting (i.e. in "Sleep Seat" it is the centre point of the spherical globe of Tool-Less fittings) projected in the Seat Track-Crown plane (Point A). It is connected with the bottom surface of the Seat-track using Multi-Point Constraints (MPC)

"Seat Pre-deformation" is the pre-requisite for the "Dynamic 16g (CS 25.562)" pulse application and "16g" needs to be applied to the seat structure that is Yawed at 10 degrees [10]. Therefore, "Seat pre-deformation" has been applied to the yawed seat structure. In order to be consistent with the Certification Specifications (CS 25.562), the deformation loads have been applied in the local co-ordinate system so that the condition of rail (in the present case is the seat track to which "PITCH" is applied) is misaligned with respect to the adjacent set of rail (in the present case is the seat track to which "ROLL" is applied) is satisfied.

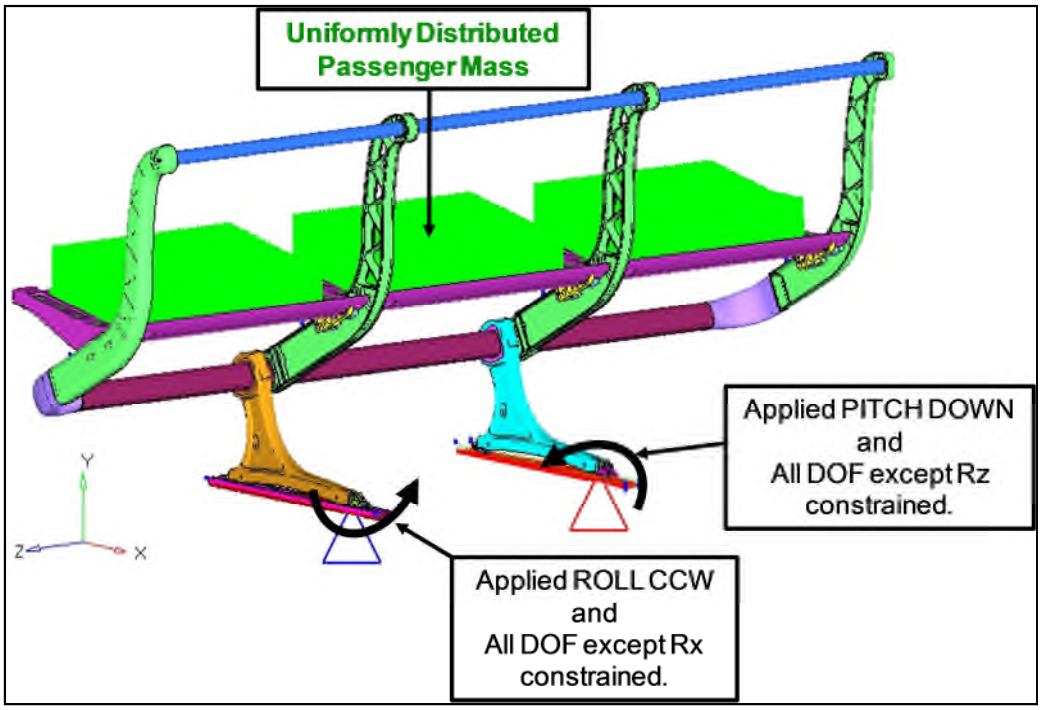

Figure Ap I-3 Definition of Seat Pre-deformation loads - 10 degree ROLL is applied in Counter Clockwise direction to the trailing leg (Leg-LHS, looking from the rear of the seat) constraining all degrees of freedom (dofs). 10 degree PITCH DOWN is applied

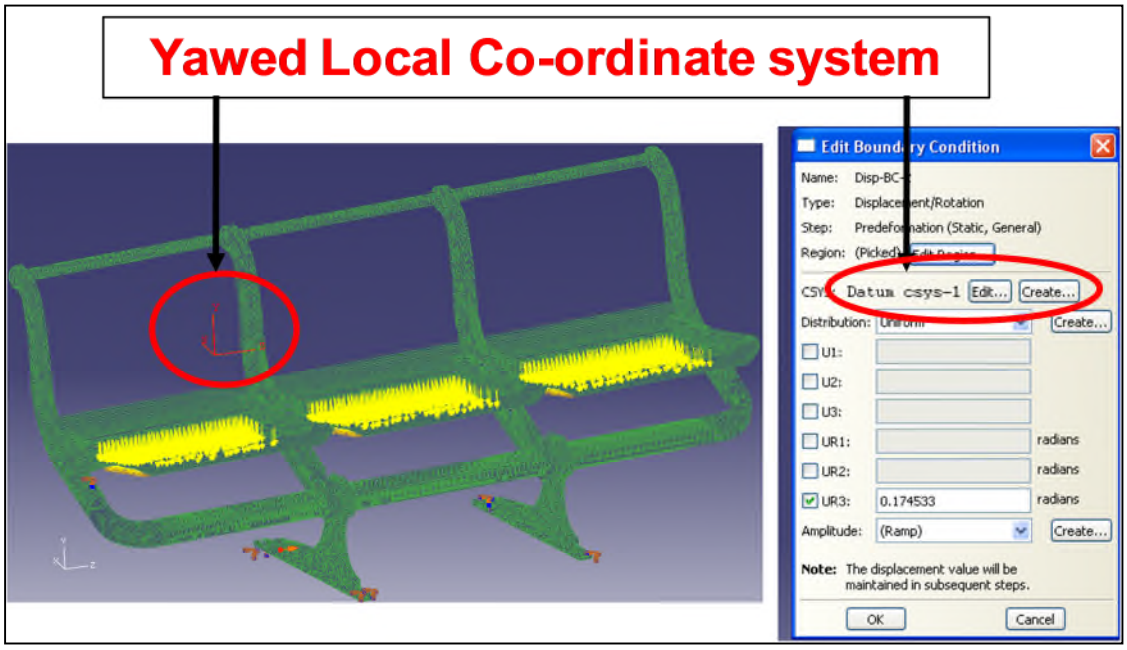

Figure Ap I-4 Seat pre-deformation loads have been applied in the "Yawed" Local Co-ordinate system (Datum csys-1) – Abaqus/CAE so that the Seat-tracks are misaligned with respect to each other as specified in CS 25.562 [8] [21].

I.2 Procedure to apply Floor-Distortion in LSDYNA

The orientation of the seat, point of application of the pre-deformation loads and choice of seat-leg to apply a 'Pitch' or 'Roll' is maintained exactly same for LS-DYNA environment as that used in the FE model of the 'Seep Seat' for the 'Pre-deformation' loadcase, built for Abaqus (Research) 6.9-3.

Following section explains the procedure adopted to apply the 'Pre-deformation' loads for both of the LSDYNA (Implicit way as well as Explicit way) environments. The point A (Figure Ap I-5) where the Pre-deformation loads are applied is attached to the part 'TKRB1' using *CONSTRAINED_EXTRA_NODES_SET [35]. TKRB1 is coincident with the bottom of the seat-track and is modelled with the shell elements.

TKRB1 has been assigned a 'rigid' material property and is defined as a *PART_INERTIA with the 'Point A' as the centre of gravity (CG). TKRB2 has been assigned a 'rigid' material property and is linked with TKRB1 using '*CONSTRAINED_RIGID_BODIES option; TKRB1 acting as a 'Master' rigid body. All the prescribed boundary conditions applied to the 'Master' rigid body (TKRB1 in this case) are also applicable to the 'slave' rigid body (TKRB2 in this case).

'Roll' and 'Pitch' enforced displacements are then applied using *BOUNDARY_PRESCRIBED_MOTION_RIGID [35]. The restraints,

- The point at which 'Pitch' is applied should be constrained for all the degrees-of- freedom except rotation corresponding to the 'Pitch' definition and
- The point at which 'Roll' is applied should be constrained for all the dofs except rotation corresponding to the 'Roll' definition; need a special consideration as the usual *BOUNDARY_SPC_NODE definition cannot be used to define the restraints on the nodes belonging to the rigid bodies [35].

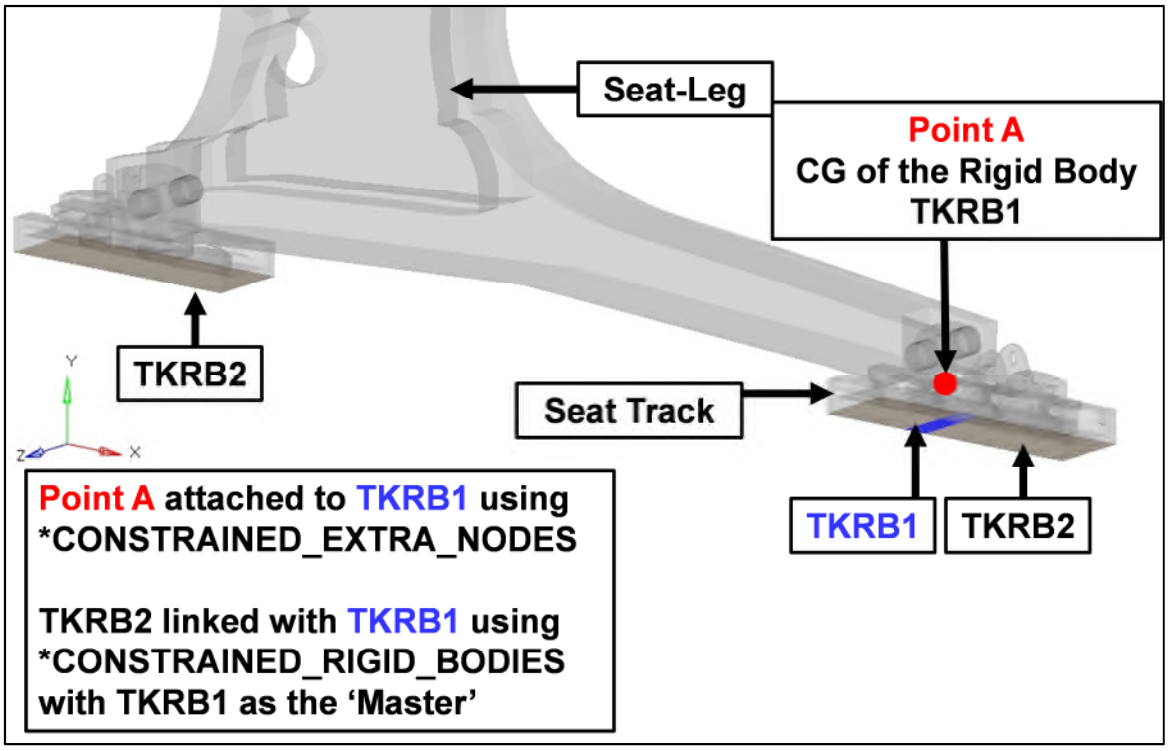

Figure Ap I-5 Seat Predeformation loads are to be applied at the pivot point of the aft fitting (i.e. in "Sleep Seat" it is the centre point of the spherical globe of Tool-Less fittings) projected in the Seat Track-Crown plane (Point A). It is connected with the bottom surface of the Seat-track using *CONSTRAINED_EXTRA_NODES_SET

These restraints are applied through *MAT_RIGID i.e. material definition for TKRB1 (Figure Ap I-6) [35]. CMO parameter on *MAT_RIGID defines the options (CON1 for the translational dof and CON2 for the rotational dof) to apply restraints to the centre of mass of the rigid body either in Global co-ordinate system (CMO =1) or in the local co-ordinate system (CMO =-1).

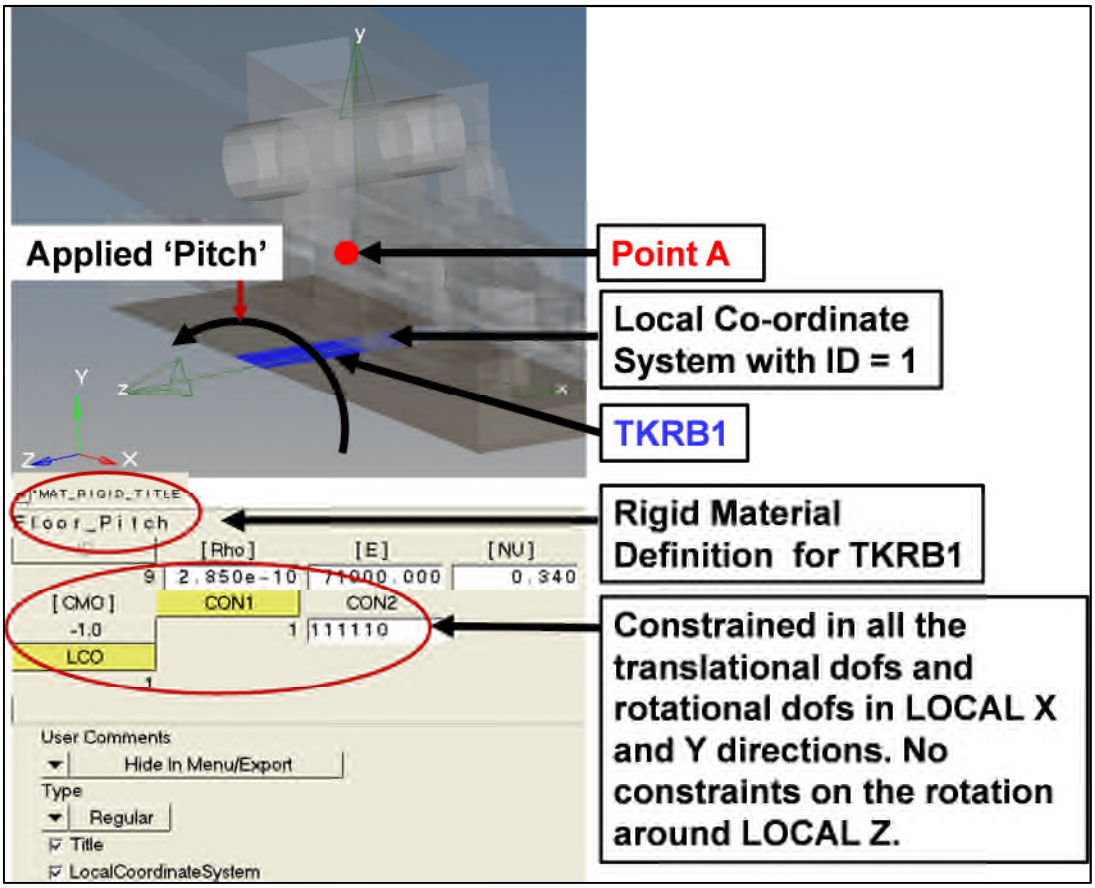

Figure Ap I-6 Floor deformation loads are applied through *MAT_RIGID. For applying 'Pitch' a local-coordinate system is defined, which ensures '10 degree YAW'. 'CON2' parameter is used to constrain all degrees-of-freedom except rotation corresponding to the 'Pitch' definition i.e. 111110 (1 stands for 'restraint' and '0' for free dof).

Such an arrangement ensures that the "Roll" and "Pitch" application point is the pivot point of the aft fitting projected in the Seat Track-Crown plane, which is in line with the requirement.

Appendix J PROCEDURE TO INITILISE THE STRESSES IN LSDYNA

In approach A (as explained in Section 9.2.2), “Floor-distortion” simulation is performed using Abaqus/ Standard. Then SIX stress components (three normal stress components and three shear stress components) along with equivalent plastic strain can be extracted either using Abaqus/CAE Report file (*.rpt) or using Altair/ Hyperview [33, 61].

J.1 Format to read initial Stress and Strain LSDYNA

*INITIAL_STRESS_SOLID [35]

Element ID	Number of Integration Points	σ_x	σ_y	σ_z	τ_{xy}	τ_{yz}	τ_{zx}	EPS
277939	1	-9.53E+00	-1.02E+01	-9.93E+00	6.83E-01	1.41E+00	7.22E-01	1.00E-03
278184	1	8.45E-02	-1.93E-01	1.39E+00	-1.28E-01	-5.29E-01	-1.91E-01	0.00E+00
278264	1	-3.64E+00	-4.58E+00	-4.03E+00	-2.24E-01	-6.54E-01	3.37E-01	4.00E-03
279544	1	-6.43E+00	-7.24E+00	-7.01E+00	6.24E-01	1.30E+00	8.41E-01	5.00E-03
280168	1	-9.96E+00	-1.04E+01	-9.88E+00	6.29E-01	1.50E+00	4.48E-01	0.00E+00
280646	1	-2.42E+00	-3.05E+00	-1.91E+00	-5.55E-01	-4.78E-01	-2.73E-01	1.00E-03
281162	1	-2.78E-02	-1.89E-01	4.56E-01	2.51E-01	2.69E-01	2.67E-01	0.00E+00
281238	1	-4.55E+00	-5.54E+00	-5.23E+00	5.21E-01	1.34E+00	5.14E-01	0.00E+00
281326	1	-6.37E+00	-7.44E+00	-6.87E+00	7.79E-01	1.70E+00	7.02E-01	4.00E-03
282554	1	-1.20E+00	-1.49E+00	-2.07E-01	-2.93E-01	-6.27E-01	-2.67E-01	0.00E+00
282798	1	-1.05E+00	-2.40E+00	-2.89E-01	2.10E-01	-2.72E-01	1.16E-01	0.00E+00

Figure Ap J-1 Format of the Control-Card “Initial_Stress_Solid/Shell" in LsDyna. This card initiates the SIX stress components and the effective plastic strain in the structure

Where,

Element ID – Unique element identification number

σ – Represents the components of normal stress in Cartesian co-ordinates

T - Represents the components of shear stress in Cartesian co-ordinates

EPS – Equivalent Plastic Strain

Please note the initial stress components for the “Shell” elements can be written in the same format with *INITIAL_STRESS_SHELL instead of *INITIAL_STRESS_SOLID [35].

File containing these two control cards can be included in the main input (keyword file, *file name*. k) file of “16g Dynamic pulse” generated by LSDYNA using [35],

*INCLUDE

file name.txt

J.2 Programme Script - FOX-PLUS

```
** Conversion.bat --- Program to Convert Abaqus Stress in LsDyna Format
foxplus fleconv
** fleconv.prg
set safe off
set date briti
set cent on
set excl on
do Nrs11le
do Nrs22
do Nrs33
do Nrs12
do Nrs23
do Nrs13
do Nrspeq
use nmsfinal
zap
append from nmstele
do Nrplpr1
clear
close all
```

```
quit

**nrs11le.prg -- Arrange Element Number and Normal Stress in X
SET EXCL ON
SELE A
USE NMSTELE
zap
APPE FROM S11ele.csv  DELIMITED
REPL ALL SRNO WITH STR(RECNO(),7)
REPL ALL F02 WITH '1'

**nrs22.prg Arrange Normal Stress in Y
SET EXCL ON
SELE A
USE NMSTELE
SELE B
USE NMS22
zap
APPE FROM S22.CSV DELIMITED
REPL ALL SRNO WITH STR(RECNO(),7)
INDE ON SRNO TO TTT

SELE A
SET RELA TO SRNO INTO B
REPL ALL F08 WITH B->F08 FOR SRNO=B->SRNO

**nrs33.prg Arrange Normal Stress in Z
SET EXCL ON
SELE A
USE NMSTELE
SELE B
```

```
USE NMS33
zap
APPE FROM S33.CSV DELIMITED
REPL ALL SRNO WITH STR(RECNO(),7)
INDE ON SRNO TO TTT

SELE A
SET RELA TO SRNO INTO B
REPL ALL F09 WITH B->F09 FOR SRNO=B->SRNO

**nrs12.prg Arrange Shear Stress in XY
SET EXCL ON
SELE A
USE NMSTELE
SELE B
USE NMS12
zap
APPE FROM S12.CSV DELIMITED
REPL ALL SRNO WITH STR(RECNO(),7)
INDE ON SRNO TO TTT

SELE A
SET RELA TO SRNO INTO B
REPL ALL F10  WITH B->F10 FOR SRNO=B->SRNO

**nrs23.prg Arrange Shear Stress in YZ
SET EXCL ON
SELE A
USE NMSTELE
SELE B
USE NMS23
```

```
zap
APPE FROM S23.CSV DELIMITED
REPL ALL SRNO WITH STR(RECNO(),7)
INDE ON SRNO TO TTT

SELE A
SET RELA TO SRNO INTO B
REPL ALL F11 WITH B->F11 FOR SRNO=B->SRNO

**nrs13.prg Arrange Shear Stress in ZX
SET EXCL ON
SELE A
USE NMSTELE
SELE B
USE NMS13
zap
APPE FROM S13.CSV DELIMITED
REPL ALL SRNO WITH STR(RECNO(),7)
INDE ON SRNO TO TTT

SELE A
SET RELA TO SRNO INTO B
REPL ALL F12 WITH B->F12 FOR SRNO=B->SRNO

**nrspeq.prg Arrange Equivalent Plastic Strain
SET EXCL ON
SELE A
USE NMSTELE
SELE B
USE NMSpeq
zap
```

```
APPE FROM peeq.CSV DELIMITED
REPL ALL SRNO WITH STR(RECNO(),7)
INDE ON SRNO TO TTT
SELE A
SET RELA TO SRNO INTO B
REPL ALL F13 WITH B->F13 FOR SRNO=B->SRNO

**nrplpr1.prg
set safe off
set echo off
set excl on
use Nmsfinal

repl all f1  with  right(space(10)+trim(f1),10)
repl all f02 with  right(space(10)+trim(f02),10)
repl all f07 with  right(space(10)+trim(f07),10)
repl all f08 with  right(space(10)+trim(f08),10)
repl all f09 with  right(space(10)+trim(f09),10)
repl all f10 with  right(space(10)+trim(f10),10)
repl all f11 with  right(space(10)+trim(f11),10)
repl all f12 with  right(space(10)+trim(f12),10)
repl all f13 with  right(space(10)+trim(f13),10)
copy to Nmkchk1
dele all for f1=space(10)
dele all for f07=' C'
pack
label form omkfle to babaomk.txt
copy to Converted.txt sdf
```

J.3 Stress and Strain Initialisation

Once the deformed seat configuration for the damaged floor condition has been obtained as the starting point of “16g” dynamic loading, next task is to involve initial stress and strain conditions. This is accomplished using the Abaqus/CAE output converted into a suitable LSDYNA format using a FOX-Plus programme developed “In-House” (as explained in Appendix J.2). Figure Ap J-2 and J-3 corroborates the accurate conversion and initialisation of stresses and strains in the structure.

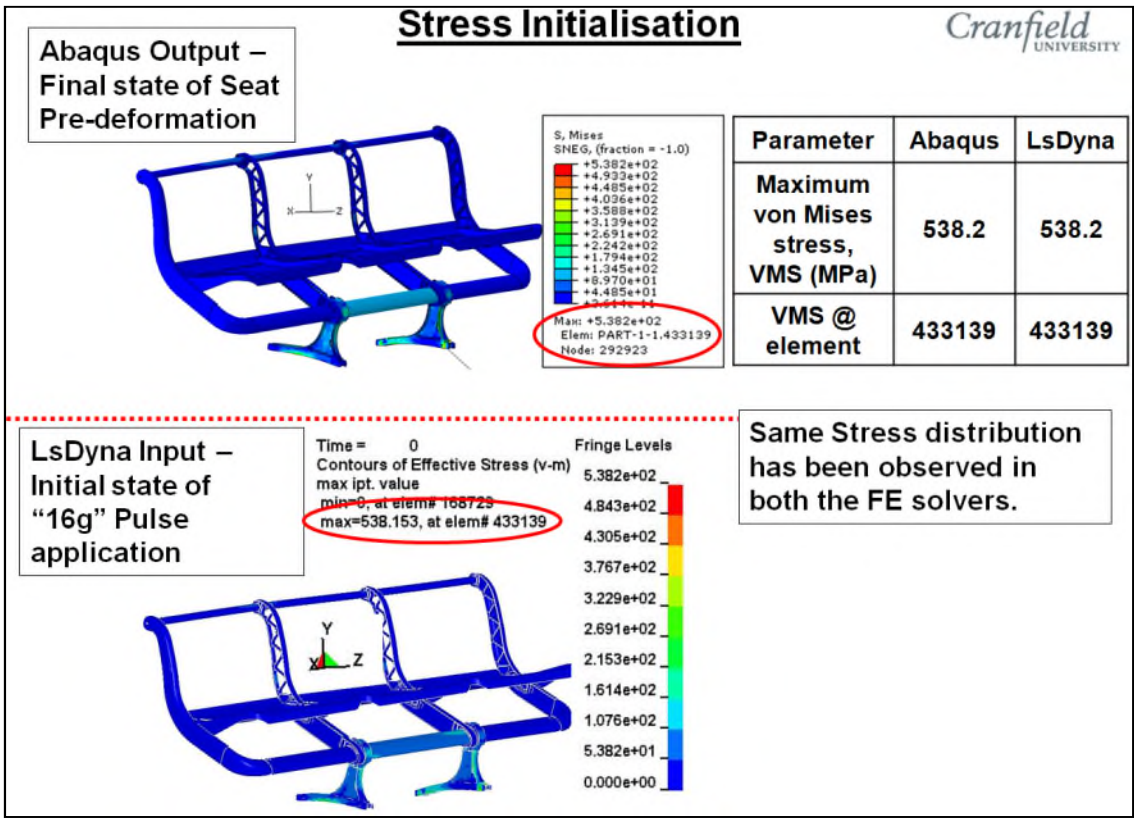

Figure Ap J-2 Stress initialisation for the yawed Seat structure with damaged floor condition (Seat Predeformation). A programme developed in-house converts the Abaqus (Research) 6.9-3 output into the required LSYNA format

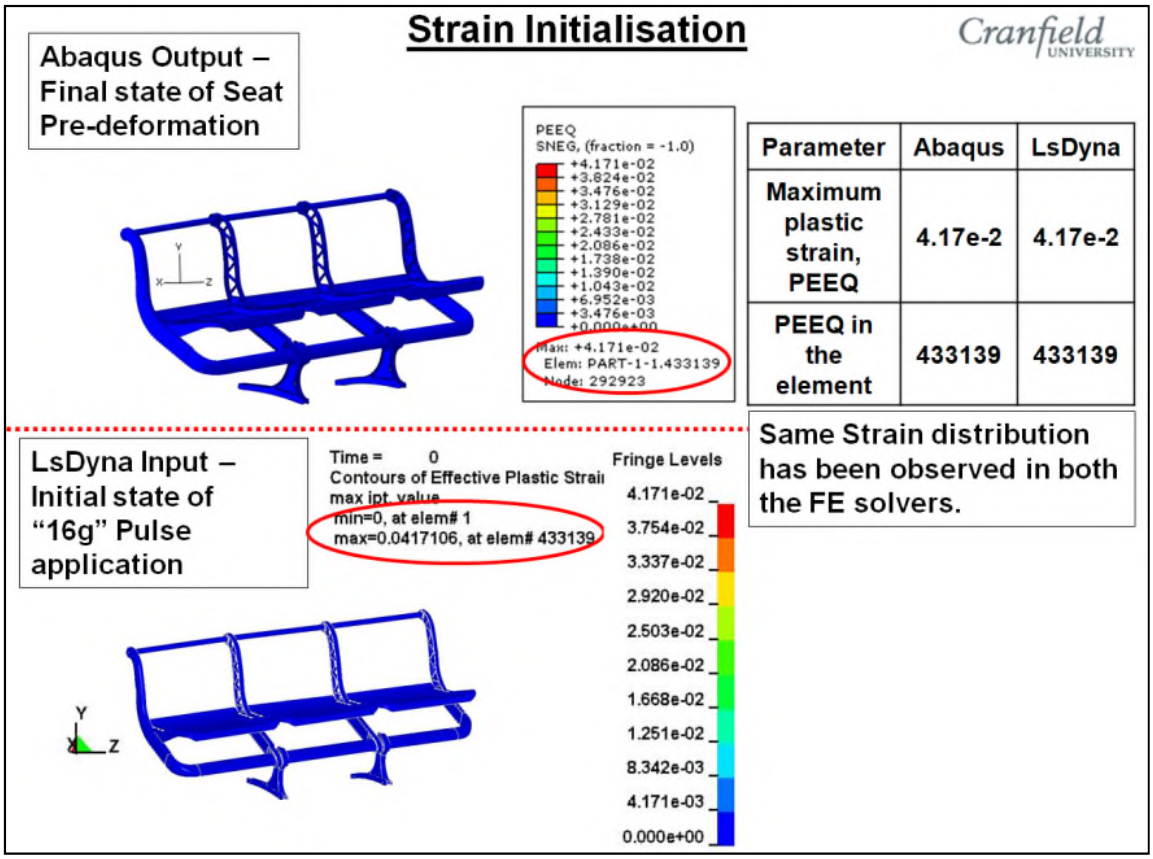

Figure Ap J-3 Strain initialisation for the yawed Seat structure with damaged floor condition (Seat Predeformation). A programme developed in-house converts the Abaqus (Research) 6.9-3 output into the required LSYNA format

Appendix K MATERIAL PROPERTIES (MECHANICAL)

Figure Ap K-1 summarise the mechanical properties of the material used for each component of the seat structure along with the material models used in LSDYNA [35, 65, 66].

Material	Density, g/cc	Modulus of elasticity , N/mm^2	Poisson's ratio	LsDyna Material Model
Al 6082 T6	2.70	7.10E+04	0.33	*MAT_PIECEWISE_ LINEAR_PLASTICITY (MAT_024)
Al 7075 T6	2.81	7.17E+04	0.33	
Al Alloy	2.85	7.10E+04	0.34	*MAT_ELASTIC (MAT_001)
CRES17-4PH (H900)	7.81	1.96E+05	0.30	

CRES17-4PH (H900)	
Yield - 1240 MPa	
Al 6082T6	
Engineering Stress, MPa	Engineering Strain
250.00	0.00
260.00	0.02
285.00	0.05
300.00	0.08
310.00	0.11

Al 7075T6	
Engineering Stress, MPa	Engineering Strain
475.73	0.00
482.63	0.02
506.76	0.04
517.11	0.06
524.00	0.08
526.00	0.10

Figure Ap K-1 Mechanical properties and the Engineering Stress-Strain

Material model used for Viton is the Mooney Rivlin.

The form of Mooney Rivlin strain energy potential [59, 60] is,

$U = C_{10} (I_1-3) + C_{01} (I_2-3) + (1/D_1) (J^{el}-1)^2$

Where,

U – Strain Energy per unit Reference Volume,

I_1 and I_2 – First and Second deviatory strain invariants defined as,

$I_1 = \lambda_1^2 + \lambda_2^2 + \lambda_3^2$ and $I_2 = (1/\lambda_1^2) + (1/\lambda_2^2) + (1/\lambda_3^2)$

λi are the principle stretches.

J – Elastic volume ratio

C_{01}, C_{10} and D_1 are the material constants

The input parameters required for the FE model of the elastomer are [35],

$C_{10} = 1.194$, $C_{01} = 0.163$ and $D_1 = 0$

For seatbelt, fabric material from LSDYNA library (MAT_034) has been used [35, 66]. A density of 890.6 Kg/m3, modulus of elasticity of 2.03 GPa and Poisson's ratio of 0.2 were input into MAT_034 [20]. The force vs. engineering strain loading and unloading curves are taken from the experimental data published by Olivares et al [20]. The seatbelt specimen is loaded at a constant displacement rate until a maximum load of 11.6 KN is reached thereafter unloading at the same displacement rate.

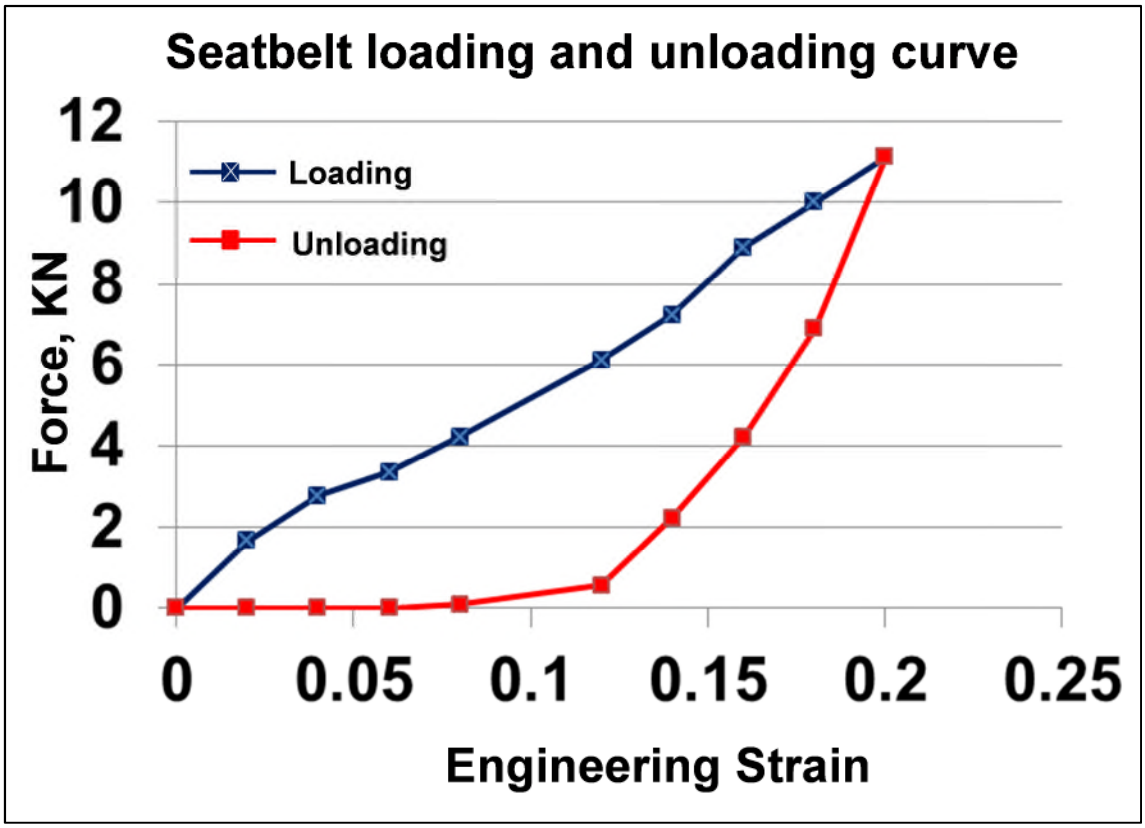

Figure Ap K-2 Force vs Engineering strain (loading and unloading) curve for seatbelt [20, 66].

Appendix L NOMENCLATURE OF THE LEG FROM "DESIGN VIEWPOINT"

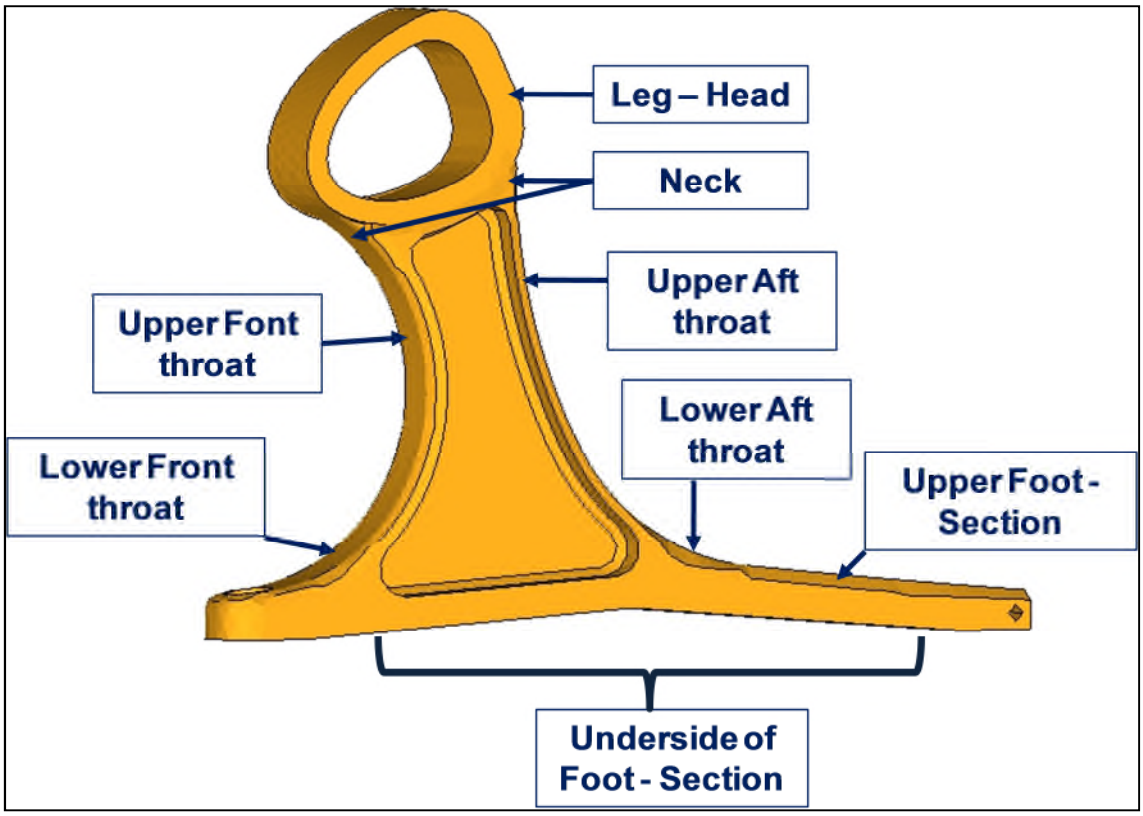

Figure Ap L-1 Nomenclature of leg from "Design Viewpoint"

Appendix M ELEMENTS OF FE MODEL- STATIC (9G) COMPLIANCE

M.1 Total mass considered

The total mass considered for the CS 25.561 consists of an occupant mass 77kg, mass of the seat structure 8.22kg (for basic fixed economy seat including restraints, cushions, food trays, all electronics and avionics items), life vest 0.9kg per passenger and mass of the in-plane literature 2.88kg per passenger. Therefore, the total mass is 89.00kg [10, 57]. This mass is then multiplied by corresponding “g” factor in the respective direction e.g. for “Forward 9g” load case, total seat mass of 87.48 kg is multiplied by a factor of (9.81*9) resulting in 7857.81N of force for each seat. Load application point is defined by Technical Standard order TSO-C39 [15] and is shown in Figure 8-12 A.

M.2 Parts Considered for FEA

The process of selecting the parts; to be considered for their FE representation; is strongly driven by what information is sought; degree of accuracy required and anticipated computational cost and capabilities of FE solver (ultimate design tool to be used).

Since certification of a Passenger-Seat is a very cost – intensive process, the modular assembly of seat structure is a basic design principle [22]. Now-a-days, airliners want to use different seat configurations on different seat track layouts. This is accomplished mainly by shifting seat spreading and using different seat legs for different seat track spacing. Therefore, identification of main structural components that carry the load from passengers to aircraft floor is an important task.

In the “Sleep Seat”, loads from the passenger are transferred to the boomerangs as the seat belts are anchored to them. Loads from all the boomerangs are then accumulated at “Forward beam”, which are then transferred to the seat track via legs. Thus the boomerang, Forward beam and the seat leg are the major load carrying members. Successful design of these

components will guarantee: adequate structural strength and functionality of seat. Therefore, these components are involved in the FE model.

Boomerangs are held together with the aft beam at the top and through seat pan near the belt anchorage. Therefore, aft beam, seat pan, seat pan attachment bracket and the corresponding spacers (connectors) are involved in the FE model.

Airline specifications demand “Seat Interface Loads (static loads imposed by the seat structure on the aeroplane floor). Therefore, tool-less fittings along with the seat track is involved in the FE model.

A Bill of materials (BOM) for the parts considered in the FE model of “Sleep Seat” is shown in Figure Ap M-1 and Figure Ap M-2. Please note that parts and material used for a particular component may vary depending on the variant of ‘Sleep Seat’.

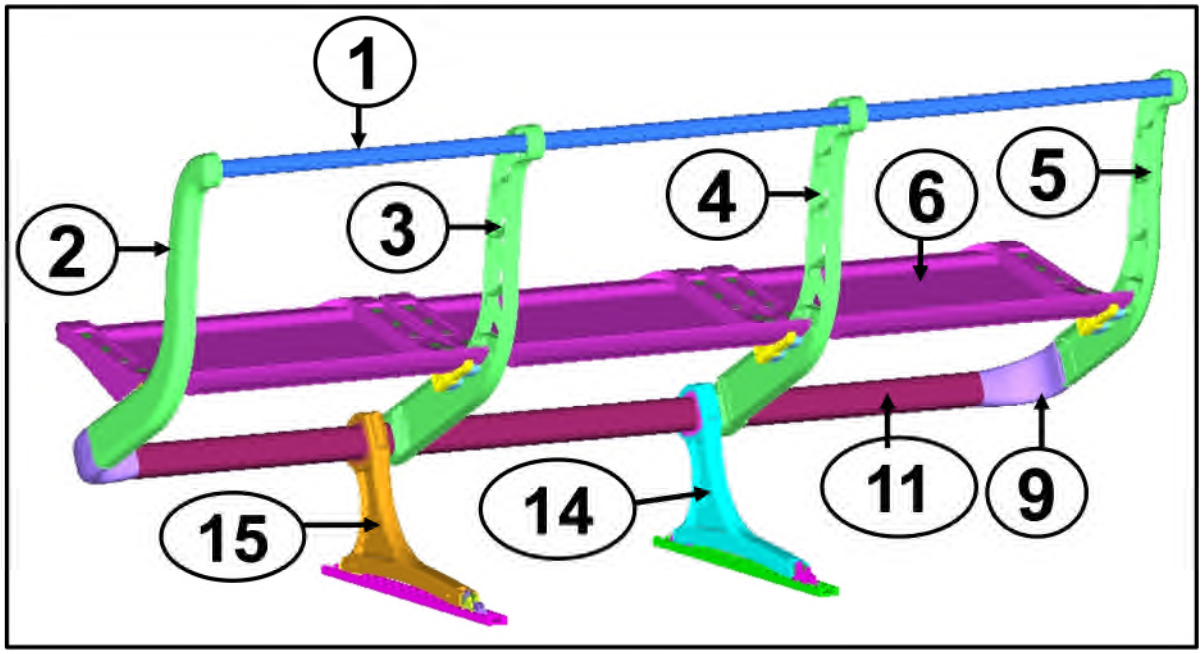

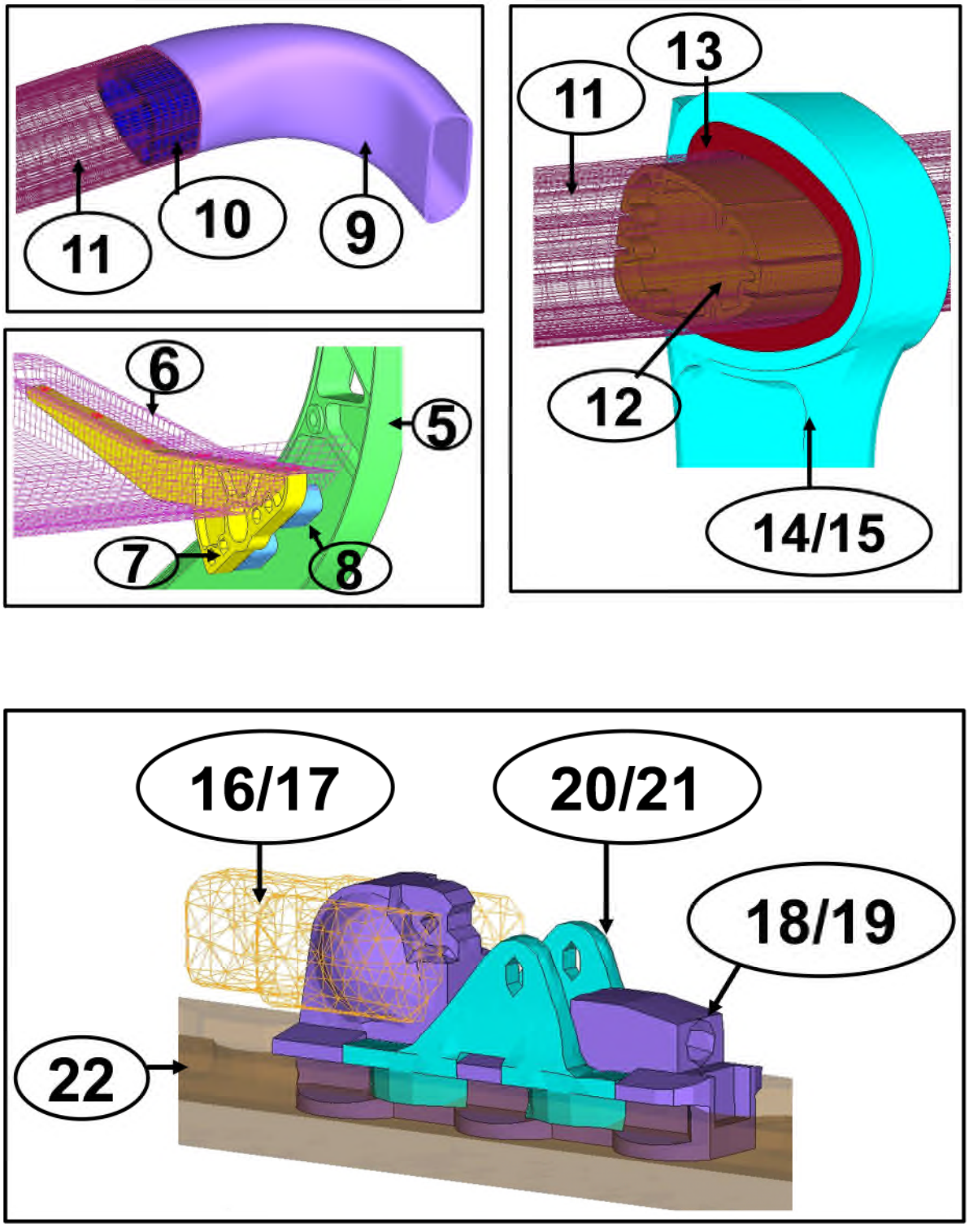

Figure Ap M-1 Nomenclature for the "Sleep Seat".

Serial Number	Component	Quantity	Material	Thickness, mm	Mass, g	Nodes	Elements	Element Type
1	Aft Beam	3	Al6082T6	1.5	173.9	6125	6076	Shell
2	LHS Side Boomerang	1	Al6082T6	2.5	573.2	28028	18934	Hexahedral
3	Center Boomerang	1	Al6082T6	2.5	573.2	28028	18934	Hexahedral
4	Offset Boomerang	1	Al6082T6	2.5	643.3	51090	33040	Hexahedral
5	RHS Side Boomerang	1	Al6082T6	2.5	689.9	57253	37989	Hexahedral
6	Seat Pan	3	Al6082T6	3.6	2799	7048	6954	Shell
7	Seat Pan Bracket	6	Al6082T6	2	118.7	8661	5462	Hexahedral
8	Connector	12	Al6082T6	Solid	19.4	801	520	Hexahedral
9	Corner	2	Al6082T6	2.5	167.8	51520	38394	Hexahedral
10	Corner Insert	2	Al6082T6	2	38.09	4800	3108	Hexahedral
11	Forward Beam	1	Al6082T6	2	1480	55877	37000	Hexahedral
12	Forward Beam Insert	2	Al6082T6	2	121.2	13272	9075	Hexahedral
13	Leg Clamp (Insert)	2	Elastomer	4/7 mm	60.67	4350	3000	Hexahedral
14	Leg - RHS	1	Al7075 T6	Solid	759	7808	24904	Tetrahedral
15	Leg - LHS	1	Al7075 T6	Solid	759	7808	24904	Tetrahedral
16	TLF Housing (FR)	2	Al7075 T6	Solid	17.07	397	1060	Tetrahedral
17	TLF Housing (RR)	2	Al7075 T6	Solid	17.35	375	1014	Tetrahedral
18	TLF (FR) - Main Body	2	CRES 17 - 4PH	Solid	88.8	2108	7237	Tetrahedral
19	TLF (RR) - Main Body	2	CRES 17 - 4PH	Solid	103.3	2075	6908	Tetrahedral
20	TLF (FR) - Retainer	2	CRES 17 - 4PH	Solid	10.7	780	2275	Tetrahedral
21	TLF (RR) - Retainer	2	CRES 17 - 4PH	Solid	28.5	942	2656	Tetrahedral
22	Seat Track	2	Al - Alloy	Solid	341	6599	20834	Tetrahedral

Figure Ap M-2 BOM (Bill of Materials) for the "Sleep Seat"

M.3 Definition of contact pairs

Non-linear Contact pairs

- Seat track and each of the main body of the tool-less fittings (TLF)
- Seat track and each of the retainer of the TLF
- Seat track and Seat leg
- Each of the retainer and the main body of the TLF
- TLF housing and main body of the TLF
- Seat Leg and TLF
- Seat leg and Outer surface of the Elastomer
- Forward beam and Inner surface of the Elastomer

Tied Contact pairs

- TLF Housing and Seat leg
- Forward beam and reinforcing inserts
- Forward beam and Connecting corners
- Forward beam and Boomerang
- Boomerang and Connecting Corners
- Boomerang and Aft beam

MPC (Multi Point Constraints) to simulate the joints between

- Boomerang and Connector (spacer)
- Connector (Spacer) and Seat Pan Attachment Bracket
- Seat Pan Attachment bracket and Seat Pan

Thus, complete seat model includes total 40 non-linear contact pairs, 12 tied contacts and 90 MPC connections.

Appendix N DEFORMATION CONTOURS OF THE TRIPLE SEAT STRUCTURE SUBJECTED TO STATIC CS25.561 INERTIA LOADS

Loadcases presented –

A. Downward 8.6g
B. Side 4g
C. Rear 1.5g
D. Upward 3g

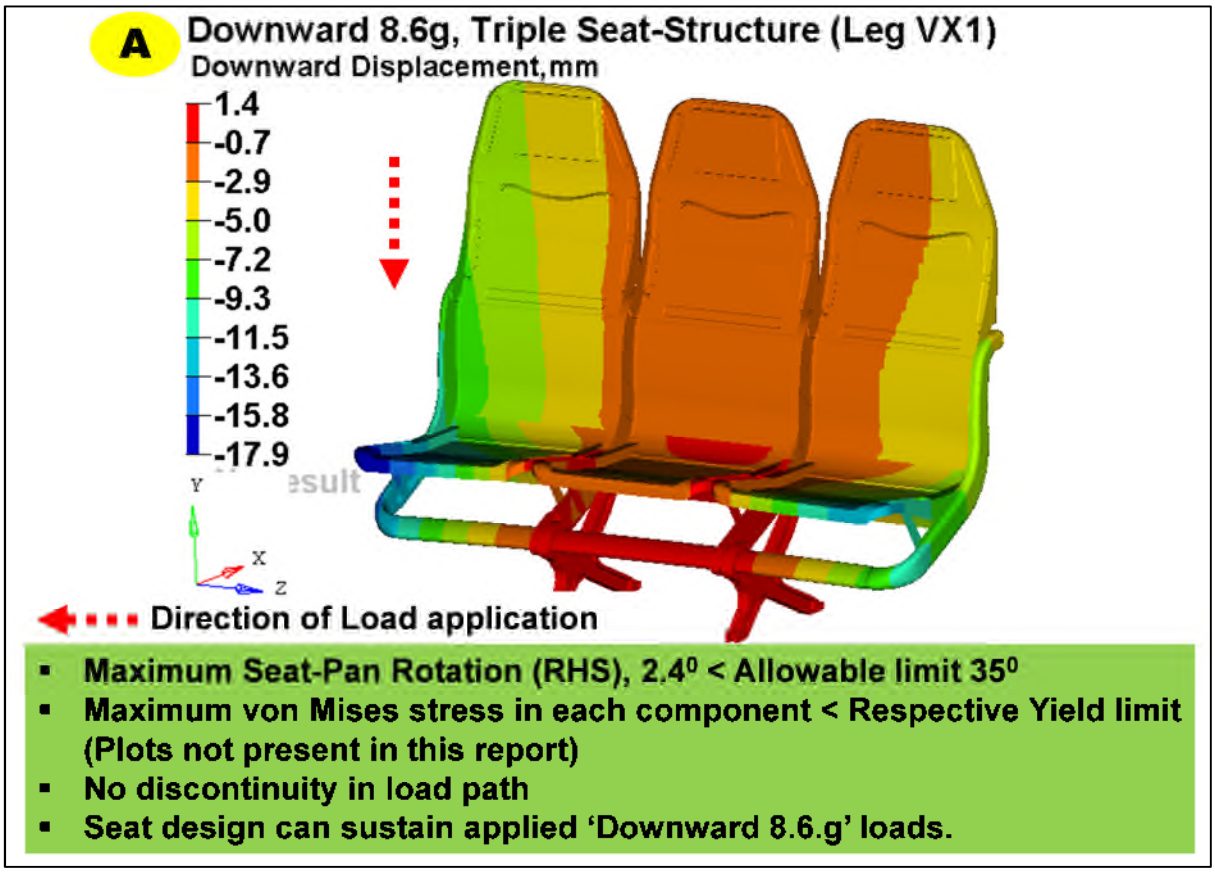

B

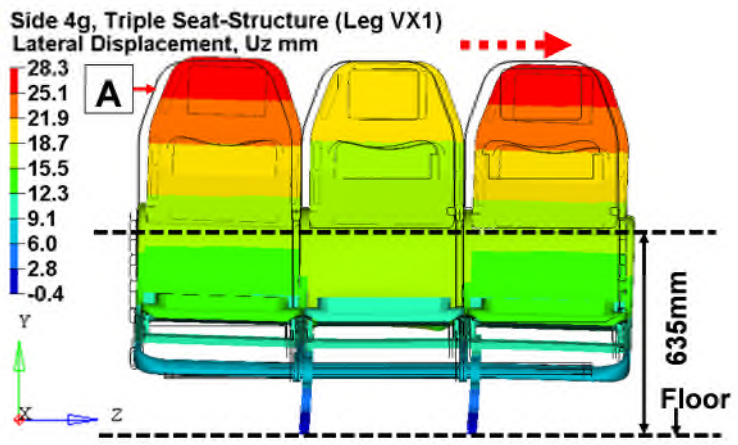

A Un-deformed Structure (Edge-View)

Direction of Load application

Distance above Floor, mm	Lateral Displacement, mm	Allowable Limit, mm
635	17.9	38
Above 635	28.3	50

- Maximum von Mises stress in each component < Respective Yield limit (Plots not present in this report)
- No discontinuity in load path
- Seat design can sustain applied 'Sideward 4g' loads.

C

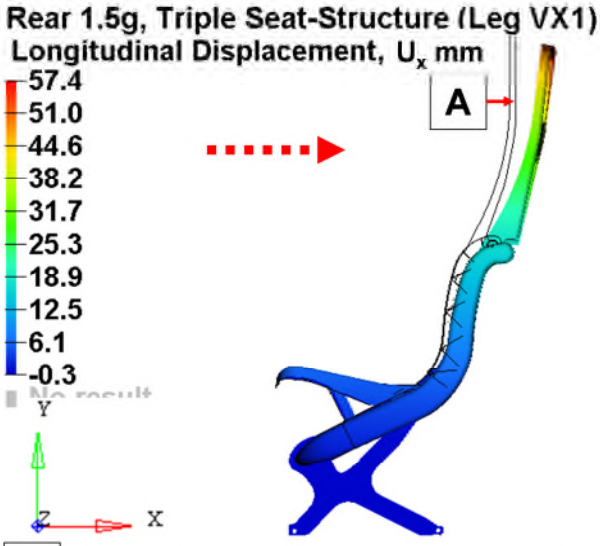

A Un-deformed Structure (Edge-View)

Direction of Load application

- Maximum longitudinal Displacement, 57.4mm < Allowable limit 75mm
- Maximum von Mises stress in each component < Respective Yield limit (Plots not present in this report)
- No discontinuity in load path
- Seat design can sustain applied 'Rearward 1.5g' loads.

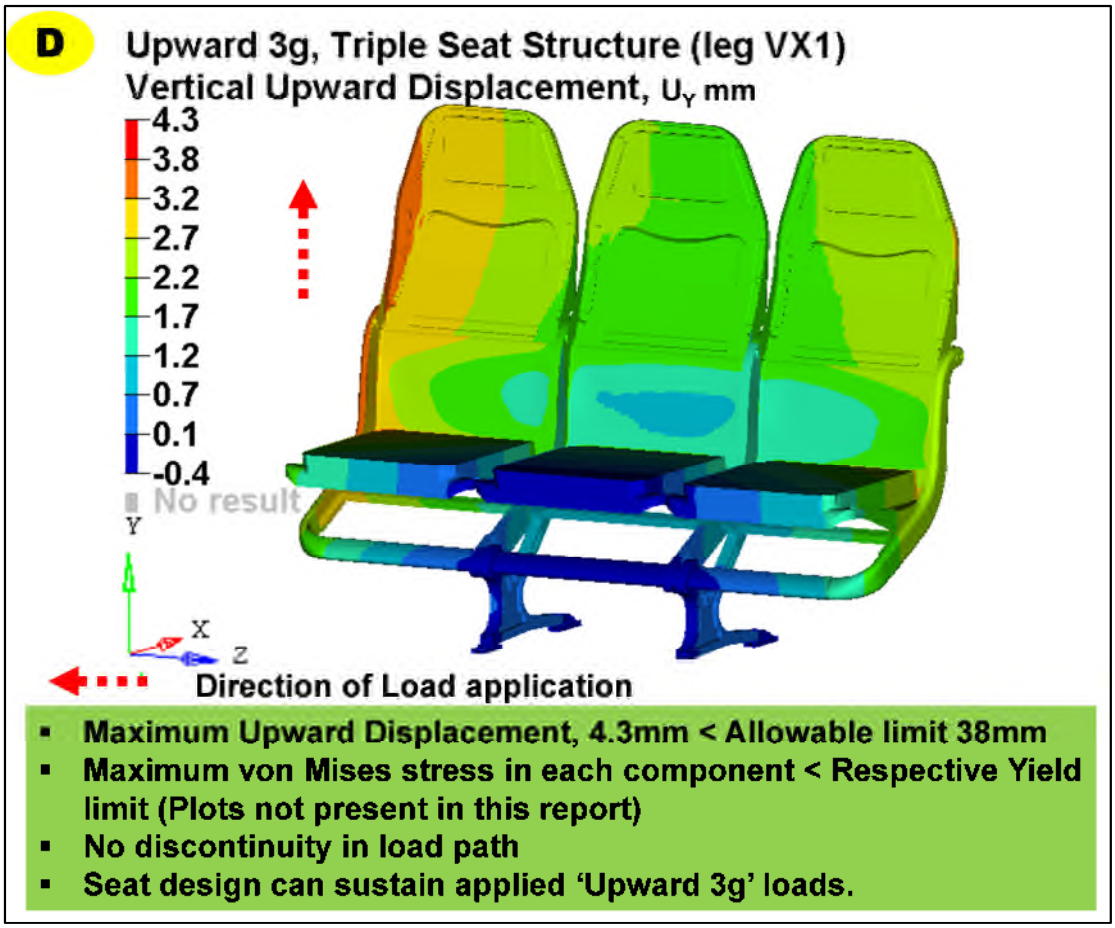

Figure Ap N-1 Overall deformation plot of triple seat-structure. Each plot summaries the maximum deformation observed and allowable limit. Loadcases A – Downward 8.6g, B – Sideward 4g, C – Rearward 1.5g and D – Upward 3g

Appendix O VMS (MPa) DISTRIBUTION PLOTS FOR PRIMARY LOAD PATH MEMBERS (CS 25.562)

Initially materials assigned for different components of seat-structure and stress-strain behaviour has been provided for interpreting the results

Components, Materials assigned and Stress-strain behaviour

Components – Seat Leg, Boomerang

Al 7075T6	
Engineering Stress, MPa	Engineering Strain
475.73	0.00
482.63	0.02
506.76	0.04
517.11	0.06
524.00	0.08
526.00	0.10

Components – Forward Beam, Mid beam, Aft beam, Seat pan

Al 6082T6	
Engineering Stress, MPa	Engineering Strain
250.00	0.00
260.00	0.02
285.00	0.05
300.00	0.08
310.00	0.11

Figure Ap O-1 Materials assigned to different components of triple seat-structure. Stress-Strain relationship has also been provided for interpreting the VMS results of dynamic '16g' simulation with damaged floor condition

O.1 Loadcase – '16g' with damaged floor condition (CS25.562)

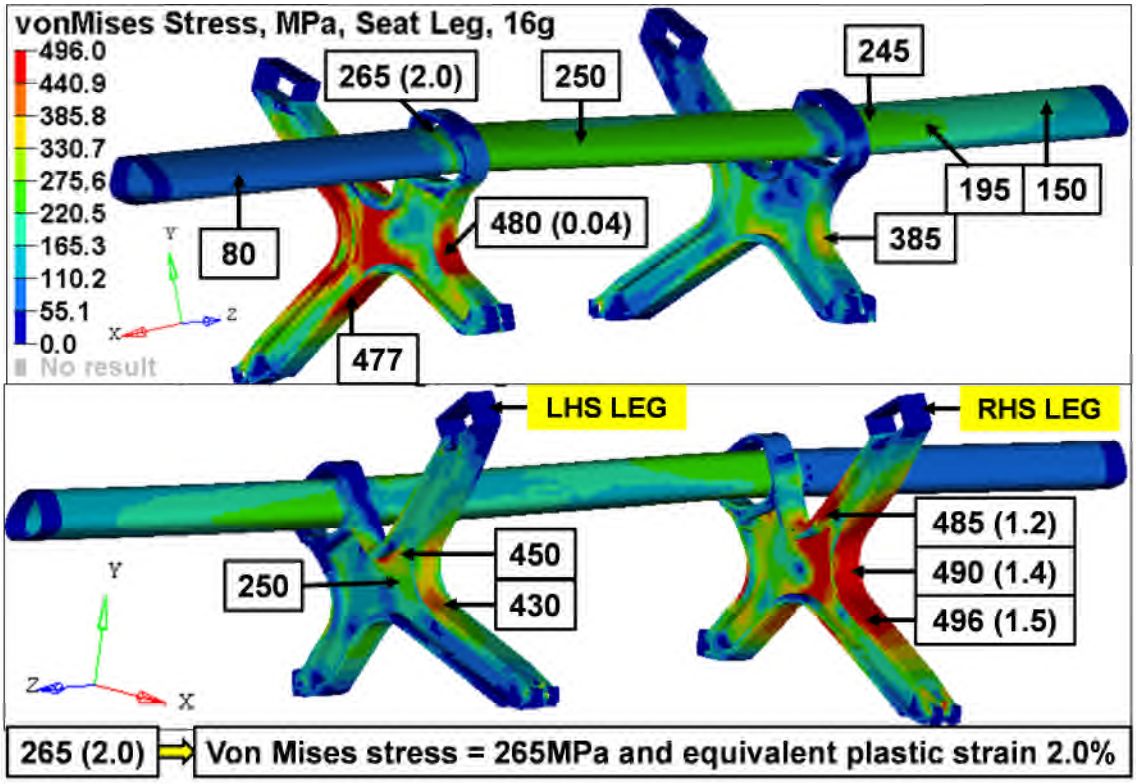

Figure Ap O-2 Von Mises plot for Seat-leg (VX1). The seat-leg can withstand the pulse without a rupture (referring Figure Ap O-1). Loadcase – Dynamic '16g' with damaged floor condition. Solver – LSDYNA

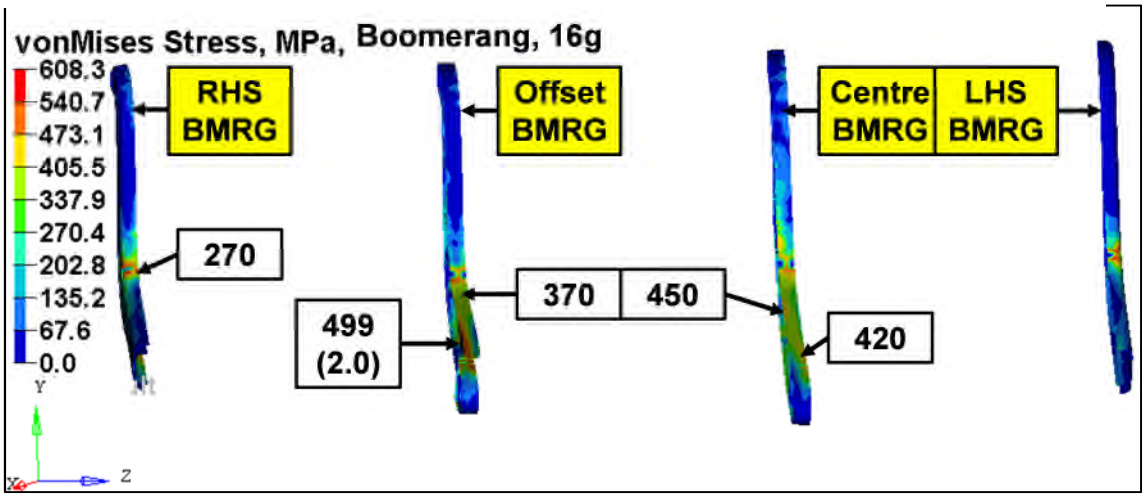

Figure Ap O-3 Von Mises plot for boomerang. It can withstand the pulse without excessive plastic deformations (referring Figure Ap O-1). Loadcase – Dynamic '16g' with damaged floor condition. Solver – LSDYNA

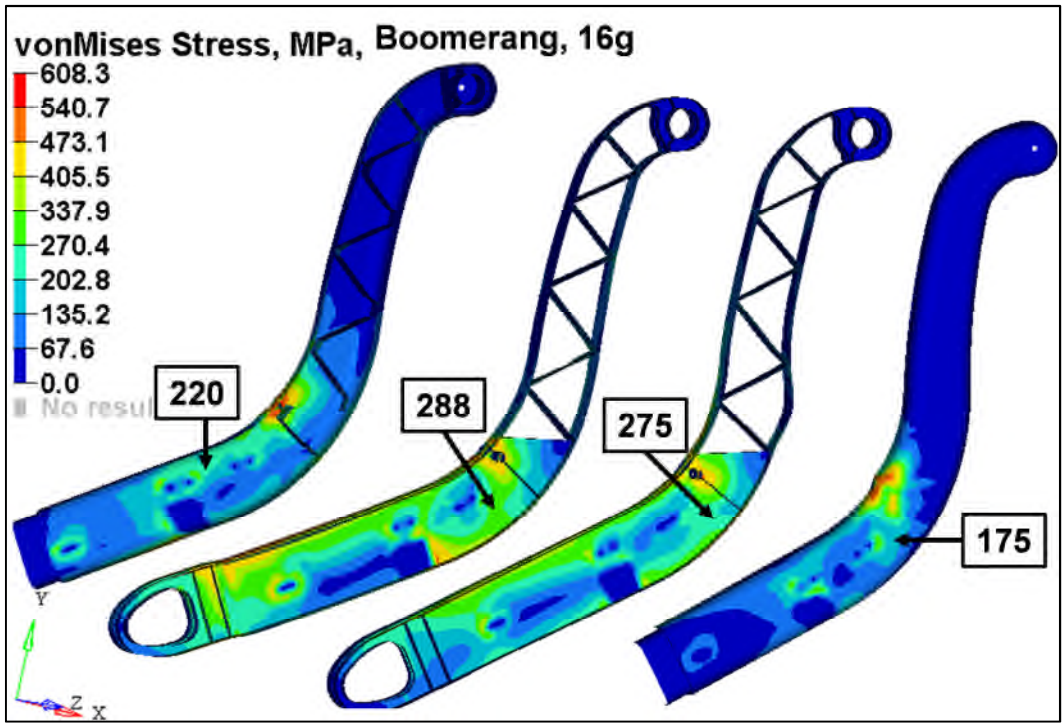

O.2 Loadcase – '14g' (CS25.562)

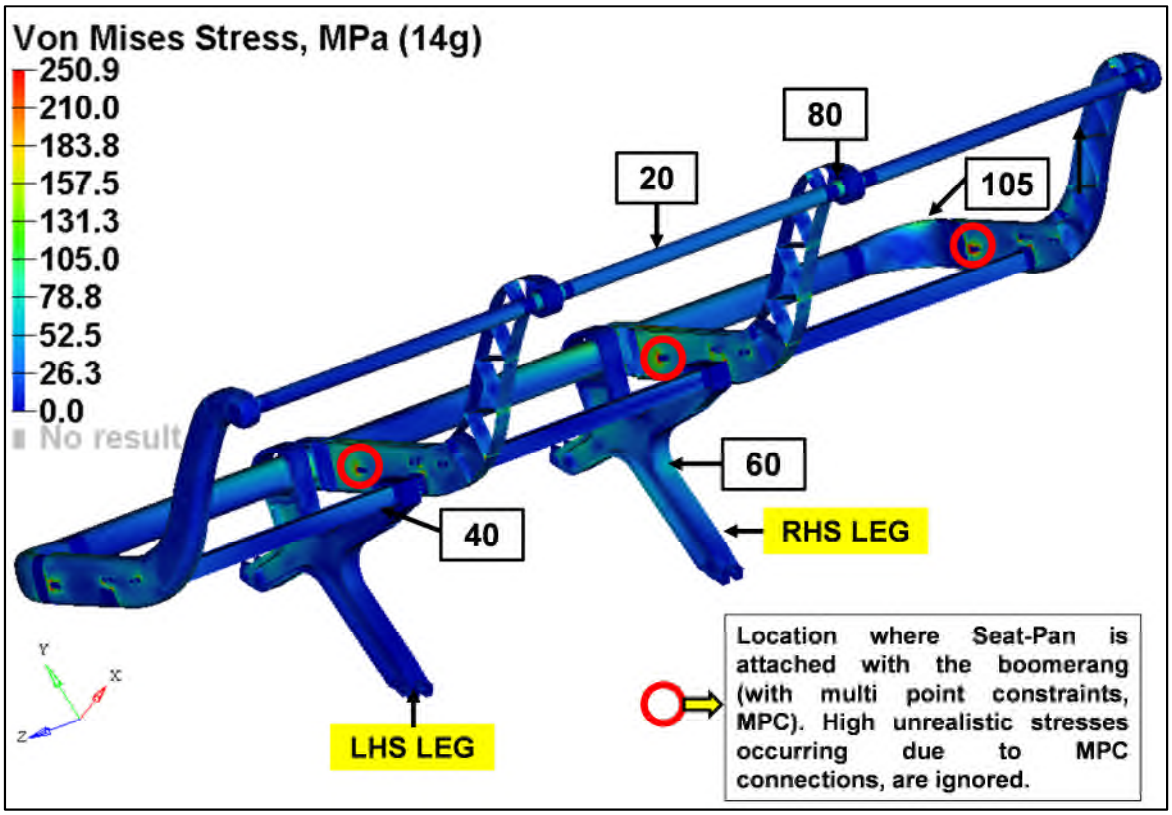

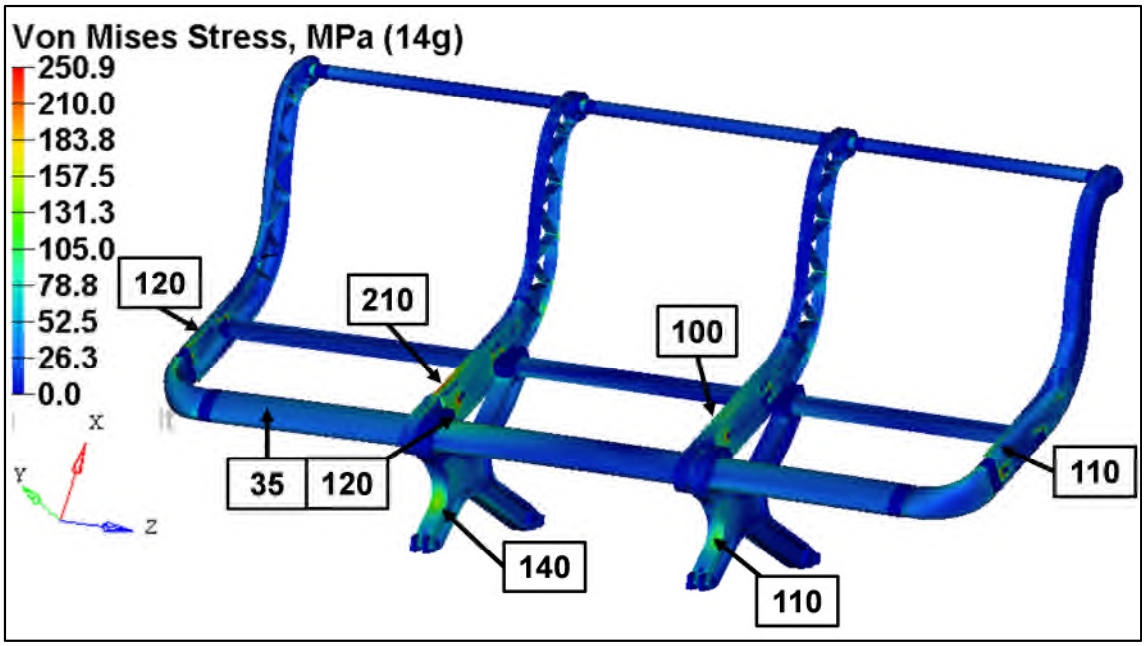

Figure Ap O-4 VMS plot for primary structure of triple seat subjected to dynamic '14g'. The structure can withstand the pulse without permanent strain and hence is safe (referring Figure Ap O-1). Solver – LSDYNA

Appendix P TIME HISTORY PLOTS FOR 16G WITH DAMAGED FLOOR CONDITION

Summary of simulation

- Triple Seat structure with three 50th percentile Hybrid numerical dummies,
- Initial velocity – 13400mm/s, Peak acceleration of “16g” achieved in 0.09s,
- Total simulation time – 0.18s. However, Simulation stops at 0.13s due to negative volume of the element situated in the shoulder of the left hand side dummy (looking the seat structure from behind).

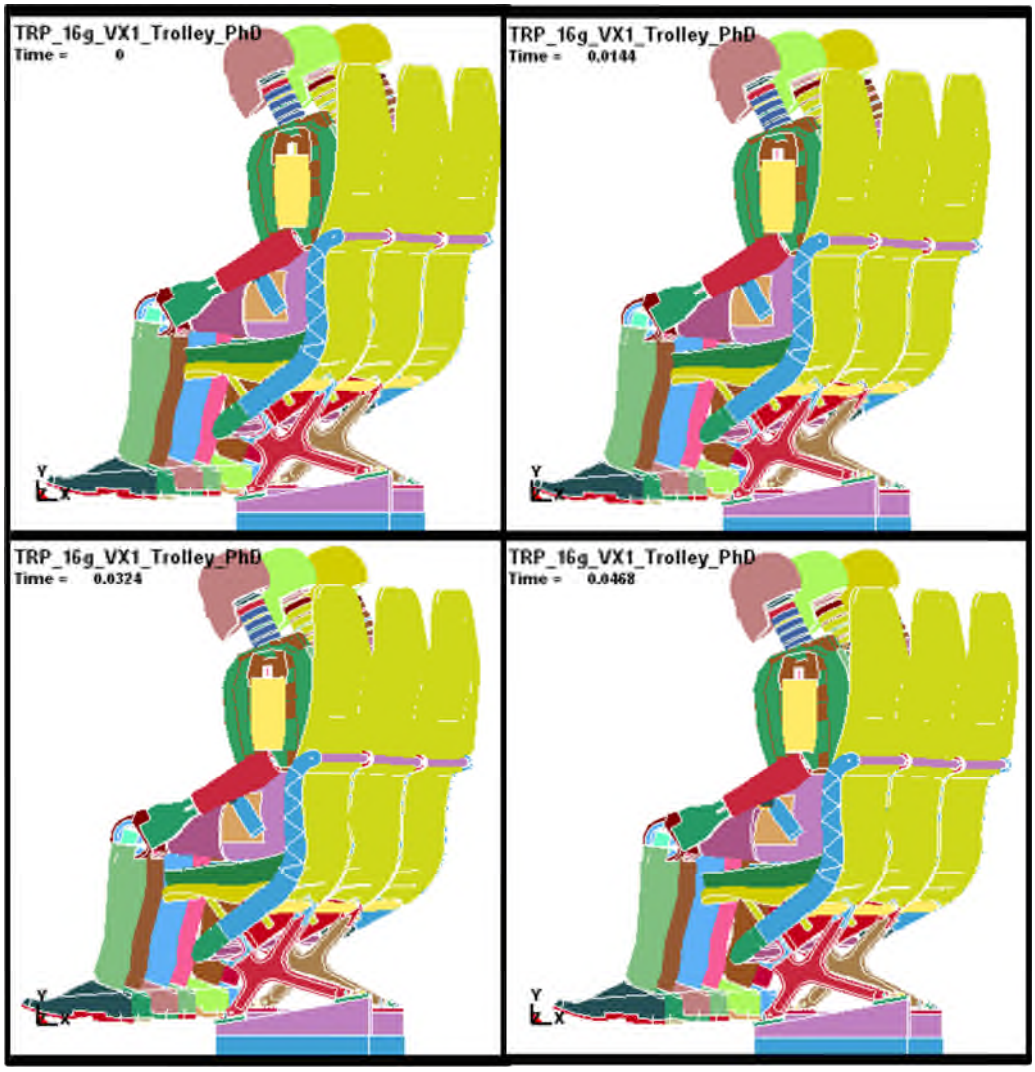

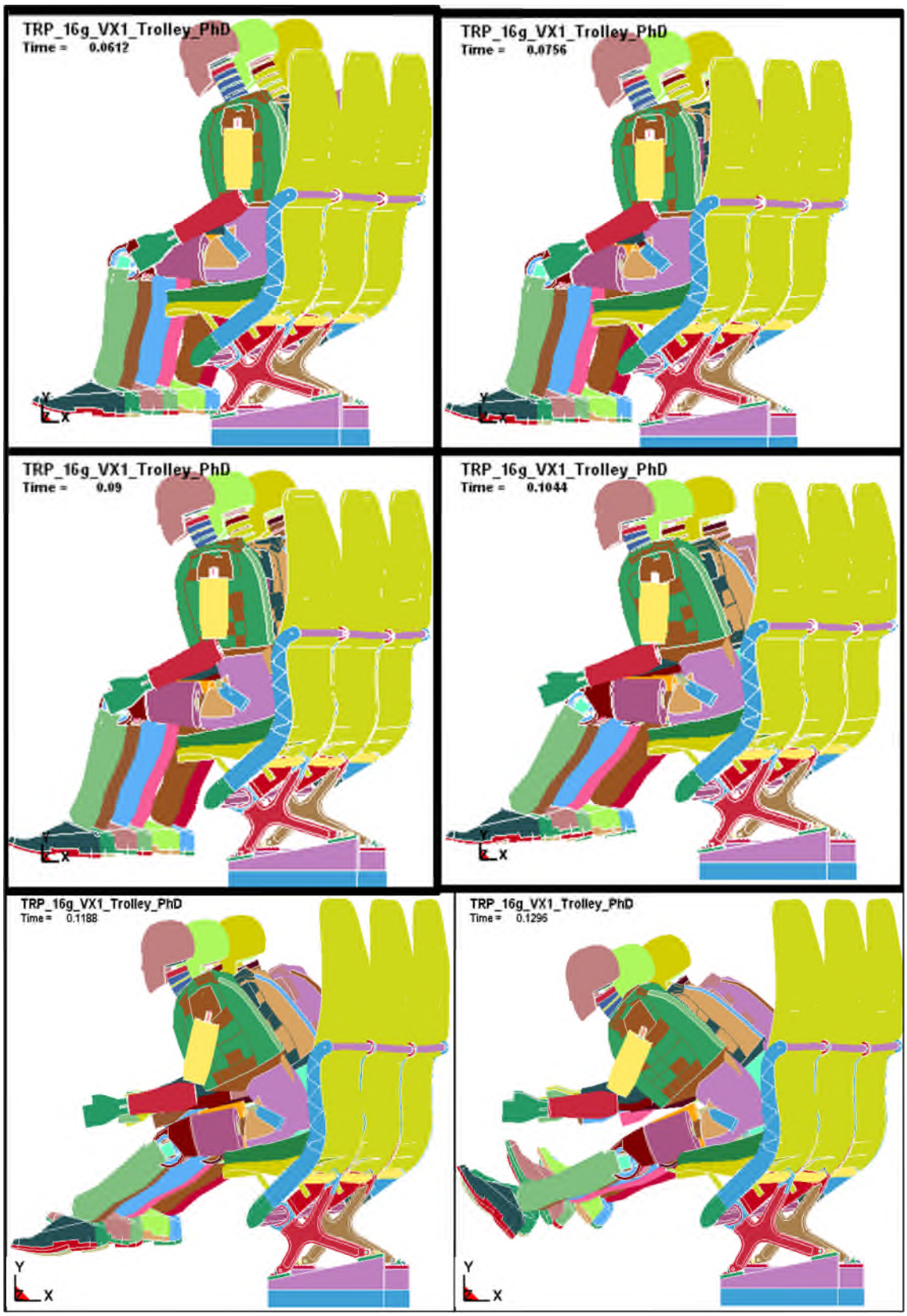

Figure Ap P-1 Time history plot of triple seat-structure with numerical dummies subjected to a dynamic '16g' pulse with damaged floor condition.